[illegible]

ProQuest LLC.
789 East Eisenhower Parkway
P.O. Box 1346
Ann Arbor, MI 48106 – 1346

THERMODYNAMICS OF INTERACTION OF MACROCYLIC LIGANDS WITH MULTIVALENT IONS AND ORGANIC MOLECULES OF BIOLOGICAL IMPORTANCE

A thesis submitted for the degree of

DOCTOR OF PHILOSOPHY

by

Marie-Claude Ritt

Department of Chemistry
University of Surrey

JANUARY 1991

ABSTRACT

The first part of this work deals with the determination of the thermodynamic parameters for the complexation of lanthanide cations (La^{3+}, Pr^{3+} and Nd^{3+}) with Cryptand-221 and Cryptand-222 in acetonitrile and propylene carbonate at 298.15 K. The complexation process between these cations and these ligands in these solvents is enthalpy-controlled. The higher stability observed for these cations and these ligands in propylene carbonate with respect to acetonitrile is attributed to the increase in entropy observed for the complexation reaction in propylene carbonate. Enthalpies of solution of lanthanide and lanthanide cryptates are reported. These data are used to derive single-ion enthalpies of transfer of La^{3+}, Pr^{3+} and Nd^{3+} from propylene carbonate to acetonitrile based on the Ph_4AsPh_4B convention. The results show that the cryptate conventions are not valid for the calculation of single-ion values for the transfer of tervalent lanthanide cations among dipolar aprotic media. Enthalpies of coordination of lanthanide(III) cryptates in the solid state are calculated.

The second part of this study aims to investigate the properties of the synthetic macrocyclic ligands such as Cryptand-222 and 18-Crown-6 towards molecules of biological importance. Stability constants (hence free energies), enthalpies and entropies of complexation of a series of DL-amino acids with 18-Crown-6 and Cryptand-222 in methanol and ethanol, as obtained from titration calorimetry, are reported. No significant variations are found in the free energies of complexation of the different amino acids and these two ligands in these solvents as a result of an enthalpy-entropy compensation effect. This effect is for the first time shown in complexation reactions involving crown ethers and cryptands.

The thermodynamic parameters of transfer of amino acids and their complexes with 18-Crown-6 and Cryptand-222 from methanol to ethanol have been calculated. Possible correlations between complexation and transfer data for the amino acids, the ligands and the amino acid-macrocyclic ligand complexes are investigated. The implications of these results to processes of biological importance are discussed.

As a continuation of this study, the possibility of selectively extracting amino acids from methanol by polymeric resins containing crown ethers as anchor groups is investigated.

ACKNOWLEDGEMENTS

I would firstly like to express my profound gratitude to my supervisor Dr Angela Danil de Namor. Her guidance, unfailing support and characteristic care have been of inestimable value to me.

Particular thanks are also due to my colleagues and friends for their assistance and encouragement throughout the whole period of my PhD. I would especially like to mention Franz Fernandez, Rafic Traboulssi and Jing Ping Zhang, whose understanding and generous cooperation I have valued very highly.

I would like to thank the technical staff of the Chemistry Department. The assistance of Dr David Lewis of the Biochemistry Department in the computer molecular modelling is sincerely acknowledged.

My heartfelt thanks to Prof Marie-José Schwing of the European Higher Institute of Chemistry of Strasbourg for the cordial welcome in her laboratory, where a part of this work has been carried out. I would like to take this opportunity to thank her, as well as Dr Françoise Arnaud and the staff of the Laboratoire de Chimie-Physique for their amiability and support shown during my stay in Strasbourg.

Finally, my sincere gratitude goes to the European Economic Community and the British Council for the financial support given to this project.

To My Loving Parents

TABLE OF CONTENTS

CHAPTER 1

INTRODUCTION

1.1 The Macrocyclic Ligands

1.1.1 Origin and General Aspects of Host-Guest Chemistry

The outset of host-guest chemistry dates back to the end of the nineteenth century when Emil Fischer enunciated his famous lock-and-key principle, referring to the stereo-electronic fit between enzymes and their bound substrates[1]. But, it was undoubtedly the discovery in the sixties of the fully artificial macrocyclic molecules which was the trigger for the extraordinary development of this area of research. Since then, host-guest chemistry has become one of the most promising and fascinating fields of study which led to the award of the 1987 Nobel Prize to its pioneers Pedersen, Lehn and Cram.

In 1967, Charles J. Pedersen reported the synthesis of the first neutral artificial molecule capable of complexing the alkali-metal ions[2]. This compound was an aromatic 18-membered ring: the macrocyclic polyether Dibenzo-18-Crown-6 (Fig. 1.1). This discovery was indeed fundamental as until then, only some naturally occurring antibiotics such as valinomycin and nonactin (Fig. 1.2) were known to form stable complexes with the non-transition metal cations[3,4] .

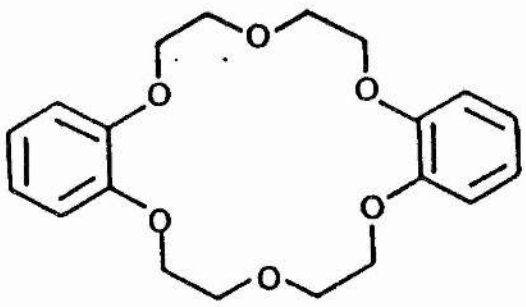

Figure 1.1 Structure of Dibenzo-18-Crown-6

The Dibenzo-18-Crown-6 turned out to complex very strongly and selectively alkali-metal cations, and it became clear that the complexation site was the hole of the macrocyclic ring. Pedersen then developed a large series of similar compounds which he called "crown ether"[5]. These are aromatic or saturated rings of various sizes, each one being designed to accommodate a particular cation in preference to others. A selection of the most commonly used crown ethers is presented in Fig. 1.3. Their names according to Pedersen's nomenclature system (ring substituent, number of ring members, number of oxygen atoms in the main ring) are also included in this figure.

Jean-Marie Lehn's idea was that three-dimensional molecules would be more selective complexing agents, and on this basis he synthesized, in 1968, the cryptands[6,7] (Fig. 1.4). The inclusion complexes formed with metal ions (cryptates) are highly structured. The bound ions are entirely surrounded by the cryptand. The properties of these ligands will be discussed in detail in this thesis (Chapter 2).

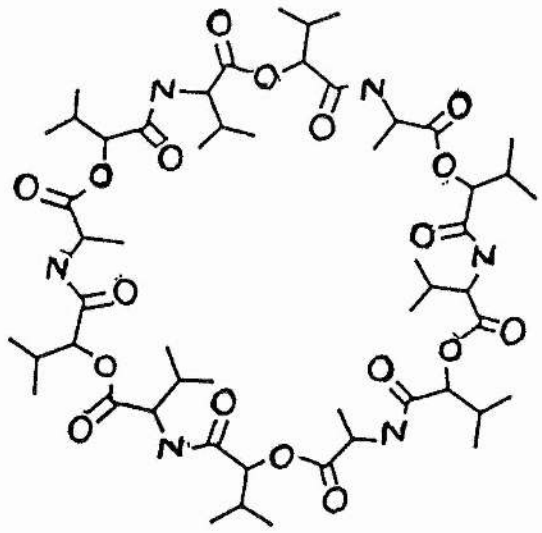

Valinomycin

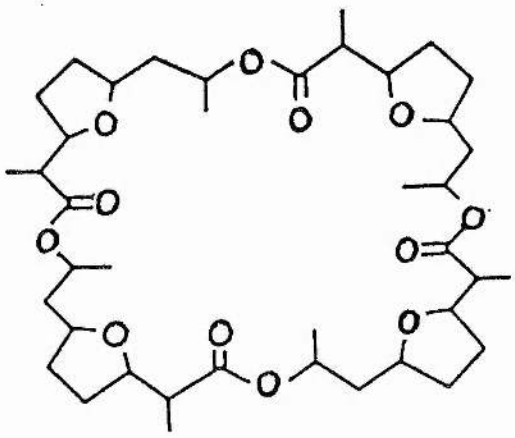

Nonactin

Figure 1.2 Structures of some naturally occurring antibiotics

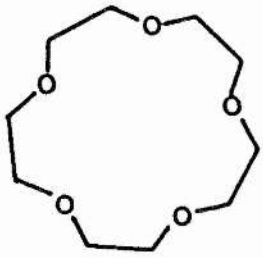

15 Crown 5

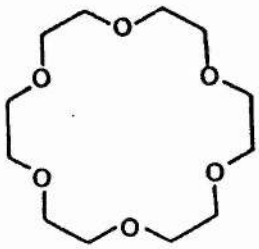

18 Crown 6

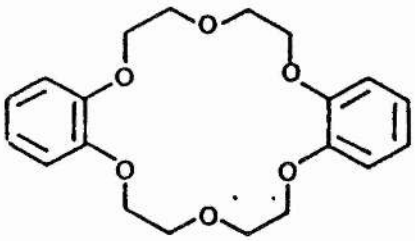

Dibenzo 18 Crown 6

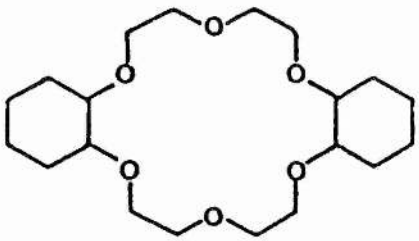

Dicyclohexyl 18 Crown 6

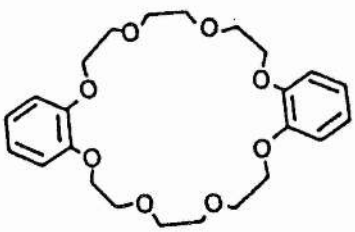

Dibenzo 24 Crown 8

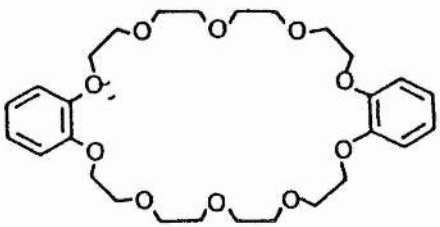

Dibenzo 30 Crown 10

Figure 1.3 Structure of the Crown Ethers

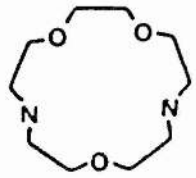

Cryptand 21

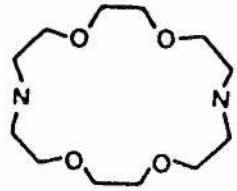

Cryptand 22

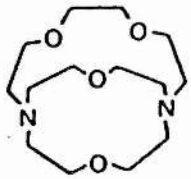

Cryptand 211

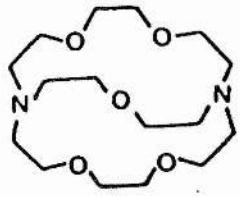

Cryptand 221

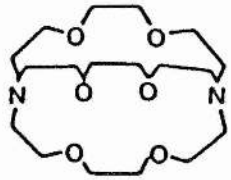

Cryptand 222

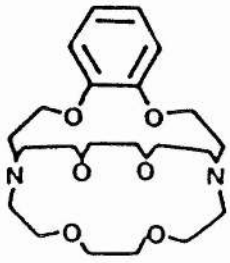

Benzo Cryptand 222

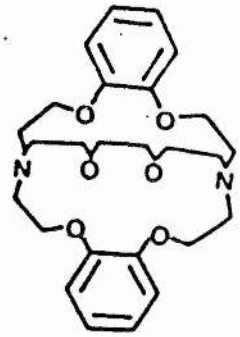

Dibenzo Cryptand 222

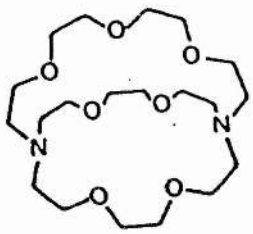

Cryptand 322

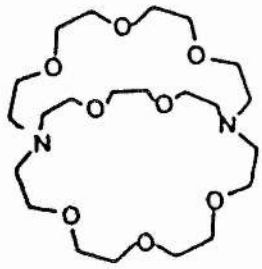

Cryptand 332

Figure 1.4 Structure of the Cryptands

A great number and variety of ligands of this type with various complexing and selectivity properties have since been developed. Their architecture are usually very sophisticated which may allow the complexation inside their structure of not only spheroidal metallic cations but also all kind of cationic, anionic or neutral species of organic, inorganic or biological nature.

Much of this work may be attributed to Donald J. Cram who notably designed and synthesized the spherands[8,9] (Fig. 1.5). These are fully preorganized ligands, their cavity being built in such a way that the coordination sites are strictly in the required positions for the complexation of the guest. Other well known families of macrocycles include the half-preorganized hemispherands[10] and the cryptaspherands[11] also developed by Cram (Fig. 1.6); and the non-cyclic podands developed by Vögtle and Weber[12,13].

The binding strength of these ligands with the metal cations can generally be classified as follow: spherands > cryptaspherands > cryptands > hemispherands > crown ethers > podands. This sequence illustrates clearly that the essential criteria for the successful design of strongly binding hosts is their preorganization. "To complex, hosts must have binding sites which cooperatively contact and attract binding sites of guests without generating strong non-bonding repulsions"[14,15]. Cram carried out the separation of racemic mixtures of amino acids following the concept that chiral hosts selectively bind guests of same chirality[16,17].

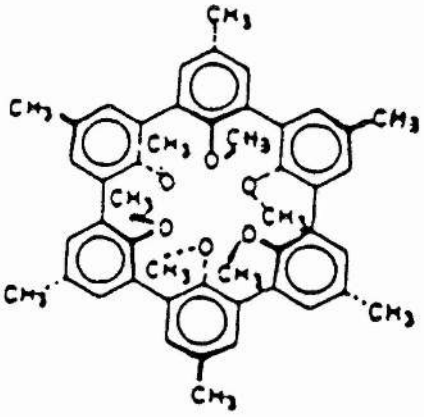

Spherand

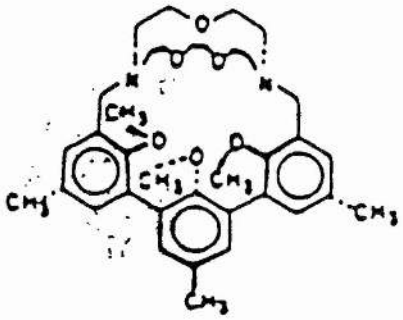

Cryptaspherand

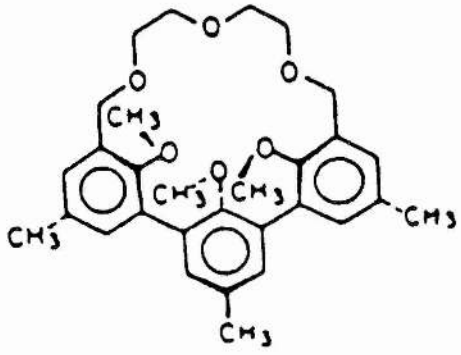

Hemispherand

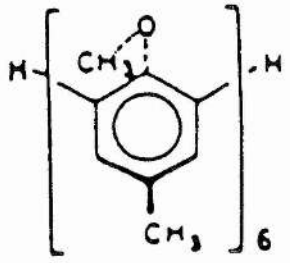

Podand

Figure 1.5 Structure of other macrocyclic ligands

1.1.2 Binding Properties

The understanding of the type of interactions governing the complexation of host molecules with smaller guest molecules is the fundamental feature of supramolecular (or host-guest) chemistry. Unlike the conventional molecular chemistry, the intermolecular binding forces between hosts and guests are essentially non-covalent, in fact they are very similar to the interactions found in biological systems.

Metal ions are bound to the macrocyclic ligands by electrostatic forces between the positive charged ion and the negative dipolar charges of the donor atoms (usually oxygen, nitrogen and/or sulphur) of the ring. This type of binding is the strongest non-covalent interaction, and generally very stable complexes are formed between metal cations and macrocyclic ligands.

The strength of hydrogen bonds are about one tenth of the strength of normal covalent bonds. However, stable complexes between hydrogen bonding species and macrocyclic ligands can be formed, especially when more than one bond is involved in the interaction.

Van der Waals' forces resulting from attractive interactions between induced dipoles of weakly polar covalent bonds (such as C-H) may also be responsible for host-guest binding.

Positively charged ligands such as polyamides presenting cationic binding sites may interact with anions via ion-pairing.

Apolar species may associate in polar medium via hydrophobic interactions. This kind of binding is the major organizing influence in the arrangement of the structures of biological species such as proteins and nucleic acids.

1.1.3 Applications

1.1.3.1 Complexing Agents in Living Systems

Metal cations, in particular the alkali and alkaline-earth ions, have a great importance in most of the mineral and biological systems. These cations play a role in many vital processes such as protein synthesis, transmission of nerve impulses (Na^+, K^+), muscle contraction (Ca^{2+}) or as enzyme activators. Macrocyclic ligands were found to be the first efficient complexing agents for alkali and alkaline-earth metal cations and obviously a considerable amount of research has been carried out in order to gain more information about the coordination chemistry of these cations with these ligands.

The biomimetic applications of the macrocycles were soon put to the fore. Most macrocyclic ligands exhibit hydrophobic groups at their external surface which make them soluble in lipids and fats. They are therefore capable to diffuse in biological membranes and can be used as transmembranar carriers for the encapsulated hydrophilic ion which is hold in the polar internal part of the ligand. This property is also characteristic of some natural antibiotics[3], which possess the ability to induce the transport of K^+ across the lipophilic membrane of mitochondria.

Macrocyclic ligands may therefore serve as models for biologically important species which contain metal ions in macrocyclic environment such as heme protein, cytochromes or chlorophyll. These ligands enable also to develop synthetic carriers which could find medical applications,such as for in tumour treatment where complexed radioactive species might be able to penetrate the immune system and destroy the target cells. Organ imaging which consists of finding out what organs look like, could be another straightforward application.

1.1.3.2 Extracting Agents and Carrier Molecules

The extraction process consists in the tranfer of a species usually from an aqueous phase to an organic water-immiscible phase (benzene, dichloromethane, chloroform, n-hexane...) containing the macrocyclic ligand. The process can be represented by:

$$S_{(aq)} + L_{(org)} \rightleftharpoons S.L_{(org)} \qquad 1.1$$

where S is the substrate and L the macrocyclic ligand.

Process 1.1 can be decomposed into:

a) the tranfer of the guest species from the aqueous phase into the organic phase

$$S_{(aq)} \longrightarrow S_{(org)} \qquad 1.2$$

b) the complexation of the guest molecule with the macrocyclic ligand in the organic phase

$$S_{(org)} + L_{(org)} \longrightarrow S.L_{(org)} \qquad 1.3$$

The transport process is closely related to the extraction process. It consists in the transfer of a substrate accross a membrane phase with the assistance of a carrier molecule. The membrane phase is usually represented by a layer of an organic water immiscible solvent of low dielectric constant (liquid membrane) separating two aqueous phases. The first step in this process is analogous to Process 1.2. The mechanism in the membrane phase involves four main steps as schematically illustrated in Fig. 1.6:

i) formation of the carrier-substrate complex at one interface

ii) diffusion of the complex through the membrane

iii) release of the substrate at the other interface

iv) back diffusion of the free carrier

From the numerous studies, it was shown in particular that the extrability of the cation varies with the stability of the complex[19,20]. A higher stability of the complex usually results in a more efficient extraction. Surprisingly, the cation with the highest transport rate is not the most stable one. The rate of transport depends on several factors, especially the activity of the carrier in the organic phase and the nature of the coextracted anion. An efficient and selective carrier should have the following features:

i) form stable and selective complexes with the substrate

ii) show fast exchange kinetics at the interface

iii) have a lipophilic outer surface so as to be soluble in organic media

iv) be of not too large size so as to diffuse rapidly

Therefore, a compromise between thermodynamic (stability) and kinetics (exchange rate) of complexation is required. According to Lamb et al.[21], the empirical result is that the optimum stability constant value for efficient transport is about 5.5 to 6 log units.

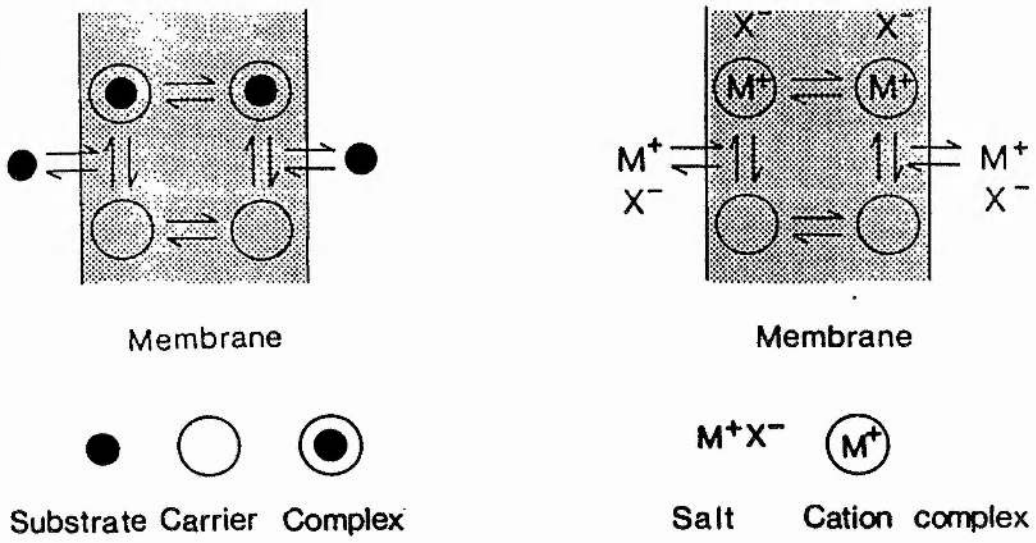

Figure 1.6 Mechanism of carrier mediated transport of a substrate through a membrane[18]

Recently, the possible use of polymeric resins containing macrocyclic ligands as anchor groups for extracting agent has been investigated. The interest of these polymers lies in their ability to be used on an industrial scale because of their easy recycling. They also offer a more realistic model of the biological membranes. The extraction of 1:1 electrolytes from aqueous and non-aqueous solutions by resins containing Dibenzo-18-Crown-6 as anchor groups has been discussed by Danil de Namor and Sigstad[22].

1.1.3.3 Catalysts

In recent years, supramolecular catalysis has become a very important field of research. The aim is to create artificial enzymes capable of mimicking the properties of the natural enzymes such as:

i) to reproduce natural phenomena in order to get a deeper understanding of the biological processes

ii) to use the artificial enzymes as abiotic catalysts, i.e. to use the activities of these enzymes in non-biological environment where the natural enzymes would loose their properties

iii) to carry out reactions which would not be possible in classical synthetic chemistry

Jean-Marie Lehn 's team already developed a synthetic polyamine which is an artificial enzyme having great analogies to the natural ATPase and kinase. ATPase and kinase respectively break and reform pyrophosphate bonds (P-O-P) which are fundamental processes in biology because they are responsible for the release of large amounts of energy in the cells[23,24,25]. Modified crown ethers may serve as artificial peptidase, the enzymes capable of breaking proteins in their amino acids. This topic is currently investigated by Cram[26] and Lehn[27,28].

1.1.3.4 Other Applications

Macrocyclic ligands have also found use in various other areas such as:

i) solubilizing agents for polar compounds in low-polarity solvents[2]

ii) dissociation of ion-pairs in solution, anion activation (increase of the activity coefficient of the anion)[29]

iii) elaboration of ion-selective electrodes, using macrocyclic antibiotics[30,31] or crown ethers[32].

CHAPTER 2

LITERATURE REVIEW ON METAL CATION - MACROCYCLIC LIGAND INTERACTIONS

A literature survey on the previous studies concerning univalent and divalent macrocyclic complexes, with an emphasis on crown ethers and cryptands is presented. A great number of books and reviews on this subject are available; the most recent ones were published by Izatt et al.[33], Bunzli and Wessner[34], Vögtle et al.[35], Lindoy[36] and others.

2.1 Factors Determining Cation Selectivity and Complex Stability

2.1.1 Respective Sizes of Cation and Ligand Ring/Cavity

At the beginning of macrocyclic chemistry, it was postulated that it is the size of the intramolecular site of the ligand which discriminates between the different cations. Most macrocycles (crown ethers and cryptands) form 1:1 inclusion complexes with the alkali and alkaline-earth metals where the bound ion lies inside a planar structure (ring or loop) in the case of crown ethers, and inside a three-dimensional structures (cavity) in the case of the cryptands. This was confirmed by X-Ray crystallographic studies[37-44].

Within the same category of cations, it was observed that in general selectivity peaks are reached when the metal ionic radius is close to the ligand intramolecular radius, as illustrated in Fig. 2.1. The greater stability achieved in this case is the result of a more favourable enthalpy of

complexation (greater electrostatic bond energy). When the respective sizes of the cation and the ligand are too different, the macrocycle must undergo conformational changes which lowers the stability constant of the complex as a result of an unfavourable entropic term.

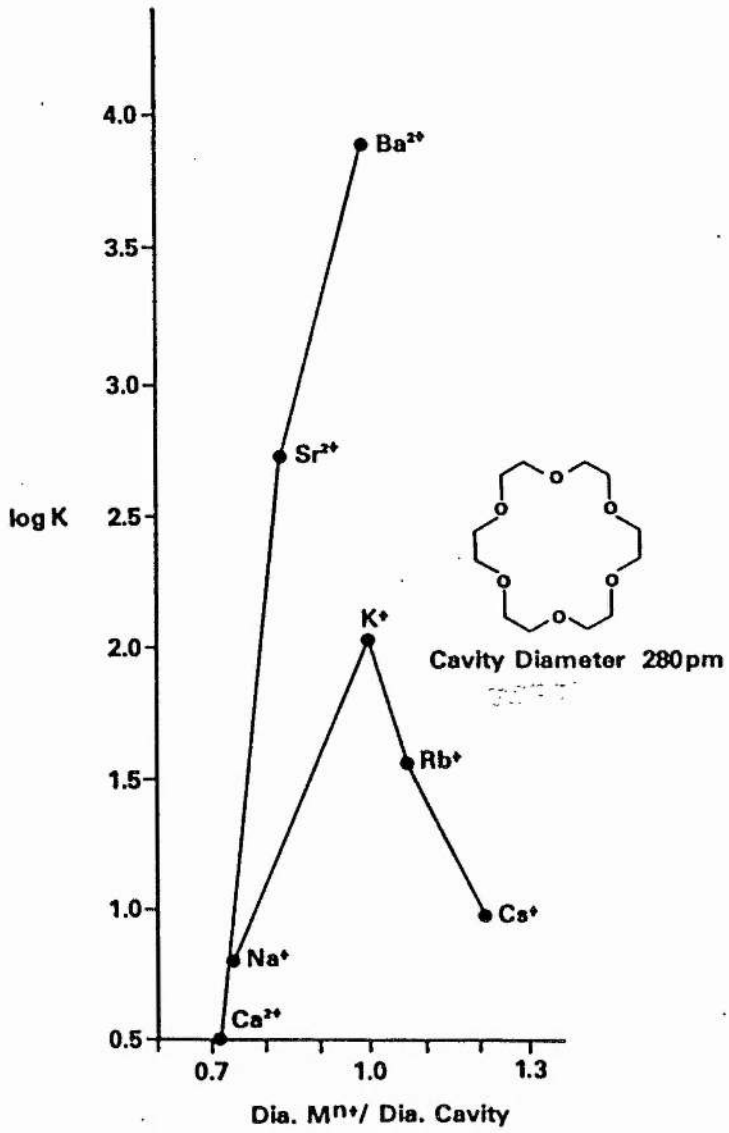

Figure 2.1 Selectivity of 18-Crown-6: log K values for reaction of 18-Crown-6 with metal cations in water at 298.15 K vs the ratio of the ionic cation diameter to the 18-Crown-6 ring diameter[45]

It was noted that the selectivity is more or less pronounced depending on the ring size of the ligand: larger rings and smaller ones seem to be less selective. Therefore, it was concluded that the size criteria is essentially valid for ligands whose ring or cavity size is similar to the range of cation size (alkalis: 0.76 to 1.67 Å; alkaline-earth: 0.72 to 1.35 Å)[46]. This means that the cryptands 222, 221 and 211 with cavity radii of 1.40. 1.10 and 0.80 Å respectively and 18-Crown-6 with a ring size of 1.3 Å present the best selectivities and stabilities for the alkali and alkaline-earth metals.

A deep examination at the thermodynamic parameters of complexation ($\Delta_c G°$, $\Delta_c H°$, $\Delta_c S°$) revealed that the size criteria is an oversimplification. It was noted that for example the complexation of Na^+ with Cryptand-221 in water is entropically controlled despite the size compatibility of the two molecules[47]. Another surprising observation is that the macrocyclic ligands display higher selectivities for the alkaline-earth metals than for the alkali metals, as reflected in the steepness of the curves in Fig. 2.1, although the difference in size along the alkali series is greater than for the alkaline-earth series. It was also observed that in the case of divalent transition and post-transition metals, the size relationship no longer holds with the cryptand[48,49]. This was explained by the partially covalent character of the bonds between the transition metal cations and the nitrogen atoms of the cryptand.

Although the size relationship between cation and ligand cavity or ring size seems the obvious parameter determinant in the complex stability, the arguments mentioned above indicate that other parameters might be important. In recent publications, it has been demonstrated that the size criteria no longer is the predominant parameter in macrocyclic complexation. This will be discussed in the next paragraphs.

2.1.2 Charge of the Cation

A greater influence of the charge of the bound cation on the magnitude of the stability is expected, due to the electrostatic nature of the metal-ligand interactions.

Cryptands form complexes, in general of higher stabilities with the divalent cations compared to the monovalent ones[50]. These ligands also display higher selectivities with these ions. The greater affinity of the ligand for the alkaline-earth cations is favoured by a more negative enthalpy of complexation[51]. The need of desolvation of the cation prior to the complexation has an important effect on the stability of the complex. Heavily solvated cations need to undergo a greater desolvation than poorly solvated ones; this results in a stabilizing effect on the complex (positive entropy term). Therefore, large bivalent cations have in general higher stabilities than monovalent ones of similar size, whereas the opposite is true when comparing small cations of different charges. For example, Izatt et al.[52,53] noted that 18-Crown-6 preferably complexes, in water, sodium and barium with respect to calcium and potassium which have similar sizes. Higher stabilities for the small monovalent lithium than for magnesium were observed with the cryptands 211 and 221. Cryptand-211 shows a higher selectivity for sodium than for calcium[54]. Cox et al.[55] explained that kinetic parameters are responsible for these stability inversions. The M^{2+}/M^{+} selectivity can be written as a ratio of their stability constants (K) with the appropriate ligand as shown by:

$$\frac{K(M^{2+}L)}{K(M^{+}L)} = \frac{k_f(M^{2+}L)/k_f(M^{+}L)}{k_d(M^{2+}L)/k_d(M^{+}L)} \qquad 2.1$$

where k_f and k_d are respectively the formation and the dissociation rate constants. Both k_f and k_d are lower for the divalent cations than for the

monovalent ones. The magnitude of *Eqn. 2.1* depends on whether the higher decrease is observed for k_f or k_d on moving from an univalent to a bivalent cation.

2.1.3 Donor Atoms and Flexibility of the Ligand

Substitution of a donor atom of the ligand by another might greatly alter the stabilities of the macrocyclic complexes. It is known that oxygen containing ligands are able to interact with the alkali and the alkaline-earth metals whereas ligands containing nitrogen atoms show a preference for silver, transition and heavy metal cations. It was noted[56] that macrocyclic ligands containing sulphur atoms form strong complexes with Ag^+ and Hg^{2+} cations but weaker complexes are known between these ligands and Tl^+ and Pb^{2+}. Frensdorff[57] concluded that interactions other than electrostatics may occur between the nitrogen and sulphur containing ligands and some transition metal cations. The magnitude of the stability constant of the complex is also related to the electronegativity of the ligand donor atoms. More electronegative donor atoms will enhance the electrostatic interactions between ligand and cation. Thus, the stability will be a result of a very favourable enthalpy of complexation.

The number of donor atoms of a macrocyclic ligand may vary from 4 to 11, in average it is 6 or 8 (e.g. for 18-Crown-6 and Cryptand-222). It was noted that without change of size, the increase of the number of donor atoms has a favourable effect on complex stability due to a more favourable enthalpy of complexation[58].

Important conformational changes of the ligand upon complexation have been observed. Thus, in the solid state, Dibenzo-30-Crown-10 has been found to wrap completely the potassium cation to form a very stable complex despite the incompatibility in size between the cation and the

ligand ring[59]. Selectivity is obviously reduced for the very flexible ligands such as the large crown ethers which can adapt themselves to any cation.

Cryptands can be found in three different conformations as illustrated in Fig. 2.3. X-Ray studies have shown that in the solid state, the free and the complexed ligand adopt always the endo-endo configuration[43]. This configuration is also expected in solution, as suggested by NMR studies[60]. Cryptands are less flexible than crown ethers, yet they can adapt sufficiently to the larger cations such as cesium[39]. In the case of too flexible ligands, intramolecular repulsions between the lone pairs of the donor atoms may occur which would destabilize the complex. In the case of rigid and very preorganized ligands like the spherands, the intramolecular repulsions exist already before the complexation. Mathieu et al.[47] suggested a cumulative effect between ligand ring or cavity size (reflected in the enthalpy term) and ligand flexibility (reflected in the entropy term) which respectively are responsible for the preselection and the final selection of a ligand for a particular cation.

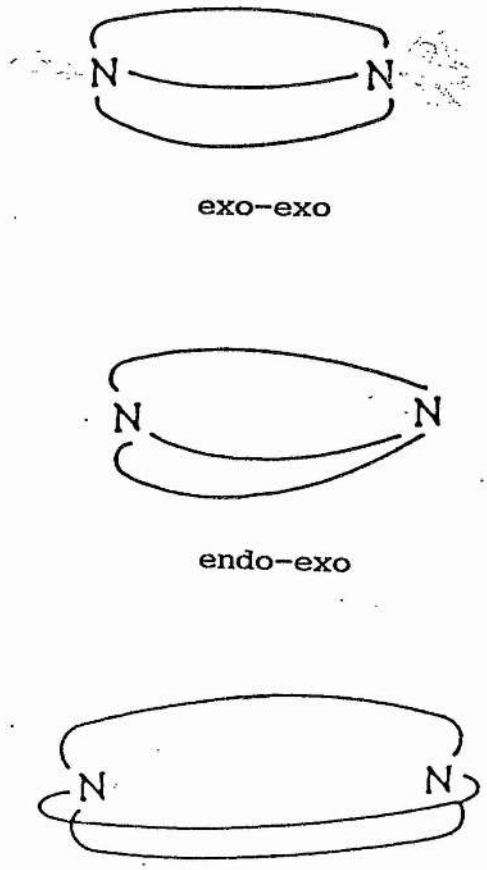

Figure 2.3 Conformations of the Cryptands

2.1.4 Substitution of the Macrocyclic Ring

Macrocyclic ligands can bear side ring substituents, in general aromatic or acyclic rings. Substituted ligands are of course more rigid than their non-substituted counterparts. In the case of benzo-substituted ligands, electrons from the basic oxygen donor atoms of the macrocyclic ring are withdrawn by the benzene groups, thus decreasing the strength of the metal-ligand interactions. The electronic as well as the steric effects of the side rings may therefore alter both the selectivity and the stability of the macrocyclic ligands with the metal cations.

Detailed studies of Dibenzo-crown ether and Dibenzo-cryptand complexes with the alkali metals in a series of non-aqueous solvents have been carried out by Danil de Namor et al.[61,62]. These authors observed a decrease in stability with Dibenzo-18-Crown-6 and Dibenzo-Cryptand-222 with respect to 18-Crown-6 and Cryptand-222. They attributed this loss in stability to an unfavourable entropic contribution as a result of the decrease in ligand flexibility. Different selectivity patterns are observed for Dibenzo-Cryptand-222 with respect to Cryptand-222 with the alkali metals in methanol[63]. For Dibenzo-18-Crown-6 in methanol, the selectivity sequence is $K^+ > Na^+ > Cs^+$ whereas for 18-Crown-6 it is $K^+ >> Cs^+ > Na^+$[64]. Cox et al.[65] reported that the side ring substituents reduce the stability of the alkali cryptates in methanol, by reducing the formation rate and increasing the dissociation rate of the complexes.

2.1.5 Solvent

The complexation between a macrocyclic ligand and a metal cation involves a competition between the ligand and the solvent for the free cation. The binding properties of a ligand depend therefore very much on the reaction medium, especially when desolvation of the cation prior to complexation is required.

Cox et al.[66] observed large variations in the stability constants of the alkali cryptates with the solvent, up to 9 orders of magnitude (in log units) for a particular complex. The stability constants are usually lowest in water and highest in the non-aqueous solvents, particularly in acetonitrile and propylene carbonate. The dielectric constants and the donor number of the different solvents give a good indication on the strength of the ion-solvent interactions (Table 2.1).

Table 2.1 Dielectric constants (ε) and donor number of some solvents (Donor No according to Gutmann and Wychera[67])

Solvent	**Donor No**	ε
Water	18.0	78.39
Acetonitrile (AN)	14.1	37.5
Propylene Carbonate (PC)	15.1	66.1
Dimethylsulfoxide (DMSO)	29.8	46.68
N,N-Dimethylformamide (DMF)	26.6	36.71
Methanol (MeOH)	25.7	32.70
Ethanol (EtOH)	30.0	24.55

The stability sequence for a given alkali cryptate is in general PC, AN > MeOH, EtOH > DMF, DMSO > Water. Further studies confirmed this sequence for the alkaline-earth cations with an inversion for water and DMSO[50]. The same order, not including DMF, is observed for the divalent heavy metal cations (Pb^{2+}, Cd^{2+}, Cu^{2+} and Zn^{2+})[49].

Crown ethers are less sensitive to solvent variations. Frensdorff[64] pointed out that with the crown ethers, the cation does not need a full desolvation since it is still in contact with the solvent in the direction perpendicular to the plane of the ring. In contrast, the complexation with cryptands requires partial or complete stripping of the solvation shell to form inclusion complexes. This effect is also observed with the macrocyclic antibiotics which despite their planar structure can fold around the ion and wrap it completely[29]. Small cations are more subject to solvent variations than larger ones. This is due to the strong electric field of small ions which attract solvent molecules especially dipolar ones. Therefore, in solvents of high polarity, the size of the cation is a very important factor for the complex stability, and desolvation of the cation is the stability determining step in the complexation process.

Solvation effects are often discussed in terms of thermodynamic cycle between a reference solvent (s_1) and another solvent (s_2)[68]:

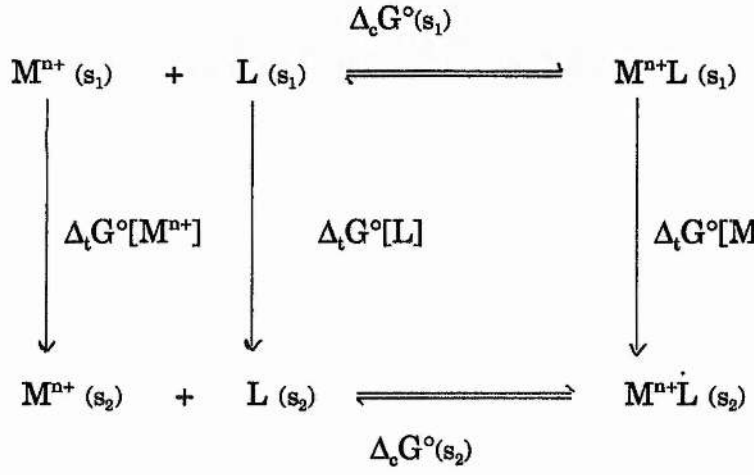

2.2

Gutknecht et al.[69] showed that the difference between the free energies of transfer of the metal ion cryptate and Cryptand-222 ($\Delta_tG°[M^+222]$ - $\Delta_tG°[222]$) respectively, and the corresponding enthalpies of transfer, are constant between water and several non-aqueous solvents (DMF, DMSO, PC, AN) for Ag^+, K^+ and Tl^+. Lejaille et al.[70] proposed then a new extra-thermodynamic assumption which enables the calculation of transfer parameters for single-ion values. This assumption, currently known as the cryptate convention, states that a cryptand L and a metal ion cryptate M^+L undergo the same solvation changes when transferred from a solvent to another. They showed that $\Delta_tG°[M^+L]$ - $\Delta_tG°[L]$ between dipolar aprotic solvents is very small[71]. The cryptate convention can be represented by (also in terms of enthalpy and entropy):

$$\Delta_tG°[M^+L]\ (s_1 \longrightarrow s_2) \approx \Delta_tG°[L]\ (s_1 \longrightarrow s_2) \qquad 2.3$$

and

$$\Delta_tG°[M^+L]\ (s_1 \longrightarrow s_2) \approx 0 \qquad 2.4$$

The single ion free energy of transfer ($\Delta_tG°$) can be calculated from the thermodynamic cycle (2.12) as,

$$\Delta_tG°[M^+]\ (s_1 \longrightarrow s_2) = \Delta_cG°\ (s_1) + \Delta_tG°[M^+L]\ (s_1 \longrightarrow s_2) - \Delta_cG°\ (s_2) - \Delta_tG°[L]\ (s_1 \longrightarrow s_2) \qquad 2.5$$

From *Eq. 2.3*, it can be derived that:

$$\Delta_tG°[M^+]\ (s_1 \longrightarrow s_2) = \Delta_cG°\ (s_1) - \Delta_cG°\ (s_2) \qquad 2.6$$

where $\Delta_c G°$ are the free energy of complexation in the appropriate solvent. The validity of *Eq. 2.6* has been verified in dipolar aprotic media[62,73,72]. In the same solvents, the validity of *Eq. 2.6* has also been verified in terms of enthalpy by Danil de Namor et al.[61,74-76]. These authors also demonstrated that the cryptate conventions (*Eqs. 2.3* and *2.4*) are not valid in transfers from water. *Eq. 2.6* can therefore be used for the calculation of the single-ion quantities for univalent cations among dipolar aprotic solvents. It is important now to test whether or not the cryptate conventions can be used to derive single-ion quantities for multivalent ions.

From *Eq. 2.4* it can be derived that:

$$\Delta_t G°[M^+L].X^- \ (s_1 \longrightarrow s_2) \ = \ \Delta_t G°[X^-] \ (s_1 \longrightarrow s_2) \qquad 2.7$$

which can be used to calculate single-ion values for the transfer of anions[77].

A linear correlation between entropies of complexation of metal(I) cations and Cryptand-222 and entropies of solvation of these cations has recently been shown by Danil de Namor[79] (Fig. 2.3). For the general process of cryptate formation:

$$M^+ \ (g) \ + \ 222 \ (s) \longrightarrow \ M^+222 \ (s) \qquad 2.8$$

which can be decomposed into:

$$M^+ (g) \longrightarrow M^+ (s) \qquad 2.9$$

and

$$M^+ (s) + 222 (s) \longrightarrow M^+222 (s) \qquad 2.10$$

The entropy of cryptate formation $\Delta_{cf}S°$ for the Process 2.7 is constant, independently of the metal cation and the solvent (AN, PC, DMF, DMSO, MeOH, $MeNO_2$). Danil de Namor put then forward the following identity:

$$\Delta_c S° = \text{const.} - \Delta_{solv} S° \qquad 2.11$$

This correlation has also been verified with Dibenzo-cryptand-222 and the same cations in the same solvents[61]. Its validity leads to the conclusion that the cation looses its solvation shell completely when entering the cavity of the cryptand or the dibenzo-cryptand.

Eq. 2.11 can be used for the evaluation of the entropy of solvation of cations(I) from entropy of complexation for these two ligands (Cryptand-222 and Dibenzo-Cryptand-222) with the metal(I) cations in dipolar aprotic media, and vice versa. The validity of this correlation indicates that the solvation of the cation plays a predominant role in the complexation process between metal(I) cations and cryptands in dipolar aprotic media.

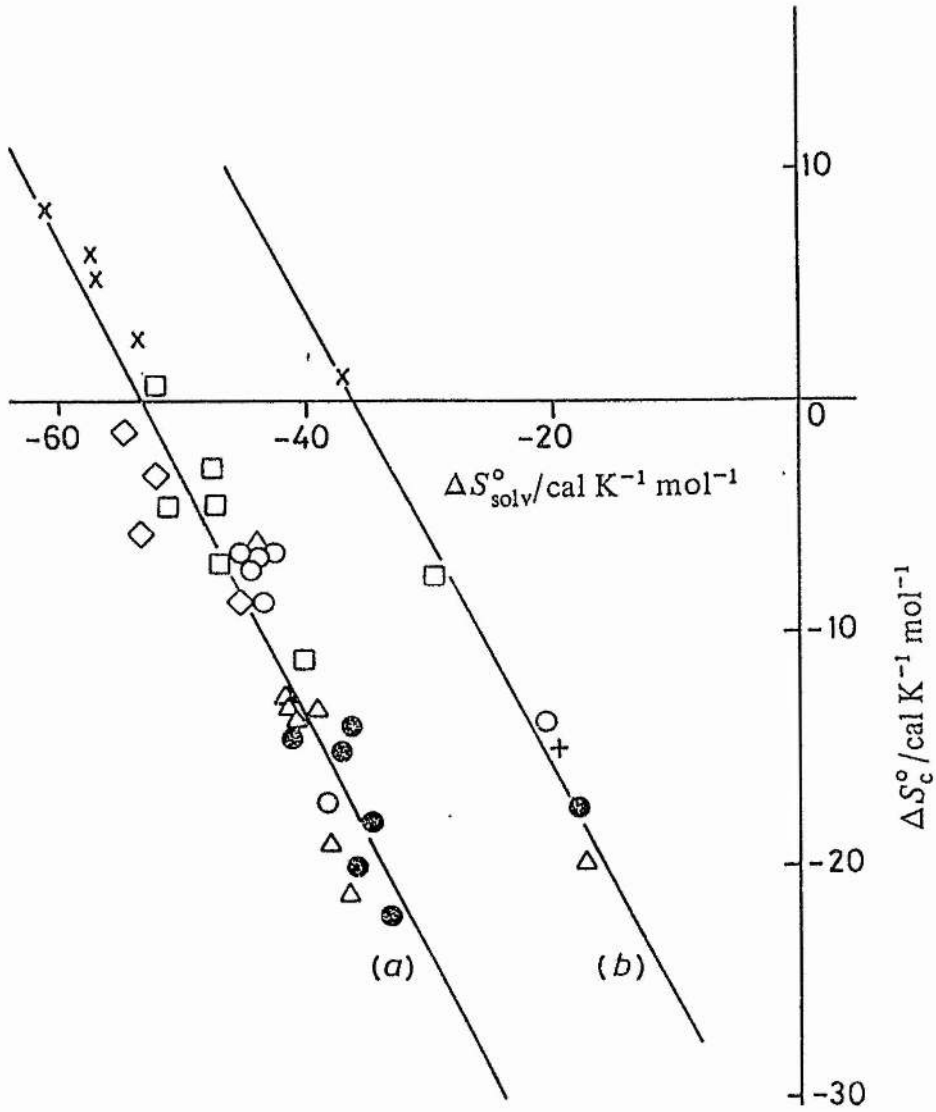

Linear correlation between entropies of complexation of cryptand 222 with metal ions and entropies of solvation of these ions (*a*) in non-aqueous solvents and (*b*) in water. ×, Li^+; □, Na^+; ○, K^+; △, Rb^+; ●, Cs^+; ◇, Ag^+; +, Tl^+.

Figure 2.3 Linear correlation between $\Delta_c S°$ and $\Delta_{solv} S°$[79]

2.1.6 Counter-Anion

It has been shown, by X-Ray studies, that in the solid state the counter-anion may still be bounded to the complexed cation in order to complete the coordination shell of the cation[47]. In solution, particularly, in solvents of low dielectric constant a macrocyclic ligand could in theory form complexes with both the free cation and the ion-pair. These associations depend of course very much on the reaction medium. In most solvents, it is generally assumed that ion-pair formation is negligible, and the effect of the anion is minimized by working in high dilution conditions or by choosing anions such ClO_4^- or NO_3^- whose salts are predominantly dissociated in solutions.

Studies of anion effects on the stabilities of macrocyclic complexes are rare. However, it has been shown that in general the stabilities of metal-ion cryptates are independent of the anion[79].

2.1.7 Stoichiometry of the Complex

Cryptands form almost universally 1:1 complexes. Crown ethers do form other complexes. Pedersen[5] reported 2:1 and 3:2 polyether-metal cation complexes for the K^+, Rb^+ and Cs^+ complexes with Dibenzo-18-Crown-6. These ions are located between two crown ethers as in a "sandwich" structure (Fig 2.4). Dinuclear 2:1 and protonated 1:1:1 complexes were also reported in the case of transition and heavy metal complexes[49].

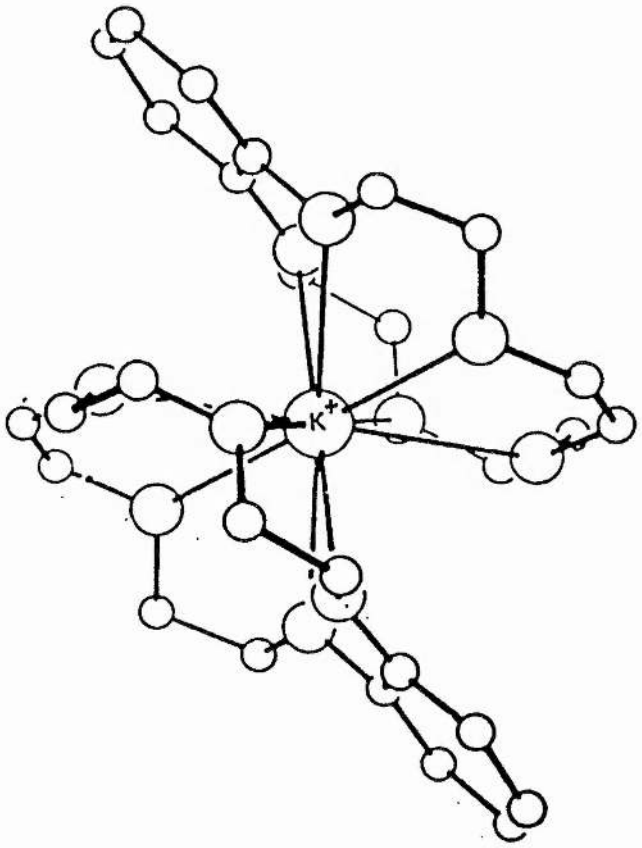

$(K\text{-}15\text{-}Crown\text{-}5)^+$ with the K^+ sandwiched

between two ether ligands

Figure 2.4 Sandwich structure

2.2 Macrocyclic and Macrobicyclic Effects

The *macrocyclic effect* describes the greater stability of complexes with cyclic ligands over those of open chain ligands of similar structure. It was first observed by Cabbines and Margerum[80] who found that the copper-tetramine complex is much more stable than with its non-cyclic counterpart. An enhancement of 10^3 to 10^4 of the stabilities of alkali-crown ether complexes is observed when compared to their open chain analogs[81]. The ring formation seems to add strength to the complexation. Linear polyethers are unable to envelop the cation as fully as the cyclic ones due to the electrostatic repulsions between their terminal groups. Macrocyclic ligands such as crown ethers and cryptands are also less solvated than the non-cyclic ones, thus complex formation requires less solvation bond breaking which results in an increase in the stability of the complex. Therefore, this process is usually more enthalpically favoured. An unfavourable entropy term also hampers a good complex stability when linear ligands are forced to adopt a cyclic structure.

The *macrobicyclic effect* is an extension of the macrocyclic effect. It is also called *cryptate effect* because it has been observed for the metal ion cryptates[82]. The large increase in stability observed for metal ion cryptates over metal ion crown ether complexes are caused by the three-dimensional cavity of the cryptand which favours the contact between cation and the donor sites of the ligand, and isolates the cation from the surrounding solvent. The macrobicyclic effect is stronger for the monovalent than for the divalent cations of similar size due to increasing cation-solvent interactions, due to the cation charge. It was shown in several papers that this effect is a result of enthalpic stabilization[48,83].

2.3 Lanthanide-Cryptand Interactions

2.3.1 The Lanthanide Metals

2.3.1.1 Chemical Properties

The lanthanide (Table 2.1) are the f-type transition metals in the periodic table. They are characterized by the only partially filled 4-f subshell. Their atomic numbers are ranging from 57 to 71. The ground state electronic configuration of lanthanum (La) is that of xenon with three extra valency electrons $5d^16s^2$. Throughout the series, the additional electrons tend to be added to the inner shell 4-f rather than to the 5-d shell, despite the fact that the 5-s and 5-p levels have already been filled. As a result, the number of valency electron remains unchanged along the series.

The lanthanide are essentially trivalent element (except for cerium which is tetrapositive) due to the removal of the $5d^16s^2$ electrons, so are their oxides of general formula Ln_2O_3. Higher valencies are found in the dark coloured oxides Pr_60_{11} and Tb_4O_7. Divalent europium, ytterbium and samarium were characterized. The tendency of these elements to be divalent in metallic salts is caused by the enhanced electronic stability associated with complete single ($4f^7$) or double ($4f^{14}$) occupancy of the orbitals. As the size of atoms and ions are determined by both, the nuclear charge and the number of occupancy of the electronic shell, an increase in size is usually observed with an increase in atomic number (Fig. 2.5). However, the sizes of the lanthanide elements decreases along the series. This effect is known as the lanthanide contraction and is caused by the fact that the addition of electrons to the shielded 4-f orbitals (higher energy levels) cannot compensate for the effect of increased nuclear charge (contractive effect due to enhanced electrostatic attractions). The lanthanide contraction is responsible for the small variations in the properties of these elements.

Table 2.5 The lanthanide elements

Name	Symbol	Atomic number	Atomic radius	Ionic radius
Lanthanum	La	57	1.887	1.061
Cerium	Ce	58	1.82	1.034
Praseodymium	Pr	59	1.828	1.013
Neodymium	Nd	60	1.821	0.995
Promethium	Pm	61	———	0.979
Samarium	Sm	62	1.802	0.964
Europium	Eu	63	2.042	0.950
Gadolinium	Gd	64	1.802	0.938
Terbium	Tb	65	1.782	0.923
Dysprosium	Dy	66	1.773	0.908
Holmium	Ho	67	1.766	0.894
Erbium	Er	68	1.757	0.881
Thulium	Tm	69	1.746	0.869
Ytterbium	Yb	70	1.940	0.858
Lutetium	Lu	71	1.734	0.848

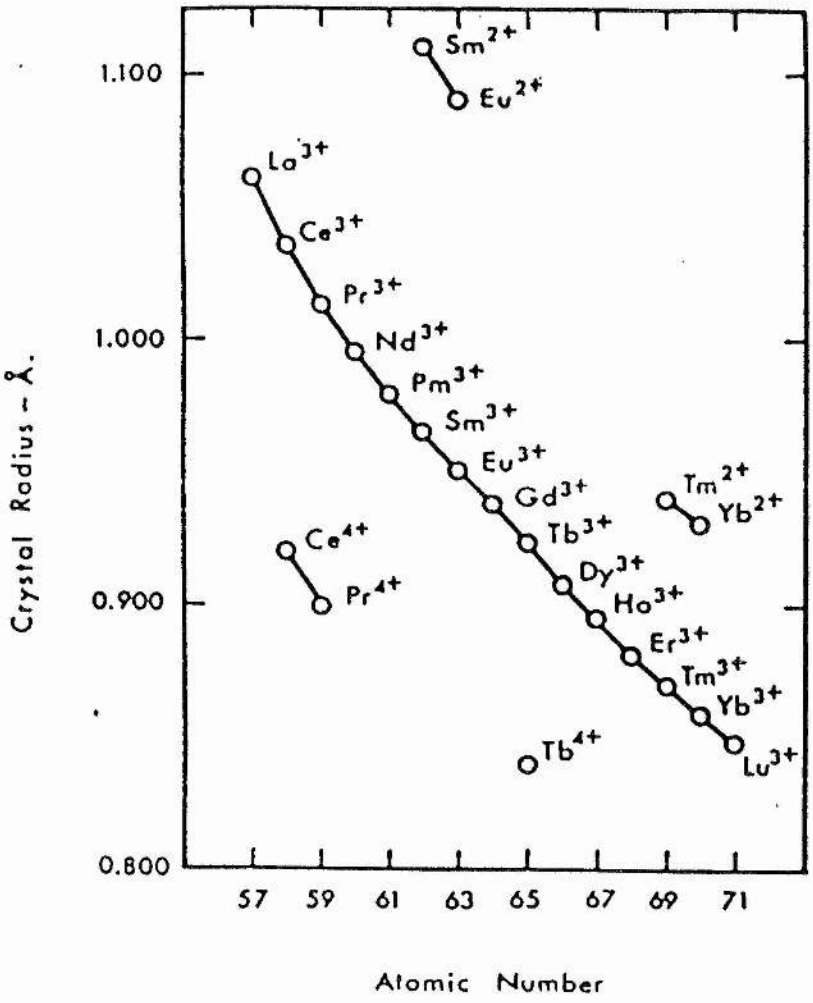

Figure 2.5 The lanthanide contraction

2.3.1.2 Applications of the Lanthanides and their Cryptates

The lanthanides are also called rare earths although they exist in nature in almost unlimited quantities. The three major applications of these metals are found in metallurgy, catalysis and glass/ceramics.

In *metallurgy*, they are used as scavengers for oxygen or sulphur. They are also used in production of magnesium alloys. The lanthanide oxides are used in cracking as well as in heterogenous and homogenous *catalysis*. In the *glass and ceramic industries*, the lanthanides are highly efficient glass polishing components. They are used as decolouring or colouring agents for glass (especially Nd and Pr oxides), in the preparation of low-dispersion, high refraction optical glass, or enamel opacifiers.

Due to their para- and ferromagnetic properties, lanthanides find also applications in other highly specialized areas such as in phosphors, electronics, magnetics, optoelectronic (e.g. microwave devices and magnetic core materials). Many applications are based on their absorption and emission of radiation (electroluminescent displays, fluorescent lamps).

Complexes of the lanthanides with cryptands have also found many applications, e.g. as ion-selective electrodes for the rare earths, as tracers in biological systems, as redox reagents in studies of electron transfer kinetics, as chemical shift reagents in NMR spectroscopy.

2.3.2 Structure of the Lanthanide Cryptates

Some lanthanide cryptates have been isolated and their solid-state structure investigated by X-Ray crystallography[84,85]. These studies have shown that the complexed lanthanide cation lies always inside the cryptand cavity in the endo-endo configuration, as in the cryptate complexes with other metals.

Due to the high coordination number of the lanthanides (up to 12) the cation is not only bound to the donor atoms of the ligand but also the counter-anion which are interposed in the gaps between the ligand bridges. Solvent molecules may also occupy empty cavities inside the complex structure. Hart et al.[85] have identified the lanthanum-222 cryptate as $[La(NO_3)_2222]_3[La(NO_3)_6].2MeOH$ (Fig 2.6). Ciampolini et al.[84] found interposed acetonitrile molecules in the solid europium-222 cryptate (Fig. 2.7).

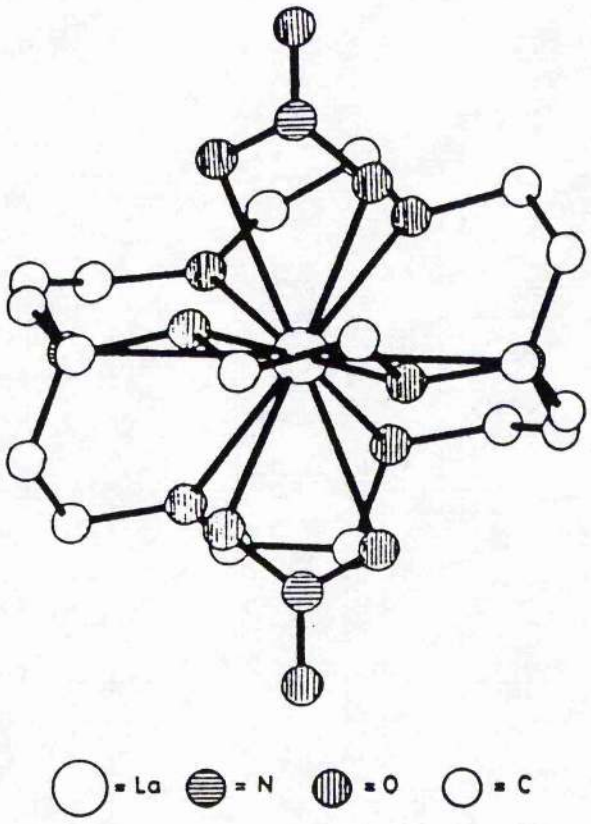

Figure 2.6 Structure of lanthanum-222 cryptate [85]

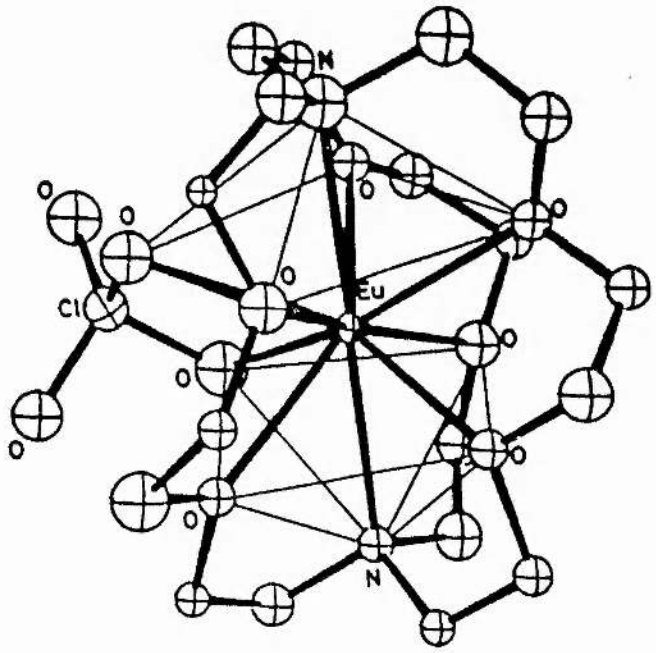

Figure 2.7 Structure of europium-222 cryptate [84]

2.3.3 Solution Thermodynamics of Lanthanide(III) Cryptates

Stability constants of the 1:1 lanthanide(III) cryptates have been determined in a number of solvents (Water, PC, DMSO, MeOH, DMF) using electrochemical or spectrophotometric methods (Table 2.2). In a few studies, the enthalpy ($\Delta_c H°$) and the entropy ($\Delta_c S°$) for the complex formation of cryptands with the lanthanides have been derived by the use of van't Hoff's isochores. These literature data are reported in Table 2.3.

It was found that the tervalent lanthanide cations exhibit the highest stabilities ever observed for metal ion cryptates. This is due to their size similar to those of Ca^{2+} and Na^{+} which are particularly adapted to Cryptand-221, and mainly to their high charge density which favours strong attractive electrostatic bonding. Cryptands are much better complexing agents for the lanthanides than the crown ethers[86]. The experiments were usually carried out at constant ionic strength. It was shown that the ionic strength has no influence on the stability of the lanthanide cryptates[87].

The major result derived from these data is the lack of cation selectivity observed in the aqueous as well as in the non-aqueous solvents studied. This rather surprising property of the lanthanides was attributed to the small difference in size between these cations (about 0.1 Å whereas for the alkalis it is 0.3 Å and for the alkaline-earths 0.2 Å). Burns and Baes[88] also suggested that the tervalent lanthanide cryptates in solution might have different structural features than the univalent and divalent cryptates. The complexed ion could be only partially desolvated and could still be in contact with the solvent.

In general, Cryptand-221 (cavity radius=1.1 Å) displays greater affinity for the lanthanides than Cryptand-222 (cavity radius=1.4 Å) due to the better match between the cavity of Cryptand-221 and the size of these cations. Taking into account the sizes of the different cryptands and their ability to

change conformation upon complexation, the general trend for their stabilities with the lanthanides is:

$$Ln^{3+}221 > Ln^{3+}222 > Ln^{3+}211$$

Surprisingly in N,N-Dimethylformamide, a reverse order was observed[89]:

$$Ln^{3+}211 > Ln^{3+}221 > Ln^{3+}222$$

In DMSO and in water, no real ligand selectivity was noted[88,90].

Variations of up to 16 log units in the stability constants of lanthanide cryptates as a result of a change in the reaction medium have been reported. The observed sequence is:

$$PC > MeOH > Water > DMSO > DMF$$

In propylene carbonate (PC), the complexation process involving lanthanide(III) cations and cryptands seems to be enthalpically governed whereas the same process in water it is entropically controlled (see Table 2.3). A deeper insight in these parameters is necessary due to the great inaccuracy of their determination.

Slow kinetics of complexation were noted in propylene carbonate[87]. This is a result of the slow removal of the lanthanide solvation shell. Consequently, the ligand is not able to replace immediately these solvation shells. However, kinetics studies in water indicate partial desolvation of the lanthanides upon complexation[91].

Table 2.2 Stability constants (log K_s) of tervalent lanthanide cryptates at 298.15 K

Solvent		Cation	21	22	211	221	222	Ref.
Water	I=0.25	La^{3+}				6.59	6.45	a
		Pr^{3+}				6.58	6.37	a
		Sm^{3+}			6.8	6.76	5.94	a
		Eu^{3+}				6.8	5.90	a
		Gd^{3+}				6.7		a
		Tb^{3+}				6.6		a
		Ho^{3+}			6.21		6.2	a
		Er^{3+}				6.60		a
		Tm^{3+}			6.8	6.88		a
		Yb^{3+}			6.51			a
		Lu^{3+}			6.55			a
	I=0	Eu^{3+}				5.94	3.37	g
DMSO	I=0	Pr^{3+}			3.86	3.47	3.22	b
		Nd^{3+}			3.97	3.01	3.26	b
		Gd^{3+}			3.87	3.26	3.45	b
		Ho^{3+}			3.80	3.11	3.47	b
		Yb^{3+}			4.43	4.00	4.11	b
	I=0.02	Yb^{3+}					3.00	b
Propylene Carbonate	I=0.1	La^{3+}	14.4	16.5	15.1	18.6	16.1	d
		La^{3+}					12.91	c
		Ce^{3+}					14.20	c
		Pr^{3+}	14.5	16.1	15.51	18.7	15.9	d
		Pr^{3+}					15.88	c
		Sm^{3+}	14.9	16.5	15.3	19.0	17.3	d
		Sm^{3+}					15.99	c
	I=0.9	Sm^{3+}					16.39	c
	I=0.1	Eu^{3+}	14.6	16.5	15.2	19.0	17.2	d
		Gd^{3+}		16.5	15.4		16.8	d
		Tb^{3+}					16.58	c
		Dy^{3+}	15.1	16.9	15.4	19.0	17.1	d
		Er^{3+}	14.8	16.9	15.5	19.2	16.8	d
		Yb^{3+}	15.4	16.9	15.6	19.1	18.0	d
		Yb^{3+}					17.56	c
Methanol	I=0.05	La^{3+}	7.08			8.28		e
		Pr^{3+}	7.94			9.31		e
		Nd^{3+}	7.86			9.86		e
		Sm^{3+}	7.00			9.70		e
		Eu^{3+}	8.59			10.57		e
		Gd^{3+}	7.67			10.14		e
		Tb^{3+}	8.29			10.26		e
		Dy^{3+}	8.96			10.45		e
		Ho^{3+}	8.81			10.86		e
		Er^{3+}	8.66			10.78		e
		Tm^{3+}	9.46			11.61		e
		Yb^{3+}				12.00		e
DMF		Sm^{3+}		≤2	4.06	2.9	2.7	f
		Eu^{3+}		≤2	4.69	3.2	2.9	f
		Yb^{3+}		≤2	4.52	3.3	2.9	f

References: (a) 88, (b) 90, (c) 87, (d) 93, (e) 92, (f) 89, (g) 91

Table 2.3 Thermodynamic parameters for the complexation of tervalent lanthanide cryptate at 298.15 K

Solvent	Cryptate complex	$-\Delta_c G^\circ$ kJ/mol	$-\Delta_c H^\circ$ kJ/mol	$\Delta_c S^\circ$ J/mol.K	Ref.
Water	Eu^{3+}222	19.24	-16.74	121.3	a
	Eu^{3+}221	33.89	-7.95	140.2	a
PC	La^{3+}222	91.63	77.40	46.0	b
	La^{3+}222	73.64	54.39	62.8	c
	Ce^{3+}222	80.75	76.57	14.6	c
	Pr^{3+}222	90.79	104.60	-41.8	b
	Pr^{3+}222	86.19	94.56	-28.0	c
	Sm^{3+}222	91.21	96.23	-16.7	c
	Sm^{3+}222	93.30	96.23	-8.8	c
	Tb^{3+}222	94.97	104.18	-30.9	c
	Er^{3+}222	99.23	112.97	-50.2	b
	Yb^{3+}222	99.16	106.69	-23.8	c
	Pr^{3+}221	108.36	138.07	-100.4	b
	Er^{3+}221	110.04	146.44	-117.1	b
	Pr^{3+}211	88.28	28.87	200.8	b
	Er^{3+}211	88.28	37.66	163.2	b
	Pr^{3+}22	91.63	129.70	-129.7	b
	Er^{3+}22	96.65	154.81	-192.5	b

References: (a) 91, (b) 93, (c) 87

2.3.4 Stabilities of Lanthanide(II) Cryptates

Yee et al.[91] investigated the possibility of stabilizing the +II oxidation state of the lanthanides. They have reduced by polarography in a reversible manner, europium(III) and ytterbium(III) cryptates into europium(II) and ytterbium(II) cryptates according to the general process represented below. The stabilities in water of the divalent lanthanide complexes were found to be up to 10^7 higher than those of the corresponding tervalent cryptates (Table 2.4).

$$\begin{array}{ccc} Ln^{3+} + e^- & \rightleftharpoons & Ln^{2+} \\ + & & + \\ L & & L \\ \downarrow & & \downarrow \\ Ln^{3+}L + e^- & \rightleftharpoons & Ln^{2+}L \end{array} \qquad 2.12$$

Similar studies in different reaction media (MeOH, PC, DMF) have been carried out by Marolleau et al.[89]. The general conclusion was that like in water, the stabilities of the reduced lanthanide cryptates are much higher than those for the corresponding lanthanide(III) cryptates. The striking feature in these results (Table 2.4) is that the cryptands display a relatively good cation selectivity with the lanthanide(II) cations. The lower charge density of the divalent cations is probably compensated by the size factor (better match between lanthanide(II) ion and cryptand cavity). Moreover, due to their charge the lanthanide(II) cations are less solvated than the lanthanide(III) cations. Therefore, with cryptands complexation is more favoured for the former than for the latter cation.

Yee et al.[91] compared the stability constants of the complexes of europium(II) and strontium(II), which are of similar size, with the 221 and

222 cryptands. It was interesting to note that the europium(II) cryptates are significantly more stable than the strontium(II) cryptates. These authors concluded that these findings were due to a weak covalent bonding between the oxygen and nitrogen atoms of the ligand with the unfilled 4-f orbitals of europium(II). More positive values of the enthalpy and entropy of complexation were observed for europium(III) than for europium(II) cryptates. This is mainly due to the solvation effect which is less pronounced for the divalent lanthanides.

Table 2.4 Stability constants of lanthanide(II) cryptates at 298.15 K

Solvent	Cation	22	221	222	Ref.
Water	Eu^{2+}		9.34	10.51	a
DMF	Sm^{2+}	≤ 4.2	10.0	13.2	b
	Eu^{2+}	≤ 5.3	10.6	14.8	
	Yb^{2+}	≤ 6.8	11.2	14.3	
MeoH	Sm^{2+}		11.9		c
	Eu^{2+}		12.77		

References: (a) 91, (b) 89, (c) 92

2.3.5 Macrocyclic Effect

A macrobicyclic effect is observed in methanol and propylene carbonate for the 211 lanthanide cryptates when compared to the corresponding 21 cryptates. Stabilities increase by a factor up to 10^5 for the bicycles with respect to the monocycles[92,93]. In propylene carbonate, this increase was attributed to a more favourable enthalpy contribution. Only a small macrobicyclic effect is observed with Cryptand-222 and the lanthanide cryptates in propylene carbonate and DMF. This suggests a difference in the solution behaviour of the Cryptand-222 lanthanide complexes with respect to the Cryptand-221 complexes[89].

2.3.6 Interactions with Small Anions

Cryptands are an efficient way of shielding the encapsulated cation from the surrounding solvent. However it has been shown that in solution, the complexed lanthanide cation can still be associated to small anions such as F^-, OH^- or Cl^-[91]. It appeared that one or two anions are able to approach closely or even contact the europium(III) or the ytterbium(III) cations despite their encapsulation within the cryptand cavity. These associations are supposed to be either direct cation-anion pairing or solvent separated ion pairing.

2.4 Purpose of the Present Work

Macrocyclic ligands offer almost unlimited research targets. Besides the design and synthesis of new receptor molecules, the essential feature is the study of their interactions with guest molecules. Like the majority of reactions that are of chemical or biological interest, complexation between host and guest occurs in solution. Thermodynamic studies are important to understand these associations, particularly to find the stabilities of the complexes as well as the origin of these stabilities. The reaction media is of course not inert and therefore might alter or strongly modify the characteristics of the binding. Detailed analyses of the complexation process and information on the structure of the complex in solution may be derived from the thermodynamic parameters.

Up to now, the most extensive studies involved the alkali and the alkaline-earth metal cations as guest with the crown ethers and the cryptands as hosts. The main conclusions drawn from these investigations have been discussed in this chapter. The idea of the present work was to broaden these studies to the tervalent cations and to bioorganic molecules, as well as to emphasize new aspects of the commonly used macrocyclic ligands.

The work is divided in two parts:

i) The tervalent lanthanide cations resemble to the alkali and alkaline-earth metal cations through their similarities in size and electropositivities. The study of their interactions with the cryptands seemed a logical extension of the work undertaken with the univalent and divalent cations. Moreover, the chemistry of the lanthanide compounds has attracted considerable practical and theoretical interest in recent years. Therefore, it was decided to determine all the thermodynamic parameters for the formation of lanthanide cryptates in two dipolar aprotic media using potentiometric and calorimetric techniques.

For the univalent cations, single-ion values for the transfer among dipolar aprotic solvents have been derived from complexation data for these ions with Cryptand-222 (see section 2.1.5). These parameters are extremely useful for the study of ion-solvent interactions, as well as to understand some fundamental processes such as the transport of ions across cell membranes. Up to now, there has been only limited information on transfer values for multivalent ions. The major aim of this part of the work was to obtain single-ion values for the tervalent lanthanide cations. Two different methods have been considered:

a) using the following thermodynamic cycle, by combining complexation data and transfer parameters for the lanthanide cryptates

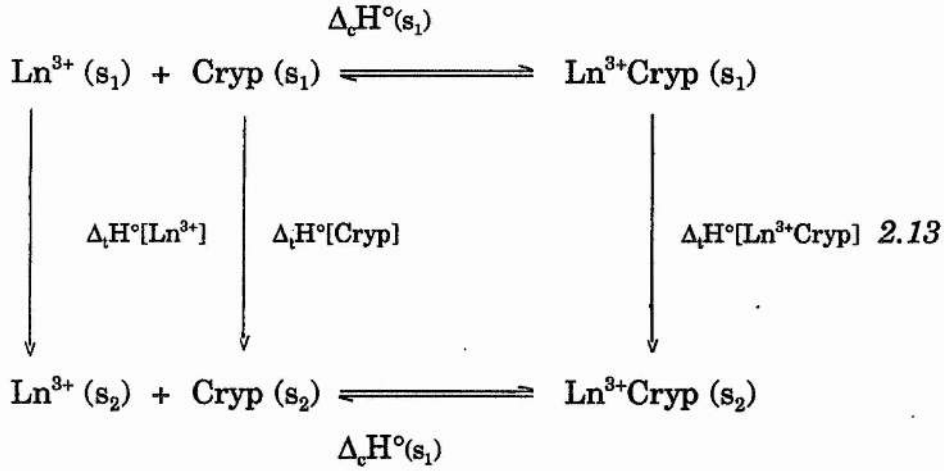

2.13

$$\Delta_t H°[Ln^{3+}]_{(s_1 \to s_2)} = \Delta_c H°(s_1) - \Delta_c H°(s_2) - \Delta_t H°[Cryp]_{(s_1 \to s_2)} + \Delta_t H°[Ln^{3+}Cryp]_{(s_1 \to s_2)} \quad \textit{2.14}$$

b) by direct measurements of the standard enthalpies of solution ($\Delta_s H°$) of the lanthanide(III) salts (LnX_3) and combination of these data with single-ion values ($\Delta_t H°$) for the anion based on the Ph_4AsPh_4B convention:

$$\Delta_t H°[Ln^{3+}]_{(s_1 \rightarrow s_2)} = \Delta_s H°[LnX_3]_{(s_2)} - \Delta_s H°[LnX_3]_{(s_1)} - 3.\Delta_t H°[X^-]_{(s_1 \rightarrow s_2)} \quad \textit{2.15}$$

ii) Macrocyclic ligands e.g. the crown ethers are capable to form stable isolable complexes with alkylammonium salts[94] and other organic ammonium cations[95] via hydrogen bonding. The idea was that other biological important species could interact in a similar manner with these ligands. Therefore, it was decided to explore the possibility of using cryptands and crown ethers as receptors for amino acids. This study could be of significant importance to several areas of research, such as:

a) the transport of amino acids across cell membranes

b) the solubility enhancement of amino acids in organic solvents

c) the use of crown ethers and cryptands for amino group protection in peptide synthesis

d) the separation of amino acids and their isomeric forms.

Therefore the thermodynamic parameters ($\Delta_c G°$, $\Delta_c H°$, $\Delta_c S°$) for the complexation of the amino acids with 18-Crown-6 and Cryptand-222 have been determined in the alcohols. In order to get a deeper insight of this process, the transfer parameters of the different species involved in the reaction have also been investigated.

Finally the possibility of using polymeric crown ethers as extracting agents for amino acids is considered.

CHAPTER 3

EXPERIMENTAL PROCEDURES

A. EXPERIMENTAL PROCEDURES FOR THE STUDY OF LANTHANIDE CATIONS-CRYPTAND INTERACTIONS

3.1. Purification of the Solvents

3.1.1 Propylene Carbonate

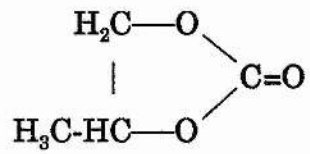

Figure 3.1: Formula of Propylene Carbonate

Propylene carbonate (PC) or 4-methyl-1,3-dioxolan-2-one is an non-toxic, odourless, colourless, aprotic solvent with a wide liquid range, a large dipole moment and a relatively high dielectric constant. Propylene carbonate readily dissolves many organic compounds and some inorganic salts. Due to its high dielectric constant, many of the dissolved ionic compounds are extensively dissociated. Some physical properties of propylene carbonate are summarized in Table 3.1.

Table 3.1 Physical properties of propylene carbonate

Freezing temperature	-49.2 °C	
Boiling temperature	241.7 °C	
Density	1.198 g/cm^3	at 760 mmHg
Viscosity	2.530 cP	at 25°C .
Dielectric constant	64.92	at 25°C
Dipole moment	4.94 D	
Debye-Hückel constants	A 0.6858 $mol^{-1/2}.l^{1/2}$	
	B 0.3629 $cm^{-1}.mol^{-1/2}.l^{1/2}$	

Commercial propylene carbonate contains in general many impurities such as water, CO_2, allyl alcohols,propylene oxides,1,2-propanediol and others still unidentified. The procedure used in this work for the purification of propylene carbonate is that suggested by Gosse and Denat[96]. This is described as follows,

a) PC (Fluka) was first treated for 12 hours with solid potassium permanganate

b) the solution was then filtered over a sintered glass funnel (porosity 4) and the permanganate was removed by heating it at 120°C for 4 hours

c) a second filtration removed MnO_2

d) the solution was distilled under reduced pressure (fast distillation) at about 70°C, taking care that the temperature did not exceed 120°C otherwise PC would be decomposed

e) the solvent was then passed through an alumina column and distilled a second time (slow distillation)

The water content of the distillate was checked by Karl-Fischer titration and found to be below 0.04%.

3.1.2 Acetonitrile

Acetonitrile (AN) or Methyl cyanide (CH_3CN) is one of the most important members of the class of dipolar aprotic solvents. It is used extensively as a reaction medium in synthesis and for mechanistic studies, as well as in electrochemistry, spectroscopy and liquid chromatography. Acetonitrile is an excellent solvent for many covalent compounds and for certain types of ionic compounds. Some of its properties are listed in Table 3.2.

Table 3.2 Physical properties of acetonitrile

Freezing temperature		- 45.7 °C	
Boiling temperature		81.6 °C	
Density		0.7766 g/cm$_3$	at 760 mmHg
Viscosity		0.344 cP	at 25°C
Dielectric constant		36.00	at 25°C
Dipole moment		4.10 D	
Debye-Hückel constants	A	1.6440 $mol^{-1/2}.l^{1/2}$	
	B	0.4857 $cm^{-1}.mol^{-1/2}.l^{1/2}$	

The common impurities found in acetonitrile are water, propionitrile, acrylonitrile, allyl alcohol, acetone and benzene. These can easily be removed by fractionally distilling acetonitrile after drying it with P_2O_5.

3.2 Synthesis and Characterization of Lanthanide(III) Trifluoromethanesulfonate complexes with Cryptands

3.2.1 Preparation of the Lanthanide Trifluoromethanesulfonate salts.

The lanthanide(III) trifluoromethanesulfonate (triflate) salts, having general formula $Ln(CF_3SO_3)_3$ were prepared according to the method of Massaux and Duyckaerts[97].

3.2.1.1 Materials

Trifluoromethanesulfonic acid (Fluka Purum) was used. The lanthanide oxides were supplied by Rhône-Poulenc (99.999%).

3.2.1.2 Synthesis

A mixture of trifluoromethanesulfonic acid (about 7 g) and lanthanide oxide in slight excess (about 3 g) was refluxed in the presence of a minimum of water. The resulting solution was heated until neutralization. The oxide in excess was filtered over a sintered glass funnel (porosity 4). The solid triflate was obtained after evaporation of the water in a rotating evaporator (Buchi) and dried in vacuum at room temperature.

3.2.1.3 Characterization

i) Characterization of the lanthanide by complexometric titration with EDTA[98]. The lanthanide triflate (≈ 0.2 g) was dissolved in water (100 ml). The pH was adjusted to 6 with an acetate buffer. After the addition of 50 mg of xylenol orange (1% xylenol orange, 99% potassium nitrate), the solution was titrated with EDTA (0.1 $mol.dm^{-3}$) until yellow coloration.

The EDTA was previously standardized with a $ZnCl_2$ solution (0.1 mol.dm^{-3}). The $ZnCl_2$ solution (5 ml) was diluted in water (100 ml). After neutralization with NaOH, the solution was titrated with EDTA in the presence of a buffer-indicator tablet (Merck) and ammonia (1 ml at 25%) until green coloration. Analytical data for the lanthanide triflates are shown in Table 3.3.

Table 3.3 Analytical Data for $Ln(CF_3SO_3)_3$

Cation	MW	Colour	$\%Ln_{found}$	$\%Ln_{calc}$
La	586.12	white	23.42	23.70
Pr	588.12	pale green	23.55	23.95
Nd	591.45	pale lilac	24.09	23.95

ii) spectral measurements (Infra-Red) of the triflate salts (Table 3.4). The specta are shown in Appendix A.

3.2.2 Preparation of the Lanthanide Cryptates.

The cryptates were prepared according to a method suggested by Seminara and Musumeci[99].

3.2.2.1. Materials

The cryptands (Kryptofix Merck) were used without further purification. The lanthanide triflates were first treated with trimethyl orthoformate

(Fluka Purum) to ensure anhydrous conditions for the synthesis. Methanol (Merck "getrocknet") contained less than 0.01% water.

3.2.2.2. Dehydration of the triflates

The synthesis of the lanthanide cryptates from hydrated salts could be hampered by partial hydrolysis of the cation to form hydroxy-compounds and by the N-protonation of the ligand to form N-protonated species.

The anhydrous salts were obtained by refluxing the hydrated solutions with trimethyl orthoformate which reacts with water,

$$Ln(CF_3SO_3)_3,aH_2O + a\ CH(OCH_3)_3 \longrightarrow Ln(CF_3SO_3)_3,aCH_3OH + a\ CH_3OH + a\ HCOOCH \qquad 3.1$$

0.5 ml of trimethyl orthoformate were mixed with 1 mmol of triflate in 20 ml methanol and refluxed for 15 min.

3.2.2.3. Synthesis of the cryptates

Kryptofix (1 mmol) was added to the lanthanide triflate solution (rigorously equimolar quantities) and refluxed for 30 min. The lanthanide cryptates precipitated very slowly: the crystallization was therefore induced by concentrating the solution to 5 ml. The cryptates were obtained after evaporation of the methanol. The crystals were washed with methanol and dried in vacuum at room temperature during 24 hours. All products were crystalline powders, the colour of which is characteristic of the cation.

3.2.2.4. Characterization of the Elements

The lanthanide analyses were carried out by complexometric titration with EDTA as described before. Because of the remarkable kinetic inertness of the lanthanide cryptates[100],complete dissociation occurred only a few hours after solubilization. It can nevertheless be accelerated in basic medium or by heating the solution. The cryptate complex (≈ 10 mg) was diluted in water (30 ml). The resulting solution was heated during 30 min, and then cooled before its titration with 0.1 M EDTA.

Elemental carbon, hydrogen and nitrogen analyses were performed at the Microanalyses Departments of EHICS, Strasbourg. Results are reported in Table 3.4.

Table 3.4 Microanalyses of the Lanthanide Cryptates (in parenthesis, the calculated values)

	%C	%H	%N	%Ln
La221(CF_3SO_3)$_3$	24.40(24.49)	3.42(3.47)	2.95(3.01)	14.82(14.91)
Pr221(CF_3SO_3)$_3$	24.72(24.77)	3.50(3.47)	3.02(3.01)	15.26(15.30)
Nd221(CF_3SO_3)$_3$	24.62(24.68)	3.42(3.46)	2.98(3.03)	15.60(15.62)
La222(CF_3SO_3)$_3$	26.01(26.01)	4.19(4.17)	2.75(2.75)	14.29(13.68)
Pr222(CF_3SO_3)$_3$	27.35(26.69)	4.26(4.29)	2.98(2.70)	14.09(13.61)
Nd222(CF_3SO_3)$_3$	26.45(26.34)	4.09(4.03)	2.83(2.79)	14.62(14.38)

3.2.2.5. Spectral Characteristics.

The Infra-Red spectra of all cryptates and of some triflate salts were recorded on a Perkin-Elmer 457 spectrophotometer, using KBr pellets. Some of these spectra are shown in Appendix A. The characteristic modes for the free ligand and the cryptates are reported in Table 3.5.

The observed peaks are in agreement with the data reported by Seminara and Rizzarelli[101] for the triflate salts, and by Seminara and Musumeci for the cryptates[99].

The characteristic modes for the triflate salts are:

-SO_3 stretching modes at 1270-1265 cm^{-1} and 1038-1035 cm^{-1}
-SO_3 deformation mode at 640-638 cm^{-1}
-SO_3 binding mode at 530-528 cm^{-1}
-SO_3 rocking mode at 352-350 cm^{-1}
-CF_3 stretching mode and -SO_3 modes overlapping near 1250 cm^{-1}
C-S stretching mode at 780-775 cm^{-1}

The characteristic modes for the ligand are:

C-O-C and C-N-C stretching modes around 1250 and 1100 cm^{-1}
C-H bending mode at 950-900 cm^{-1}

The C-0-C and C-N-C modes of the free ligand shift upon complexation towards lower frequencies (20-40 cm^{-1}): the C-N mode shifts towards higher frequencies (10-30 cm^{-1}).

Table 3.5 Characteristic modes for the free ligand and the lanthanide cryptates

	Modes (cm^{-1})		
	C-0-C	**C-N-C**	**C-H**
222	1120	1250	915
221	1115	1255	940
La221(CF_3SO_3)$_3$	1070	1230	950
Pr221(CF_3SO_3)$_3$	1070	1220	950
Nd221(CF_3SO_3)$_3$	1070	1230	950
La222(CF_3SO_3)$_3$	1070	1230	950
Pr222(CF_3SO_3)$_3$	1110	1225	950
Nd222(CF_3SO_3)$_3$	1110	1225	960

3.3 Potentiometry

3.3.1. Potentiometric Method for the Determination of Lanthanide Cryptate Stabilities. Fundamentals.

This method is based on a competitive reaction between the lanthanide cation (Ln^{3+}) and a auxiliary cation (X^+) when they are complexed by a cryptand (Cryp). It is commonly used due to the difficulty to measure directly the lanthanide concentrations. On the other hand, it is easy to follow the concentrations of some cations such as silver (Ag^+) or potassium (K^+) with ion-selective electrodes.

The process under study for the formation of 1:1 complexes may be written as:

$$X^+L\ (s) + Ln^{3+}\ (s) \rightleftharpoons Ln^{3+}L\ (s) + X^+\ (s) \qquad 3.2$$

Its stability constant K_s is then determined:

$$K_s = \frac{a_{Ln^{3+}L} \cdot a_{X^+}}{a_{X^+L} \cdot a_{Ln^{3+}}} = \frac{K_{(Ln^{3+}L)}}{K_{(X^+L)}} \qquad 3.3$$

In practice, $K_{(Ln^{3+}L)}$ and $K_{(X^+L)}$ should be of a similar magnitude or if they are slightly different, the experimental should be carried out with an excess of the metal whose stability is lowest. It has been shown that Ag^+ and K^+ suited best as auxiliary cations for these type of compounds in the solvent studied[92,93]. Once K_s and $K_{(X^+L)}$ are known, $K_{(Ln^{3+}L)}$ can easily calculated.

3.3.2. Experimental Procedures

The following electrochemical cells were used:

a) Ag_{solid} / $AgClO_4$ [Ag^+], Ln^{3+} [Ln^{3+}], Et_4NClO_4 (10^{-1} mol.dm^{-3}) //
Et_4NClO_4 (10^{-1} mol.dm^{-3}) // Et_4NClO_4 (9.10^{-2} mol.dm^{-3}),
$AgClO_4$ (10^{-2} mol.dm^{-3}) / Ag_{solid}

for the determination of the stability constants of Ln^{3+}221 in acetonitrile and Ln^{3+}221 and Ln^{3+}222 in propylene carbonate

b) K_{solid} / $KClO_4$ [K^+], Ln^{3+} [Ln^{3+}], Et_4NClO_4 (10^{-1} mol.dm^{-3}) //
Et_4NClO_4 (10^{-1} mol.dm^{-3}) // Et_4NClO_4 (9.10^{-2} mol.dm^{-3}),
$AgClO_4$ (10^{-2} mol.dm^{-3}) / Ag_{solid}

for the determination of the stability constants of Ln^{3+}222 in acetonitrile

A silver electrode (Metrohm) was always used as the reference. The titration electrode was either a silver electrode or a potassium glass electrode. They were connected to a Tacussel Isis 20000 multimeter. The reference and titration cells made of quartz were linked together by a salt bridge of Et_4NClO_4 10^{-1} mol.dm^{-3}. They were wrapped in thermostated jackets and maintained at 25.0 ± 0.1°C with a water bath (Haake FJ).

Before each measurement, a calibration of the titration electrode was carried out in order to check its response, particularly the linearity of the Nernst equation E=f[log(cK^+, cAg^+)] and its slope (equals to 59.2 mV at 25°C). If necessary, a correction was applied to adjust the slope.

For the calibration of the electrode, small quantities of AgClO4 or KClO4 (10^{-2} mol.dm^{-3} were added to a solution (10 ml) of lanthanide (≈25 mg) and Et_4NClO_4 (10^{-1} mol.dm^{-3}) in the titration cell until equimolar concentrations of lanthanide and Ag^+/K^+. The stability constant of the process 3.1 was then determined by titrating the solution with a 10^{-2} mol.dm^{-3} cryptand solution. The potential of the cell was followed as a function of volume of cryptand added.

The supporting-electrolyte Et_4NClO_4 (Fluka Purum) was recrystallized twice in water, washed with acetone and dried in a desiccator, then under vacuum at room temperature for several days.

Silver perchlorate (Fluka Puriss.) and potassium perchlorate (Prolabo-Normapur) were dried under vacuum at least 24 hours before the preparation of the solutions.

3.3.3 Interpretation of the Data

The results were interpreted by computer with the calculation program Miniquad[102]. This program is one of many for the computation of the stability constants of complex compounds in solution. It has the advantage that systems containing any number of reactant species and all kind of potentiometric data including multi-reactant and multi-electrode systems can be solved.

Miniquad is based on an iterative process which minimizes the sum of the squares of the differences between calculated and measured concentrations, and optimizes the values of the constants and the concentrations of all the species in solution.

3.4 Solution Calorimetry

Calorimetry has its roots at the end of the eighteenth century when Crawford, Lavoisier and Laplace measured the heat quantities generated by animal respiration. It is one of the oldest scientific measurements but surprisingly, its wide development only occurred in the past fifty years. Today, calorimeters are used for two major purposes, either as an instrument for the determination of thermodynamic data or as a general analytical tool.

3.4.1 Adiabatic and Isoperibol Calorimeters

A calorimeter is an instrument for measuring heat effects accompanying chemical or physical processes. There are several types of calorimeters in practical use, generally these can be classified under two major headings: adiabatic calorimeters and heat-conduction calorimeters.

In adiabatic calorimetry, there is little or no heat transfer at all between the calorimetric reaction vessel and its surroundings. The heat generated by a transformation is contained within the calorimeter. A general design is shown in Figure 3.2.

This type of instrumentation has not found any application in analytical chemistry. They are used for measurements of reactions of long duration and in cases where the temperature at which the measurements are made is very different from the room temperature.

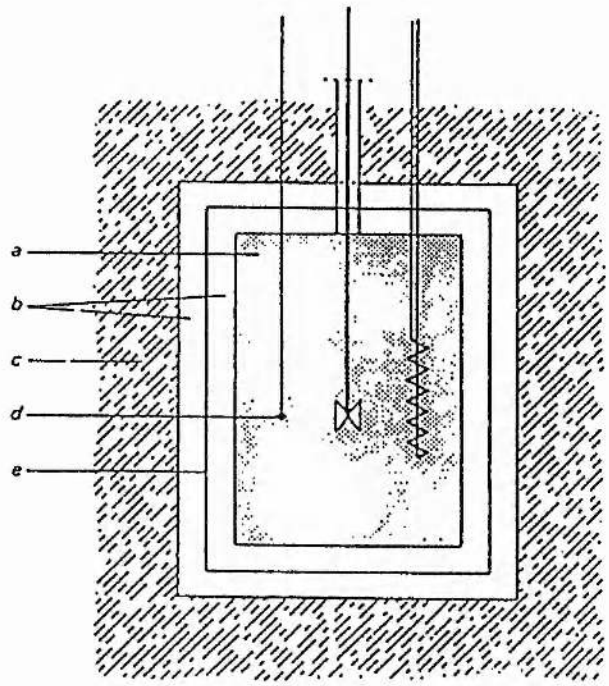

Adiatatic shield calorimeter: (*a*) calorimeter vessel, (*b*) air gap or vacuum, (*c*) thermostated bath or block, (*d*) thermometer, (*e*) adiabatic shield with heater winding.

Figure 3.2 Adiabatic Calorimeter

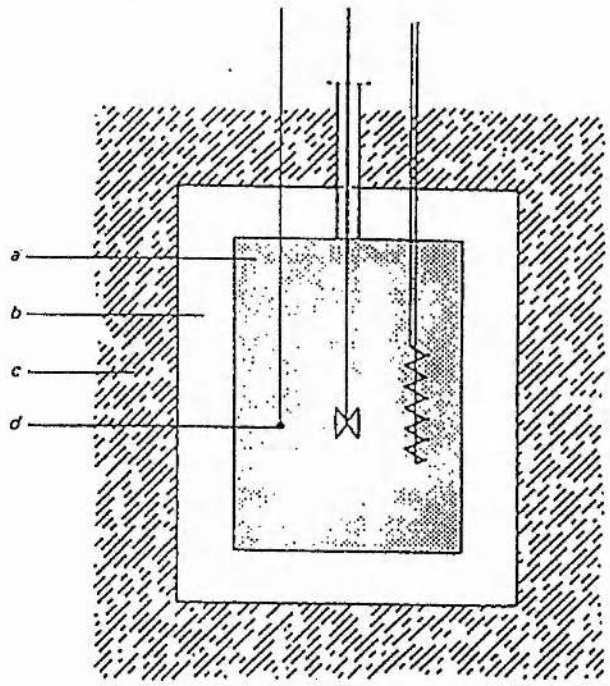

Isoperibol calorimeter: (*a*) calorimeter vessel, (*b*) air gap or vacuum, (*c*) thermostated bath or block, (*d*) thermometer.

Figure 3.3 Isoperibol Calorimeter

Isoperibol calorimeters also called constant-temperature calorimeters, are a variant of the adiabatic calorimeters. These are one of the simplest and most commonly used type of heat-conduction calorimeters. Their design is shown in Figure 3.3. A temperature change between the reaction vessel and its surroundings occurs during the experiment and heat exchange takes place.

This kind of calorimeters are in frequent use as reaction and solution calorimeters. These are very accurate for fast processes. For very short reactions, these calorimeters are equivalent to an adiabatic system.

Other variants of heat-conduction calorimeters are the thermopile conduction calorimeter and the thermoelectric pump calorimeter[103].

3.4.2. Calorimetric Measurements

Carrying out a calorimetric experiment amounts to measure temperature changes. But, in isoperibol calorimetry, the temperature change which occur when a reaction takes place in the vessel is not only due to the heat involved in that process. It is also due to other factors such as the heat generated inside the vessel (heat of stirring, heat developed by the thermistor) and mainly to the heat exchange between the vessel and its surroundings. This heat exchange called heat-leak is caused by the non-ideality of the calorimetric system. It is usually significant for accurate measurements.

3.4.2.1. The Heat Exchange

Heat is mainly transferred by three different mechanisms:

a) Radiation: heat is radiated from one body at one temperature to a cooler body at another temperature. Radiation follows Stefan-Boltzman T^4 law, it is proportional to T^4-T_s^4 where T and T_s are respectively the temperatures of the calorimeter and of the surrounding shields.

b) Convection: it is the result of mass transfer in a fluid from one region at one temperature to another at another temperature. It is generated either by stirring (forced convection) or by gravitational forces acting because of different densities of the fluid (free convection). This type of heat transfer is very complex because it depends on the geometry and the temperature distributions.

c) Conduction: the conduction through matter (air, metallic wires and leads, support, etc...) depends on the temperature difference ΔT between the vessel and the shield. At low temperatures, it is the main source of heat transfer and it is directly proportional to ΔT.

The total exchange of thermal power is then:

$$P_t = P_r + P_{cv} + P_{cd} \qquad 3.4$$

(where r, cv and cd stand for radiation, convection and conduction)

The laws governing these transfers are different for the three mechanisms. As conduction is more important than radiation and convection at low

temperatures, the total heat exchange can be expressed as a good approximation by Newton's law of cooling. This law states that the rate of cooling of a hot body is directly proportional to the temperature difference between this body and its surroundings. A linear relationship between the thermal power transfer and the temperature difference can be expressed as follows:

$$P_t = h.(T_s - T) \qquad 3.5$$

where h is the heat transfer coefficient.

The calorimetric experiment consists of taking time-temperature data points in order to get a time-temperature plot (Figure 3.4) from which the heat involved in the reaction can be calculated. The actual temperature rise during the reaction is given by:

$$\Delta T = T_e - T_b + \Delta T_{ex} \qquad 3.6$$

T_b and T_e are the temperatures at the beginning and at the end of the reaction; ΔT_{ex} is the temperature change due to the heat-leak.

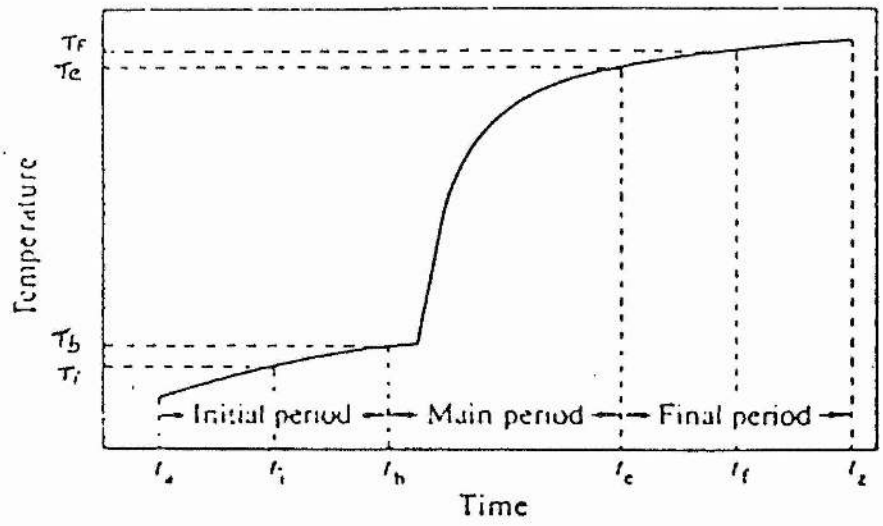

Figure 3.4 Typical Time-Temperature Curve

Determination of T_b, T_e and ΔT_{ex}

The calorimetric experiment can be divided into three different parts, as illustrated in Figure 3.4 : the initial, the main (in which the reaction takes place) and the final periods. When no reaction takes place, during the initial and the final periods, the equation for the rate of the temperature change can be expressed as:

$$g = dT/dt = P/\varepsilon + h/\varepsilon.(T_s-T) \qquad 3.7$$

$$= u + K.(T_s-T) \qquad 3.8$$

P is the total power generated in the vessel, T_s the temperature of the calorimetric shield and T the temperature inside the reaction vessel, h the heat-transfer coefficient, ε the heat capacity of the calorimeter so that

$$u = P/\varepsilon \qquad 3.9$$

where u is the total heat developed in the vessel and K, the cooling constant of the calorimeter is defined as

$$K = h/\varepsilon \qquad 3.10$$

The total heat developed (u) is generally constant for each calorimetric equipment (when solvent, compounds and ampoule are the same). It can be

calculated from the thermal conductivities in a small range of temperature. K should not deviate more than 1% for identical ε. In macro-combustion calorimeters, K is of the order of 10^{-3} to 10^{-4} s^{-1}.

P can be determined when the calorimetric vessel is left undisturbed for a long time and the equilibrium is reached:

$$g = dT/dt = 0, \quad \text{at } T=T_\infty \qquad 3.11$$

therefore,

$$P = h.(T_\infty - T_s) \qquad 3.12$$

From equation 3.7, 3.10 and 3.12:

$$g = dT/dt = h/\varepsilon.(T_\infty - T) \qquad 3.13$$

$$= K.(T_\infty - T) \qquad 3.14$$

or for the initial and final periods:

$$g_i = K.(T_\infty - T_i) \qquad 3.15$$

$$g_f = K.(T_\infty - T_f) \qquad 3.16$$

During the initial and final periods, the temperature change is only due to the heat-leak and represented by equations 3.15 and 3.16. From the measurements during these periods, it is possible to obtain values for g, K

and T_∞ and to calculate afterwards T_b and T_e, the temperatures at the beginning and the end of the reaction.

The integration of equations 3.15 and 3.16 gives:

$$T_\infty - T_i = (T_\infty - T_b).\exp[\ -K(t_i - t_b)\ ] \qquad 3.17$$

$$T_\infty - T_f = (T_\infty - T_e).\exp[\ -K(t_f - t_e)\ ] \qquad 3.18$$

These equations describe how the temperature in the vessel approaches that of the surrounding water bath, everything left undisturbed. As K is very small, equations 3.17 and 3.18 can be approximated by a linear relation:

$$T_{i,f} = a + g_{i,f}.t \qquad 3.19$$

$$(dT/dt)_{i,f} = g_{i,f} \qquad 3.20$$

which gives $$T_\infty = g_{i,f}/K + T_{i,f} \qquad 3.21$$

thus $$K = (g_i - g_f)/(T_f - T_i) \qquad 3.22$$

Tb and Te are then obtained by extrapolating at the time t_b and t_e, the slope T versus exp[-Kt] using a least-square method (Figure 3.4).

ΔT_{ex}, the temperature change due to the heat-leak, can be obtained by two different methods: Dickinson's or Regnault-Pfaundler's.

3.4.2.2. Regnault-Pfaundler's Method[104]

From equation 3.13,

$$\Delta T = -K\int_{t_b}^{t_e}(T_\infty - T).dt \qquad 3.23$$

$$\Delta T = -K.(T_\infty - T).(t_e - t_b) \qquad 3.24$$

$$\Delta T = -K.(T_\infty - T_m).\Delta t \qquad 3.25$$

Δt is the length of the main period, and

$$T_m = \frac{1}{(t_e - t_b)}\int_{t_b}^{t_e} T dt \qquad 3.26$$

If n-1 observations T_1, T_2,...T_{n-1} were done during the main period, between t_b and t_e, the trapezoidal equation can be used to calculate T_m. It gives:

$$T_m = \frac{T_b + 2.(T_1 + T_2 + ... + T_{n-1}) + T_e}{2n} \qquad 3.27$$

and if n-1 is odd, Simpson's one-third rule can be applied:

$$T_m = \frac{T_b + 4.(T_1 + T_3 + ... + T_{n-1}) + 2.(T_2 + T_4 + ... + T_{n-2}) + T_e}{3n} \qquad 3.28$$

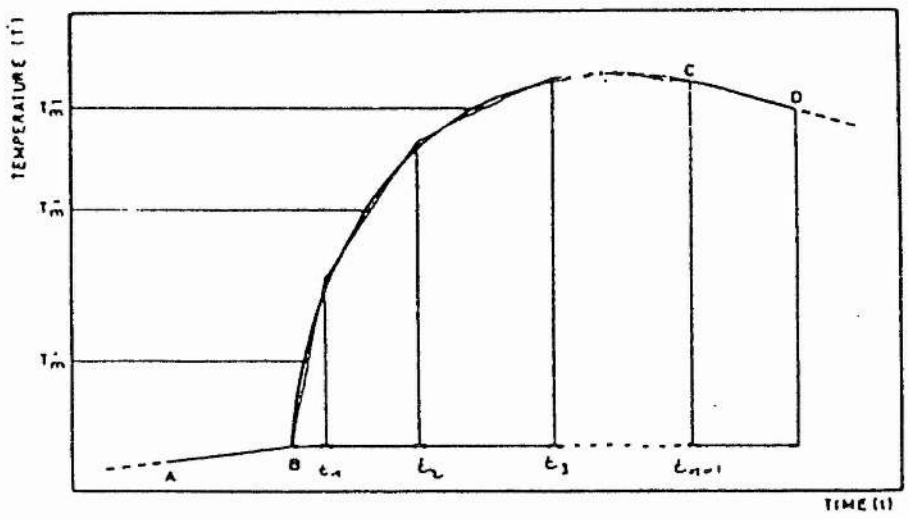

Figure 3.5 Diagram showing the Regnault-Pfaunder method

3.4.2.3. Dickinson's Method

This method[105] introduced by Challower et al.[106] is actually a variant of Dickinson's original method[107]. It consists of extrapolating at the beginning and at the end of the main period the tangents to the time-temperature curve. The difference is then equal to the corrected temperature change.

A typical time-temperature curve obtained with an isoperibol calorimeter is shown in Figure 3.4. The heat-leak is given by:

$$\Delta T_{ex} = -K\int_{t_b}^{t_e}(T_\infty - T)dt \qquad 3.29$$

By splitting ΔT_{ex} into four integrals:

$$\Delta H_{ex} = -K\,[\int_{t_b}^{t_x}(T_\infty - T_i)dt - \int_{t_b}^{t_x}(T - T_i)dt + \int_{t_x}^{t_e}(T_\infty - T_f)dt - \int_{t_x}^{t_e}(T_f - T)dt] \qquad 3.30$$

T_i, T_e and T_f are the temperatures in the initial, main and final periods respectively. t_x is the time selected so that:

$$\int_{t_b}^{t_x}(T - T_i)dt = \int_{t_x}^{t_e}(T_f - T)dt \qquad 3.31$$

as shown in Figure 3.6; the areas A and B are then equal.

$$\Delta H_{ex} = -K\left[\int_{t_b}^{t_x}(T_\infty - T_i)dt + \int_{t_x}^{t_e}(T_\infty - T_f)dt\right] \qquad 3.32$$

Using equation 3.17 and 3.18:

$$T_\infty - T_i = (T_\infty - T_b).\exp[-K(t_i - t_b)] \qquad 3.33$$

$$T_\infty - T_f = (T_\infty - T_e).\exp[-K(t_f - t_e)] \qquad 3.34$$

and after integration:

$$\int_{t_b}^{t_x}(T_\infty - T_b)dt = -(T_\infty - T_b).\exp\left[\frac{-K(t_x - t_b) - 1}{K}\right] \qquad 3.35$$

$$\int_{t_x}^{t_e}(T_\infty - T_e)dt = -(T_\infty - T_e).\exp\left[\frac{-K(t_x - t_e) - 1}{K}\right] \qquad 3.36$$

so that finally:

$$\Delta T = T_e - T_b + \Delta T_{ex}$$

$$= - (T_\infty - T_e).\exp[\ -K.(t_x-t_e)\ ] + (T_\infty - T_b).\exp[-K.(t_x-t_b)] \quad 3.37$$

This method for the determination of ΔT is long and complex. Therefore, the calculation of ΔT must done by computer. In practice a graphical method of extrapolation can be considered, as illustrated in Figure 3.7. For very fast reactions it can be assumed that $t_x \approx t_e \approx t_b$. The corrected temperature change is then the difference of the extrapolation of the linear parts to the time at which the areas A and B are equal.

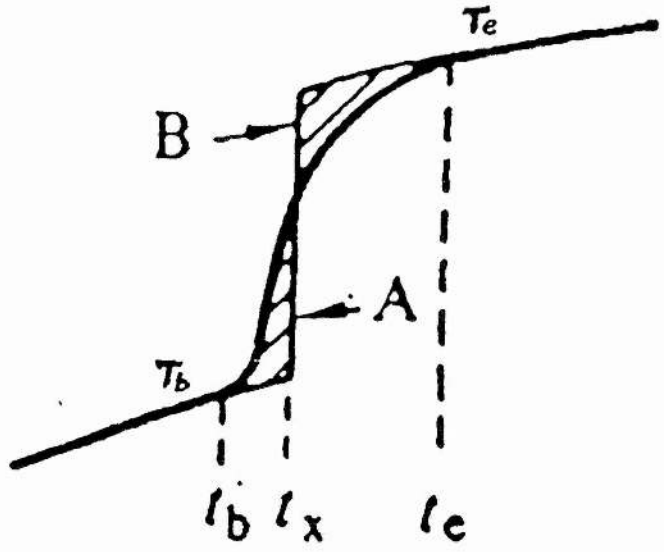

Figure 3.6 Diagram showing the Dickinson method

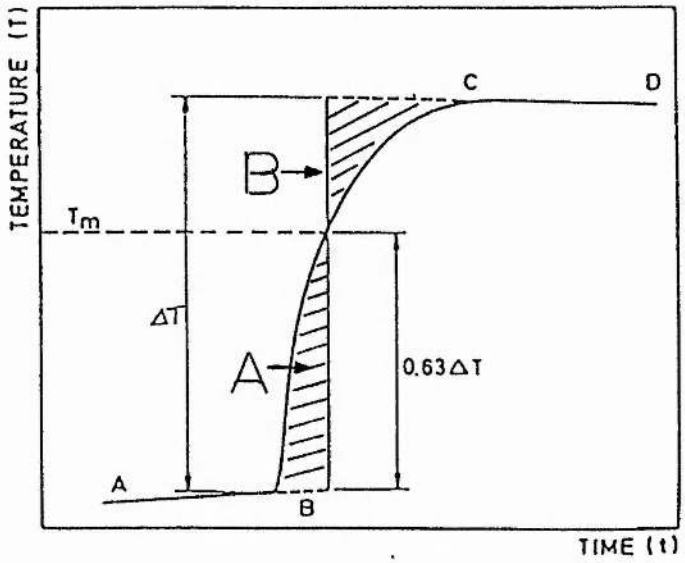

Figure 3.7 Diagram showing the graphical extrapolation method of Dickinson

3.4.3. The calorimeters

In this work, two different solution calorimeters of the isoperibol type have been used: the "LKB 8700 Precision Calorimetric System" and the "Tronac 450 Calorimeter". Their descriptions follow.

3.4.3.1. The LKB 8700 Precision Calorimetric System

The LKB model 8700 (Figure 3.8) is a reaction and solution calorimeter originally designed by Sünner and Wadsö[108,109]. It is designed for studying fast processes -no longer than 30 minutes- and for working at atmospheric pressure over a temperature range varying from 0 to 50°C.

The calorimeter is composed of a reaction vessel (the calorimeter itself) and a surrounding shield which is a thermostated water bath. The vessel consists of thin-walled glass (volume 100 ml) and it is equipped with a temperature sensor (thermistor of 2,000 ohms), a heater (approximately 50 ohms) and a stirrer made of 18 carat gold. The stirrer is also used as the holder for the cylindrical glass ampoules. The chromium plated brass cylinder is immersed with the vessel in the water bath which temperature is controlled by a thermistor and regulated by proportional heating. The temperature of the vessel is measured by the thermistor which forms one of the arms of a manually balanced Wheatstone bridge, and detected by an electrical galvanometer. The heater is used for electrical calibration experiments. Its resistance is checked using a potentiometer by comparison with a 50 ohms resistance included in the calorimetric circuit.

The calorimeter is also equipped with a timer in order to measure the heating times during calibration runs. The reaction starts by breaking a glass ampoules which contain the compound being studied against a sapphire tipped rod sealed at the bottom of the vessel.

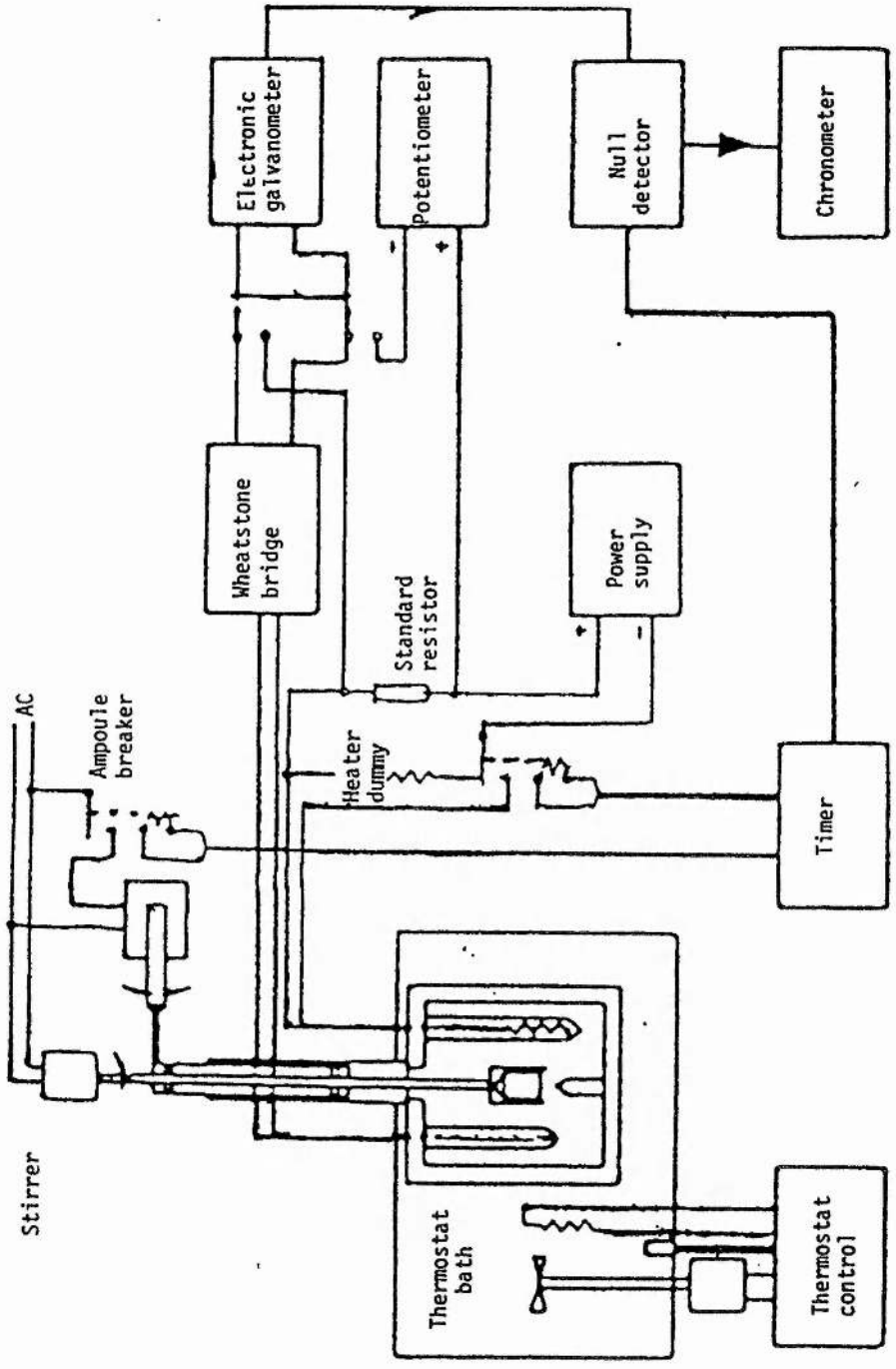

Figure 3.8 LKB 8700 Precision Calorimetric System

3.4.3.2. The Tronac 450 Calorimeter

The Tronac 450 is a commercial version of the solution calorimeter originally designed by Christensen and Izatt[110]. This calorimeter can also be used as a titration calorimeter.

The electronic assembly of the calorimeter consists of a constant temperature water bath (25°C) with a capacity of 50 litres, a motor driven stirrer, a cooled-heater assembly, a bath temperature central probe and a precision temperature controller which maintains the bath within 0.0001°C.

The reaction vessel is a rapid response glass vacuum Dewar of 50 ml of volume. The ampoule-breaker consists of a stainless steel motor, that holds the ampoule in such a way that it does not touch the walls of the reaction vessel. When the hammer is released by the burette-ampoule switch, the ampoule is crushed between the plunger and stirring blade assembly. Glass ampoules of 1 ml of volume were used and properly sealed.

The calorimeter header shaft comprises the stirrer blade assembly together with the thermistor and the heater. A strip chart recorder is connected to the recorder terminals. The latter provide the output voltage from the Wheatstone bridge which indicates the change of temperature from the reaction vessel contents. The heating intervals are accurately measured by the timer connected to the electronic assembly.

3.4.4. The Calorimetric Experiment

3.4.4.1. Determination of the Heat Capacity of the Calorimeter

In a calorimetric experiment, the heat quantities involved in the change of state of a compound are measured by comparative methods. The observed heat effect is compared with the effect of a known amount of heat obtained by some kind of calibration. In modern calorimetry, the calibration energy is always supplied by electrical heating (Joule effect).

During a calibration experiment, the calibration constant or heat capacity of the calorimeter ε is determined. ε is characteristic of each calorimetric system and it is used as a proportional factor in the calculation of the heat of a reaction:

$$\varepsilon = Q_{calib}/\Delta T_{calib} \qquad 3.38$$

where Q_{calib} is the known heat input during the calibration experiment and ΔT_{calib} the corresponding temperature change.

During the calibration experiment, a known current flows through a known resistance during a known length of time. The amount of electrical energy necessary to duplicate or to nullify -respectively for endothermic and exothermic processes- the thermal heat occurred in the experimental run gives the quantity of heat evolved or absorbed.

$$Q_{calib} = I^2.R.t \qquad 3.39$$

$$= (V_1.V_2.t)/R \text{ (Joules)} \qquad 3.40$$

I: calibration current (A)

R: heater resistance (Ω)

t: heating time (s)

V_1 and V_2: voltages taken in the heater voltage positions (V)

In the previous calculations, the heat evolution has always been considered in terms of temperature change. But in practical use, resistance changes are measured with a thermistor which is a semi-conductor. The thermistor resistance R is not directly proportional to the temperature but follows an exponential path:

$$R = A.\exp[B/T] \qquad 3.41$$

For a given solvent, A and B are constants.

In order to determine A and B for a particular solvent, the reaction vessel containing the solvent is left undisturbed for a long time, usually overnight. The equilibrium resistance R is found by adjusting the resistance dials to equilibrate the Wheatstone bridge. This is done at two different temperatures of the water-bath.

Derivation of R gives,

$$dR/dT = \frac{-A.B.\exp[B/T]}{T^2} = \frac{-B.R}{T^2} \qquad 3.42$$

thus,

$$\Delta R/\Delta T = \frac{-R_m.B}{T_m^2} \qquad 3.43$$

where R_m is the mean resistance during the experimental run:

$$R_m = \frac{R_i+R_f}{2} \qquad 3.44$$

and T_m the mean temperature during the experimental run:

$$T_m = \frac{T_i+T_f}{2} \qquad 3.45$$

therefore,

$$\Delta T = \frac{\Delta R.T_m^2}{R_m} \qquad 3.46$$

which can be approximated as

$$\Delta T = \Delta R/R_m \qquad 3.47$$

if T_m^2 is assumed to be constant during the experiment

Expression 3.47 can be used for the calculation of the heat of calibration:

$$Q_{calib} = \varepsilon.(\Delta R/R_m)_{calib} \qquad 3.48$$

The heat evolution Q_r for the studied process can be calculated knowing the calibration constant of the calorimeter:

$$Q_r = \varepsilon.\Delta T_r \qquad 3.49$$

$$= \varepsilon.(\Delta R/R_m)_r \qquad 3.50$$

The molar enthalpy change for the reaction is then:

$$\Delta H = Q_r/n \qquad 3.51$$

n being the molar quantity of the studied species.

3.4.4.3 Miscellaneous Corrections

Apart from the temperature correction for the heat-leak applied to non-adiabatic calorimetric systems, a number of other heat effects may occur during the experiment for which a correction must be made.

i) Heat of ampoule-breaking

The calorimetric experiments are usually initiated by breaking a glass ampoule in the vessel. There is then a heat effect for which a correction must sometimes be made. The amount of this correction was determined

experimentally (Table 3.6) by breaking empty but sealed ampoules in the vessel containing the solvent. The heat change varies with the solvent.

Table 3.6 Heat of ampoule-breaking in different solvents at 298.15 K

Solvent	**Q (J)**
Acetonitrile	-0.063
Propylene Carbonate	0.188
Methanol	0.263
Ethanol	0.166

ii) Heat of stirring

Heat can be generated by friction between the solvent and the ampoule. It can be different for the unbroken and the broken ampoule, depending also on the speed of stirring. This heat effect can easily be detected on the chart. If there is a difference between the steepness of the curve before and after the experimental run, a correction must be made. Generally there is no heat effect of this kind.

iii) Heat caused by incompletely filled ampoules

The ampoules used are usually not completely filled and therefore contain some air which will pass through the calorimetric liquid. This heat effect is generally small and it is included in the ampoule-breaking correction.

3.4.4.3 Practical Use of the Calorimeters

The reaction vessel was first cleaned with distilled water, then with acetone and finally dried with nitrogen. The solvent (50 ml for the Tronac, 100 ml for the LKB) was pipetted into the vessel; the ampoules (capacity: 1 ml, were blown in a mould from selected thin walled glass tubing) containing the compound were sealed and fixed onto the ampoule holder. The temperature inside the vessel was then adjusted to 25°C by heating (using the calorimetric heater) or cooling (with iced water).

The vessel was then immersed in the water-bath and left for about 15 minutes in order to stabilize the system. The experiment consisted of taking time-temperature measurements which were also recorded on a chart. The proper reaction was started by breaking the glass ampoule. The calibration experiment was carried out under similar conditions as the experimental run. This was usually done after the reaction.

3.4.5 Standard Reactions

To check the accuracy and the reproducibility of the calorimetric measurements, standard reactions have been carried out. These are detailed as follows.

3.4.5.1 Heat of Solution of Potassium Chloride in Water at 298.15 K

Mishchenko and Kaganovich[111] suggested in 1949 that the dissolution of KCl in water can be used as a standard process to calibrate reaction calorimeters.

$$KCl\ (solid) + 200\ H_2O \longrightarrow KCl,200\ H_2O \qquad 3.52$$

A value of 17.54 $kJ.mol^{-1}$ for this process at 298.15 K was reported by these authors.

The results using the Tronac 450 calorimeter are shown in Table 3.7. The value obtained (17.57 $kJ.mol^{-1}$) is in excellent agreement with the value reported by Mishchenko and Kaganovich. Other literature are reported in Table 3.8 [125].

Table 3.7 Heat of solution of KCl in water at 298.15 K

[KCl] /mol.dm^{-3}	$\sqrt{c}$	$\Delta_s H$ /kJ.mol^{-1}
$5.03\ 10^{-2}$	0.224	17.98
$5.69\ 10^{-2}$	0.238	17.84
$5.33\ 10^{-2}$	0.231	17.53
$5.66\ 10^{-2}$	0.238	17.13
$6.81\ 10^{-2}$	0.261	17.37

$\Delta_s H° = 17.57 \pm 0.33$ kJ.mol^{-1}

Table 3.8 Literature values for the standard enthalpy of solution of KCl in water at 298.15 K [125]

Authors	$\Delta_s H°$ /**kJ.mol^{-1}**
Brönsted	17.43 ± 0.08
Cohen and Kooy	17.96 ± 0.02
Shibata and Terasaki	17.42 ± 0.08
Slansky	17.05 ± 0.16
Kapustinskii and Drakin	17.22 ± 0.10
Hutchinson and White	17.24 ± 0.10
Coops, Balk and Tolk	17.08 ± 0.08
Sunner and Wadsö	17.26 ± 0.02
Coops, Somsen and Tolk	17.19 ± 0.02
Talakin et al.	17.10 ± 0.10

3.4.5.2 Heat of Solution of THAM in 0.1 M Hydrochloric Acid at 298.15 K

Irving and Wadsö[112] suggested in 1964 the reaction of Tris-Hydroxymethyl-Amino-Methane (THAM) with 0.1 M HCl can be used as a standard reaction in calorimetry.

$$H_2NC(CH_2OH)_3 + H_3O^+ \longrightarrow H_3N^+C(CH_2OH)_3 + H_2O \quad 3.53$$

The enthalpy of solution of reaction 3.53 is $\Delta H° = -29.73$ kJ.mol^{-1} according to these authors.

The results obtained with the Tronac are shown in Table 3.9, those obtained with the LKB are listed in Table 3.10. There is an excellent agreement between these values (-29.65 and -29.73 kJ.mol^{-1}) and those reported by some other authors (Table 3.11).

Table 3.9 Standard enthalpy of reaction of THAM with 0.1 M HCl at 298.15 K, using the Tronac 450 calorimeter

[THAM] /mol.dm^{-3}	ΔH /kJ.mol^{-1}
3.64 10^{-2}	-29.63
3.17 10^{-2}	-29.85
1.21 10^{-2}	-29.38
2.78 10^{-2}	-29.74

$\Delta H° = -29.65 \pm 0.20$ kJ.mol^{-1}

Table 3.10 Standard enthalpy of reaction of THAM with 0.1 M HCl at 298.15 K,using the LKB 8700 calorimeter

[THAM] /mol.dm^{-3}	ΔH /kJ.mol^{-1}
3.02 10-2	-29.72
2.59 10-2	-29.72
3.00 10-2	-29.74
2.97 10-2	-29.75

$\Delta H° = -29.74 \pm 0.01$ kJ.mol^{-1}

Table 3.11 Literature values for the standard enthalpy of reaction of THAM with 0.1 M HCl at 298.15 K

Authors	$\Delta H°$ /kJ.mol^{-1}	Ref.
Irving and Wadsö	-29.73 ± 0.02	113
Gunn	-29.73 ± 0.02	114
Sunner and Wadsö	-29.75 ± 0.01	109
Irving and Wadsö	-29.76 ± 0.01	117
Ojelund and Wadsö	-29.75 ± 0.02	115
Irving and Sousa	-29.75 ± 0.01	117
Hill et al.	-29.74 ± 0.01	116
Bidokhti	-29.75 ± 0.02	117
Ghousseini (Tronac)	-29.69 ± 0.07	118
Traboulssi (Tronac)	-29.70 ± 0.06	119
(LKB)	-29.74 ± 0.02	119
This work (Tronac)	-29.65 ± 0.20	
(LKB)	-29.73 ± 0.01	

B. EXPERIMENTAL PROCEDURES FOR THE STUDY OF AMINO ACID-MACROCYCLIC LIGAND INTERACTIONS

3.5 Purification of the Alcohols

Methanol (HPLC Grade) and Ethanol (Aldrich) were purified from water according to the procedure described by Vogel[120]. For methanol, the procedure involves the following reactions:

$$2CH_3OH + Mg\ (solid) \longrightarrow H_2\ (g) + Mg(OCH_3)_2 \qquad 3.54$$

$$Mg(OCH_3)_2 + 2H_2O \longrightarrow 2CH_3OH + Mg(OH)_2\ (solid) \qquad 3.55$$

Reaction 3.54 proceeds readily since the magnesium (Mg) is activated with iodine (I_2) and the water content does not exceed 1%. Subsequent interaction between magnesium methoxide [$Mg(OCH_3)_2$] and water gives the highly insoluble magnesium hydroxide [$Mg(OH)_2$] and methanol (CH_3OH) of high purity.

Magnesium (5 g) and iodine (0.5 g) were added to 50 ml of methanol, the mixture was then gently heated until all of the iodine had disappeared and, the magnesium had been totally converted into magnesium methoxide. The new mixture was refluxed for 30 minutes. Following this, methanol was further purified by fractional distillation. Only the middle fraction of the distillate was collected and used. Ethanol was purified according to the same method. The water content of the purified alcohols was checked by Karl Fischer titration and was found to be less than 0.02%.

The physical constants of methanol and ethanol are reported in Table 3.12.

Table 3.12 Physical properties of methanol and ethanol at 298.15 K

	Methanol	**Ethanol**
Molecular weight	32.04	46.07
Freezing temperature (°C)	-97.8	-114.5
Boiling temperature (°C)	64.6	78.3
Density (g/cm^3) at 760 mmHg	0.7866	0.7851
Viscosity (cP) at 25°C	0.5445	1.089
Dielectric constant at 25°C	32.70	24.55
Dipole moment (D)	1.70	1.69
Debye-Hückel constants A ($mol^{-1/2}.l^{1/2}$)	1.8950	2.914
B ($cm^{-1}.mol^{-1/2}.l^{1/2}$)	0.5093	0.5878

3.6 Purification of Other Reagents Used

a) 18-Crown-6 (Aldrich 99.9%) was purified by sublimation[2] in an apparatus schematically shown in Figure 3.9. The ligand was heated for about 2 hours at about 420 K at a vacuum pressure of 0.05 to 0.1 mmHg. After sublimation of the crown, crystals were formed on the cold finger. The crystals were then collected and dried under vacuum. The purity of the crown ether was checked by microanalyses ($\%C_{found}$ 54.57,$C_{calc.}$ 54.53; $\%H_{found}$ 9.23,$H_{calc.}$ 9.15) and by verification of the melting point (311-312 K) [2].

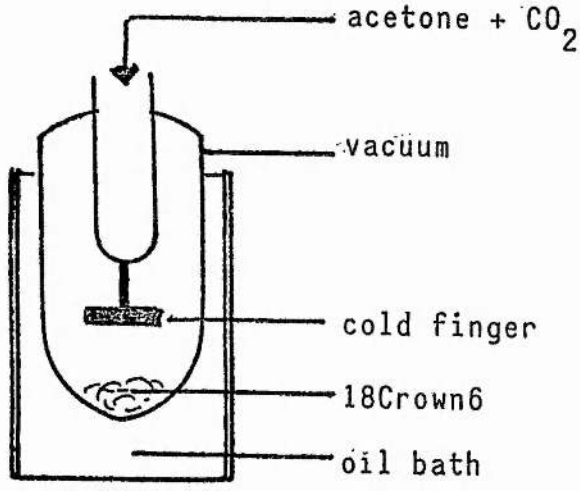

Figure 3.9 Apparatus used for the sublimation of 18-Crown-6

b) Cryptand-222 (Kryptofix Merck) was dried under vacuum at room temperature before use.

c) The amino acids (Sigma) were all dried under vacuum at 100°C before use. Their solutions were made up and left for several days in a thermostated and ultrasonic bath (25.0 ± 0.1°C) due to their slow dissolution in the alcohols.

d) The resin (polydibenzo-18-crown-6, Fluka) was dried prior to use in a drying pistol at 100°C with phosphorous pentoxide.

3.7 Synthesis of the amino acid-macrocyclic ligand (18-Crown-6 or Cryptand-222) complexes

Equimolar quantities of the amino acid and the macrocyclic ligand were mixed in a small volume (20 ml) of methanol and heated until complete dissolution of the amino acid. The resulting solution was then concentrated to induce the precipitation of the complex. The colourless crystals which were deposited were washed with cold methanol and finally dried under vacuum at room temperature for several days. The purity of all the samples was checked by microanalyses (Tables 3.13 and 3.14)

Table 3.13 Microanalyses of amino acid-18 Crown 6 complexes (in parenthesis, the calculated values)

	%C	%H	%N
DL-ALA-18C6	50.18(50.95)	8.62(8.77)	3.96(3.96)
GLY-18C6	49.23(49.54)	8.49(8.63)	4.23(4.12)
DL-ILE-18C6	54.35(54.65)	9.43(9.44)	3.25(3.53)
DL-LEU-18C6	54.35(54.65)	9.44(9.44)	3.51(3.53)
DL-PHE-18C6	58.75(58.72)	8.12(8.23)	2.95(3.25)
DL-TRP-18C6	58.35(58.95)	7.92(7.76)	6.18(5.97)
DL-VAL-18C6	52.73(53.52)	9.12(9.26)	4.00(3.67)

Table 3.14 Microanalyses of amino acid-Cryptand-222 complexes (in parenthesis, the calculated values)

	%C	%H	%N
DL-ALA-222	54.42(54.12)	9.06(9.33)	9.64(9.02)
GLY-222	53.78(53.19)	9.14(9.17)	9.25(9.30)
DL-ILE-222	56.80(56.77)	10.24(9.75)	8.43(8.24)
DL-LEU-222	57.07(56.77)	9.35(9.74)	8.25(8.27)
DL-PHE-222	59.86(59.86)	8.56(8.76)	7.78(7.75)
DL-VAL-222	55.96(55.96)	9.77(9.62)	8.77(8.51)

3.8 Solubility measurements

For the solubilities measurements, saturated solutions of the amino acids and their complexes with 18-Crown-6 and Cryptand-222 were left in a thermostated bath (25.0 ± 0.1°C) for several days in order to reach equilibrium. Aliquots were removed and analyzed by the gravimetric method described below. Solubility measurements were done by triplicate.

Amino acid concentrations were determined by gravimetry. A sample (10-30 ml) of the solution to be analyzed was taken and the solvent evaporated on a hot plate. The amino acid residue obtained was then accurately weighed (± 0.00001 g). This procedure was repeated at least twice, and an average of these measurements was taken to calculate the solubility for the appropriate compound.

3.9 Partition Experiment

An accurately weighed amount of 18-Crown-6 (0.09793 g) was left in a tetradecane-ethanol (10/5 ml) mixture in a thermostated bath (25 ± 0.1°C) under constant shaking for several days. A sample of the ethanolic phase was then analyzed and the concentration of 18-Crown-6 determined by a calorimetric method.

18-Crown-6 was complexed with an amino acid (DL-Phenylalanine) for which the log K_s and the ΔH values have been calculated previously. The heat measured, corrected by the heat of the different side effects, enabled the calculation of the concentration of the complex formed [LHAa] and therefore the initial concentration of the ligand in ethanol $[L]_o$ using the formula 3.56:

$$[L]_o = [LHAa].(1+\frac{1}{K.([HAa]_o-[HAa])}) \qquad 3.56$$

$[LHAa]_o$ being the initial concentration of the amino acid.

3.10 Capacity Measurements of §DB18C6 with Amino Acids in Methanol at 298.15 K

An accurately weighed (± 0.0001 g) amount of resin was transferred to a container containing an accurately analyzed solution (50 ml) of the amino acid to be extracted. The solution was left in a thermostated bath (25 ± 0.1 °C), under periodic stirring. After a few days, an aliquot (25 ml) of the solution was taken and analyzed. A further volume (25 ml) was added to the resin and the solution was left in the thermostated bath for a few days more. This procedure was followed subsequently until no further uptake was observed. Not less than two separate experiments were set up.

3.11 Spectrophotometry

UV spectroscopy was the analytical technique used to determine the concentrations of the aromatic amino acid DL-Phenylalanine in methanol, ethanol and propan-2-ol in the presence of different concentrations of the macrocyclic polyether 18-Crown-6.

A series of solutions containing various amounts of 18-Crown-6 ($\approx 10^{-3}$ to 6.10^{-2} mol.dm^{-3}) and the amino acid in excess ($\approx 10^{-1}$ mol.dm^{-3}) were

left for one week in closed vessels (20 ml) under constant shaking in a thermostated bath (25.0 ± 0.1°C). The undissolved amino acid was then filtered off over sintered glass funnel (porosity 4). The concentration of the amino acid in solution was determined by UV absorption on a Shimadzu UV-240 or a Cary-17D spectrophotometer. The spectra were recorded between 300 and 220 nm where DL-Phenylalanine absorbs. The optical densities (OD) were printed at regular wavelength intervals.

The molar extinction coefficient (ε) of DL-Phenylalanine in methanol, ethanol and propan-2-ol was first determined using reference solutions of known molarity (Table 3.15). The wavelength of maximum absorbance λ_{max} was found to be 258 nm; Beer-Lambert's law was applied:

$$OD = \varepsilon \, . \, c \, . \, l \qquad\qquad 3.57$$

where c is the concentration of the amino acid in mol.dm^{-3} and l the length of the absorption layer (cm).

Table 3.15 Extinction coefficients of DL-Phenylalanine in the alcohols at 298.15 K

	OD	[PHE] mol.dm^{-3}	l cm	ε dm^3.mol^{-1}.cm^{-1}
MeOH	0.104	$2.76 \cdot 10^{-4}$	2	18
EtOH	0.128	$3.63 \cdot 10^{-4}$	2	176
PrOH	0.020	$7.36 \cdot 10^{-5}$	2	136

3.12 pH titration of amino acid solution containing 18-Crown-6

Amino acids (Glycine, DL-Alanine, DL-Phenylalanine) stock solutions (10^{-3} mol.dm^{-3}) were prepared in methanol. An excess of perchloric acid $HClO_4$ (2.10^{-3} mol.dm^{-3}) was added. Tetraethylammonium perchlorate (Et_4NClO_4 8.10^{-3} mol.dm^{-3}) as the supporting-electrolyte in order to keep the ionic strength at 10^{-2} mol.dm^{-3} was used.

The titration experiments were carried out with a titroprocessor Metrohm (Dosimat E635) equipped with an automatic microburette. The titration vessel was thermoregulated at 25.0 ± 0.1°C. A computing system allowed the plotting of the titration curves, the printing of the pH values and the calculation of the pKas. A glass electrode Metrohm in which the saturated KCl solution has been replaced by a 10^{-2} mol.dm^{-3} Et_4NClO_4 methanolic solution was used as titration electrode. The junction potentials have been taken into account for the determination of the pH values in methanol:

$$pH_{real} = pH_{meas.} + a + b.10^{-pHmeas.} \qquad 3.58$$

The constants a (0.452) and b (-45.25) were determined with two reference solutions at pH = 2 ($HClO_4$ 10^{-2} mol.dm^{-3}) and at pH = 3 ($HClO_4$ 10^{-3} mol.dm^{-3}, Et_4NClO_4 9.10^{-3} mol.dm^{-3}).

The amino acid stock solution (5 ml) was titrated with tetraethylammonium hydroxide (Et_4NOH) as a base (3.88 10^{-2} mol.dm^{-3}). The molarity of the base was previously checked with a phthalic acid $KHC_8H_4O_4$ solution of known molarity (1.87 10^{-3} mol.dm^{-3}). A series of solutions made up from the stock solution and containing different concentrations of 18-Crown-6 (≈10^{-3} to 10^{-2} mol.dm^{-3}) were titrated with Et_4NOH. All the pKas listed were refined with the calculation program Miniquad[102].

3.13 Titration Calorimetry

3.13.1 Principles of the technique

Titration calorimetry has been developed by Izatt and co-workers in the 70's for the simultaneous determination of the stability constant (hence free energy) and enthalpy values in the complexation process involving macrocyclic ligands[121-123]. This technique measures the temperature changes produced during the course of the titration. The data are then interpreted in form of a thermogram i.e. a plot of the heat evolved versus the number of moles of titrant added (Figure 3.10).

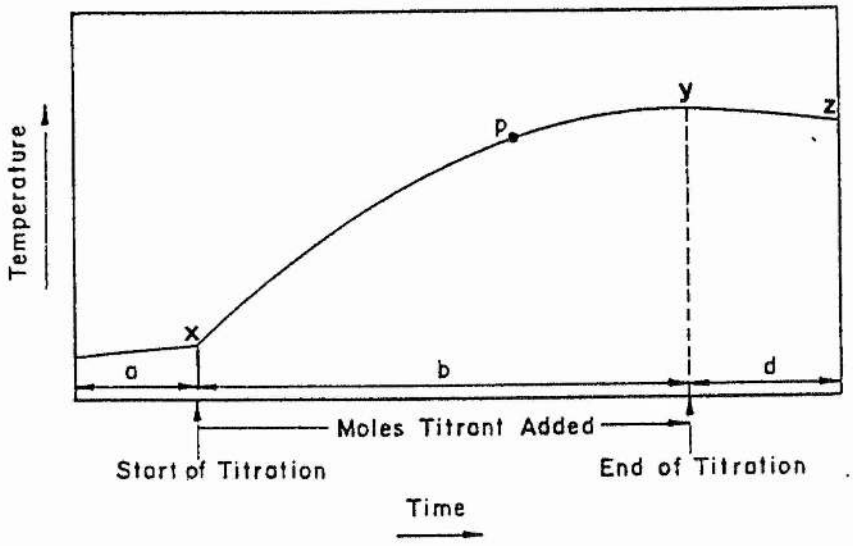

Figure 3.10 Typical thermogram

A thermogram can be obtained by two different means:

i) by incremental addition of the titrant into the reaction vessel. The temperature change is recorded after each titrant addition then readjusted to its initial value. This method only allows a limited number of data points to be obtained . It has the advantage that the overall temperature change is slight and temperature dependent corrections (e.g. heat leak) are kept small.

ii) by continuous addition of the titrant into the reaction vessel. The titrant is added at a constant rate and the temperature is recorded continuously. This produces a complete record of the reaction and allows an unlimited number of data points. The disadvantage of this method is that the overall temperature change might be large so that temperature dependent corrections can usually not be neglected. A quick response of the measuring device is also needed.

The range of applicability of titration calorimetry is within certain limits. The technique can be used for the simultaneous determination of the stability constant (log K_s) and enthalpy (ΔH) values provided that the complexation process does not occur at 100%. The Figure 3.11 shows that the curvature of the thermogram is related to the K_s value, when ΔH is assumed constant. The stability constant of the complex should be between 1 and 6 log units. If log $K_s > 6$, it would be difficult to make accurate calculations of K_s due to the ambiguity of differentiating between the curves(Figure 3.11). Very small heat is evolved in complexes characterized by small enthalpies of complexation and therefore, these measurements can be subject to considerable error. For low stability constants (log $K_s < 1$), the percentage of complexation that can be achieved can be relatively small. Consequently, extrapolation to 100% complexation could lead to inaccurate enthalpy data.

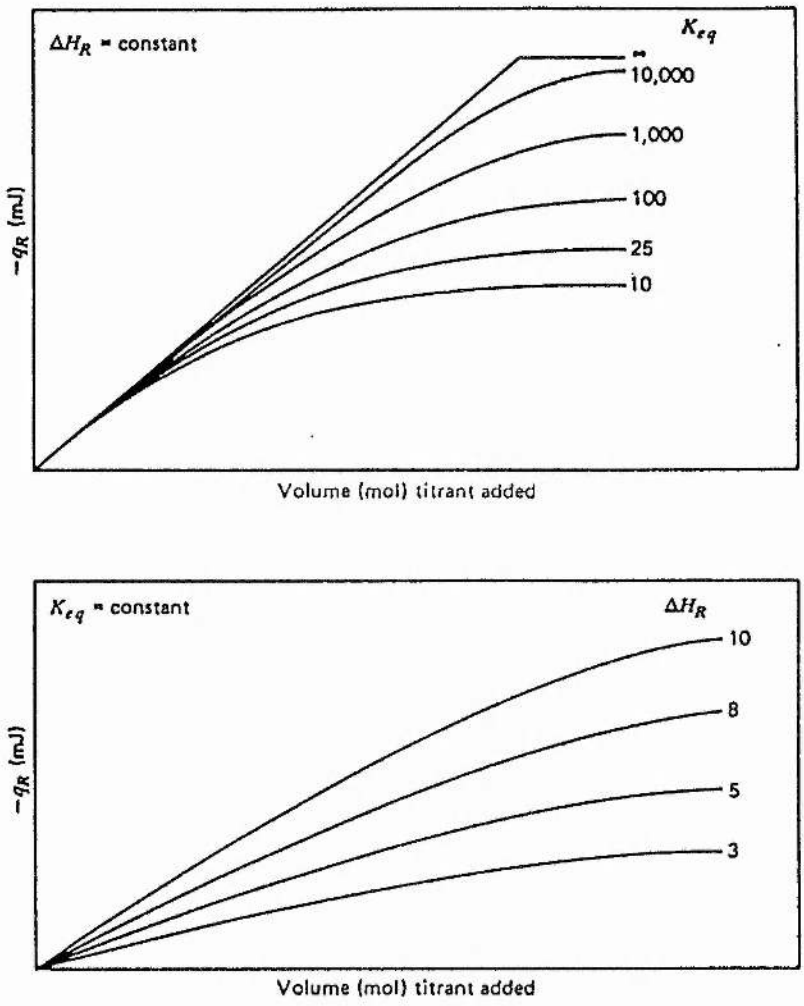

Figure 3.11 Dependence of calorimetric data on K_a and ΔH

3.13.2 Analysis of the thermogram

The temperature versus time curve (Fig. 3.10) is converted into a heat versus mole of titrant added curve using Regnault-Pfaundler or Dickinson's methods of calculation. These were described in Sections 3.4.2.2 and 3.4.2.3.

A typical thermogram is composed of three main regions (Figure 3.10)

i) the prereaction (region "a") where the heat effects are those occurring before the titration begins (heat leak and mechanical heat effects)

ii) the main period (region "b") where the heat change is due to the reaction taking place, plus other heat effects due to the heat of dilution of the titrant and the titrate or the heat resulting from a temperature difference between the titrant and the titrate.

iii) the postreaction (region "c") after the titration, where the temperature change is caused by similar effects to those described in (i).

Approximate calculation of the equilibrium constant

The interpretation of the titration data consists of the determination of ΔH and log K_s values for the complexation process being studied. For each of the data points, the measured heat (Q_p) is related to the enthalpy of complexation and to the number of moles (n_p) of the complex formed from the start of the titration to point p, as illustrated in Fig. 3.10:

$$Q_p = \Delta H \times n_p$$

or for i reactions, $Q_p = \Sigma_i (\Delta H_i \times n_{i,p})$ *3.59*

n_p can be derived from the equilibrium constant K_s for the reaction. In our case, K_s is not known. Calculations were done by approximating K_s and derive from it the corresponding value of n_p; thus a ΔH value can be obtained at a given data point from equation 3.59. For a set of data points ΔH should be constant. If such is not the case, a new value of K_s is chosen and the corresponding ΔH values are calculated. This iterative procedure is followed until a K_s value is found which yields to the same ΔH value at each data point throughout the titration experiment. The computer program for the calculation of log K_s and $\Delta_c H°$ developed by J.D. Lamb[124] considers the following steps:

i) For a given log K_s value, the concentration of the different species in the reaction vessel are calculated, taking into account their activity coefficients as obtained from the extended Debye-Hückel equation (see section 4.1).

ii) Calculation of the corresponding ΔH values for the chosen K_s for at each data point

iii) Evaluation of the error square σ sum for the average of the ΔH values

iv) Minimization of σ by a least-square analysis of equation 3.60 using an iterative procedure to find the best values of K_s and ΔH

$$\sigma = \Sigma_p \ [Q_p - \Sigma_i(\Delta H_i \times n_{i,p})]^2 \qquad 3.60$$

An example of calculation is shown in Appendix B.

3.13.3 Heat corrections

The heat measured for a given complexation process does not only involve the heat of complexation itself but also a number of other heat effects generated by side processes. Some of these heat effects are similar to those encountered in solution calorimetry especially the heat-leak and the mechanical heats occurred in the vessel (heat of stirring, resistance across the thermistor...) which are corrected in the same way. Other heat effects which are typical of titration calorimetry must also be considered. These are the heats of dilution of the titrant and the titrate, the heat occurred from the temperature difference between the titrant and the titrate, the heat contributed from other reactions.

3.13.3.1 Heat of dilution of the titrant and the titrate

This heat effect is due to the chemical changes such as solvation, hydrolysis or ion-pairing which might occur in the reaction vessel when the titrant is added to the titrate. It is concentration dependent and can be determined experimentally or from available data[125-127].

3.13.3.2 Temperature difference between titrant and titrate

The mixing of the titrant and the titrate can produce extra-heat if these are not kept at the same temperature. This effect can be minimized by immersing the burette in the thermostated bath of the calorimeter so that titrant and titrate are kept at the same temperature.

3.13.3.3 Heat contributed from other reactions

If reactions other than the ones of interest occur in the calorimetric vessel, their heat contribution must be corrected for. The commonly encountered

side reactions are hydrolysis, proton ionization and metal-ligand interactions. In the present work, no effect of this type had to be considered.

3.13.4 The Hart Scientific 5021 Calorimeter

3.13.4.1 Description

The Hart Scientific 5021 titration calorimeter is an isothermal/isoperibol calorimeter with similar features to that of the Tronac 450 calorimeter described earlier (section 3.4.3.2). A schematic view is shown in Figure 3.12. Instead of an ampoule breaking system, the Hart calorimeter is equipped with a burette which is connected by teflon tubes to the reaction vessel. The calorimeter is also equipped with a computing system which allows precise injections of the titrant during an accurately known amount of time.

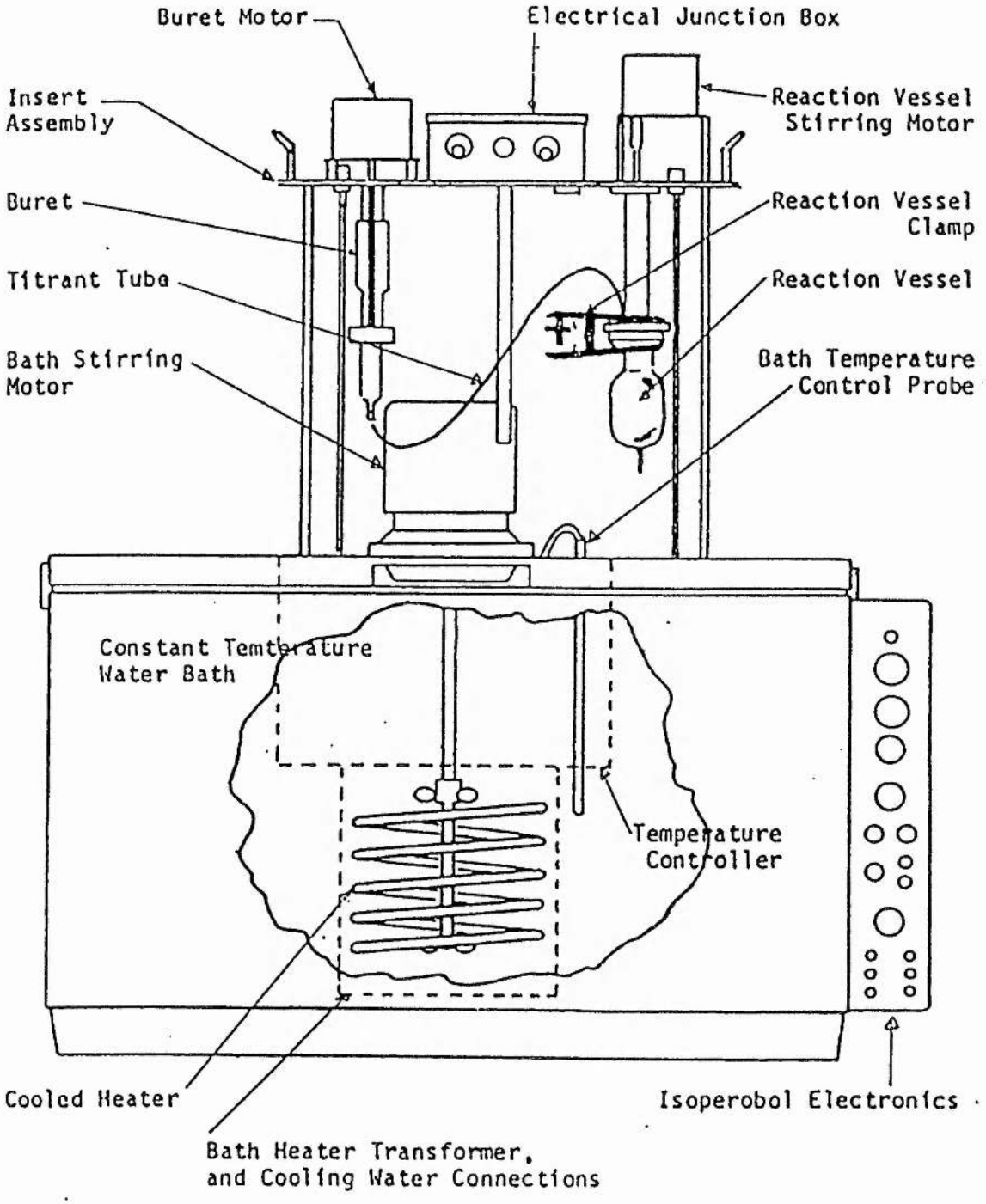

Figure 3.12 The Hart Scientific 5021 Calorimeter

3.13.4.2 Experimental procedure

Amino acid solutions (50 ml) in methanol and ethanol were placed into the reaction vessel of the calorimeter. The burette was loaded with a solution of the ligand in the appropriate solvent. The whole assembly (vessel and burette) was then immersed into the calorimetric bath and left for several minutes until thermal equilibrium was reached. The titrant was added and the temperature change monitored on a chart strip recorder. An electrical calibration was carried out after each addition and the temperature of the vessel was readjusted to its initial value. The ligand was added until the end of the reaction when all the amino acid was complexed and no heat was observed.

3.13.5 Calibration of the equipment

3.13.5.1 Burette calibration

The burette has been calibrated by weighing accurately amounts of distilled water delivered by it over several time intervals, at different delivery rates (50,100,200,400 steps/second). The burette delivery rate (BDR) is then expressed in units of volume per units of time. BDR is calculated by using the following equation:

$$BDR = W/\rho \,.\, \theta \qquad 3.61$$

where W is the weight of water (g), ρ the density of water at 25°C (0.9970 g/cm^3) and θ the time (s) during which water was delivered. The BDR values found were respectively 6.61 ± 0.01, 13.15 ± 0.02, 26.25 ± 0.04 and 53.57 ± 0.09 µl/s for delivery rates of 50, 100, 200, and 400 steps/sec. These are represented in Figure 3.13. These data are the result of three independent determinations.

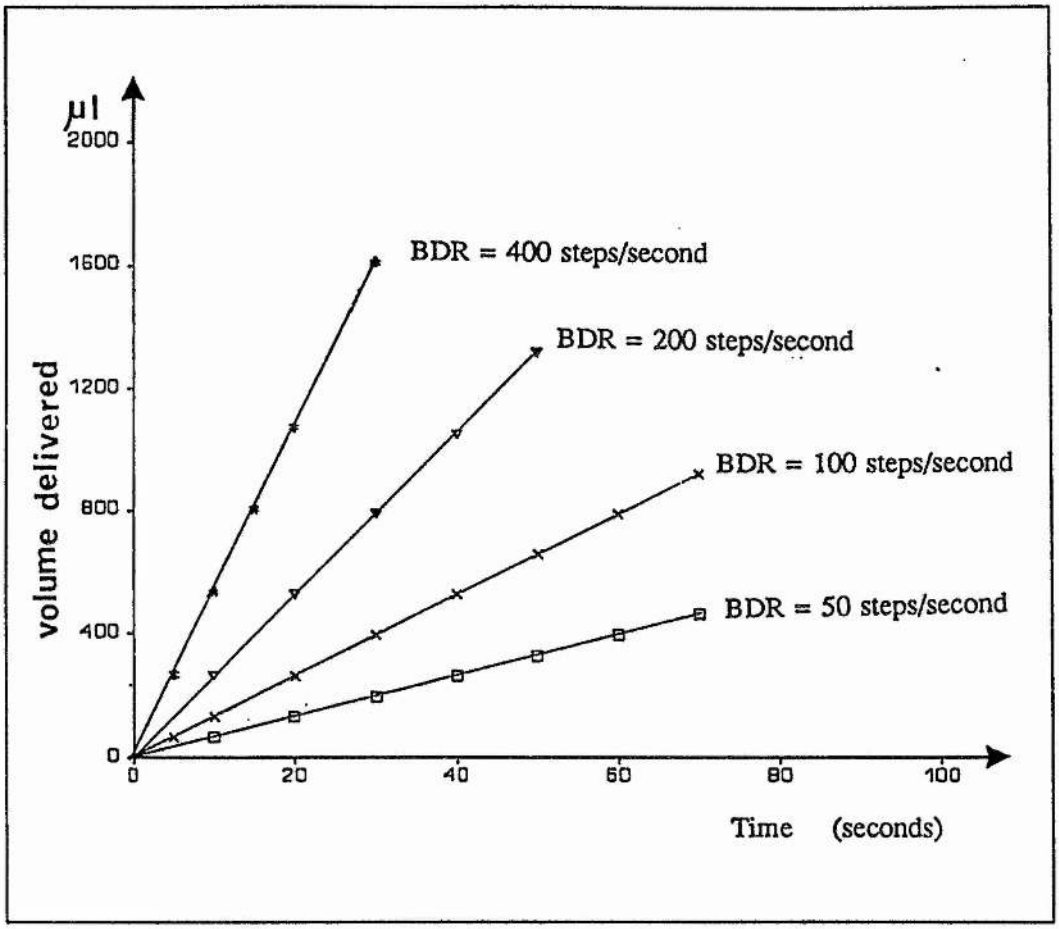

Figure 3.13 Burette Calibration Curves at Different Delivery Rates at 298.15 K

3.13.5.2 Standard reactions

In order to check the accuracy and the reproducibility of the calorimetric system, particularly the electrical heater and the measuring devices, the heat of reaction of well known chemical standard reactions have been measured.

The reaction between $HClO_4$ and NaOH in water is recommended as a standard chemical reaction in titration calorimetry[128].

$$HClO_4\ aq + NaOH\ aq \longrightarrow NaClO_4\ aq + H_2O \qquad 3.62$$

An aqueous solution of $HClO_4$ (0.355 $mol.dm^{-3}$) was incrementally added to 50 ml of NaOH (0.1 $mol.dm^{-3}$). The heats of reaction measured are reported in Table 3.16. The standard enthalpy of this reaction (ionization of water) was found to be -55.30 ± 0.19 $kJ.mol^{-1}$. This is in good agreement with the values reported by Vanderzee and Swanson[129] (- 55.80 $kJ.mol^{-1}$), Hale et al.[130] (-55.79 $kJ.mol^{-1}$) and Hansen and Lewis[131] (-55.8 $kJ.mol^{-1}$).

Table 3.16 Enthalpy of Formation of Water at 298.15 K

Moles added	Q_f/J	$\Delta_f H°$ /kJ.mol^{-1}
2.35 10^{-5}	-1.3045	-55.51
2.35 10^{-5}	-1.2937	-55.05
2.35 10^{-5}	-1.2989	-55.27
2.35 10^{-5}	-1.3066	-55.60
2.35 10^{-5}	-1.3007	-55.34
2.35 10^{-5}	-1.2937	-55.05
2.35 10^{-5}	-1.2989	-55.27
2.35 10^{-5}	-1.3007	-55.34

$\Delta H° = -55.30 \pm 0.19$ kJ.mol^{-1}

CHAPTER 4

THERMODYNAMICS OF INTERACTION BETWEEN LANTHANIDE(III) CATIONS AND CRYPTANDS IN DIPOLAR APROTIC MEDIA

4.1 Macrocyclic Complexation: General Process

The interactions of a metallic salt ($M^{n+}nX^-$) and a macrocyclic ligand (L) in a solvent (s) can be described as follow:

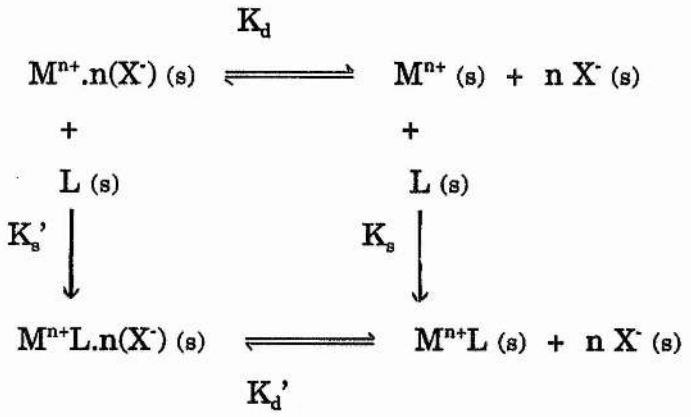

4.1

K_s and K_s' are the stability constants for the free cation and the ionic-pair with the ligand L; and K_d and K_d' the dissociation constants of the free ion-pair and the complexed ion-pair respectively.

In polar solvents, K_s is usually the only stability constant of importance since

the salt can be considered as fully dissociated in these media. However, in some cases ion-pair formation takes place and should also be taken into account. In apolar solvents, K_s' would be the predominant stability constant.

In dipolar aprotic solvents, the process under study can be written as:

$$M^{n+}\ (s) + L\ (s) \overset{K_s}{\rightleftharpoons} M^{n+}L\ (s) \qquad 4.2$$

This equilibrium is characterized by the thermodynamic stability constant:

$$K_s = \frac{a_{M^{n+}L}}{a_{M^{n+}}.a_L} = \frac{[M^{n+}L]}{[M^{n+}].[L]} x \frac{\gamma_{M^{n+}L}}{\gamma_{M^{n+}}.\gamma_L} \qquad 4.3$$

where a_i, γ_i and [i] are respectively the molar activity, the mean ionic activity coefficient on the molar scale and the concentration of the species i in $mol.dm^{-3}$.

In highly dilute solutions, the activity coefficient for the uncharged ligand γL is often given as unity (γL=1). The activity coefficients of the free and the complexed cation γM^{n+} and $\gamma M^{n+}L$ can be estimated from the Debye-Hückel equation. The Debye-Hückel equation functionalizes the electrostatic effect of the ionic atmosphere and deducts it from the chemical potential of these ions. Its extended form can be written as:

$$\log \gamma_{\pm} = \frac{-A.|z_+.z_-|.\sqrt{I}}{1+B.a.\sqrt{I}} \qquad 4.4$$

where

$$A = \frac{1.8246\ 10^6}{(T.\varepsilon_r)^{3/2}}\ mol^{-1}.l^{1/2}.K^{3/2} \qquad 4.5$$

and

$$B = \frac{50.29\ 10^8}{(T.\varepsilon_r)^{1/2}}\ cm^{-1}.mol^{-1/2}.l^{1/2}.K^{1/2}. \qquad 4.6$$

ε_r is the dielectric constant of the reaction medium and a the ion size parameter. The ionic strength defined on the molar scale is given by:

$$I=\tfrac{1}{2}.\Sigma_i\ m_i z_i^2 \qquad 4.7$$

At constant ionic strength, it is usually assumed that γM^{n+} equals $\gamma M^{n+}L$, despite different ion size-parameters for the free ion and the complex. The determination of the stability constant enables the calculation of the free energy $\Delta_c G°$ for the studied process:

$$\Delta_c G° = -RT.\ln K_s \qquad 4.8$$

$$= -\ 2.303\ RT.\log K_s \qquad 4.9$$

This expression is made by the contribution of the enthalpy ($\Delta_c H°$) and the entropy ($\Delta_c S°$) of complexation:

$$\Delta_c G° = \Delta_c H° - T.\Delta_c S° \qquad 4.10$$

The thermodynamic parameters can be obtained by a variety of experimental methods. Commonly used techniques for the determination of the stability constant (log K_s) include electrochemistry (potentiometry, conductance, polarography, cyclic voltammetry) or spectroscopy (Nuclear Magnetic Resonance, Visible-Ultraviolet, Electron-Spin Resonance). Stability constants between 1 and 6 log units can also be derived from calorimetric measurements.

A commonly used method to obtain enthalpy data is to derive them from the variation of the stability constant with the temperature using the van't Hoff isochore (plot of log K_s vs 1/T). This can be expressed as:

$$d(\ln K_s)/dT = \Delta_c H°/RT^2 \qquad 4.11$$

However, the temperature dependence is weak in many cases. Therefore, this method is unreliable in many solvents, especially in highly volatile solvents which only allow a very narrow temperature range to work on. The calorimetric technique was chosen to determine the enthaply data reported in this thesis. This is by far the best method available to obtain these quantities. The theory of calorimetry and the experimental procedures were described in detail in section 3.5.

4.2 Thermodynamic Parameters for the Complexation of Lanthanide(III) cations in Acetonitrile and Propylene Carbonate at 298.15 K

4.2.1 Stability Constants of Lanthanide Cryptates in Acetonitrile and Propylene Carbonate at 298.15 K

The stability constants of lanthanide (La^{3+}, Pr^{3+}, Nd^{3+}) cations with Cryptand-222 and Cryptand-221 were determined in acetonitrile (AN) and propylene carbonate (PC), using a potentiometric method of competition with an auxiliary cation (K^+ or Ag^+). The stability constants of the auxiliary cation with the appropriate cryptand in the appropriate solvent are reported in Table 4.1. These data were used to calculate the stabilities of the lanthanide cryptates which are listed in Table 4.2. Only 1:1 lanthanide-cryptand complexes were formed as deduced from the Miniquad calculations.

The stability constants in acetonitrile are the first set of data to be reported for this kind of complexes in this solvent. In propylene carbonate, some values are already available in the literature. All the values reported here have been taken as an average of not less than two independent measurements.

For the lanthanide salts, the trifluoromethanesulphonic anion ($CF_3SO_3^-$) was chosen as the counter-anion. According to Seminara and Rizzarelli[101], $CF_3SO_3^-$ is a non-coordinating anion with the lanthanide complexes. These observations are based on Infra-Red, absorption and emission f-f spectra studies which showed that the sulphonate group of the anion is not bound to the lanthanide in complexes with 8-coordinating ligands.

The ionic strength was maintained constant during all the experiments at 0.1 $mol.dm^{-3}$ with tetraethylammonium perchlorate (Et_4NClO_4). From previous

studies, it seems that the effect of the supporting-electrolyte on the stability constants of the complexes is negligible.

Equilibrium was usually reached quickly; no particular kinetics were observed with Cryptand-221, though with Cryptand-222 several minutes were necessary to get a stable reading on the multimeter. It should be pointed out that the kinetics involved in the process refers to the competition reaction between the lanthanide and the auxiliary cation for the ligand and not to the proper complexation of the lanthanide cryptates.

Table 4.1 Stability constants (log K_s) of silver and potassium cryptates in acetonitrile and propylene carbonate at 298.15 K

Cryptate Complex	Acetonitrile	Propylene Carbonate
[Ag^+222]	8.9 [a]	16.30 [b]
[Ag^+221]	11.1 [a]	18.80 [c]
[K^+222]	11.4 [a]	

(a): ref. 143; (b): ref. 93; (c): ref. 92

Table 4.2 Stability constants (log K_s) of lanthanide cryptates in acetonitrile and propylene carbonate at 298.15 K

Cryptate	Acetonitrile	Propylene Carbonate
La^{3+}222	10.81 ± 0.01 [a]	16.1 ± 0.4 [c]
Pr^{3+}222	11.01 ± 0.01 [a]	15.90 [c]
Nd^{3+}222	11.06 ± 0.01 [a]	15.99 ± 0.01 [a]
La^{3+}222	11.39 ± 0.03 [a]	18.56 ± 0.02 [b]
Pr^{3+}222	11.52 ± 0.03 [a]	18.70 ± 0.06 [b]
Nd^{3+}222	11.65 ± 0.04 [a]	18.73 ± 0.01 [a]

(a): average values of at least two determinations; (b): ref. 92; (c): ref. 93

The lack of metal ion selectivity reported for the lanthanide cryptates in solvents such as water, N,N-Dimethylformamide, dimethylsulfoxide, methanol and propylene carbonate is also observed in acetonitrile. This confirms the unusual behaviour of these cations with these ligands, although the very close stability constants found for La^{3+}, Pr^{3+} and Nd^{3+} may certainly be attributed to the similarity of the ionic radii of these cations (La^{3+}: 1.06 Å, Pr^{3+}: 1.01 Å, Nd^{3+}: 0.99 Å)[132]. But the size factor is not the predominant parameter: Cryptand-221 (ionic radius: 1.1 Å) should be better adapted to the lanthanide cations than Cryptand-222 (ionic radius: 1.4 Å). In propylene carbonate, the 222 cryptates are effectively more stable for about 2.5 log units than the corresponding 221 cryptates, whereas in acetonitrile this difference is not appreciable. It can therefore be concluded that in acetonitrile the stability constants of the lanthanide cryptates are ligand independent.

The results also show that the stability constants in propylene carbonate are considerably higher than in acetonitrile. This was expected from the solvating properties of these two solvents. For the lanthanide cryptates, the solvent sequence is as follows:

$$PC >> AN > MeOH > H_2O > DMSO > DMF$$

4.2.2 Standard Enthalpies of Complexation of Lanthanide Cryptates in Acetonitrile and Propylene Carbonate at 298.15 K

The standard enthalpies of complexation ($\Delta_c H°$) of the lanthanide cryptates were obtained by calorimetric measurements carried out at different ratios of metal/ligand concentrations. The total heat observed (Q) was corrected by the heat due to the ampoule- breaking (0.1883 J in acetonitrile; -0.0607 J in propylene carbonate) and the heat of solution of the ligand in the appropriate solvent. The heats of solution of Cryptand-222 were taken from the literature[75] (34.47 $kJ.mol^{-1}$ in propylene carbonate; 32.93 $kJ.mol^{-1}$ in acetonitrile). For Cryptand-221, literature values were not available; therefore, the data reported in Table 4.3 and Table 4.4 for acetonitrile and propylene carbonate respectively are the result of this work. The enthalpies of reaction ($\Delta_r H$) which include the enthalpies of complexation of the lanthanide cryptates ($\Delta_c H$) and the enthalpies of solution of the cryptand ($\Delta_s H°$) are shown Tables 4.5-4.16. The enthalpies of complexation are summarized in Table 4.17.

No variation of $\Delta_c H°$ was noted with the change of concentrations of the electrolyte. Formations of ion-pairs was reduced to a minimum by using a non-coordinating anion ($CF_3SO_3^-$) and by working with very diluted solutions. Because of the high stability constants observed for the lanthanide cryptates in acetonitrile and propylene carbonate, the measured $\Delta_c H°$ always corresponded to 100% of ligand complexed when using a slight excess in the concentration of metal cation with respect to the ligand. In all cases, $\Delta_c H°$ was taken as the average of at least four determinations. For comparison, the $\Delta_c H°$ values obtained from the temperature dependence of the stability constant are included in Table 4.17.

Kinetics of complexation were mentioned by some authors, notably by Guillain et al.[87]. These authors noted that the complexation process of the lanthanide cryptates seems to be greatly hampered by the low formation

rate of these complexes, due to the slow removal of the solvation shell of the highly charged lanthanides. This effect was indeed observed in the present study for the smaller lanthanide cations such as the europium(III) cation. For this cation $\Delta_c H°$ could not be determined as the equipment used (macrocalorimeters) is designed for fast processes. An attempt to measure $\Delta_c H°$ in N,N-Dimethylformamide was also unfruitful. N,N-Dimethylformamide is known to be a very powerful solvating media and in this solvent the kinetics of complexation are even slower. Therefore, the enthalpy measurements were limited to the larger cations of the lanthanide series and to the less solvating solvents in the dipolar aprotic range (acetonitrile and propylene carbonate).

A general analysis of the enthalpies of complexation confirms the trend already observed by Guillain et al.[87] and Arnaud-Neu et al.[93], $\Delta_c H°$ becoming more negative (more favourable) along the lanthanide series. $\Delta_c H°$ measures the difference in strength between cation-ligand bonds and cation-solvent bonds, in other words $\Delta_c H°$ is a good indication of the affinity of the cation for the ligand in a particular reaction medium. The higher charge density of small cations enhances the electrostatic cation-ligand interactions and $\Delta_c H°$ becomes more favourable despite the poor fit between these cations and the cryptands.

The rather intriguing observation derived from these results is that:

$$\Delta_c H°(AN) \approx \Delta_c H°(PC) \qquad 4.13$$

This was observed with Cryptand-221 and Cryptand-222.

Table 4.3 Standard enthalpy of solution of Cryptand-221 in acetonitrile at 298.15 K

[221] /mol.dm^{-3}	Q /J	$\Delta_s H$ /kJ.mol^{-1}
1.07 10^{-3}	0.117	2.19
1.57 10^{-3}	0.176	2.24
1.09 10^{-3}	0.125	2.34

$\Delta_s H° = 2.26 \pm 0.08$ kJ.mol^{-1}

Table 4.4 Standard enthalpy of solution of Cryptand-221 in propylene carbonate at 298.15 K

[221] /mol.dm^{-3}	Q /J	$\Delta_s H$ /kJ.mol^{-1}
0.76 10^{-3}	0.050	1.36
1.42 10^{-3}	0.092	1.30
1.45 10^{-3}	0.100	1.37

$\Delta_s H° = 1.34 \pm 0.04$ kJ.mol^{-1}

Table 4.5 Standard enthalpy of complexation of La^{3+} with Cryptand-222 in acetonitrile at 298.15 K

$[La^{3+}]$ /mol.dm^{-3}	[222] /mol.dm^{-3}	Q /J	$\Delta_r H$ /kJ.mol^{-1}
$8.02\ 10^{-4}$	$4.94\ 10^{-4}$	-1.122	-45.42
$9.92\ 10^{-4}$	$5.37\ 10^{-4}$	-1.196	-44.52
$9.98\ 10^{-4}$	$6.24\ 10^{-4}$	-1.427	-45.78
$1.10\ 10^{-3}$	$7.39\ 10^{-4}$	-1.694	-45.80

$\Delta_r H° = -45.38 \pm 0.59$ kJ.mol^{-1}

$\Delta_c H° = -78.36 \pm 0.58$ kJ.mol^{-1}

Table 4.6 Standard enthalpy of complexation of La^{3+} with Cryptand-222 in propylene carbonate at 298.15 K

$[La^{3+}]$ /mol.dm^{-3}	[222] /mol.dm^{-3}	Q /J	$\Delta_r H$ /kJ.mol^{-1}
$1.77\ 10^{-3}$	$3.18\ 10^{-4}$	-0.687	-43.13
$2.11\ 10^{-3}$	$5.15\ 10^{-4}$	-1.104	-42.87
$2.85\ 10^{-3}$	$5.84\ 10^{-4}$	-1.261	-43.19

$\Delta_r H° = -43.06 \pm 0.16$ kJ.mol^{-1}

$\Delta_c H° = -77.53 \pm 0.16$ kJ.mol^{-1}

Table 4.7 Standard enthalpy of complexation of Pr^{3+} with Cryptand-222 in acetonitrile at 298.15 K

$[Pr^{3+}]$ /mol.dm^{-3}	[222] /mol.dm^{-3}	Q /J	$\Delta_r H$ /kJ.mol^{-1}
$7.60\ 10^{-4}$	$2.33\ 10^{-4}$	-1.393	-59.63
$1.07\ 10^{-3}$	$2.12\ 10^{-4}$	-1.277	-60.12
$1.99\ 10^{-3}$	$4.78\ 10^{-4}$	-2.883	-60.31
$2.07\ 10^{-3}$	$5.57\ 10^{-4}$	-3.291	-59.01

$\Delta_r H° = -59.77 \pm 0.57$ kJ.mol^{-1}

$\Delta_c H° = -92.72 \pm 0.58$ kJ.mol^{-1}

Table 4.8 Standard enthalpy of complexation of Pr^{3+} with Cryptand-222 in propylene carbonate at 298.15 K

$[Pr^{3+}]$ /mol.dm^{-3}	[222] /mol.dm^{-3}	Q /J	$\Delta_r H$ /kJ.mol^{-1}
$2.59\ 10^{-3}$	$5.44\ 10^{-4}$	-3.224	-59.26
$2.90\ 10^{-3}$	$8.07\ 10^{-4}$	-4.970	-61.59
$3.08\ 10^{-3}$	$9.30\ 10^{-5}$	-0.563	-60.51
$3.96\ 10^{-3}$	$5.12\ 10^{-4}$	-3.063	-59.76

$\Delta_r H° = -60.28 \pm 1.00$ kJ.mol^{-1}

$\Delta_c H° = -94.77 \pm 1.00$ kJ.mol^{-1}

Table 4.9 Standard enthalpy of complexation of Nd^{3+} with Cryptand-222 in acetonitrile at 298.15 K

$[Nd^{3+}]$ /mol.dm^{-3}	[222] /mol.dm^{-3}	Q /J	$\Delta_r H$ /kJ.mol^{-1}
$1.76\ 10^{-3}$	$3.08\ 10^{-4}$	-2.210	-71.74
$2.58\ 10^{-3}$	$3.24\ 10^{-4}$	-2.308	-71.09
$3.28\ 10^{-3}$	$4.94\ 10^{-4}$	-3.525	-71.32
$3.87\ 10^{-3}$	$3.18\ 10^{-4}$	-2.273	-71.42

$\Delta_r H° = -71.39 \pm 0.25$ kJ.mol^{-1}

$\Delta_c H° = -104.35 \pm 0.25$ kJ.mol^{-1}

Table 4.10 Standard enthalpy of complexation of Nd^{3+} with Cryptand-222 in propylene carbonate at 298.15 K

$[Nd^{3+}]$ /mol.dm^{-3}	[222] /mol.dm^{-3}	Q /J	$\Delta_r H$ /kJ.mol^{-1}
$6.80\ 10^{-4}$	$1.25\ 10^{-4}$	-0.886	-70.97
$1.57\ 10^{-3}$	$3.13\ 10^{-4}$	-2.202	-70.26
$1.81\ 10^{-3}$	$3.74\ 10^{-4}$	-2.604	-69.54
$2.06\ 10^{-3}$	$4.17\ 10^{-4}$	-2.963	-70.94

$\Delta_r H° = -70.43 \pm 0.67$ kJ.mol^{-1}

$\Delta_c H° = -104.89 \pm 0.67$ kJ.mol^{-1}

Table 4.11 Standard enthalpy of complexation of La^{3+} with Cryptand-221 in acetonitrile at 298.15 K

$[La^{3+}]$ /mol.dm^{-3}	[221] /mol.dm^{-3}	Q /J	$\Delta_r H$ /kJ.mol^{-1}
$1.75\ 10^{-3}$	$9.54\ 10^{-4}$	-3.581	-75.13
$1.80\ 10^{-3}$	$4.10\ 10^{-4}$	-1.560	-76.03
$2.05\ 10^{-3}$	$8.33\ 10^{-4}$	-3.150	-75.57
$2.40\ 10^{-3}$	$1.85\ 10^{-3}$	-7.033	-75.99
$2.50\ 10^{-3}$	$1.91\ 10^{-3}$	-7.205	-75.61

$\Delta_r H° = -75.67 \pm 0.37$ kJ.mol^{-1}

$\Delta_c H° = -77.90 \pm 0.46$ kJ.mol^{-1}

Table 4.12 Standard enthalpy of complexation of La^{3+} with Cryptand-221 in propylene carbonate at 298.15 K

$[La^{3+}]$ /mol.dm^{-3}	[221] /mol.dm^{-3}	Q /J	$\Delta_r H$ /kJ.mol^{-1}
$2.20\ 10^{-3}$	$6.30\ 10^{-4}$	-2.359	-74.99
$2.52\ 10^{-3}$	$1.19\ 10^{-3}$	-4.481	-75.20
$3.15\ 10^{-3}$	$1.65\ 10^{-3}$	-6.280	-76.03
$3.28\ 10^{-3}$	$1.46\ 10^{-3}$	-5.472	-75.36
$3.70\ 10^{-3}$	$1.28\ 10^{-3}$	-4.873	-75.72

$\Delta_r H° = -75.46 \pm 0.41$ kJ.mol^{-1}

$\Delta_c H° = -76.77 \pm 0.46$ kJ.mol^{-1}

Table 4.13 Standard enthalpy of complexation of Pr^{3+} with Cryptand-221 in acetonitrile at 298.15 K

$[Pr^{3+}]$ /mol.dm^{-3}	[221] /mol.dm^{-3}	Q /J	$\Delta_r H$ /kJ.mol^{-1}
$1.45\ 10^{-3}$	$5.41\ 10^{-4}$	-2.452	-90.60
$1.52\ 10^{-3}$	$5.41\ 10^{-4}$	-2.468	-91.22
$1.77\ 10^{-3}$	$1.05\ 10^{-3}$	-4.790	-91.21
$1.85\ 10^{-3}$	$5.41\ 10^{-4}$	-2.460	-90.91
$1.94\ 10^{-3}$	$8.75\ 10^{-4}$	-3.995	-91.31

$\Delta_r H° = -91.05 \pm 0.29$ kJ.mol^{-1}

$\Delta_c H° = -93.30 \pm 0.37$ kJ.mol^{-1}

Table 4.14 Standard enthalpy of complexation of Pr^{3+} with Cryptand-221 in propylene carbonate at 298.15 K

$[Pr^{3+}]$ /mol.dm^{-3}	[221] /mol.dm^{-3}	Q /J	$\Delta_r H$ /kJ.mol^{-1}
$2.28\ 10^{-3}$	$6.24\ 10^{-4}$	-2.803	-89.86
$2.47\ 10^{-3}$	$1.14\ 10^{-3}$	-5.159	-90.59
$2.48\ 10^{-3}$	$1.38\ 10^{-3}$	-6.242	-90.42
$3.10\ 10^{-3}$	$1.43\ 10^{-3}$	-6.334	-88.71
$3.16\ 10^{-3}$	$9.89\ 10^{-4}$	-4.456	-90.11

$\Delta_r H° = -89.94 \pm 0.74$ kJ.mol^{-1}

$\Delta_c H° = -91.25 \pm 0.75$ kJ.mol^{-1}

Table 4.15 Standard enthalpy of complexation of Nd^{3+} with Cryptand-221 in acetonitrile at 298.15 K

$[Nd^{3+}]$ /mol.dm^{-3}	[221] /mol.dm^{-3}	Q /J	$\Delta_r H$ /kJ.mol^{-1}
1.25 10^{-3}	9.20 10^{-4}	-4.828	-104.23
1.62 10^{-3}	1.28 10^{-3}	-6.744	-104.97
1.76 10^{-3}	1.01 10^{-3}	-5.305	-104.88
2.10 10^{-3}	1.95 10^{-3}	-10.192	-104.54
2.40 10^{-3}	2.01 10^{-3}	-10.539	-104.56

$\Delta_r H° = -104.63 \pm 0.30$ kJ.mol^{-1}

$\Delta_c H° = -106.90 \pm 0.37$ kJ.mol^{-1}

Table 4.16 Standard enthalpy of complexation of Nd^{3+} with Cryptand-221 in propylene carbonate at 298.15 K

$[Nd^{3+}]$ /mol.dm^{-3}	[221] /mol.dm^{-3}	Q /J	$\Delta_r H$ /kJ.mol^{-1}
1.69 10^{-3}	4.60 10^{-4}	-2.397	-103.58
2.67 10^{-3}	5.50 10^{-4}	-2.841	-102.99
2.77 10^{-3}	1.97 10^{-3}	-10.225	-103.56
3.22 10^{-3}	2.08 10^{-3}	-10.677	-102.28
3.68 10^{-3}	7.60 10^{-4}	-3.933	-103.70

$\Delta_r H° = -103.22 \pm 0.58$ kJ.mol^{-1}

$\Delta_c H° = -104.56 \pm 0.62$ kJ.mol^{-1}

Table 4.17 Standard enthalpy of complexation of lanthanide(III) cations with cryptands in acetonitrile and propylene carbonate at 298.15 K

Cation	Ligand	Solvent	$\Delta_c H°$/ kJ.mol^{-1}
La^{3+}	221	AN	-77.90 ± 0.46
La^{3+}	222	AN	-77.36 ± 0.58
La^{3+}	221	PC	-76.77 ± 0.46
La^{3+}	222	PC	-77.53 ± 0.16
			(-54.39)[a]
Pr^{3+}	221	AN	-93.30 ± 0.37
Pr^{3+}	222	AN	-92.76 ± 0.58
Pr^{3+}	221	PC	-91.25 ± 0.91
Pr^{3+}	222	PC	-94.77 ± 1.00
			(-104.6)[b],(-94.14)[a]
Nd^{3+}	221	AN	-106.90 ± 0.37
Nd^{3+}	222	AN	-104.35 ± 0.25
Nd^{3+}	221	PC	-104.56 ± 0.63
Nd^{3+}	222	PC	-104.89 ± 0.67

(a): ref.87; (b): ref. 93

4.2.3 Standard Entropies of Complexation of Lanthanide(III) Cations and Cryptands in Acetonitrile and Propylene Carbonate at 298.15 K

Combination of the stability constants (hence the free energy of complexation, $\Delta_c G°$) and the standard enthalpies of complexation ($\Delta_c H°$) enables the calculation of the entropies of complexation $\Delta_c S°$ for the lanthanide cryptates. All these thermodynamic parameters are listed in Table 4.18 and represented in form of graphics in Fig. 4.1 and Fig. 4.2.

The general trend is a decrease (more defavourable) of the entropy of complexation from La^{3+} to Nd^{3+}. The entropy term in a macrocyclic complexation process is mainly originated by two different effects:

i) The change of the state of solvation of the free cation, due to the release of coordinated solvent molecules when entering the ligand cavity. This effect is favourable and is expressed as a positive $\Delta_c S°$.

ii) The change in internal entropy of the ligand, due to reorientation, rigidification and conformational changes. This factor is defavourable and is expressed as a negative $\Delta_c S°$.

In the complexation process between the alkali metal cations and Cryptand-222 in dipolar aprotic media[74-77], it was shown from a linear correlation between the entropies of complexation and the entropies of solvation that the alkali metal ions loose their solvation shells completly when entering the cavity of the cryptand (Chapter 2, Eqn. 2.11). Therefore, the entropies of complexation ($\Delta_c S°$) become regularly less positive or more negative as the cation becomes larger. This is due to the larger entropic gain for the complexation of small cations which display large entropies of solvation.

Along the lanthanide series, the cations become smaller as a result of the lanthanide contraction. Small cations have very high charge densities and are therefore more solvated than larger ones. If the lanthanide cations are

fully desolvated in the complexation process with cryptands in acetonitrile and propylene carbonate, an increase in $\Delta_c S°$ is expected from La^{3+} to Nd^{3+}. The opposite trend observed (Table 4.18) leads to the suggestion that the lanthanide cations retain a part of their solvation shell when complexed by the cryptands.

$\Delta_c S°$ being mainly negative indicates also that structural modifications of the ligand occur, these are more pronounced for the smaller lanthanides.

Table 4.18 Thermodymnamic parameters for the complexation of lanthanide(III) cryptates in acetonitrile and propylene carbonate at 298.15 K

Cryptate Complex	**$\Delta_c G°$/kJ.mol^{-1}**	**$\Delta_c H°$/kJ.mol^{-1}**	**$\Delta_c S°$/J.K^{-1}.mol^{-1}**
	ACETONITRILE		
La^{3+}222	-61.71	-78.36	-55.6
Pr^{3+}222	-62.84	-92.76	-100.4
Nd^{3+}222	-63.14	-104.35	-138.5
La^{3+}221	-65.02	-77.91	-43.1
Pr^{3+}221	-65.77	-93.30	-92.5
Nd^{3+}221	-66.48	-106.90	-135.5
	PROPYLENE CARBONATE		
La^{3+}222	-91.92	-77.53	+48.1
Pr^{3+}222	-90.75	-94.77	-13.4
Nd^{3+}222	-91.29	-104.89	-45.2
La^{3+}221	-105.94	-76.77	+97.9
Pr^{3+}221	-106.73	-91.25	+51.9
Nd^{3+}221	-106.90	-104.56	+7.9

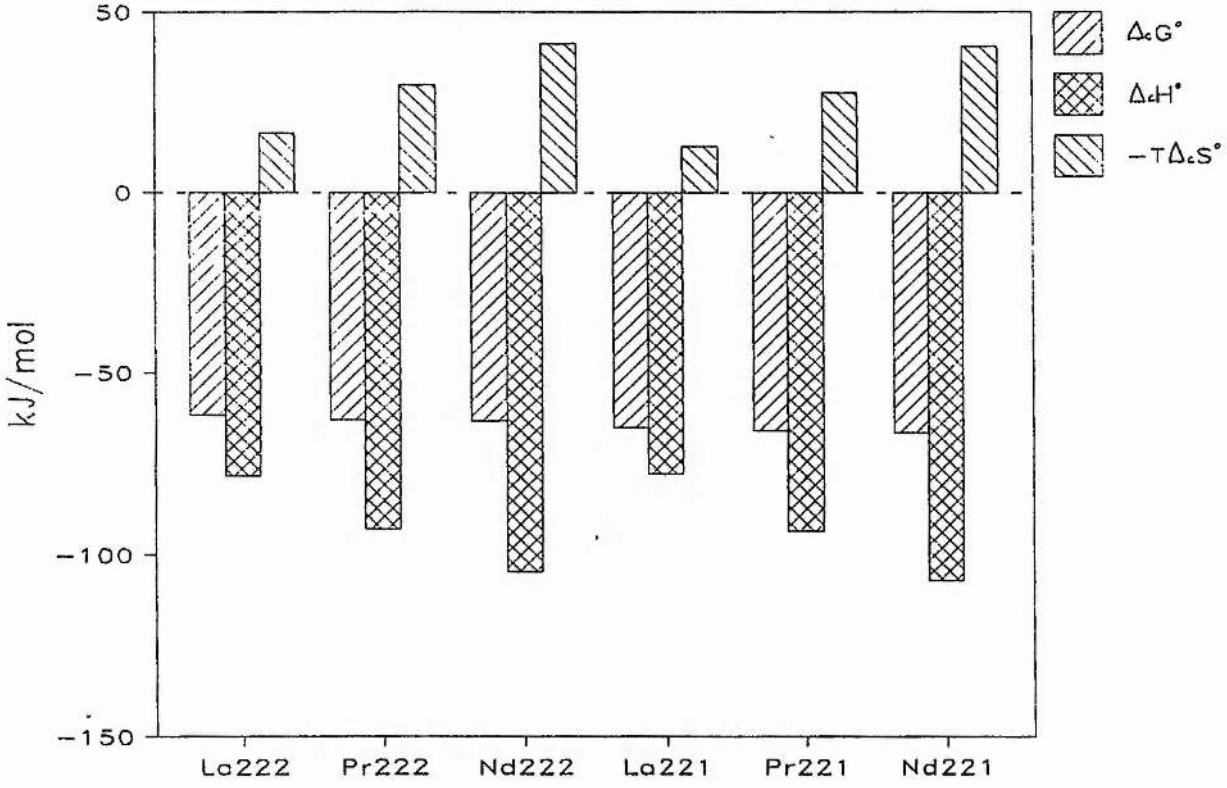

Figure 4.1 Thermodynamic parameters for the complexation of lanthanide(III) cations with cryptands in acetonitrile at 298.15 K

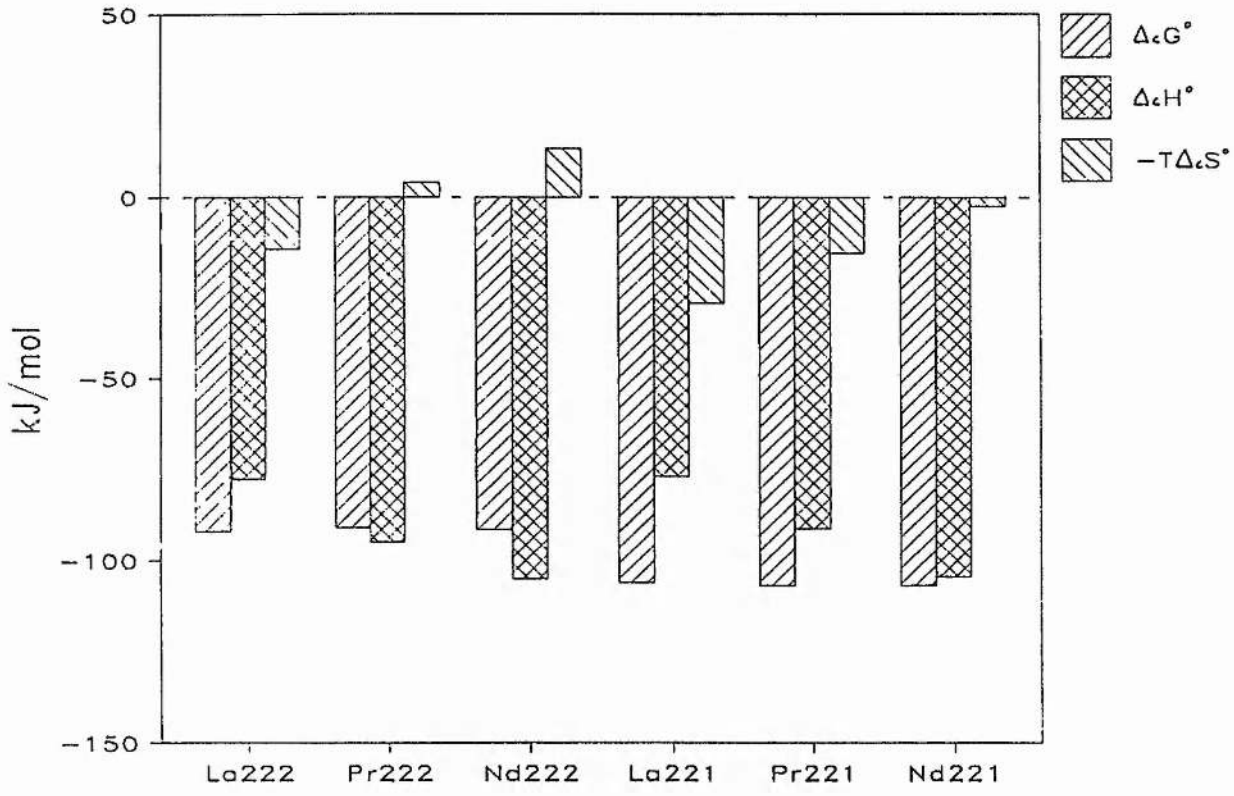

Figure 4.2 Thermodynamic parameters for the complexation of lanthanide(III) cations with cryptands in propylene carbonate at 298.15 K

The general analysis of the parameters in Table 4.18 results in two combinations of $\Delta_c H°$ and $\Delta_c S°$:

i) In acetonitrile, a favourable process in terms of enthalpy ($\Delta_c H° < 0$) and unfavourable in terms of entropy ($\Delta_c S° < 0$) is observed.

ii) In propylene carbonate, the process is favoured in terms of enthalpy ($\Delta_c H° < 0$) and in terms of entropy ($\Delta_c S° > 0$) for the complexes with Cryptand-221 and for La^{3+}222 but enthalpy controlled, whereas the Pr^{3+}222 and the Nd^{3+}222 cryptates are only enthalpy stabilized.

Macrocyclic complexation in non-aqueous media is usually enthalpy stabilized ($\Delta_c H°< 0$) and entropy destabilized ($\Delta_c S°< 0$)[61,74-76]. Entropy stabilization is sometimes found for complexes of small cations such as for the Li^{+}222 cryptate in propylene carbonate and acetonitrile[75], or in heavily solvating media such as for the Eu^{3+}222 cryptate in water[91]. In these cases, the entropic gain can be mostly attributed to the desolvation of the complexed cation. Stabilities originated exclusively from a positive entropic term can also be observed when the cation-ligand binding is weak ($\Delta_c H°$ small or even positive) [33]. In this case, the favourable entropy of complexation is not only due to the desolvation of the cation but also to the greater degree of freedom of the complex formed.

For the lanthanide cryptates, positive $\Delta_c S°$ are observed in propylene carbonate for La^{3+}222, La^{3+}221 and Pr^{3+}221; negative $\Delta_c S°$ are observed for the other complexes in acetonitrile and propylene carbonate. The difference in $\Delta_c S°$ observed between acetonitrile and propylene carbonate may be associated to the state of solvation of the lanthanide cations. The results seems to indicate that the lanthanide cations are more heavily solvated in propylene carbonate than in acetonitrile. The more positive $\Delta_c S°$ in propylene carbonate corresponds to a greater release of solvents molecules which seem to be responsible for the greater stabilization of the lanthanide cryptates in this solvent with respect to acetonitrile. A steric factor may also be of a

significant importance. Propylene carbonate molecules are relatively larger than acetonitrile molecules, therefore the metal cation must loose more solvent molecules when entering the ligand cavity in propylene carbonate. The more favourable $\Delta_t S°$ observed for Cryptand-221 can be explained by the need of a greater desolvation of the lanthanide cations when entering this ligand cavity.

The results suggest that the lanthanide cations retain a part of their solvation shell when complexed by the cryptands. This observation supposes the existence of interactions between the complexed lanthanide and the reaction medium. Single-ion transfer parameters for the free and the complexed lanthanide would be extremely useful to understand these interactions.

4.3 Standard Enthalpies of Transfer for the Lanthanide(III) Cations from Propylene Carbonate to Acetonitrile at 298.15 K

4.3.1 Theoretical Considerations

4.3.1.1 Standard Enthalpy of Solution and Single-Ion Transfer Enthalpy

Thermodynamic transfer parameters ($\Delta_t G°$, $\Delta_t H°$ and $\Delta_t S°$) are extremely useful to correlate properties between solvents and to investigate the theoretical aspects of solution such as ion-ion or ion-solvent interactions. The thermodynamic cycle previously used for the calculation of single-ion values[68] for monovalent cations among dipolar aprotic solvents is now extended to tervalent cations. The thermodynamic cycle is considered here from propylene carbonate (PC) to acetonitrile (AN).

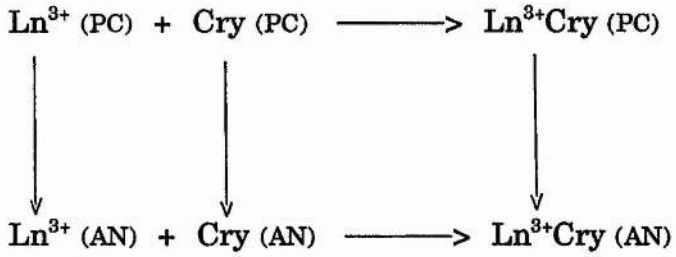

4.13

The standard enthalpy of transfer ($\Delta_t H°$) for an electrolyte, from propylene carbonate to acetonitrile, is given by:

$$\Delta_t H° \text{ (PC->AN)} = \Delta_s H° \text{ (AN)} - \Delta_s H° \text{ (PC)} \qquad 4.14$$

where $\Delta_s H°$ are the standard enthalpies of solution of the electrolyte in the appropriate solvent. $\Delta_s H°$ are obtained, using the Debye-Hückel theory, by extrapolating to infinite dilution the enthalpies of solution $\Delta_s H$ measured at different electrolyte concentrations or strictly speaking the ionic strength.

$$\Delta_s H = \Delta_s H° - \Delta_D H \qquad 4.15$$

Expression 4.15 is derived from the Debye-Hückel limiting law, valid at low concentrations only[133]. $\Delta_D H$ is the enthalpy of dilution of the compound and is directly proportional to the square root of the ionic strength ($\sqrt{I}$). The plot of $\Delta_s H$ against $\sqrt{I}$ follows a straight line and its extrapolation to zero gives the standard enthalpy of solution of the electrolyte ($\Delta_s H°$).

For the interpretation of the solvation phenomena or the other interactions taking place in solution, it is more useful to consider the enthalpy of transfer

for the single-ions rather than for the electrolytes. The standard enthalpy of transfer ($\Delta_t H°$) for single-ions can not be measured, nor can their standard enthalpy of solution ($\Delta_s H°$). Therefore, extrathermodynamic assumptions have been introduced to split the medium effect for an electrolyte into values for the individual ions.

4.2.1.2 Extrathermodynamic Assumptions

Extrathermodynamic assumptions were first proposed for the estimation of the transfer free energies and the transfer activity coefficients of single-ions. They have than been extended to the enthalpies and entropies of transfer[134]. Most of these assumptions are based on the equal sharing of the enthalpy of transfer between two ions or an ion-molecule pair. These ions or molecules are usually very large, of a low surface-charge density; they have their active atoms enclosed in the same inert, organic group in order to minimize specific interactions between then and the solvent.

The most popular extrathermodynamic assumption is the reference electrolyte assumption[135]. This assumption states that for a 1:1 electrolyte, the standard enthalpy of transfer of the anion equals that of the cation. The tetraphenylarsomium-tetraphenylborate (Ph_4As^+/Ph_4B^-) assumption [$\Delta_t H°(Ph_4As^+) = \Delta_t H°(Ph_4B^-)$] has been widely used and most of the data reported in aqueous as well as in non-aqueous solvents have been derived from it. Another variant is the tetraphenylphosphonium-tetraphenylborate assumption [$\Delta_t H°(Ph_4P^+) = \Delta_t H°(Ph_4B^-)$] which gives similar results[136].

The anion-molecule assumptions, as for example the tetraphenylmethane-tetraphenylborate (Ph_4B^-/Ph_4C) assumption and the cation-molecule assumptions, as for example the tetraphenylarsonium-tetraphenylmethane (Ph_4As^+/Ph_4C) assumption are limited to solvents with comparable dielectric constants[137]. The electrostatic interactions of the ion with the solvent have

to remain unchanged during the transfer as it is for the neutral species. This problem is not encountered with the reference electrolyte assumption for which the electrostatic contribution can be omitted as one is dealing with two ions. The ion-molecule assumptions are therefore less reliable. For instance, the Strehlow assumption[138] which considers the ferrocene-ferricinium couple $[Fe(C_5H_5)_2/Fe(C_5H_5)^{2+}]$ as a solvent independent reference electrode, gives slightly different results than the Ph_4As^+/Ph_4B^- assumption[139].
The assumption of the negligible liquid junction potential between Ag^+/Ag electrodes in two non-aqueous solvents connected with a salt bridge of 0.1 $mol.dm^{-3}$ of tetraethylammonium picrate gives similar results to those obtained with the Ph_4As^+/Ph_4B^- assumption[140].

These extrathermodynamic assumptions, as well as some other methods of calculating single-ion transfer values such as the linear correspondence method, the extrapolation method and the reference ion method have been reviewed and discussed by Marcus[141]. This author recommended the tetraphenylarsonium-tetraphenylborate assumption. This assumption was also recommended by Cox et al.[134]. Therefore, the data in this work will be based on this assumption.

4.3.2 Single-Ion $\Delta_f H°$ Values for the Tervalent Lanthanide Cations as Obtained via the Thermodynamic Cycle

The synthesis and isolation of the solid lanthanide cryptates (section 3.2.2) allowed the measurement of their enthalpies of solution in acetonitrile and propylene carbonate by calorimetry at 298.15 K (Tables 4.21-4.32). The enthalpies of solution ($\Delta_s H$) were determined at different electrolyte concentrations. By plotting the $\Delta_s H$ against the square root of the ionic strength, straight lines were obtained. An example is shown in Fig. 4.3.

Extrapolation of this lines to zero concentration (infinite dilution) gave the standard enthalpies of solution ($\Delta_s H°$). These data are reported in Table 4.33, assorted with their standard deviations calculated via: $\sigma\Delta_s H° = \sigma\Delta_s H.\sqrt{(1-r^2)}$.

The standard enthalpies of solution obtained for the lanthanide cryptates in acetonitrile and propylene carbonate are all positive. The interpretation of the enthalpies of solution are often difficult as they are a combination of two opposing processes:

i) An unfavourable process of separating the ions from the lattice into a non-coordinating state (lattice effect)

ii) A favourable process of solvating the separate ions (solvation effect)

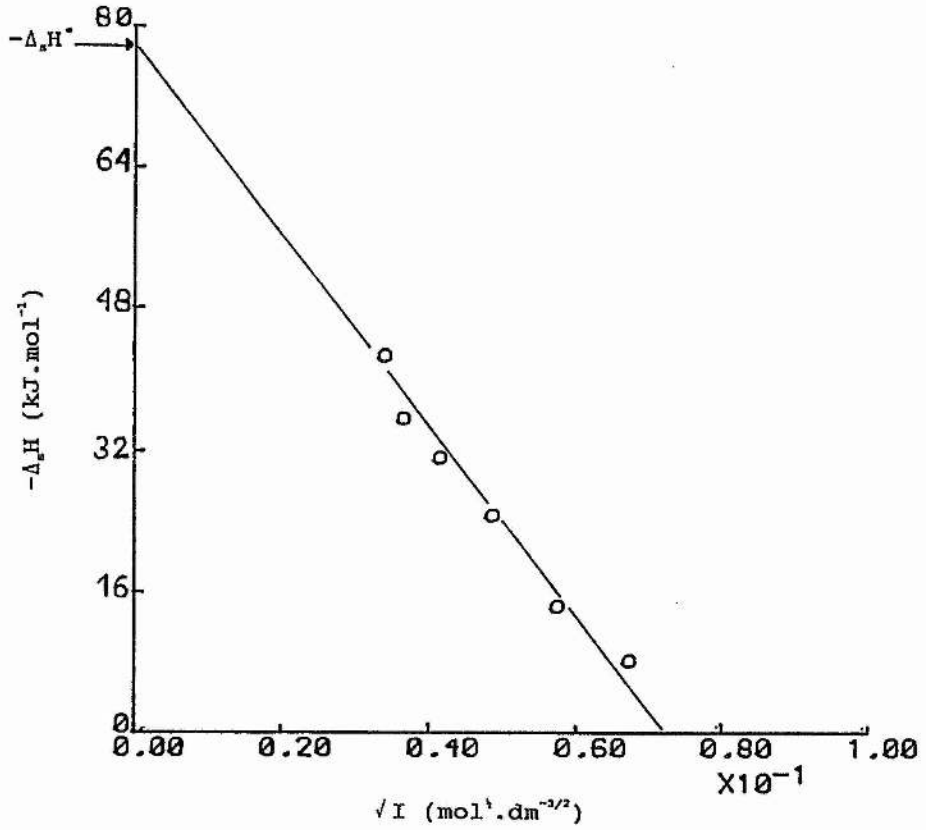

Figure 4.3 Plot of $\Delta_s H$ versus $\sqrt{I}$ for Nd221$(CF_3SO_3)_3$ in propylene carbonate

To split $\Delta_t H°$ into their ionic contributions, $\Delta_t H°$ for the trifluoromethanesulphonic anion was determined. This value was obtained after measuring the $\Delta_s H°$ values for sodium trifluoromethanesulphonate ($NaCF_3SO_3$) in acetonitrile and propylene carbonate (Tables 4.19 and 4.20) and combination of these values with the $\Delta_t H°$ value, based on the Ph_4As^+/Ph_4B^- assumption for the sodium cation (Na^+) from propylene carbonate to acetonitrile[75]:

$$\Delta_t H°[Na^+]\ (PC->AN) = -3.43\ kJ.mol^{-1} \qquad 4.16$$

It was found that:

$$\Delta_t H°[CF_3SO_3^-]\ (PC->AN) = \Delta_s H°[NaCF_3SO_3]\ (AN) - \Delta_s H°[NaCF_3SO_3]\ (PC) - \Delta_t H°[Na^+]\ (PC->AN) \qquad 4.17$$

$$= -1.71\ kJ.mol^{-1}$$

This small contribution for $CF_3SO_3^-$ was expected as bulky ions are not very affected by solvent changes. It has been subtracted from the overall $\Delta_t H°$ values for the lanthanide cryptates in order to obtain the $\Delta_t H°$ values for the complexes lanthanide cations. These data are included in Table 4.33.

The transfer data for the uncomplexed lanthanide cations were calculated by a rearrangement of the thermodynamic cycle (see Eq. 2.5 in Chapter 2).

$$\Delta_t H°[Ln^{3+}]\ (PC->AN) = -\Delta_c H°(AN) + \Delta_c H°(PC) + \Delta_t H°[Ln^{3+}Cry]\ (PC->AN) - \Delta_t H°[Cry]\ (PC->AN) \qquad 4.18$$

where Cry stands for Cryptand-221 and Cryptand-222 and the $\Delta_c H°$ values correspond to the enthalpies of complexation reported in Tables 4.4-4.16. The $\Delta_t H°$ for the lanthanide cations are listed in Table 4.34.

Two sets of data were obtained for the transfer values of the lanthanide(III) cations, using the thermodynamic cycle involving Cryptand-221 and Cryptand-222. The values obtained should be the same regardless the ligand. These are indeed in excellent agreement (Table 4.34). The interpretation of these results can be directly related to ion solvation phenomena, including effects that may have the cation on the solvent surrounding it (solvent structure, dielectric saturation...) and cation-solvent interactions. The $\Delta_t H°$ values for the free lanthanide cations are all positive in the transfer process from propylene carbonate to acetonitrile. This is an indication that in enthalpy terms, propylene carbonate is the solvent preferred energetically for the lanthanides. The enthalpy of solvation involves breaking of solvent-solvent bonds (endothermic effect) and ion-solvent interactions (exothermic effect), therefore the results reported here suggests that the solute-solvent interactions (solvation of the ions) are more emphasized in propylene carbonate than in acetonitrile. This suggestion agrees with the donor number of the two solvents[67] (acetonitrile: 14.1; propylene carbonate: 15.1) and with the structural characteristics of these solvents.

Table 4.19 Standard enthalpy of solution of $NaCF_3SO_3$ in acetonitrile at 298.15 K

$[NaCF_3SO_3]$ mol.dm^{-3}	$\sqrt{I}$ mol$^{1/2}$.dm$^{-3/2}$	Q J	$\Delta_s H$ kJ.mol^{-1}
2.64 10^{-3}	0.051	0.240	0.91
2.77 10^{-3}	0.052	0.239	0.86
3.19 10^{-3}	0.056	0.299	0.94
6.07 10^{-3}	0.077	0.545	0.94
6.68 10^{-3}	0.081	0.589	0.88

$\Delta_s H° = 0.92 \pm 0.04$ kJ.mol^{-1}

Table 4.20 Standard enthalpy of solution of $NaCF_3SO_3$ in propylene carbonate at 298.15 K

$[NaCF_3SO_3]$ mol.dm^{-3}	$\sqrt{I}$ mol$^{1/2}$.dm$^{-3/2}$	Q J	$\Delta_s H$ kJ.mol^{-1}
1.23 10^{-3}	0.035	0.912	7.44
2.67 10^{-3}	0.047	1.024	4.51
2.35 10^{-3}	0.048	1.002	4.27
2.74 10^{-3}	0.052	1.539	5.61
7.15 10^{-3}	0.084	3.865	5.40
7.30 10^{-3}	0.085	4.085	5.59

$\Delta_s H° = 6.06 \pm 1.09$ kJ.mol^{-1}

Table 4.21 Standard enthalpy of solution of [La222(CF_3SO_3)$_3$] in acetonitrile at 298.15 K

[La222(CF_3SO_3)$_3$] mol.dm^{-3}	√I mol$^{1/2}$.dm$^{-3/2}$	Q J	$\Delta_s H$ kJ.mol^{-1}
3.82 10^{-4}	0.048	0.619	32.37
5.01 10^{-4}	0.055	0.812	32.46
6.21 10^{-4}	0.061	1.042	33.62
9.97 10^{-4}	0.077	1.862	37.36

$\Delta_s H° = 23.18 \pm 0.58$ kJ.mol^{-1}

Table 4.22 Standard enthalpy of solution of [La222(CF_3SO_3)$_3$] in propylene carbonate at 298.15 K

[La222(CF_3SO_3)$_3$] mol.dm^{-3}	√I mol$^{1/2}$.dm$^{-3/2}$	Q J	$\Delta_s H$ kJ.mol^{-1}
2.88 10^{-4}	0.041	0.213	14.82
3.43 10^{-4}	0.045	0.297	17.39
5.40 10^{-4}	0.057	0.519	19.19
1.13 10^{-3}	0.082	1.326	23.47
1.73 10^{-3}	0.102	2.456	28.32

$\Delta_s H° = -7.24 \pm 0.72$ kJ.mol^{-1}

Table 4.23 Standard enthalpy of solution of [Pr222(CF_3SO_3)$_3$] in acetonitrile at 298.15 K

[Pr222(CF_3SO_3)$_3$]	√I	Q	$\Delta_s H$
mol.dm^{-3}	mol$^{1/2}$.dm$^{-3/2}$	J	kJ.mol^{-1}
4.12 10^{-4}	0.016	0.046	21.66
5.16 10^{-4}	0.017	0.050	20.79
8.48 10^{-4}	0.023	0.084	20.14
1.23 10^{-3}	0.027	0.129	20.79

$\Delta_s H° = 21.92 \pm 0.63$ kJ.mol^{-1}

Table 4.24 Standard enthalpy of solution of [Pr222(CF_3SO_3)$_3$] in propylene carbonate at 298.15 K

[Pr222(CF_3SO_3)$_3$]	√I	Q	$\Delta_s H$
mol.dm^{-3}	mol$^{1/2}$.dm$^{-3/2}$	J	kJ.mol^{-1}
1.09 10^{-4}	0.026	0.234	-43.02
1.73 10^{-4}	0.032	0.439	-43.83
1.85 10^{-4}	0.033	0.385	-41.55
1.98 10^{-4}	0.035	0.510	-45.53
6.52 10^{-4}	0.063	0.171	-52.52
9.95 10^{-4}	0.077	0.222	-44.86

$\Delta_s H° = -44.43 \pm 1.55$ kJ.mol^{-1}

Table 4.25 Standard enthalpy of solution of [Nd222(CF_3SO_3)$_3$] in acetonitrile at 298.15 K

[Nd222(CF_3SO_3)$_3$]	√I	Q	$\Delta_s H$
mol.dm^{-3}	mol$^{1/2}$.dm$^{-3/2}$	J	kJ.mol^{-1}
2.07 10^{-4}	0.035	0.029	1.50
3.54 10^{-4}	0.046	0.065	1.85
4.18 10^{-4}	0.050	0.046	1.11
6.61 10^{-4}	0.063	0.008	0.12

$\Delta_s H° = 3.81 \pm 0.41$ kJ.mol^{-1}

Table 4.26 Standard enthalpy of solution of [Nd222(CF_3SO_3)$_3$] in propylene carbonate at 298.15 K

[Nd222(CF_3SO_3)$_3$]	√I	Q	$\Delta_s H$
mol.dm^{-3}	mol$^{1/2}$.dm$^{-3/2}$	J	kJ.mol^{-1}
2.47 10^{-4}	0.038	1.418	-34.50
4.12 10^{-4}	0.050	1.142	-46.22
6.00 10^{-4}	0.060	1.464	-24.40
8.78 10^{-4}	0.073	0.322	-3.70

$\Delta_s H° = -95.18 \pm 2.26$ kJ.mol^{-1}

Table 4.27 Standard enthalpy of solution of [La221(CF_3SO_3)$_3$] in acetonitrile at 298.15 K

[La221(CF_3SO_3)$_3$]	$\sqrt{I}$	Q	$\Delta_s H$
mol.dm^{-3}	mol$^{1/2}$.dm$^{-3/2}$	J	kJ.mol^{-1}
2.43 10^{-4}	0.038	2.334	19.21
3.06 10^{-4}	0.043	2.468	16.10
3.46 10^{-4}	0.046	2.761	15.96
4.41 10^{-4}	0.051	3.405	15.45
5.52 10^{-4}	0.057	3.845	13.94
5.85 10^{-4}	0.059	3.707	12.67

$\Delta_s H° = 27.61 \pm 0.71$ kJ.mol^{-1}

Table 4.28 Standard enthalpy of solution of [La221(CF_3SO_3)$_3$] in propylene carbonate at 298.15 K

[La221(CF_3SO_3)$_3$]	$\sqrt{I}$	Q	$\Delta_s H$
mol.dm^{-3}	mol$^{1/2}$.dm$^{-3/2}$	J	kJ.mol^{-1}
2.28 10^{-4}	0.037	-0.029	-2.78
4.12 10^{-4}	0.050	-0.062	-2.98
5.06 10^{-4}	0.055	-0.079	-3.18
7.39 10^{-4}	0.067	-0.121	-3.37
9.98 10^{-4}	0.077	-0.192	-3.88

$\Delta_s H° = -1.71 \pm 0.08$ kJ.mol^{-1}

Table 4.29 Standard enthalpy of solution of [Pr221(CF_3SO_3)$_3$] in acetonitrile at 298.15 K

[Pr221(CF_3SO_3)$_3$] mol.dm^{-3}	√I mol$^{1/2}$.dm$^{-3/2}$	Q J	Δ_sH kJ.mol^{-1}
8.40 10^{-5}	0.022	0.092	22.20
1.12 10^{-4}	0.026	0.117	20.99
1.60 10^{-4}	0.031	0.155	19.66
2.45 10^{-4}	0.038	0.293	24.04

$\Delta_s H° = 18.20 \pm 1.63$ kJ.mol^{-1}

Table 4.30 Standard enthalpy of solution of [Pr221(CF_3SO_3)$_3$] in propylene carbonate at 298.15 K

[Pr221(CF_3SO_3)$_3$] mol.dm^{-3}	√I mol$^{1/2}$.dm$^{-3/2}$	Q J	Δ_sH kJ.mol^{-1}
1.30 10^{-5}	0.009	-0.234	-35.89
1.66 10^{-5}	0.010	-0.305	-36.66
6.17 10^{-5}	0.019	-0.117	-38.19
7.17 10^{-5}	0.021	-0.144	-40.26
8.50 10^{-5}	0.022	-0.165	-39.02

$\Delta_s H° = -44.31 \pm 1.08$ kJ.mol^{-1}

Table 4.31 Standard enthalpy of solution of [Nd221(CF_3SO_3)$_3$] in acetonitrile at 298.15 K

[Nd221(CF_3SO_3)$_3$] mol.dm^{-3}	√I mol$^{1/2}$.dm$^{-3/2}$	Q J	Δ_sH kJ.mol^{-1}
1.01 10^{-4}	0.024	0.079	16.33
1.64 10^{-4}	0.031	0.121	14.83
2.55 10^{-4}	0.039	0.171	13.56
3.33 10^{-4}	0.045	0.205	12.29
4.06 10^{-4}	0.049	0.205	10.28
7.13 10^{-4}	0.065	0.301	8.49

$\Delta_s H° = 21.04 \pm 0.50$ kJ.mol^{-1}

Table 4.32 Standard enthalpy of solution of [Nd221(CF_3SO_3)$_3$] in propylene carbonate at 298.15 K

[Nd221(CF_3SO_3)$_3$] mol.dm^{-3}	√I mol$^{1/2}$.dm$^{-3/2}$	Q J	Δ_sH kJ.mol^{-1}
1.93 10^{-4}	0.034	-4.301	-44.58
2.25 10^{-4}	0.037	-4.201	-37.34
2.89 10^{-4}	0.042	-4.728	-32.73
3.96 10^{-4}	0.049	-5.108	-25.80
5.52 10^{-4}	0.057	-0.219	-15.04
7.56 10^{-4}	0.067	-3.255	-8.62

$\Delta_s H° = -77.36 \pm 1.96$ kJ.mol^{-1}

Table 4.33 Standard enthalpies of solution of lanthanide cryptates and cryptands in acetonitrile (AN) and propylene carbonate (PC) at 298.15 K. Derived standard enthalpies of transfer from propylene carbonate to acetonitrile

Cryptate	$\Delta_s H°$ /kJ.mol^{-1}		$\Delta_t H°$ /kJ.mol^{-1}
	AN	PC	
La222$(CF_3SO_3)_3$	23.18 ± 0.58	-7.24 ± 0.71	30.42
Pr222$(CF_3SO_3)_3$	21.92 ± 0.62	-44.43 ± 1.55	66.36
Nd222$(CF_3SO_3)_3$	3.81 ± 0.41	-95.18 ± 2.25	98.99
La221$(CF_3SO_3)_3$	27.86 ± 0.75	-1.71 ± 0.08	29.58
Pr221$(CF_3SO_3)_3$	18.28 ± 1.67	-44.31 ± 1.13	62.59
Nd221$(CF_3SO_3)_3$	21.04 ± 0.50	-77.36 ± 2.00	98.41
Cryptand 222	32.93[a]	34.47[a]	-1.55
Cryptand 221	2.26 ± 0.08	1.34 ± 0.04	0.92

Table 4.34 Calculated enthalpies of transfer of lanthanide(III) cations from propylene carbonate to acetonitrile at 298.15 K

Cation	via cycle 222	via cycle 221
La^{3+}	37.11	34.98
Pr^{3+}	71.04	68.91
Nd^{3+}	105.18	105.02

4.3.3 Single-Ion Values Obtained dy Direct Measurements

The enthalpies for the transfer of lanthanide(III) cations from propylene carbonate to acetonitrile have also been determined by direct measurements of the enthalpies of solution of lanthanide trifluoromethanesulphonate salts in these two solvents (Tables 4.35-4.40). Large variations of $\Delta_s H$ were observed with the change of electrolyte concentration, due to the large dilution effect of the tervalent cations. Therefore the standard enthalpies of solution ($\Delta_s H°$) extrapolated from the least square plot of $\Delta_s H$ versus $\sqrt{I}$ are within a relatively great uncertainty. These data are listed in Table 4.41. The contribution of the counter-anion ($CF_3SO_3^-$) has been subtracted using the data based on the Ph_4As^+/Ph_4B^- convention (section 4.2.2), the standard enthalpies of transfer of the cations are included in Table 4.41.

Comparison of these data and the data obtained via the thermodynamic cycle (section 4.2.2) show that the calculation of the single-ion values via the thermodynamic cycle can be applied to the tervalent cations. An average of the three independent sets of data was taken (Table 4.42). The comparison of these data with the $\Delta_t H°$ values for the complexed lanthanide cations indicate that for the transfer between propylene carbonate and acetonitrile:

$$\Delta_t H°[Ln^{3+}Cry]\ (PC\text{->}AN) \approx \Delta_t H°[Ln^{3+}]\ (PC\text{->}AN) \qquad 4.19$$

The validity of identity 4.19 suggests that propylene carbonate and acetonitrile are able to selectively recognise the presence of the tervalent lanthanide cations.

It was already assumed from the complexation data that the lanthanide cations may still be able to interact with the surrounding reaction media when they are complexed by the cryptands. This suggestion is confirmed by

the transfer data reported here. Exclusive complexes have also been considered from the fact that no macrobicyclic effect was observed with the tervalent lanthanide cations and Cryptand-222 [93]. But this interpretation does not hold as in the case of Cryptand-221, similar single-ion values for the transfer of the lanthanides have been found than with Cryptand-222, despite the existence of a macrobicyclic effect for this cryptand. Therefore, it was suggested on the basis of the results reported in this thesis that the lanthanide cryptates form inclusive complexes with only partial removal of the cation solvation shell.

The entropies of cryptate formation for the lanthanide cryptates in acetonitrile and propylene carbonate were not calculated due to the unavailability of the entropies of solvation of the lanthanide cations in these solvents.

Considering that,

$$\Delta_t H°[\text{Cryp}]_{(PC->AN)} \approx 0 \qquad 4.20$$

and identity 4.19, it becomes clear that

$$\Delta_c H°(AN) = \Delta_c H°(PC) \qquad 4.21$$

This identity (4.21) is experimentally verified by the results shown in section 4.1. The validity of identity 4.21 suggests that Cryptand-221 and Cryptand-222 exhibit similar affinities for the tervalent lanthanide cations in propylene carbonate and acetonitrile.

As a consequence of identities 4.19 and 4.21, the cryptate conventions (see Chapter 2, Eqns. 2.3 and 2.4) are not valid for the calculation of single-ion values for the lanthanide cations among dipolar aprotic solvents.

Table 4.35 Standard enthalpy of solution of $La(CF_3SO_3)_3$ in acetonitrile at 298.15 K

$[La(CF_3SO_3)_3]$ mol.dm^{-3}	$\sqrt{I}$ mol$^{1/2}$.dm$^{-3/2}$	Q J	$\Delta_s H$ kJ.mol^{-1}
7.06 10^{-4}	0.065	-1.314	-37.21
9.66 10^{-4}	0.076	-1.619	-33.56
1.48 10^{-3}	0.094	-0.766	-10.44
2.28 10^{-3}	0.117	-0.791	-6.67

$\Delta_s H° = -78.95 \pm 5.39$ kJ.mol^{-1}

Table 4.36 Standard enthalpy of solution of $La(CF_3SO_3)_3$ in propylene carbonate at 298.15 K

$[La(CF_3SO_3)_3]$ mol.dm^{-3}	$\sqrt{I}$ mol$^{1/2}$.dm$^{-3/2}$	Q J	$\Delta_s H$ kJ.mol^{-1}
5.46 10^{-4}	0.057	-2.330	-85.49
7.92 10^{-4}	0.068	-7.477	-40.96
1.31 10^{-3}	0.089	-4.470	-68.60
2.52 10^{-3}	0.123	-6.539	-40.96

$\Delta_s H° = -108.03 \pm 2.30$ kJ.mol^{-1}

Table 4.37 Standard enthalpy of solution of $Pr(CF_3SO_3)_3$ in acetonitrile at 298.15 K

$[Pr(CF_3SO_3)_3]$ mol.dm^{-3}	$\sqrt{I}$ mol$^{1/2}$.dm$^{-3/2}$	Q J	$\Delta_s H$ kJ.mol^{-1}
1.79 10^{-4}	0.033	-0.422	-47.30
2.36 10^{-4}	0.037	-0.506	-42.91
2.92 10^{-4}	0.042	-0.502	-34.48
4.33 10^{-4}	0.051	-0.494	-22.91
6.47 10^{-4}	0.062	-0.632	-19.56
7.87 10^{-4}	0.069	-0.460	-11.72

$\Delta_s H° = -77.15 \pm 3.00$ kJ.mol^{-1}

Table 4.38 Standard enthalpy of solution of $Pr(CF_3SO_3)_3$ in propylene carbonate at 298.15 K

$[Pr(CF_3SO_3)_3]$ mol.dm^{-3}	$\sqrt{I}$ mol$^{1/2}$.dm$^{-3/2}$	Q J	$\Delta_s H$ kJ.mol^{-1}
1.33 10^{-4}	0.028	-0.690	-104.09
2.03 10^{-4}	0.035	-0.899	-88.32
2.10 10^{-4}	0.035	-0.933	-88.77
2.78 10^{-4}	0.041	-1.175	-84.56
3.21 10^{-4}	0.044	-1.280	-79.65
4.18 10^{-4}	0.050	-1.556	-74.46
5.33 10^{-4}	0.056	-1.661	-62.32

$\Delta_s H° = -138.07 \pm 2.46$ kJ.mol^{-1}

Table 4.39 Standard enthalpy of solution of $Nd(CF_3SO_3)_3$ in acetonitrile at 298.15 K

$[Nd(CF_3SO_3)_3]$ mol.dm^{-3}	$\sqrt{I}$ mol$^{1/2}$.dm$^{-3/2}$	Q J	$\Delta_s H$ kJ.mol
$8.80\ 10^{-5}$	0.023	-0.493	-56.37
$1.06\ 10^{-4}$	0.025	-0.494	-46.62
$7.93\ 10^{-4}$	0.069	-2.611	-32.93
$1.23\ 10^{-3}$	0.086	-3.251	-26.40
$1.54\ 10^{-3}$	0.096	-1.899	-18.76

$\Delta_s H° = -62.26 \pm 3.26$ kJ.mol^{-1}

Table 4.40 Standard enthalpy of solution of $Nd(CF_3SO_3)_3$ in propylene carbonate at 298.15 K

$[Nd(CF_3SO_3)_3]$ mol.dm^{-3}	$\sqrt{I}$ mol$^{1/2}$.dm$^{-3/2}$	Q J	$\Delta_s H$ kJ.mol
$1.81\ 10^{-4}$	0.033	-2.297	-127.06
$2.75\ 10^{-4}$	0.041	-2.589	-94.08
$3.33\ 10^{-4}$	0.045	-3.054	-91.75
$4.66\ 10^{-4}$	0.053	-3.657	-78.36
$6.79\ 10^{-4}$	0.064	-3.782	-55.65
$6.96\ 10^{-4}$	0.064	-3.887	-55.78
$1.02\ 10^{-3}$	0.078	-5.284	-51.91
$1.11\ 10^{-3}$	0.082	-4.958	-55.65

$\Delta_s H° = -162.17 \pm 8.83$ kJ.mol^{-1}

Table 4.41 Standard enthalpies of solution of lanthanide(III) trifluoromethanesulphonate salts in acetonitrile and propylene carbonate at 298.15 K

Cryptate Complex	$\Delta_s H°$ /kJ.mol^{-1}		$\Delta_t H°$ /kJ.mol^{-1}
	Acetonitrile	Propylene Carbonate	
$La(CF_3SO_3)_3$	-78.95 ± 5.39	-108.90 ± 2.30	29.95
$Pr(CF_3SO_3)_3$	-77.15 ± 3.00	-138.07 ± 2.46	60.83
$Nd(CF_3SO_3)_3$	-62.26 ± 3.26	-162.17 ± 8.83	99.91

Table 4.42 Single-ion $\Delta_t H°$ values for the transfer of tervalent lanthanide cations from propylene carbonate to acetonitrile at 298.15 K in kJ.mol^{-1}

Cation	Via Cycle	Direct Measurements	Average
La^{3+}	37.11 [a]	35.10	35.73 ± 0.92
	34.98 [b]		
Pr^{3+}	71.04 [a]	66.02	68.66 ± 2.00
	68.91 [b]		
Nd^{3+}	105.18 [a]	105.14	105.10 ± 0.08
	105.02 [b]		
La^{3+}222	32.72	35.56	34.14
Pr^{3+}222	66.44	71.55	68.99
Nd^{3+}222	104.14	104.18	104.16
La^{3+}221	34.89	34.77	34.85
Pr^{3+}221	64.89	67.78	66.32
Nd^{3+}221	103.72	103.59	103.68

(a) : via cycle involving Cryptand-222 (from Table 4.34)

(b) : via cycle involving Cryptand-221 (from Table 4.34)

4.4 Standard Enthalpies of Coordination of Lanthanide(III) Cryptates in the Solid State

The complexation of the lanthanide cryptates in the solid state can be represented by the following process:

$$Ln(CF_3SO_3)_3\ (solid) + Cry\ (solid) \longrightarrow Ln.Cry.(CF_3SO_3)_3\ (solid) \qquad 4.22$$

This process can be decomposed into the following thermodynamic cycle which is a modified form of the thermodynamic cycle[68] previously introduced (Chapter 2, Section 2.1.5):

$$\begin{array}{ccccc} Ln(CF_3SO_3)_3\ (solid) & + & Cry\ (solid) & \longrightarrow & Ln.Cry.(CF_3SO_3)_3\ (solid) \\ \downarrow & & \downarrow & & \downarrow \\ Ln^{3+}\ (s) + 3.CF_3SO_3^-\ (s) & + & Cry\ (s) & \longrightarrow & Ln^{3+}.Cry\ (s) + 3.CF_3SO_3^-\ (s) \end{array} \qquad 4.23$$

The standard enthalpy of coordination ($\Delta_{c,solid}H°$) of the lanthanide cryptates in the solid state can calculated as:

$$\Delta_{c,solid}H° = \Delta_sH°[Cry]\ (s) + \Delta_sH°[Ln(CF_3SO_3)_3]\ (s) + \Delta_cH°(s) - \Delta_sH°[Ln.Cry.(CF_3SO_3)_3] \qquad 4.24$$

Cox and Schneider[143] used Eqn. *4.24* for the calculation of the thermodynamic parameters of coordination in the solid state of metal(I) cryptates. *Eqn. 4.24*

was applied here to the tervalent lanthanide cations by using the thermodynamic cycle in propylene carbonate and in acetonitrile. As the $\Delta_{c,solid}H°$ for a particular cryptate complex are independent of the reaction medium, the equation can be used to check the accuracy of $\Delta_sH°$ and $\Delta_cH°$ values reported here. The results are shown in Table 4.43.

Table 4.43 Standard enthalpies of coordination of lanthanide(III) cryptates in the solid state at 298.15 K

Cryptate Complex	$\Delta_{c,solid}H°$ /kJ.mol^{-1}
La222$(CF_3SO_3)_3$	-144.72 [a]
	-147.57 [b]
Pr222$(CF_3SO_3)_3$	-153.93 [a]
	-156.90 [b]
Nd222$(CF_3SO_3)_3$	-137.40 [a]
	-137.48 [b]
La221$(CF_3SO_3)_3$	-182.63 [a]
	-182.46 [b]
Pr221$(CF_3SO_3)_3$	-183.67 [a]
	-186.48 [b]
Nd221$(CF_3SO_3)_3$	-188.03 [a]
	-187.94 [b]

(a) : derived from $\Delta_cH°$ and $\Delta_sH°$ values in propylene carbonate (Tables 4.17, 4.33 and 4.41)

(b) : derived from $\Delta_cH°$ and $\Delta_sH°$ values in acetonitrile (Tables 4.17, 4.33 and 4.41)

It can be seen that the $\Delta_{c,solid}H°$ values which were derived from the thermodynamic cycle in acetonitrile are in excellent agreement with those derived from the cycle in propylene carbonate. The striking difference between these data and the data found in solution is the greater stabilisation, in the enthalpic sense, of the lanthanide 221 cryptates with respect to the corresponding lanthanide 222 cryptates. This reflects the greater affinity of the lanthanide cations for Cryptand-221 than for Cryptand-222 as a result of a better cation-cavity size match. In general, the $\Delta_{c,solid}H°$ values are appreciably higher than the values obtained in solution. This might be due to the fact that the process in the solid state does not involve any competition reaction with the solvent.

CHAPTER 5

AMINO ACID - MACROCYCLIC LIGAND INTERACTIONS

5.1 Generalities

5.1.1 The Amino Acids

Amino acids are the basic structural units of proteins which play crucial roles in virtually all biological processes. They are water-soluble organic compounds that possess both a carboxyl (-COOH) and an amino ($-NH_2$) group attached to the same carbon atom called the α-carbon (Fig. 5.1). The amino acids can be represented by the general formula:

$$\mathbf{R\text{-}CH(NH_2)COOH}$$

where R may be hydrogen or an organic group.

(zwitterion).

Figure 5.1 Structure of the un-ionized and zwitterion forms of an amino acid.

Through the formation of peptide bonds, amino acids join together in short chains (peptides) or much longer chains (polypeptides or proteins). Proteins are composed of various proportions of about twenty commonly occurring amino acids (Table 5.1) and it is the sequence of these amino acids which determines the shape, properties and hence biological role of the proteins.

Amino acids in solution at neutral pH are predominantly dipolar ions (zwitterions) rather than un-ionized molecules. In the dipolar form of an amino acid, the amino group is protonated (NH_3^+) and the carboxyl group is dissociated (COO^-). These ionization state varies with the pH.

The tetrahedral array of four different groups about the α-carbon confers asymmetry to the molecule and therefore optical activity (Figure 5.2).

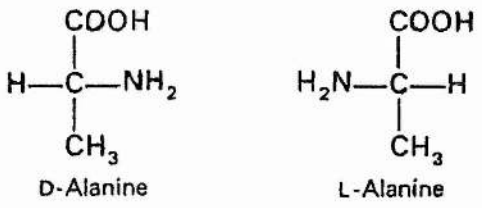

Figure 5.2 Absolute configurations of the L- and D-isomers of amino acids

Table 5.1 Amino acids constituent of proteins, classified according to the nature of their side chain

Aliphatic (proline could also be included here)

glycine (gly)

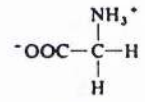

nonpolar neutral nonessential

alanine (ala)

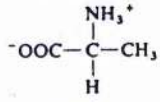

nonpolar neutral nonessential

valine (val)

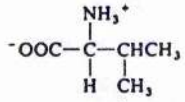

nonpolar neutral essential

leucine (leu)

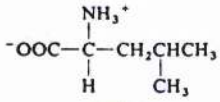

nonpolar neutral essential

isoleucine (ile)

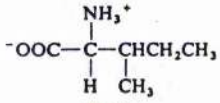

nonpolar neutral essential

Aromatic (histidine could be also included here)

phenylalanine (phe)

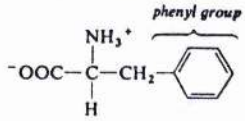

nonpolar, neutral, essential

tyrosine (tyr)

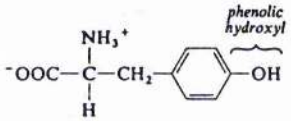

polar, nonessential weakly acidic

tryptophan (trp)

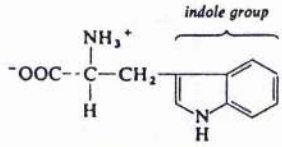

nonpolar, neutral, essential

Acidic (and corresponding neutral amides)

aspartic acid (asp)

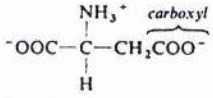

polar, acidic, nonessential

asparagine (asn)

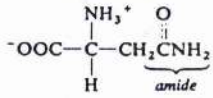

polar, neutral, nonessential

glutamic acid (glu)

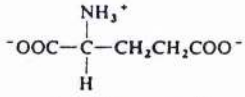

polar, acidic, nonessential

glutamine (gln)

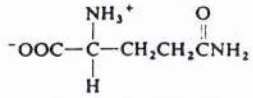

polar, neutral, nonessential

Basic

arginine (arg)

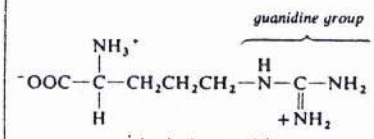

polar, basic, essential

histidine (his)

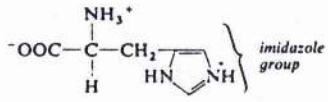

polar, weakly basic, essential

lysine (lys)

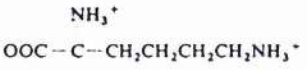

polar, basic, essential

Imino

proline (pro)

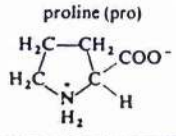

nonpolar neutral nonessential

Hydroxyl (tyrosine could also be included here)

serine (ser)

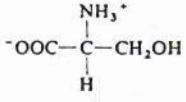

polar neutral nonessential

threonine (thr)

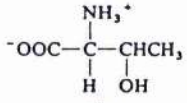

polar neutral essential

Sulfur

cysteine (cys)

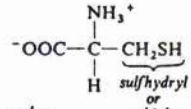

polar weakly acidic nonessential

methionine (met)

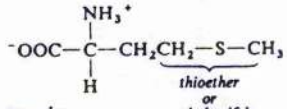

nonpolar neutral essential

5.1.2 Literature Review

The interactions of amino acids with the classic macrocyclic ligands such as the crown ethers and the cryptands, have not been extensively studied. Actually, very few information is available in the literature and the only work done so far has been reported by Bidzilya and co-workers.

Bidzilya and Oleksenko[144] reported the synthesis and isolation in the solid state of the complexes formed between various type of amino acid derivates (K^+, Ca^{2+}, Na^+ and Cl^- salts) and macrocyclic polyethers. The characterization of the physical and chemical properties of these complexes has been carried out by Infra-Red and NMR spectroscopy, mass spectroscopy and elemental analysis.

Three types of complexes between amino acids and 18-Crown-6 were suggested:

a) LHAa type complexes with the electrically neutral (zwitterionic) form of the amino acid in which L represents the macrocyclic ligand and HAa the amino acid.

b) MLAa type complexes in which the amino acid is in its anionic form (Aa^-) and M^+ is a metal cation

c) LH_2Aa^+ type complexes in which the amino acid is in its protonated form (H_2Aa^+).

PMR measurements showed that 1:1 complexes were formed with all amino acids and amino acid derivates studied.

The same authors reported in another paper[145] the stability constants of the complexes between the neutral aromatic amino acids and the macrocyclic polyethers 18-Crown-6 and 15-Crown-5 in methanol at 298.15 K (Table 5.2). These data were derived from a UV-spectrophotometric method. It was observed that 18-Crown-6 is a better receptor for these amino acids than 15-

Crown-5. This was attributed to the greater ring size of 18-Crown-6 which can be better adapted to the size of the amino group presumed to be the active site of the amino acid.

Table 5.2 Stability constants (log K_s) of amino acid-crown ether complexes in methanol at 298.15 K

Amino Acid	18-Crown-6	15-Crown-5
DL-Tyrosine	2.84	1.53
DL-Phenylalanine	2.52	1.51
DL-Tryptophan	2.49	1.09

The slightly higher stability constant observed with 18-Crown-6 for DL-Tyrosine was attributed to the possibility of interactions between the hydroxyl group (-OH) of the amino acid side chain and the macrocyclic ring.

The other interesting observation in this study was the increase in the solubilities of the free amino acids, in methanol, in presence of 18-Crown-6 and 15-Crown-5.

Bidzilya with other co-workers[146] studied also the complexation of amino acids with 18-Crown-6 and Dibenzo-18-Crown-6 in acetonitrile using NMR spectroscopy. This study was carried out in acidic medium because of the insolubility of the amino acid in pure acetonitrile. Because of the amphiphilic character of the aromatic amino acids (PHE, TRP and TYR)

and the benzo substituted crown ethers, it was suggested that hydrophobic and "stacking" interactions between the aromatic rings might occur, as illustrated in Fig. 5.3. Therefore, the authors suggested that the binding of the aromatic amino acids with benzo crown ethers takes place on two sections:

a) The amino group ($-NH_3^+$) of the amino acid binds the oxygen atoms of the crown ether ring

b) The intramolecular stacking reaction takes place between the aromatic group of the amino acid and the aromatic substituent of the crown ether, in a non-coplanar manner.

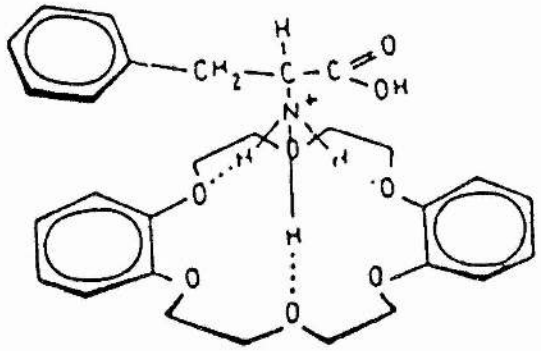

Figure 5.3 Structure of the complex of phenylalanine with dibenzo-18-crown-6

An increase in the overall stability was observed with these type of complexes (Table 5.3) when compared to the complexes with the non-aromatic amino acids.

Table 5.3 Stability constants (log K_s) of amino acid-crown ether complexes in acetonitrile at 298.15 K

Amino Acid	Dibenzo-18-Crown-6	18-Crown-6
DL-Phenylalanine	2.68	2.49
DL-Tyrosine	2.72	———
DL-Alanine	2.55	———

Detailed thermodynamic parameters of complexation for the amino acid-macrocyclic ligand complexes are non-existent. Nevertheless, great emphasis has been made in the literature[95,147-154,161-164] on the complexation of the macrocyclic polyethers with protonated amines, which have similar binding features than the amino acids. Thus, Izatt et al.[95] determined by titration calorimetry the thermodynamic parameters for the complexation of thirty organic ammonium cations with 18-Crown-6 in methanol at 298.15 K. Some of these data are shown in Table 5.4. These authors have analyzed the results in terms of the number of hydrogen bonds available for interaction and the steric hindrance of the guest molecules. According to their interpretation, the electronic factors have no significant effect. It was also noted that the type of anion had no influence on the complex stability and that ion pairing is negligible in methanol. The complexation process was in all cases enthalpy stabilized ($\Delta H < 0$) and entropy destabilized ($\Delta S < 0$).

Table 5.4 Stability constants (log K_s), enthalpy and entropy values for the complexation of RNH_3^+ and $R_2NH_2^+$ cations with 18-Crown-6 in methanol at 298.15 K [95]

Cation	log K_s	$\Delta_c G°$/kJ.mol^{-1}	$\Delta_c H°$/kJ.mol^{-1}	$\Delta_c S°$/J.K^{-1}.mol^{-1}
NH_4^+	4.27	-24.36	-38.78	-48.3
$HONH_3^+$	3.99	-22.77	-37.70	-35.7
$CH_3NH_3^+$	4.25	-24.25	-44.81	-68.9
$CH_3CH_2NH_3^+$	3.99	-22.77	-44.56	-73.1
$CH_3(CH_2)_2NH_3^+$	3.97	-22.65	-42.09	-65.1
$(CH_3)_2CHNH_3^+$	3.56	-20.31	-40.37	-67.3
$(CH_3)_3CNH_3^+$	2.90	-16.55	-32.47	-53.3
$PhNH_3^+$	3.80	-21.68	-39.91	-61.2
$(CH_3)_2NH_2^+$	1.76	-10.04	-27.90	-59.9

5.2 Thermodynamic Parameters for the Complexation of Amino Acids with 18-Crown-6 and Cryptand-222 in Methanol and Ethanol at 298.15 K

5.2.1 The Active Site of the Amino Acid

The complexation of organic guest species, in particular the protonated amines RNH_3^+, by macrocyclic ligands differs in many aspects from the complexation of metal cations with these ligands, the major difference being the nature of the binding. It is believed that the binding of the organic species to the macrocyclic polyethers essentially takes place through hydrogen bonding and to a slight extent through electrostatic interactions. Timko et al.[154] estimated the relative contributions of hydrogen-bonding (N^+-H...O) and electrostatic interactions (N^+...O) to be 75% and 25% respectively in the case of the ammonium cation with the polyethers. For hosts containing 18-membered rings, CPK molecular models show that three acidic hydrogen atoms of NH_3^+ provide three hydrogen bonds[154]. In the model complexes, the remaining three oxygen atoms of the macrocycle are located at van der Waals distance from the nitrogen atoms of the guest and are able to provide three electrostatic (N^+...O) interactions. The stucture of many crystalline complexes of crown ethers with ammonium ion and substituted ammonium ions have also been reported[148-153]. All the complexes were found to have the NH_3^+ group above the plane of the crown ether ring.

It is reasonable to assume that similar interactions take place in the case of amino acid complexes with the macrocyclic ligands. Evidence that the protonated amino group ($-NH_3^+$) is the active site of the amino acid was demonstrated by using N-blocked amino acids (N-Acetyl-DL-Alanine, N-Acetyl-DL-Phenylalanine) and trying to complex them with 18-Crown-6 in methanol. The results derived from titration calorimetry (measurement of the heat of complexation) indicate that no complexation occurs between these amino acids and 18-Crown-6, due probably to the fact that the

possibility of hydrogen bond formation is partially hampered by the blockage of the amino group.

Another experimental evidence that the amino group is the active site of the amino acid was the formation of 2:1 18-Crown-6/lysine complexes. Lysine (Table 5.1) is an amino acid bearing two amino (NH_3^+) groups; one is attached to the α-carbon, the other at the end of the side chain. Lysine[18-Crown-6]$_2$ was isolated in its pure form, according to the procedure outlined in section 3.7. The elemental analyses gave 50.10 $\%C_{found}$, 5.56 $\%H_{found}$ and 4.02 $\%N_{found}$ which is in very good agreement with the calculated values (%C: 50.35, %H: 5.45, %N: 3.93).

pH titration experiments confirmed that the amino acids exist in methanol in their dipolar form (zwitterion). Glycine, DL-Alanine and DL-Phenylalanine were titrated in methanol by a base (Et_4NOH) in the presence and in the absence of 18-Crown-6. A typical titration curve is shown in Figure 5.4. The inflection points of the curve "A" (titration of the free amino acid) correspond to the following equilibria:

a) the equilibrium between the protonated form (H_2Aa^+) and the neutral form (HAa) of the amino acid,

$$H_2Aa^+ \longrightarrow HAa + H^+ \qquad 5.1$$

characterized by the apparent acid dissociation constant,

$$K_{a1} = \frac{[HAa] \cdot [H^+]}{[H_2Aa^+]} \qquad 5.2$$

b) the equilibrium between the neutral form (HAa) and the anionic form

(Aa^-) of the amino acid,

$$HAa \longrightarrow Aa^- + H^+ \qquad 5.3$$

characterized by the apparent dissociation constant,

$$K_{a2} = \frac{[Aa^-] \cdot [H^+]}{[HAa]} \qquad 5.4$$

The activities of the different species in methanol have been approximated by their concentrations.

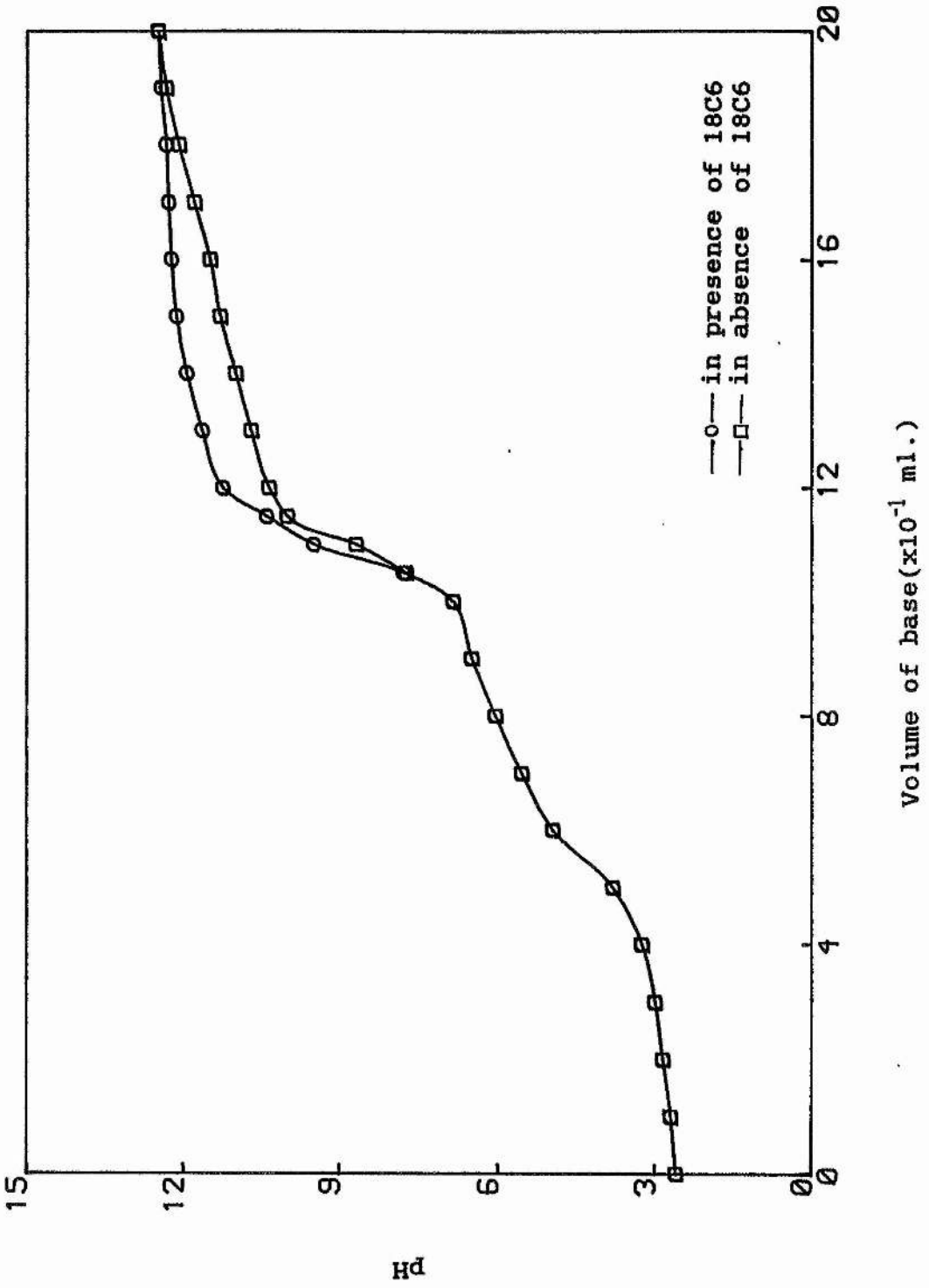

Figure 5.4 pH titration curves of amino acids (DL-Phenylalanine) in methanol in presence (curve "B") and in absence (curve "A") of 18-Crown-6

In the presence of the crown ether (curve "B"), an increase in pK_{a2} ($-\log K_{a2}$) is observed, whereas pK_{a1} ($-\log K_{a1}$) remains constant. The analysis of the shape of these curves can give an indication on which form of the amino acid complexes with the crown ether.

The interaction of the dipolar form of amino acid with 18-Crown-6 (18C6), the protonated amino group being the active site, may be represented by:

$$HAa + 18C6 \xrightarrow{K_s} 18C6.HAa \xrightarrow{K_{a2}'} 18C6 + H^+ + Aa^- \qquad 5.5$$

where

$$K_s = \frac{[18C6.HAa]}{[HAa].[18C6]} \qquad 5.6$$

and

$$K_{a2}' = \frac{[18C6].[H^+].[Aa^-]}{[18C6.HAa]} \qquad 5.7$$

K_{a2}' can be rearranged as:

$$K_{a2}' = \frac{1}{K_s}.K_{a2} \qquad 5.9$$

thus,

$$pK_{a2}' = \log K_s + pK_{a2} \qquad 5.10$$

An increase in pK_{a2}' for the amino acid in the presence of 18-Crown-6 is observed with respect to pK_{a2} in the absence of 18-Crown-6, the difference being the logarithm of the stability constant K_s of the amino acid-crown ether complex.

The results obtained here (Figure 5.4) are also an evidence that the amino acid (HAa) is present in its dipolar form in methanol, otherwise an increase in pK_{a1}' with respect to pK_{a1} is to be observed:

$$H_2Aa^+ + 18C6 \xrightarrow{K_s} 18C6.H_2Aa^+ \xrightarrow{K_{a1}'} 18C6 + H^+ + HAa \qquad 5.11$$

where

$$K_{a1}' = \frac{[18C6] \cdot [H^+] \cdot [HAa]}{[18C6 \cdot H_2Aa^+]} \qquad 5.12$$

$$K_{a1}' = \frac{[18C6] \cdot [H_2Aa^+]}{[18C6 \cdot H_2Aa^+]} X \frac{[H^+] \cdot [HAa]}{[H_2Aa^+]} \qquad 5.13$$

$$K_{a1}' = \frac{1}{K_s} \cdot K_{a1} \qquad 5.14$$

thus,

$$pK_{a1}' = \log K_s + pK_{a1} \qquad 5.15$$

If the carboxyl group of the dipolar form of the amino acid would interact with the crown ether, no variation in pK_{a2}' would be observed:

$$HAa + 18C6 \xrightarrow{K_s} HAa.18C6 \xrightarrow{K_{a2}'} H^+ + Aa^-.18C6 \qquad 5.16$$

where

$$K_{a2}' = \frac{[H^+].[Aa^-.18C6]}{[HAa.18C6]} \qquad 5.17$$

$$K_{a2}' = \frac{[H^+].[Aa^-]}{[HAa]} x \frac{[HAa].[18C6]}{[HAa.18C6]} x \frac{[Aa^-.18C6]}{[18C6].[Aa^-]} \qquad 5.18$$

$$K_{a2}' = K_{a2}.\frac{1}{K_s}.K_s \qquad 5.19$$

$$pK_{a2}' = pK_{a2} \qquad 5.20$$

This experiment provides evidence that:

a) the amino acids in methanol exist in their dipolar form (zwitterion)

b) the protonated form ($-NH_3^+$) of the amino acid interacts with the macrocyclic ligand

This experimental results are supported by computer calculations using a COSMIC package[155]. The computer model proposes the structure shown in Figure 5.5 for the amino acid (Alanine) complexed with 18-Crown-6. It is important however to point out that computer models do not take into account the reaction medium and are therefore only hypothetical models in solution.

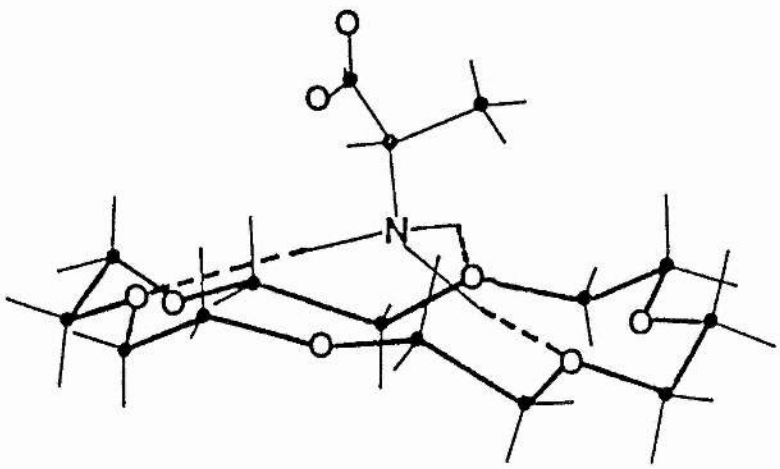

Figure 5.5 Computer model for the Alanine/18-Crown-6 complex

Figure 5.5 shows that three hydrogen atoms of NH_3^+ are located close enough to the crown ether to form hydrogen bonds with three oxygen atoms. The calculated distances of these bonds are 1.72, 1.84 and 2.26 Å. The calculated distances of the electrostatic N^+...0 bonds are 2.82, 2.96 and 3.14 Å. These distances are comparable to the hydrogen bond distances observed in the crystal structures of complexes of 18-Crown-6 with hydrazinium perchlorate (1.96, 2.07 and 2.10 Å), hydroxylammonium perchlorate (2.22, 2.16 and 2.25 Å) and methylammonium perchlorate (2.17, 2.17 and 1.98 Å)[153]. In these complexes, the N^+...O distances were in average 2.88 Å. It is also interesting to note that in the amino acid-18-Crown-6 complexes, the amino acid side chain is directed perpendicularly to the plane of the crown ether and therefore it is fully exposed to the surrounding medium.

In the case of Cryptand-222, the computer model predicts slightly different interactions. The calculated hydrogen-oxygen distances are estimated to be 1.57, 3.18 and 3.41 Å. Clearly, one hydrogen bond can be formed (1.57 Å), the distances of 3.18 and 3.41 Å are considered to be too long for hydrogen bond formation and N^+...O electrostatic interactions are more likely to occur. The predicted model for the Glycine-Cryptand 222 complex is shown in Figure 5.6.

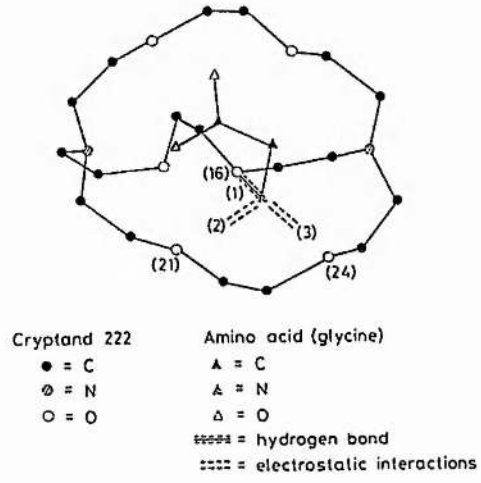

Figure 5.6 Computer modelling for the Cryptand 222-amino acid (glycine) interactions

5.2.2 Free Energies, Enthalpies and Entropies of Complexation of Amino Acids with 18-Crown-6 and Cryptand-222 in Methanol and Ethanol at 298.15 K

The thermodynamic parameters for the complexation of a series of amino acids with the macrocyclic ligands (18-Crown-6 and Cryptand-222) in methanol and ethanol were determined by titration calorimetry, as described in Section 3.13.

The amino acids are found as zwitterions ($^{+}H_3N$-CH(R)-COO^{-}) abbreviated as HAa) in the alcohols and most of their complexes formed with the macrocyclic ligands (L) are of 1:1 stoichiometry. The process studied can therefore be represented as:

$$HAa\ (s) + L\ (s) \longrightarrow LHAa\ (s) \qquad 5.21$$

This equilibrium is characterized by the thermodynamic stability constant (K_s) which can be written in terms of molar activities as:

$$K_s = \frac{a_{LHAa}}{a_L \cdot a_{HAa}} \qquad 5.22$$

or in terms of activity coefficients and concentrations:

$$K_s = \frac{\gamma_{LHAa}}{\gamma_{HAa}} \cdot \frac{[LHAa]}{[L] \cdot [HAa]} \qquad 5.23$$

In *Eqn. 5.23*, it is assumed that the activity coefficient of the ligand is equal

to unity (γ_L=1). Activity coefficients for the free amino acid (γ_{HAa}) and the complexed amino acid (γ_{LHAa}) have been taken into account for the simultaneous determination of the free energy of complexation ($\Delta_c H°$) and the enthalpy of complexation ($\Delta_c H°$). The method for the calculation of these quantities is detailed in Appendix B.

The series of the commonly occurring amino acids (Table 5.1) have been studied with 18-Crown-6 and Cryptand-222 in methanol and ethanol. The racemic mixture (DL) have been considered. Results are reported in Tables 5.5-5.8.

Table 5.5 Stability constants, free energies, enthalpies and entropies of complexation of amino acids with 18-Crown-6 in methanol at 298.15 K

Amino Acid	log K_s	$\Delta_c G°$/kJ.mol^{-1}	$\Delta_c H°$/kJ.mol^{-1}	$\Delta_c S°$/J.mol^{-1}.K^{-1}
DL-ALA	3.59±0.06	-20.48	-45.94±1.02	-85.3
DL-ARG	3.42±0.10	-19.51	-40.11±1.93	-69.0
DL-ASN	3.14±0.02	-17.91	-40.24±0.54	-72.8
DL-ASP	2.99±0.03	-17.06	-38.55±1.36	-71.9
DL-CYS	3.28±0.10	-18.71	-30.67±0.53	-40.2
DL-GLU	3.34±0.03	-19.05	-35.78±1.01	-56.1
GLY	3.98±0.03	-22.70	-53.83±0.61	-104.2
DL-HIS	3.03±0.10	-17.29	-39.20±2.11	-73.6
DL-ILE	3.17±0.04	-18.08	-36.24±1.45	-61.5
DL-LEU	3.35±0.03	-19.11	-42.47±0.69	-78.2
DL-MET	3.66±0.03	-20.88	-37.85±1.31	-56.9
DL-PHE	3.15±0.06	-17.97	-39.18±1.03	-71.1
DL-PRO	2.64±0.10	-15.06	-11.38±1.51	-80.7
DL-SER	3.37±0.04	-19.22	-38.80±0.92	-65.7
DL-THR	3.02±0.01	-17.23	-35.36±0.56	-60.7
DL-TRP	3.06±0.10	-17.45	-41.63±0.87	-81.2
DL-TYR	2.93±0.10	-16.71	-45.34±2.10	-95.8
DL-VAL	3.19±0.01	-18.20	-34.49±0.24	-54.8

Table 5.6 Stability constants, free energies, enthalpies and entropies of complexation of amino acids with 18-Crown-6 in ethanol at 298.15 K

Amino Acid	log K_s	$\Delta_c G°$/kJ.mol^{-1}	$\Delta_c H°$/kJ.mol^{-1}	$\Delta_c S°$/J.mol^{-1}.K^{-1}
DL-ALA	3.69±0.11	-20.98	-54.52±2.87	-112.1
GLY	3.81±0.09	-21.34	-64.95±0.98	-146.0
DL-ILE	3.41±0.10	-19.45	-52.89±3.69	-112.1
DL-LEU	3.62±0.01	-20.65	-50.22±0.22	-99.2
DL-PHE	3.36±0.04	-19.17	-56.67±1.08	-125.5
DL-TRP	3.42±0.02	-19.51	-53.57±3.55	-114.2
DL-VAL	3.41±0.05	-19.45	-55.27±0.55	-120.1

Table 5.7 Stability constants, free energies, enthalpies and entropies of complexation of amino acids with Cryptand-222 in methanol at 298.15 K

Amino Acid	log K_s	$\Delta_c G°$/kJ.mol^{-1}	$\Delta_c H°$/kJ.mol^{-1}	$\Delta_c S°$/J.mol^{-1}.K^{-1}
DL-ALA	3.22±0.10	-18.38	-15.40±0.94	10.0
DL-ARG	3.59±0.20	-20.48	-8.97±0.12	38.5
DL-ASN	3.32±0.03	-18.94	-19.57±0.26	-2.1
DL-ASP	4.23±0.07	-24.13	-26.80±0.56	-8.8
DL-CYS	3.36±0.03	-19.17	-15.53±0.43	12.1
DL-GLU	4.50±0.20	-25.67	-30.10±1.44	-14.6
GLY	3.48±0.01	-19.86	-41.77±0.14	-73.5
DL-HIS	3.33±0.08	-18.99	-12.15±0.62	23.0
DL-ILE	3.81±0.20	-21.73	-6.40±0.50	51.5
DL-LEU	3.38±0.20	-19.28	-9.11±0.35	33.9
DL-MET	3.58±0.04	-20.42	-4.37±0.10	53.5
DL-PHE	3.48±0.15	-19.86	-10.21±0.64	32.3
DL-PRO	2.46±0.05	-14.04	-5.20±0.56	29.6
DL-SER	3.64±0.02	-20.78	-15.74±0.23	16.9
DL-THR	3.88±0.20	-22.13	-4.26±0.16	59.8
DL-TRP	3.72±0.20	-21.23	-7.92±0.78	44.6
DL-VAL	3.16±0.03	-18.03	-4.60±0.79	44.7

Table 5.8 Stability constants, free energies, enthalpies and entropies of complexation of amino acids with Cryptand-222 in ethanol at 298.15 K

Amino Acid	log K_s	$\Delta_c G°$/kJ.mol^{-1}	$\Delta_c H°$/kJ.mol^{-1}	$\Delta_c S°$/J.mol^{-1}.K^{-1}
DL-ALA	3.38±0.10	-19.82	-19.82±0.79	-1.8
GLY	3.43±0.11	-19.57	-49.42±0.93	-100.1
DL-ILE	3.20±0.10	-18.26	-18.55±0.29	-1.0
DL-LEU	3.33±0.06	-19.00	-16.20±0.10	9.4
DL-PHE	3.16±0.10	-18.03	-19.83±0.13	-6.0
DL-VAL	3.22±0.05	-18.37	-19.66±0.55	-4.3

The most notable feature in the data reported here is the similitude of the stability constants for all amino acid (except DL-Proline) complexes with 18-Crown-6 and Cryptand-222, in the two solvents studied (methanol and ethanol). These data suggest that although these ligands can be used as receptors for the amino acids, selective complexation does not occur.

Proline differs from the other amino acids in the basic set of twenty, in that it contains a secondary rather than a primary amino group (Table 5.1). Strictly speaking, proline is an imino acid. The side chain of proline is bound to both the amino group and the α-carbon, thereby forming a cyclic structure. The results in Table 5.5 and Table 5.6 show a difference in the thermodynamic parameters of complexation for DL-Proline with respect to the other amino acids in the series. This difference is particularly marked with 18-Crown-6. A decrease in stability of about one log unit with both ligands is observed. In terms of enthalpy, a decrease of about 8 $kJ.mol^{-1}$ with Cryptand-222 and 30 $kJ.mol^{-1}$ with 18-Crown-6 is observed. This is due to the fact that proline only possesses two hydrogen atoms available for interactions which reduces considerably the strength of the binding. A steric factor may also contribute to the decrease in the stability and in the enthalpy of complexation of the process. The steric bulk of the cyclic structure about the α-carbon must hamper the complexation more than the organic groups of other amino acids.

The analysis of the enthalpy and entropy contributions to the complexation process reveals that the similitude of the free energy term is a result of a remarkable $\Delta_c H°/\Delta_c S°$ compensation effect. This effect is shown in a plot of the $\Delta_c H°$ values versus the $\Delta_c S°$ values which is a straight line (Figure 5.7). A correlation coefficient of 0.9820 and a slope of 297.6 K were calculated. The slope is known as the isoequilibrium temperature. At this temperature, all crown ether and cryptand complexes with the amino acids are considered to have identical stabilities in methanol and in ethanol. It can be noted that

in the present case the isoequilibrium temperature is almost equals to 298.15 K.

The enthalpy-entropy compensation effect has been mostly observed in complexation reactions involving cyclodextrins as macrocyclic ligands and different guests in different reaction media[157-159]. It was also noted that the ΔH-ΔS relationship in general holds for complexation of cations with crown ethers and related ligands[160]. This is the first time that this effect is observed for reactions involving crown ethers and cryptands with neutral molecules. The origin of this effect is not entirely clear. However, it seems logical that the more the host-guest complexation is enthalpically favoured (more negative ΔH), the more the process will be unfavoured entropically (less positive or more negative ΔS). An enthalpy gain from the stronger binding will be compensated by an entropy loss due to the more structured complex, and vice-versa.

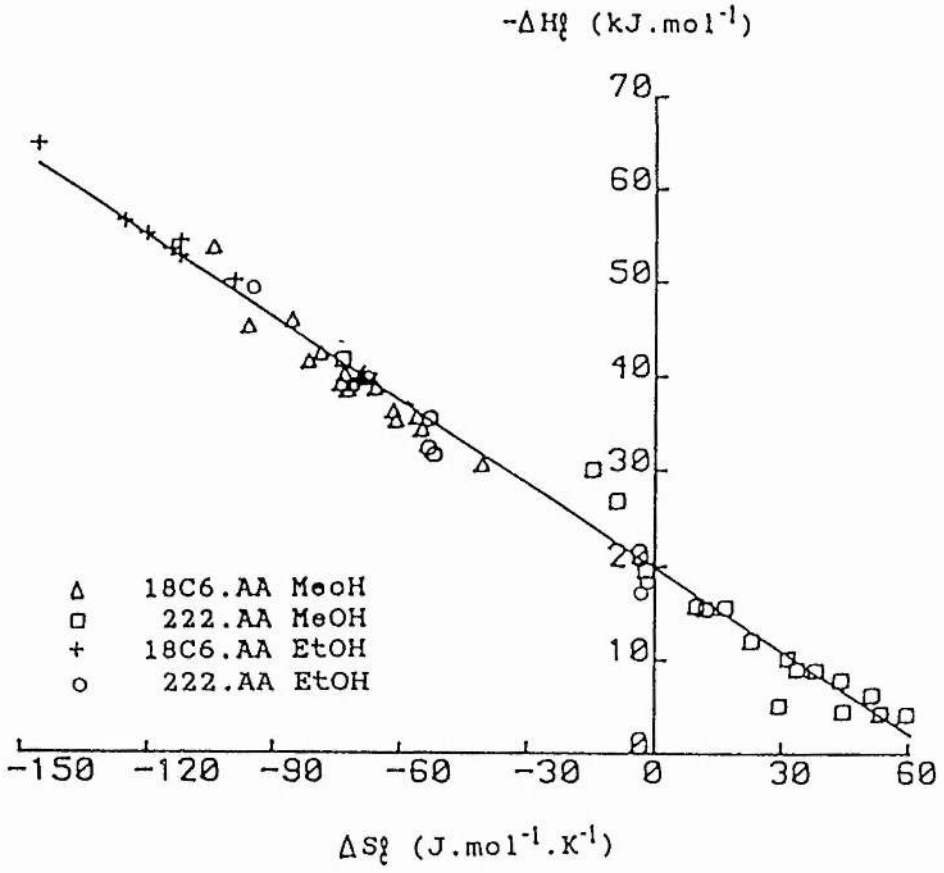

Figure 5.7 $\Delta_c H°$-$\Delta_c S°$ compensation effect for amino acid-macrocyclic ligand complexation in methanol and ethanol

The results reported here show that in all cases the complexation reaction between amino acids and crown ethers and cryptands in methanol and ethanol is enthalpically favoured ($\Delta_c H° < 0$). The complexation is entropically unfavoured with 18-Crown-6 ($\Delta_c S° < 0$), whereas with Cryptand-222, it is mostly entropically favoured ($\Delta_c S° > 0$). Unlike the free energy of complexation, the enthalpy and entropy of complexation are dependent on the nature of *i)* the guest molecule, *ii)* the ligand and *iii)* the solvent. The results are then discussed in terms of these three parameters.

i) The complexation of the amino acids with the macrocyclic ligands differ from that of the metal cations because of the different binding mechanisms involved with the two types of guests. In the metallic complexation, the size of the cation is an important factor affecting the complexation strength because the complexes formed are mostly inclusive. The amino acids are too large to fit into the ring of the crown ether or the cavity of the cryptand. Therefore, as it has been shown in the molecular models (Figure 5.5), the amino acid is lying on the top of the macrocycle forming exclusive complexes. Thus, the significant parameters related to the amino acid are likely to be:

(a) *The number of hydrogen atoms available for hydrogen bonding*
As mentioned earlier in the case of proline, the number of hydrogen bonds greatly influences the complex stability thus, the enthalpy and entropy of complexation. It is certainly the most determinant factor in this process, as it was also observed in the complexation of the primary ammonium salts with 18-Crown-6[95].

(b) The steric hindrance of host-guest approach by the amino acid
The complexes between the amino acids with 18-Crown-6 and Cryptand-222 are all exclusive (Figure 5.5), therefore the influence of the steric effect should not be very important. However, the approach to the macrocyclic ligand might be limited for some amino acids, particularly those having a bi-substituted ß-carbon such as isoleucine, threonine and valine. Slightly

less favourable (less negative) $\Delta_c H°$ values have been observed for these three amino acids with 18-Crown-6 in methanol (Table 5.5).

(c) the electronic effect

The inductive effect is enhanced as the number of successive electron donating groups attached to the α-carbon increases. The α-carbon becomes then more negative, therefore the NH_3^+ group becomes less positive. As a result, a less favourable $\Delta_c H°$ value will be observed. If the inductive effect was the only factor which contributes to the enthalpic stability of amino acids and macrocyclic ligands, the stability in enthalpic terms should decrease in the following order GLY > ALA > VAL >ILE > LEU. Clearly, this is not the case for amino acids having an aliphatic side chain. The stability in enthalpic terms for the complexes of these amino acids with 18-Crown-6 and Cryptand-222 in methanol varies as GLY > ALA > LEU > ILE > VAL. Amino acids containing substituents attached to the ß-carbon such as phenolic (TYR), phenyl (PHE), indole (TRP), hydroxyl (SER), carboxyl (ASP) or imidazole (HIS) groups do not seem to have an appreciable effect on the active site of complexation of the guest molecule and therefore, not much variations are observed in the enthalpies and entropies of complexation in methanol. This is also the case for amino acids containing substituent groups at the γ or δ carbon such as guanidine (ARG) or carboxylic (GLU) groups.

The possibility of interactions of the amino acid side chain with the macrocyclic ring must also be taken into consideration. Amino acids bearing groups with labile hydrogen atoms (-OH, -SH, $-NH_2$) might form additional hydrogen bonds with the donor atoms of the macrocyclic ligand. This could influence the stability of the complex as well as the $\Delta_c H°$ and $\Delta_c S°$ values. The results obtained with 18-Crown-6 and Cryptand-222 do not reflect any particular effect of this type. The molecular models also show that in all cases the side chain is directed perpendicularly to the plane of the macrocyclic and therefore is too far to be involved in any direct interaction with the ligand.

ii) The most striking feature in the results reported here undoubtedly is the difference in the $\Delta_c H°$ values observed between 18-Crown-6 and Cryptand-222. For the crown ether, the average $\Delta_c H°$ value obtained is about -38 $kJ.mol^{-1}$ whereas for the cryptand it is -13 $kJ.mol^{-1}$.

Unlike the guest parameters, the parameters for the host are similar to those observed in the metallic complexation i.e. ring size, number and type of donor atoms, ring number and type, ring substituent and ring conformation. Due to the nature of the complexes formed between the amino acids and the crown ethers and cryptands, it might be surprising that the size of the macrocycle plays a role in this process. The molecular models (Figure 5.5) show that the interactions occur between the donor atoms of the ligand and the protonated amino group of the amino acid (NH_3^+). Therefore, an optimum size of the macrocyclic ring exists for which the three oxygen atoms involved in the hydrogen bonding are located close enough to the active site of the amino acid. Cram and co-workers[161-163] studied the interactions of primary ammonium salts with a series of crown ethers, and found that the most stable complexes are formed with the 18-membered rings. Moreover, Bidzilya and Oleksenko[144] showed that the 15-membered ring 15-Crown-5 is not a suitable receptor for the amino acids due to its small ring size.

The enthalpies of complexation and the stability constants observed for the amino acid-crown ether complexes in methanol are of the same order of magnitude to those observed for the primary ammonium salts (RNH_3^+) with the same ligand in the same solvent[95]. This is not surprising considering that the host-guest interactions for the amino acid and the primary ammonium salts are alike. It can also be noted that the $\Delta_c H°$ values for ammonium cation-18-Crown-6 complexes are largely compensated by $\Delta_c S°$ values. Therefore the plot of $\Delta_c H°$ versus $\Delta_c S°$ shows that these data fit on the same straight line than the data obtained for the amino acid-macrocyclic ligand complexes (Figure 5.8).

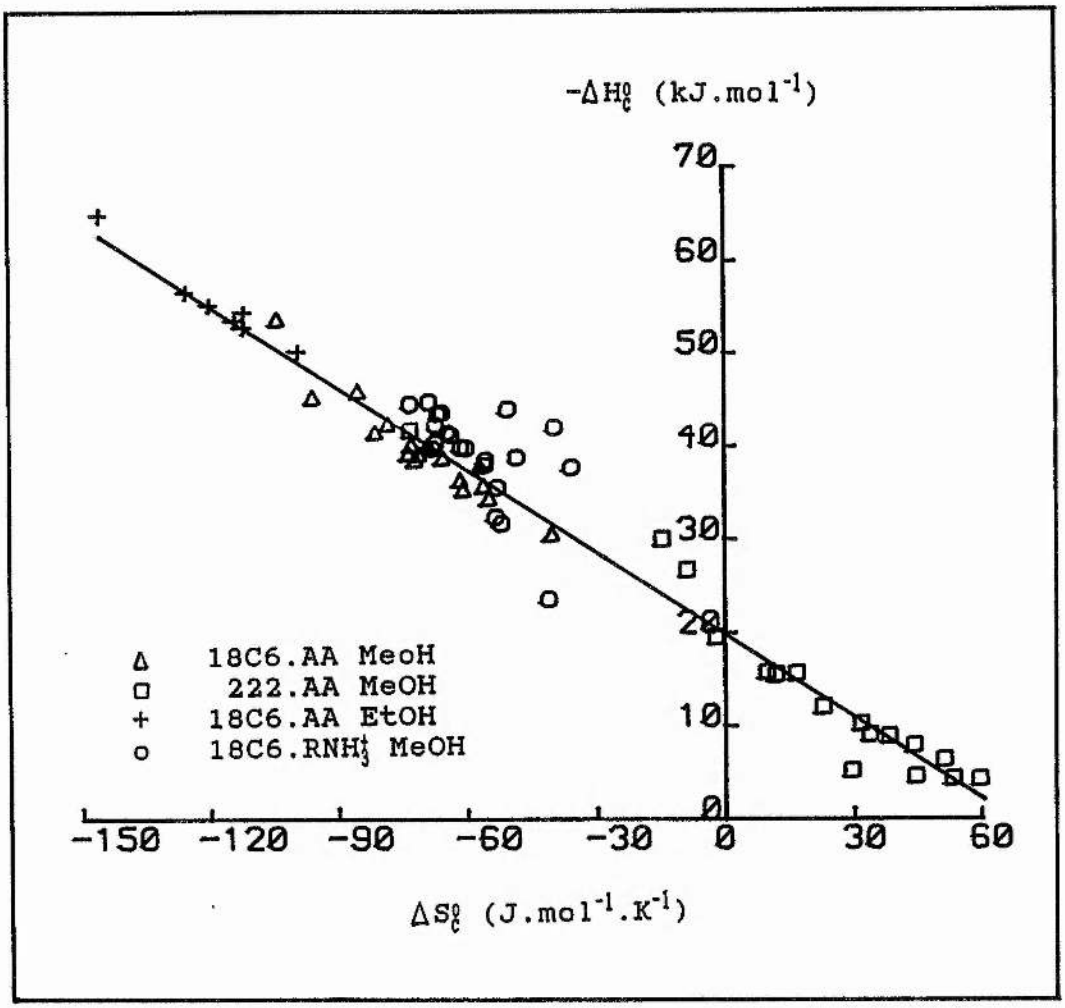

Figure 5.8 $\Delta_c H°$-$\Delta_c S°$ compensation effect for the complexation of amino acids and ammonium cations with 18-Crown-6 and Cryptand-222 in methanol and ethanol

The differences in the enthalpies of complexation of amino acids and crown ethers relative to the corresponding data for amino acids and cryptands can certainly be attributed to the different structural characteristics of the ligands. The enthalpy of complexation is mainly related to the variation in nature and energy of the interactions between the guest molecule and either the ligand or the solvent molecules. The computer molecular model predicts that for Cryptand-222, the hydrogen atoms of the NH_3^+ group are not close enough to the oxygen atoms of the ligand to form three hydrogen bonds. This is attributed to steric effects which reduce the ability of the cryptand to interact with the amino acid. Differences are also found between the entropy of complexation of amino acids and Cryptand-222 relative to 18-Crown-6. The amino acids are able to form stronger interactions with 18-Crown-6 than with Cryptand-222 (more favourable $\Delta_c H°$ values for 18-Crown-6 than for Cryptand-222). As a result, the complexes formed with the crown ether are likely to be more structured than the complexes formed with the cryptand. More favourable (more positive) $\Delta_c S°$ values are therefore obtained in the complexation process involving Cryptand-222 than for the same process involving 18-Crown-6.

iii) The determination of the thermodynamic parameters for the complexation of several amino acids with 18-Crown-6 and Cryptand-222 in ethanol enabled the study of the influence of the reaction medium on this process.

The alcohols have been chosen as reaction media because there are solubility limitations in other non-aqueous media. Amino acids are known to be mainly water-soluble compounds. Some attempts have been made in order to complex them with the crown ether in water. Unfortunately, these reactions could not be studied in macrocalorimetry. No heat of reaction could be measured either because $\Delta_c H°$ and/or log K_s are very small. Water is a good solvating medium for the amino acids, therefore a poor reaction medium for complexation.

No significant variations can be observed in the stability constants for the amino acid-macrocyclic ligand complexes in ethanol with respect to methanol. The more negative $\Delta_c H°$ values observed in ethanol is certainly related to the difference in the strength of interaction of the amino acid in these solvents. Ethanol is a less solvating medium than methanol and therefore the amino acid is less bounded to the solvent molecules and more susceptible to interact with the macrocyclic ligand in ethanol than in methanol. As a result, the $\Delta_c H°$ values are more favourable (more negative) in ethanol than in methanol. The differences observed are quite significant, up to 20 $kJ.mol^{-1}$.

In the series of amino acids studied in ethanol, the variations of the $\Delta_c H°$ values does not seem to follow a particular trend. It is actually interesting to see that, apart from glycine, the amino acids do not show any significant enthalpy variations. The factors influencing the enthalpy of complexation in methanol, in particular the electronic effects, seem to have no influence in ethanol. Inductive and charge effects are likely to decrease in ethanol due to its lower dielectric constant ($\varepsilon_{[MeOH]}$=32.70, $\varepsilon_{[EtOH]}$=24.55).

Like in methanol, the $\Delta_c H°$ and the $\Delta_c S°$ values compensate each other to give similar log K_s values (Figure 5.7).

In order to study the effect of the solvent in greater detail, it was decided to determine the transfer parameters of the uncomplexed and complexed species between methanol and ethanol, and to demonstrate as for the metal cation-cryptand interactions, the importance of the transfer data in the understanding of the complexation data.

5.3 Thermodynamic Parameters for the Transfer of Amino Acids and their Complexes with Macrocyclic Ligands between Methanol and Ethanol at 298.15 K

The transfer parameters of the different species involved in this reaction (guest, host, complex) have been determined between methanol and ethanol. The following thermodynamic cycle[68] has been considered:

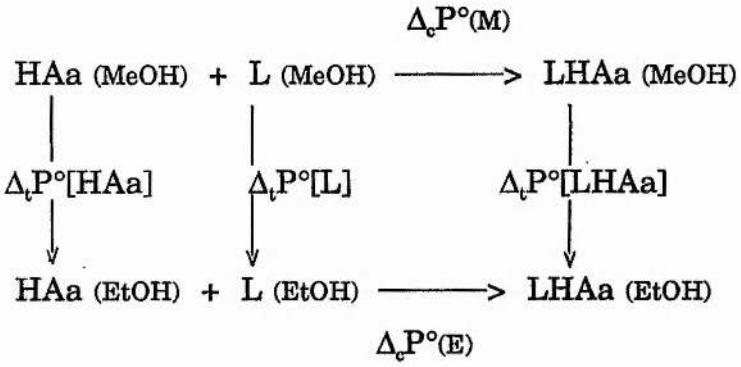

5.24

where P = G, H or S. The knowledge of these parameters might be useful for the interpretation of the complexation process, particularly to assess the influence of the reaction medium. Transfer data may also confirm some of the suggestions made in the preceding paragraph (Section 5.2).

5.3.1 Free Energies of Transfer

The free energy of transfer of a species i from a solvent s_1 to a solvent s_2 is given by:

$$\Delta_t G°[i]_{(s1->s2)} = \Delta_s G°[i]_{(s_2)} - \Delta_s G°[i]_{(s_1)} \qquad 5.25$$

$$\Delta_t G°[i]_{(s1->s2)} = -RT.\ln \frac{[i]_{(s_1)}}{[i]_{(s_2)}} \qquad 5.26$$

where $[i]_{(s_1)}$ and $[i]_{(s_2)}$ are the solubilities of the species i in the solvents s_1 and s_2 respectively.

The solubilities of seven amino acids have been measured in methanol and ethanol (section 3.8). These values are reported in Table 5.9. The free energies of solution ($\Delta_s G°$) of these amino acids in methanol and ethanol were then calculated as:

$$\Delta_s G° = -RT.\ln[HAa]_{(s)} \qquad 5.27$$

These data as well as the free energies of transfer ($\Delta_t G°$) from methanol to ethanol are listed in Table 5.10. The activity coefficients of the saturated amino acid solutions in the alcohols are assumed to be unity, as the solutes are in their standard state in these solvents.

Very few data on the solubilities of amino acids in the alcohols , particularly DL-amino acids, are available in the literature. Some values have been reported for glycine[164-166]. The value in methanol shown in Table 5.9 is in

good agreement with that reported by McMeekin et al.[166] ($4.26\ 10^{-3}$ mol.dm^{-3}). The same applies to DL-valine in ethanol ($1.08\ 10^{-3}$ mol.dm^{-3}) given by the same authors.

It can be observed from the results shown in Table 5.9 that the solubilities of the amino acids decreases from methanol to ethanol. This is not surprising considering the more hydrophobic character of ethanol. The $\Delta_t G°$ values are therefore positive in all cases which indicates an unfavourable transfer process.

Table 5.9 Solubilities of amino acids in methanol and ethanol at 298.15 K (in $mol.dm^{-3}$)

Amino Acid	Methanol	Ethanol
DL-ALA	$(8.99\pm0.18)\cdot10^{-3}$	$(1.28\pm0.34)\cdot10^{-3}$
GLY	$(4.55\pm0.21)\cdot10^{-3}$	$(1.17\pm0.06)\cdot10^{-3}$
DL-ILE	$(2.08\pm0.01)\cdot10^{-2}$	$(2.62\pm0.16)\cdot10^{-3}$
DL-LEU	$(5.98\pm0.08)\cdot10^{-3}$	$(7.39\pm0.74)\cdot10^{-4}$
DL-PHE	$(1.10\pm0.02)\cdot10^{-2}$	$(1.88\pm0.04)\cdot10^{-3}$
DL-TRP	$(3.68\pm0.17)\cdot10^{-3}$	$(4.78\pm0.18)\cdot10^{-4}$
DL-VAL	$(1.34\pm0.02)\cdot10^{-2}$	$(1.06\pm0.02)\cdot10^{-3}$

Table 5.10 Free energies of solution of amino acids in methanol and ethanol. Derived free energies of transfer from methanol to ethanol at 298.15 K (in $kJ.mol^{-1}$)

Amino Acid	Methanol	Ethanol	$\Delta_t G°$ (MeOH->EtOH)
DL-ALA	11.68	15.38	3.70
GLY	13.36	16.71	3.35
DL-ILE	9.60	14.23	4.63
DL-LEU	12.69	17.00	4.31
DL-PHE	11.18	16.48	5.30
DL-TRP	13.89	18.95	5.06
DL-VAL	10.69	16.09	5.40

Table 5.11 Solubilities of amino acid/18-Crown-6 complexes in methanol and ethanol at 298.15 K (in $mol.dm^{-3}$)

Amino Acid	Methanol	Ethanol
DL-ALA.18C6	$(2.59\pm0.02)\cdot10^{-1}$	$(3.56\pm0.02)\cdot10^{-2}$
GLY.18C6	$(1.63\pm0.02)\cdot10^{-1}$	$(2.46\pm0.18)\cdot10^{-2}$
DL-ILE.18C6	$(1.25\pm0.04)\cdot10^{-1}$	$(1.77\pm0.07)\cdot10^{-2}$
DL-LEU.18C6	$(4.14\pm0.21)\cdot10^{-2}$	$(2.05\pm0.20)\cdot10^{-2}$
DL-PHE.18C6	$(9.35\pm0.12)\cdot10^{-2}$	$(1.92\pm0.11)\cdot10^{-2}$
DL-TRP.18C6	$(3.55\pm0.14)\cdot10^{-2}$	$(1.56\pm0.01)\cdot10^{-2}$
DL-VAL.18C6	$(1.79\pm0.03)\cdot10^{-1}$	$(1.23\pm0.29)\cdot10^{-2}$

Table 5.12 Free energies of solution of amino acid/18-Crown-6 complexes in methanol and ethanol. Derived free energies of transfer from methanol to ethanol at 298.15 K (in $kJ.mol^{-1}$)

Amino Acid	Methanol	Ethanol	$\Delta_t G°$ (MeOH->EtOH)
DL-ALA.18C6	3.35	8.27	4.92
GLY.18C6	4.49	9.18	4.69
DL-ILE.18C6	5.14	10.00	4.86
DL-LEU.18C6	7.89	9.64	1.75
DL-PHE.18C6	5.87	9.80	3.93
DL-TRP.18C6	8.27	10.31	2.04
DL-VAL.18C6	4.26	10.90	6.64

Table 5.13 Solubilities of amino acid/Cryptand-222 complexes in methanol and ethanol at 298.15 K (in $mol.dm^{-3}$)

Amino Acid	Methanol	Ethanol
DL-ALA.222	$(4.47\pm0.04)\cdot10^{-2}$	$(1.04\pm0.11)\cdot10^{-2}$
GLY.222	$(4.81\pm0.30)\cdot10^{-2}$	$(8.10\pm0.08)\cdot10^{-3}$
DL-ILE.222	$(3.31\pm0.05)\cdot10^{-2}$	$(1.17\pm0.01)\cdot10^{-2}$
DL-LEU.222	$(2.16\pm0.19)\cdot10^{-2}$	$(8.30\pm0.09)\cdot10^{-3}$
DL-PHE.222	$(2.16\pm0.12)\cdot10^{-2}$	$(7.20\pm0.06)\cdot10^{-3}$
DL-VAL.222	$(3.21\pm0.12)\cdot10^{-2}$	$(1.01\pm0.13)\cdot10^{-2}$

Table 5.14 Free energies of solution of amino acid/Cryptand-222 complexes in methanol and ethanol. Derived free energies of transfer from methanol to ethanol at 298.15 K (in $kJ.mol^{-1}$)

Amino Acid	Methanol	Ethanol	$\Delta_t G°$ (MeOH->EtOH)
DL-ALA.222	7.70	11.31	3.61
GLY.222	7.52	11.93	4.41
DL-ILE.222	8.44	11.02	2.57
DL-LEU.222	9.50	11.87	2.37
DL-PHE.222	9.50	12.22	2.72
DL-VAL.222	8.52	11.38	2.86

Amino acid complexes with 18-Crown-6 and Cryptand-222 have been isolated in the solid state (section 3.7) and their solubilities determined in methanol and ethanol (Tables 5.11 and 5.13). The free energies of solution of these species as well as their free energies of transfer from methanol to ethanol have also been calculated. These data are listed in Tables 5.12 and 5.14.

The results in Tables 5.11 and 5.13 show that the complexed amino acids are much more soluble in the alcohols than the free amino acids, as a direct result from the binding of the amino acid to the macrocyclic ligand. For example in the case of glycine in methanol, the solubilities are enhanced by a factor of 35 for 18-Crown-6 and 10 for Cryptand-222 respectively.

The results enabled to:

i) compare the difference in the variation of the state of solvation of the uncomplexed and complexed amino acid upon transfer between the two alcohols

ii) test the validity of the complexation data (Tables 5.5-5.8) via the thermodynamic cycle

The free energy of transfer ($\Delta_t G°$) is the most significant parameter in the discussion of the solvation phenomena. The observation in Tables 5.10, 5.12 and 5.14 that:

$$\Delta_t G°[HAa]_{(MeOH->EtOH)} \approx \Delta_t G°[LHAa]_{(MeOH->EtOH)} \qquad 5.28$$

leads to the conclusion that the amino acids and their complexes with 18-Crown-6 and Cryptand-222 undergo similar changes in solvation when they are transferred from methanol to ethanol. This again provides some

evidence that amino acid -macrocyclic ligand complexes are exclusive. Therefore, the amino acids are most likely to be fully exposed to the reaction medium.

The availability of the stability constants (hence the free energies $\Delta_c G°$) for the complexation of amino acids with 18-Crown-6 and Cryptand-222 in methanol and ethanol enable the calculation of the $\Delta_t G°$ values for the amino acid between these solvents by an indirect method using the thermodynamic cycle (3.24) previously discussed[68]. The free energy of transfer ($\Delta_t G°$) of an amino acid between methanol and ethanol can be calculated from the following expression:

$$\Delta_t G°[HAa]_{(MeOH->EtOH)} = \Delta_c G°_{(MeOH)} - \Delta_c G°_{(EtOH)} + \Delta_t G°[LHAa]_{(MeOH->EtOH)} - \Delta_t G°[L]_{(MeOH->EtOH)} \qquad 5.29$$

$\Delta_t G°[L]_{(MeOH->EtOH)}$ for L = 18-Crown-6 was obtained from partition data of this ligand in the tetradecane-methanol[168] (0.01180) and in the tetradecane-ethanol (0.01156, see section 3.9) solvent systems. A $\Delta_t G°$ value of 0.05 $kJ.mol^{-1}$ for 18-Crown-6 from methanol to ethanol was then calculated. $\Delta_t G°[L]$ for Cryptand-222 was found to be equal to 0.12 $kJ.mol^{-1}$ [167]. The calculated free energies of transfer from methanol to ethanol of the amino acid-macrocyclic ligand complexes, using both 18-Crown-6 and Cryptand-222 as ligands are reported in Table 5.15. For comparison purposes, the $\Delta_t G°$ values obtained from direct solubility measurements of the amino acids in the two solvents are included in this table.

Table 5.15 Free energies of transfer of amino acids from methanol to ethanol at 298.15 K (in $kJ.mol^{-1}$)

Amino Acid	Direct Measurements	via cycle (18-Crown-6)[a]	via cycle (Cryptand-222)[b]
DL-ALA	3.70	4.22	4.40
GLY	3.35	2.33	4.01
DL-ILE	4.63	5.94	1.03
DL-LEU	4.31	5.80	1.45
DL-PHE	5.30	6.45	0.83
DL-TRP	5.06	7.06	———
DL-VAL	5.40	6.09	3.08

a: calculated from data in Tables 5.5, 5.6 and 5.12

b: calculated from data in Tables 5.7, 5.8 and 5.14

5.3.2 Enthalpies of Transfer

Eqn. 5.25 given in terms of free energies is now expressed in terms of enthalpies. Thus,

$$\Delta_t H°[i]\ (s_1 \rightarrow s_2) = \Delta_s H°[i]\ (s_2) - \Delta_s H°[i]\ (s_1) \qquad 5.30$$

where $\Delta_s H°$ are the enthalpies of solution of the species i in the appropriate solvent.

Due to the relatively low solubilities and the slow dissolution rate of the amino acids in the alcohols, it was not possible to carry out direct measurements of their heats of solution in these solvents. However, the amino acid complexes with the macrocyclic ligands (18-Crown-6 and Cryptand-222) are characterized by a higher solubility (Tables 5.11 and 5.13) and are readily dissolved in these media, so that their heats of solution could be determined. These data are listed in Tables 5.16-5.19.

Table 5.16 Standard enthalpies of solution of amino acid-18-Crown-6 complexes in methanol at 298.15 K

Complex	[HAa18C6] mol.dm^{-3}	$\Delta_s H°$ kJ.mol^{-1}
DL-ALA.18C6	$4.30 \cdot 10^{-4}$	34.94
	$3.62 \cdot 10^{-4}$	34.57
	$3.04 \cdot 10^{-4}$	33.75
	$2.46 \cdot 10^{-4}$	33.73
	($\Delta_s H°$=34.25±0.60 kJ.mol^{-1})	
GLY.18C6	$4.42 \cdot 10^{-4}$	34.97
	$3.58 \cdot 10^{-4}$	34.88
	$2.64 \cdot 10^{-4}$	36.00
	$2.46 \cdot 10^{-4}$	34.72
	($\Delta_s H°$=35.14±0.58 kJ.mol^{-1})	
DL-ILE.18C6	$4.04 \cdot 10^{-4}$	38.21
	$3.16 \cdot 10^{-4}$	39.39
	$2.28 \cdot 10^{-4}$	39.46
	$1.99 \cdot 10^{-4}$	40.26
	($\Delta_s H°$=39.33±0.84 kJ.mol^{-1})	
DL-LEU.18C6	$5.48 \cdot 10^{-4}$	37.35
	$5.02 \cdot 10^{-4}$	38.45
	$4.78 \cdot 10^{-4}$	38.14
	$2.70 \cdot 10^{-4}$	38.25
	($\Delta_s H°$=38.05±0.48 kJ.mol^{-1})	
DL-PHE.18C6	$3.78 \cdot 10^{-4}$	41.29
	$2.56 \cdot 10^{-4}$	40.93
	$1.44 \cdot 10^{-4}$	39.55
	($\Delta_s H°$=40.59±0.91 kJ.mol^{-1})	
DL-TRP.18C6	$4.32 \cdot 10^{-4}$	36.26
	$3.40 \cdot 10^{-4}$	36.77
	$2.64 \cdot 10^{-4}$	37.08
	($\Delta_s H°$=36.70±0.41 kJ.mol^{-1})	
DL-VAL.18C6	$2.04 \cdot 10^{-4}$	36.89
	$2.00 \cdot 10^{-4}$	38.86
	$1.91 \cdot 10^{-4}$	36.62
	($\Delta_s H°$=36.79±0.14 kJ.mol^{-1})	

Table 5.17 Standard enthalpies of solution of amino acid-18-Crown-6 complexes in ethanol at 298.15 K

Complex	[HAa18C6] mol.dm^{-3}	$\Delta_s H°$ kJ.mol^{-1}
DL-ALA.18C6	$2.60 \cdot 10^{-4}$	36.88
	$2.12 \cdot 10^{-4}$	35.42
	$1.25 \cdot 10^{-4}$	36.11
	$1.15 \cdot 10^{-4}$	36.14
	($\Delta_s H°$=36.17±0.85 kJ.mol^{-1})	
GLY.18C6	$1.96 \cdot 10^{-4}$	37.21
	$1.92 \cdot 10^{-4}$	37.53
	$1.76 \cdot 10^{-4}$	37.43
	$1.55 \cdot 10^{-4}$	36.59
	($\Delta_s H°$=37.19±0.41 kJ.mol^{-1})	
DL-ILE.18C6	$2.04 \cdot 10^{-4}$	42.41
	$1.89 \cdot 10^{-4}$	43.23
	$1.07 \cdot 10^{-4}$	43.39
	($\Delta_s H°$=43.03±0.53 kJ.mol^{-1})	
DL-LEU.18C6	$2.18 \cdot 10^{-4}$	39.66
	$1.96 \cdot 10^{-4}$	40.29
	$1.14 \cdot 10^{-4}$	40.05
	($\Delta_s H°$=39.99±0.31 kJ.mol^{-1})	
DL-PHE.18C6	$2.30 \cdot 10^{-4}$	43.34
	$1.74 \cdot 10^{-4}$	43.66
	$1.10 \cdot 10^{-4}$	43.04
	($\Delta_s H°$=43.35±0.31 kJ.mol^{-1})	
DL-TRP.18C6	$1.76 \cdot 10^{-4}$	41.36
	$1.43 \cdot 10^{-4}$	40.49
	$1.06 \cdot 10^{-4}$	41.19
	($\Delta_s H°$=41.01±0.46 kJ.mol^{-1})	
DL-VAL.18C6	$2.16 \cdot 10^{-4}$	40.63
	$1.80 \cdot 10^{-4}$	40.35
	$1.06 \cdot 10^{-4}$	40.18
	($\Delta_s H°$=40.39±0.22 kJ.mol^{-1})	
18-Crown-6	$6.40 \cdot 10^{-4}$	37.20
	$4.96 \cdot 10^{-4}$	37.07
	$4.50 \cdot 10^{-4}$	36.88
	$3.62 \cdot 10^{-4}$	37.04
	($\Delta_s H°$=37.05±0.16 kJ/mol^{-1})	

Table 5.18 Standard enthalpies of solution of amino acid-Cryptand-222 complexes in methanol at 298.15 K

Complex	[HAa222] mol.dm^{-3}	$\Delta_s H°$ kJ.mol^{-1}
DL-ALA.222	3.38 10^{-4}	31.85
	3.50 10^{-4}	34.43
	3.82 10^{-4}	38.32
	5.05 10^{-4}	31.85
	($\Delta_s H°$=33.45±1.22 kJ.mol^{-1})	
GLY.222	2.22 10^{-4}	35.35
	2.96 10^{-4}	35.82
	3.38 10^{-4}	34.45
	3.98 10^{-4}	34.95
	($\Delta_s H°$=35.14±0.57 kJ.mol^{-1})	
DL-ILE.222	2.12 10^{-4}	32.82
	2.74 10^{-4}	34.14
	3.32 10^{-4}	34.41
	3.80 10^{-4}	34.95
	($\Delta_s H°$=34.08±0.89 kJ.mol^{-1})	
DL-LEU.222	2.04 10^{-4}	35.85
	2.44 10^{-4}	36.58
	2.60 10^{-4}	37.19
	2.86 10^{-4}	37.77
	5.96 10^{-4}	35.42
	($\Delta_s H°$=37.22±0.88 kJ.mol^{-1})	
DL-PHE.222	2.92 10^{-4}	30.77
	1.71 10^{-4}	32.58
	1.89 10^{-4}	33.38
	3.94 10^{-4}	30.77
	($\Delta_s H°$=31.97±1.22 kJ.mol^{-1})	
DL-VAL.222	1.82 10^{-4}	32.82
	2.04·10^{-4}	33.61
	3.86 10^{-4}	32.56
	4.30 10^{-4}	32.14
	($\Delta_s H°$=32.59±0.70 kJ.mol^{-1})	

Table 5.19 Standard enthalpies of solution of amino acid-Cryptand-222 complexes in ethanol at 298.15 K

Complex	[HAa222] mol.dm^{-3}	$\Delta_s H°$ kJ.mol^{-1}
DL-ALA.222	1.38 10^{-4}	34.69
	1.84 10^{-4}	35.19
	2.92 10^{-4}	34.76
	2.98 10^{-4}	36.69
	($\Delta_s H°$=35.19±0.66 kJ.mol^{-1})	
GLY.222	1.05 10^{-4}	38.35
	1.19 10^{-4}	37.79
	1.56 10^{-4}	36.84
	2.04 10^{-4}	38.35
	($\Delta_s H°$=37.87±0.75 kJ.mol^{-1})	
DL-ILE.222	1.55 10^{-4}	34.46
	1.59 10^{-4}	36.65
	1.62 10^{-4}	36.91
	1.94 10^{-4}	36.72
	($\Delta_s H°$=36.68±0.18 kJ.mol^{-1})	
DL-LEU.222	1.10 10^{-4}	38.32
	1.27 10^{-4}	38.22
	1.69 10^{-4}	38.09
	7.62 10^{-5}	38.41
	($\Delta_s H°$=38.26±0.13 kJ.mol^{-1})	
DL-PHE.222	7.52 10^{-5}	35.92
	1.06 10^{-4}	36.87
	1.39 10^{-4}	36.08
	1.57 10^{-4}	34.52
	($\Delta_s H°$=35.85±0.97 kJ.mol^{-1})	
DL-VAL.222	5.18 10^{-5}	37.63
	1.23·10^{-4}	38.17
	1.35 10^{-4}	36.59
	1.78 10^{-4}	36.56
	($\Delta_s H°$=37.24±0.79 kJ.mol^{-1})	

The standard enthalpies of transfer of the amino acid-macrocyclic ligand complexes were then calculated (Table 5.20). Using the thermodynamic cycle (5.24) in terms of enthalpies, the $\Delta_t H°$ values for the free amino acids were obtained:

i) via the cycle involving 18-Crown-6 (18C6),

$$\Delta_t H°[HAa]_{(MeOH->EtOH)} = \Delta_t H°_{(MeOH)} - \Delta_t H°_{(EtOH)} + \Delta_t H°[18C6.HAa]_{(MeOH->EtOH)} - \Delta_t H°[18C6]_{(MeOH->EtOH)} \quad 5.31$$

ii) via the cycle involving Cryptand-222 (222),

$$\Delta_t H°[HAa]_{(MeOH->EtOH)} = \Delta_t H°_{(MeOH)} - \Delta_t H°_{(EtOH)} + \Delta_t H°[222.HAa]_{(MeOH->EtOH)} - \Delta_t H°[222]_{(MeOH->EtOH)} \quad 5.32$$

These data are reported in Table 5.21. Ideally, the $\Delta_t H°$ values for the amino acids should be equal independently of the ligand used in the cycle. The differences obtained for the two sets of data can be attributed to experimental errors. The standard deviations of each of the parameters used in Eqns. 5.31 and 5.32 are cummulative to give the standard deviations of the $\Delta_t H°$ values included in Table 5.21. Average values were therefore suggested and are also listed in Table 5.21.

The results show that in terms of enthalpy, the amino acids are more stable in methanol than in ethanol ($\Delta_t H°>0$). It is the lower enthalpic stability of these amino acids in ethanol which leads to the more favourable enthalpy of complexation observed for these compounds with the macrocyclic ligands in this solvent (results in section 5.2.2, pages 186-189).

A close examination of the data reported shows that:

$$\Delta_t H°[L]\ (MeOH\text{->}EtOH) \approx \Delta_t H°[LHAa]\ (MeOH\text{->}EtOH) \qquad 5.33$$

As a result, an interesting correlation (Eqn. 5.34) is found between the difference in enthalpies of complexation $\Delta(\Delta_c H°)$ in ethanol and methanol, and their corresponding $\Delta_t H°$ values. A plot of $\Delta(\Delta_c H°)$ versus $\Delta_t H°$ gives a straight line (Figure 5.9). This was observed with 18-Crown-6 and Cryptand-222.

$$\Delta_c H°(MeOH) - \Delta_c H°(EtOH) \approx \Delta_t H°[HAa](MeOH\text{->}EtOH) \qquad 5.34$$

Identity 5.33 reflects that when the protonated amino group of the amino acid is blocked (by the macrocyclic ligand), the strength of the interactions between the remaining part of the amino acid with methanol must be quite similar to that in ethanol and therefore, the transfer enthalpies of the amino acid-macrocyclic ligand complexes are similar to that of the ligand. When the amino group of the amino acid is blocked by the ligand, no direct interaction between this group and the solvent is possible. As a result, the $\Delta_t H°$ values for the amino acid-macrocyclic complexes are almost constant (Table 5.20).

Whereas the $\Delta_t H°$ values for the complexed amino acids are almost constant, the $\Delta_t H°$ values for the free amino acid vary with the nature of the amino acid side chain. $\Delta_t H°$ becomes more positive as the aliphatic chain attached to the α-carbon of the amino acid increases. It appears therefore that the variations observed in the $\Delta_t H°$ values for the aliphatic amino acids are directly related to the differences in $\Delta_c H°$ for these amino acids (section 5.2.2, pages 186-189).

Table 5.20 Standard enthalpies of transfer from methanol to ethanol of amino acid-macrocyclic ligand (18-Crown-6 and Cryptand-222) complexes at 298.15 K (in $kJ.mol^{-1}$)

Amino Acid-Crypand222	$\Delta_t H°$	Amino Acid-18Crown6	$\Delta_t H°$
DL-ALA.222	1.74	DL-ALA.18C6	1.92
GLY.222	2.73	GLY.18C6	2.05
DL-LEU.222	1.04	DL-LEU.18C6	1.95
DL-ILE.222	2.58	DL-ILE.18C6	3.70
DL-PHE.222	3.88	DL-PHE.18C6	2.76
DL-TRP.222	———	DL-TRP.18C6	4.32
DL-VAL.222	4.65	DL-VAL.18C6	3.60

Table 5.21 Standard enthalpies of transfer from methanol to ethanol of amino acids at 298.15 K (in $kJ.mol^{-1}$)

Amino Acid	via cycle (18-Crown-6)[a]	via cycle (Cryptand-222)[b]	average value
DL-ALA	8.05	5.63	6.84
GLY	10.72	9.84	10.28
DL-ILE	17.72	12.19	14.95
DL-LEU	7.25	7.58	7.41
DL-PHE	17.80	12.91	15.35
DL-TRP	13.81	———	———
DL-VAL	21.93	19.17	20.55

a: calculated from data in Tables 5.5, 5.6 and 5.20

b: calculated from data in Tables 5.7, 5.8 and 5.20

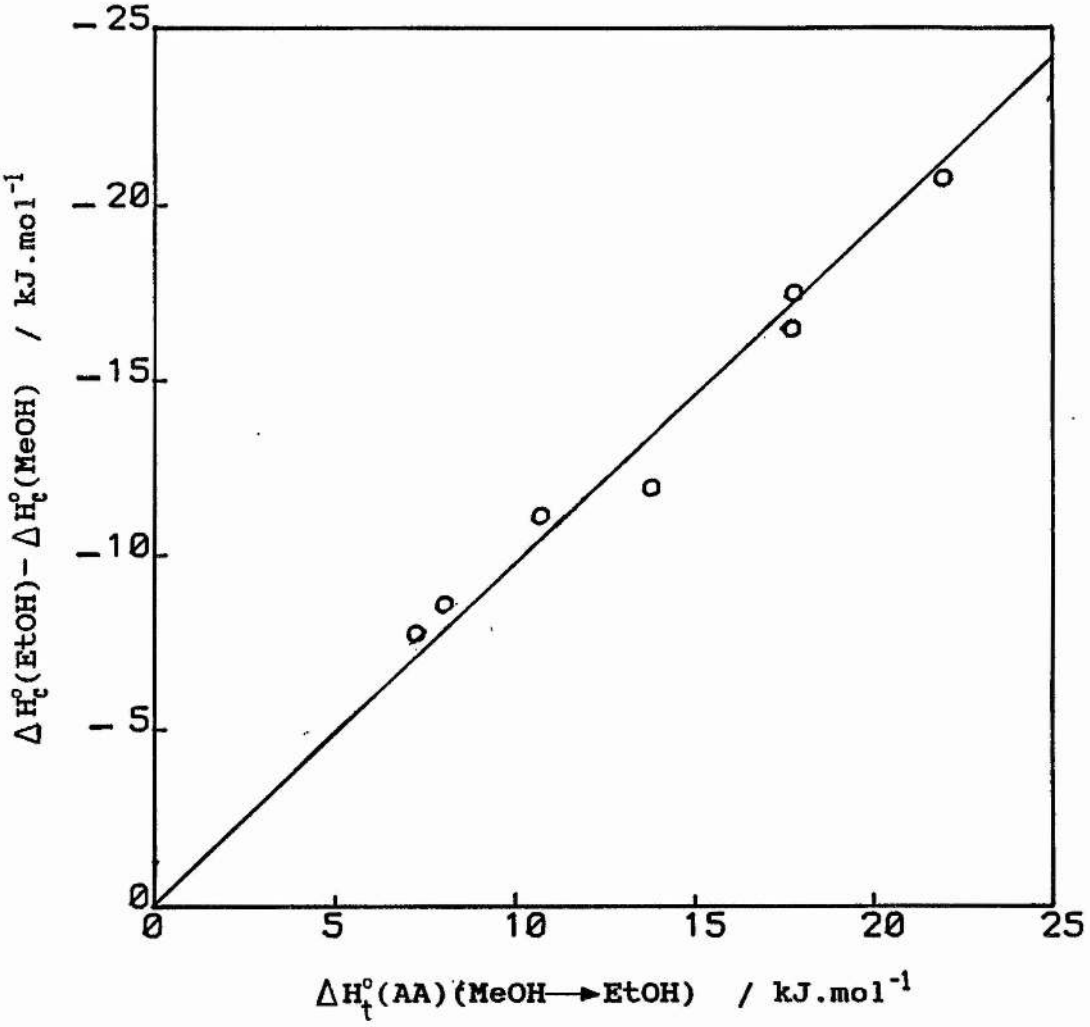

Figure 5.9 Linear correlation between $\Delta_c H°_{(MeOH)}$ - $\Delta_c H°_{(EtOH)}$ and $\Delta_t H°[HAa]$ (MeOH->EtOH) for the complexation of amino acids with macrocyclic ligands in methanol and ethanol

5.3.3 Standard entropies of transfer

The entropies of transfer of the amino acids from methanol to ethanol were derived from the free energy and enthalpy data. These are listed in Table 5.22.

Analysis of the results in Table 5.22 shows that the transfer of the free amino acids from methanol to ethanol is entropically favoured. The striking feature in these results is the difference in the $\Delta_t S°$ values for the free amino acid (positive) and for the complexed amino acid (slightly positive or slightly negative). This reflects the different environmental changes of the amino group in the amino acid (solvent) and the amino acid complex (macrocyclic ligand).

The more favourable entropy of transfer for the amino acid from methanol to ethanol results in a more favourable entropy of complexation of this amino acid in methanol than in ethanol. This observation clearly shows that the entropy term, like the enthalpy term, in the complexation process of amino acids with macrocyclic ligands reflects the competition between the ligand and the solvent for the amino acid.

Table 5.22 Standard entropies of transfer of amino acids and their complexes with 18-Crown-6 and Cryptand-222, from methanol to ethanol at 298.15 K (in $J.mol^{-1}.K^{-1}$)

HAa	$\Delta_t S^\circ$	HAa.18Crown6	$\Delta_t S^\circ$	HAa.Cryptand222	$\Delta_t S^\circ$
DL-ALA	14.6	DL-ALA.18C6	-10.1	DL-ALA.222	-6.3
GLY	24.7	GLY.18C6	-8.9	GLY.222	-5.6
DL-ILE	43.9	DL-ILE.18C6	6.5	DL-ILE.222	0.3
DL-LEU	9.9	DL-LEU.18C6	-9.8	DL-LEU.222	-4.5
DL-PHE	41.9	DL-PHE.18C6	-3.9	DL-PHE.222	3.9
DL-TRP	29.3	DL-TRP.18C6	7.6	DL-TRP.222	——
DL-VAL	55.4	DL-VAL.18C6	-10.2	DL-VAL.222	6.0

5.4 Applications to Processes of Biological Importance

5.4.1 Solubility Enhancement

As already mentioned earlier, macrocyclic ligands have the property to increase the solubilities of the species they complex. Therefore, it was decided to carry out some quantitative measurements on the increase in the solubility of amino acids in the alcohols using a UV-spectrophotometric method (section 3.11). Figures 5.10-5.12 shows the spectra of the solubility enhancement of DL-Phenylalanine in methanol, ethanol and propan-2-ol upon addition of 18-Crown-6. These solubility data were plotted as a function of the concentration of 18-Crown-6 and are shown in Figure 5.13.

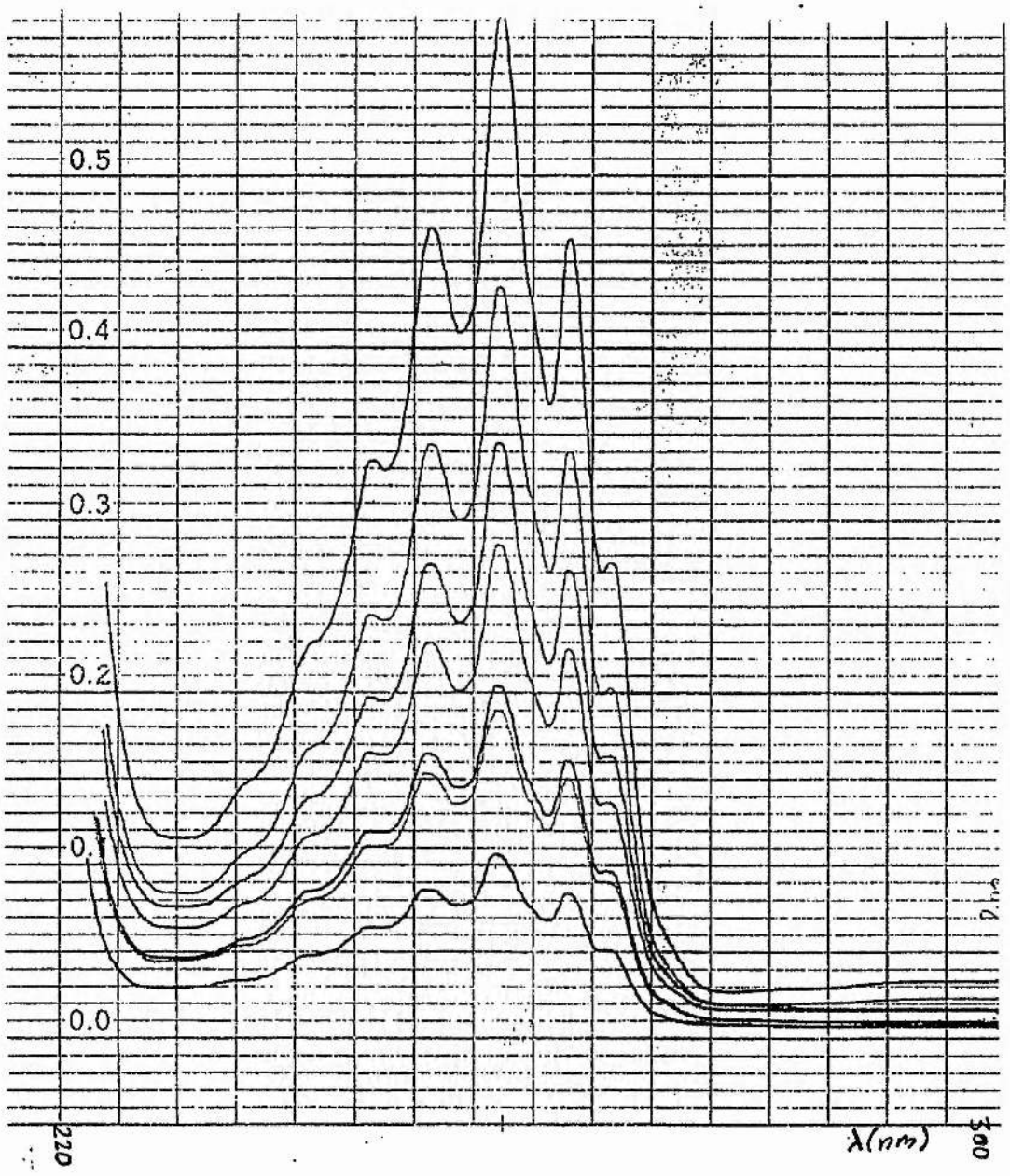

Figure 5.10 Spectrum of DL-Phenylalanine in methanol

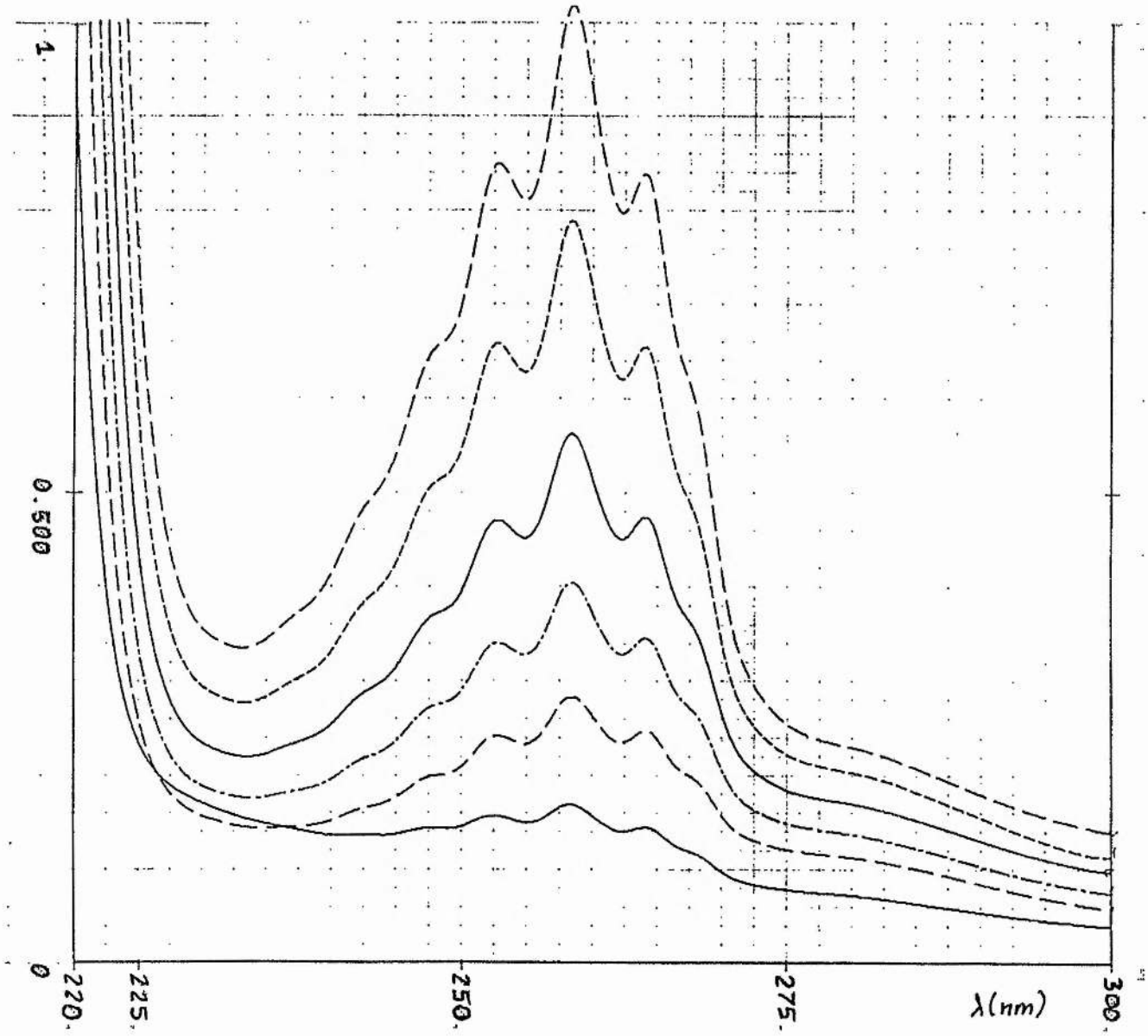

Figure 5.11 Spectrum of DL-Phenylalanine in ethanol

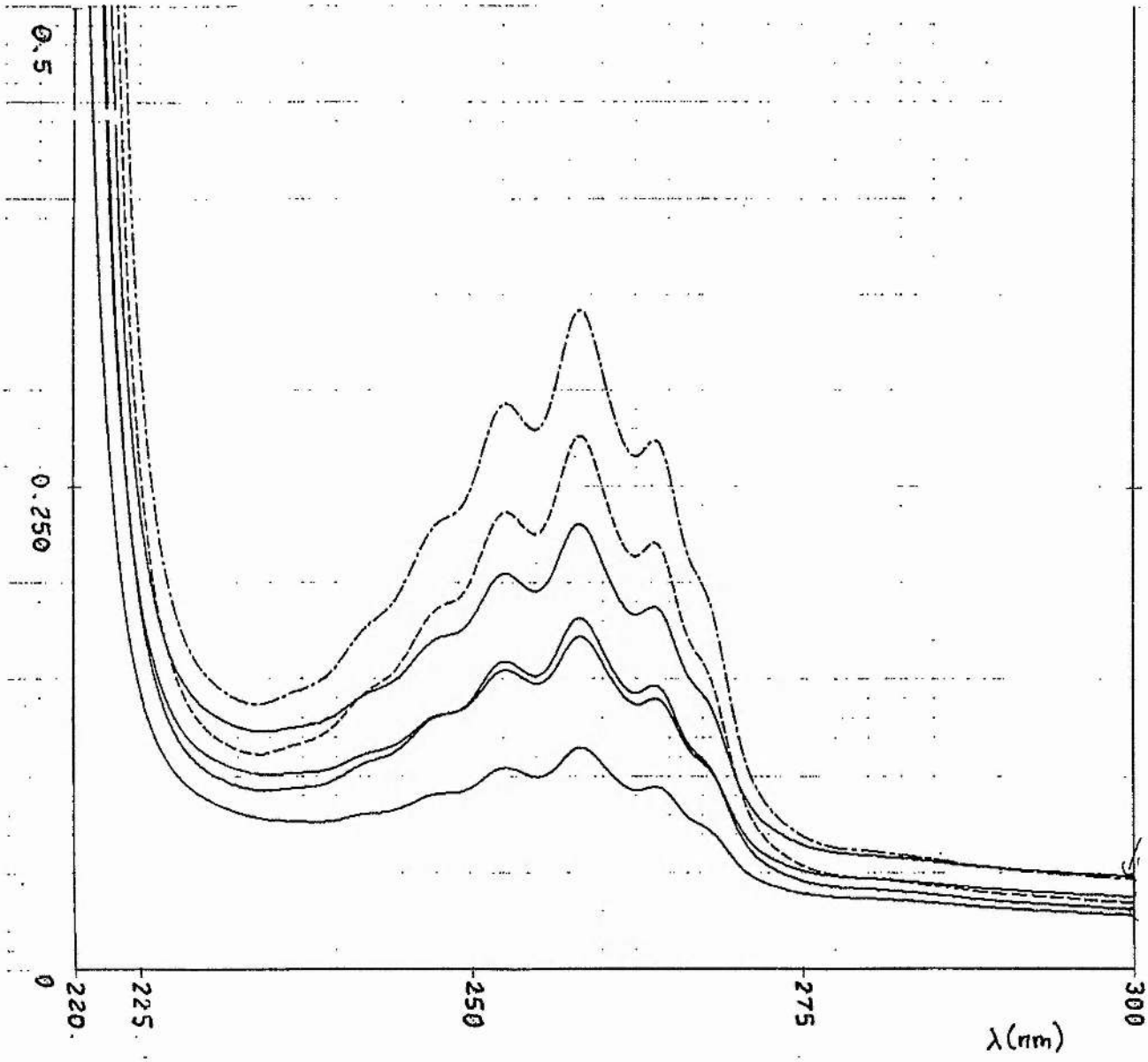

Figure 5.12 Spectrum of DL-Phenylalanine in propan-2-ol

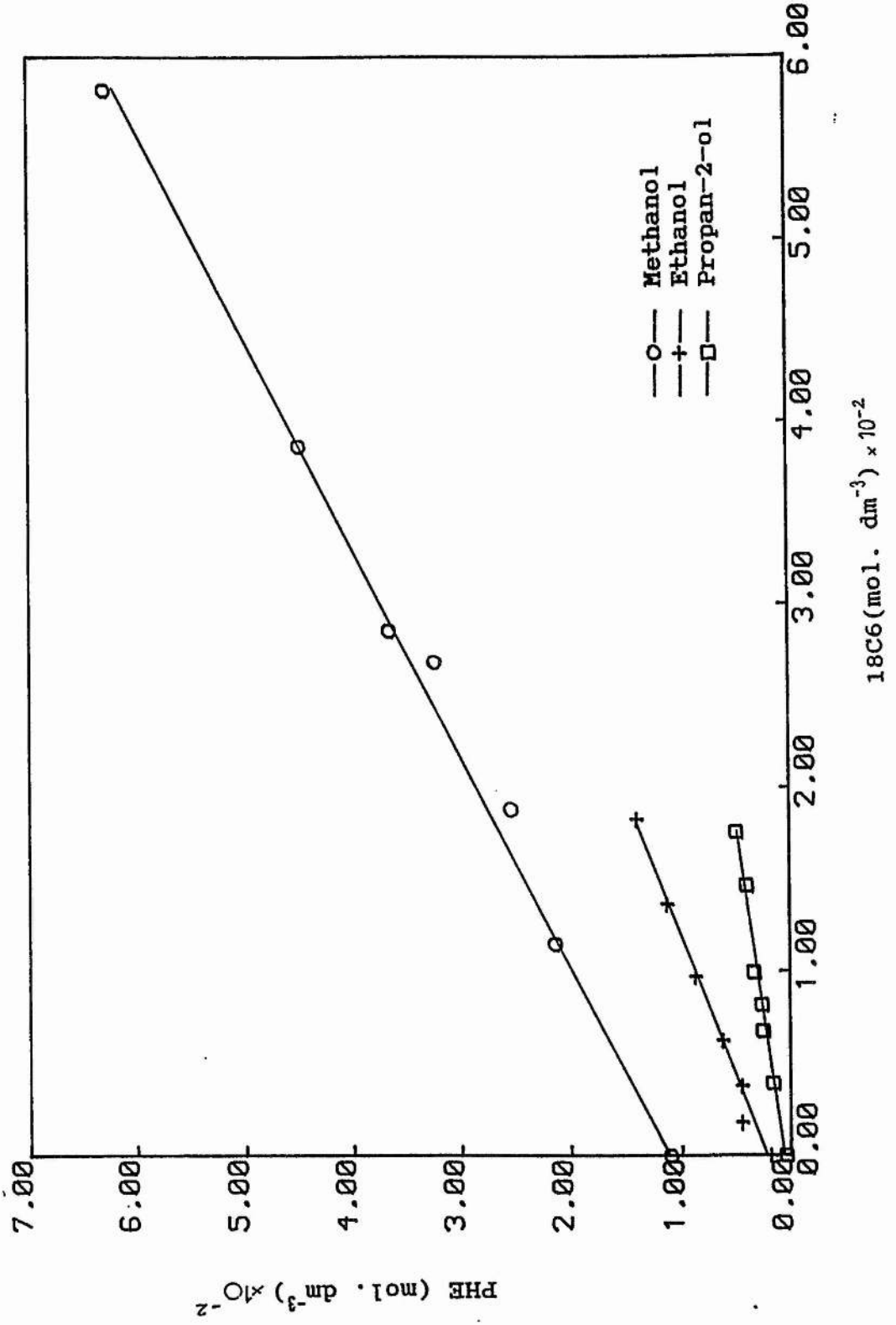

Figure 5.14 Solubility enhancement of DL-Phenylalanine as a function of 18-Crown-6 concentration

5.4.2 Extraction Process

The relevant process for the transport of amino acids across cell membranes and for the solvent extraction may be represented as:

$$HAa\ (H_2O) + L\ (s) \longrightarrow LHAa\ (s) \qquad 5.35$$

which can be decomposed into two steps:

i) the transfer of the amino acid from water to the non-aqueous solvent (s)

$$HAa\ (H_2O) \longrightarrow HAa\ (s) \qquad 5.36$$

ii) the complexation of the amino acid and the macrocyclic ligand in the non-aqueous phase

$$HAa\ (s) + L\ (s) \longrightarrow LHAa\ (s) \qquad 5.37$$

Therefore the extraction constant K_{ex} may be written as:

$$K_{ex} = K_t.K_s \qquad 5.38$$

For the determination of K_t, the solubilities of the amino acid in water (Table 5.23) and in the non-aqueous solvents (Table 5.9) must be taken into account. If the activity coefficient of the amino acids in water and in the alcohols are assumed to be unity, K_t is determined as:

$$K_t = \frac{[HAa]_{(s)}}{[HAa]_{(H_2O)}} \qquad 5.39$$

Table 5.23 Solubilities of amino acids in water at 298.15 K[169] (in mol.dm^{-3})

DL-ALA	1.8767
GLY	3.3288
DL-ILE	0.1699
DL-LEU	0.0755
DL-PHE	0.0854
DL-TRP	0.0107*
DL-VAL	0.6055

* this work

Four different processes have been considered:

i) the extraction of the amino acid from water to methanol using 18-Crown-6 as extracting agent

ii) the extraction of the amino acid from water to ethanol using 18-Crown-6 as extracting agent

iii) the extraction of the amino acid from water to methanol using Cryptand-222 as extracting agent

iv) the extraction of the amino acid from water to ethanol using Cryptand-222 as extracting agent

The results (Table 5.24-5.27) show that despite the lack of selectivity observed in the complexation processes of the amino acids with 18-Crown-6 and Cryptand-222 in methanol and in ethanol, the extraction of these amino acids from water to the alcohols by these ligands is a relatively selective process. The selectivity determinant step is the transfer of the amino acid from water to the alcohols, as reflected by the K_t values.

It must be emphasised that the processes considered here are only hypothetical since water is essentially a miscible solvent with methanol and ethanol. Therefore, other reaction media such as chloroform and octanol would be more representative of biological membranes. It would also be interesting to use other ligands such as the benzo substituted crown ethers which are only sparingly soluble in water and therefore, are better models for biological carriers.

Table 5.24 K_t, K_c and K_{ex} for the extraction of amino acids from water to methanol by 18-Crown-6, at 298.15 K

Amino Acid	K_t	K_c	K_e
DL-ALA	$4.79 \cdot 10^{-3}$	3890	18
GLY	$1.36 \cdot 10^{-3}$	9550	13
DL-ILE	$1.22 \cdot 10^{-1}$	1479	80
DL-LEU	$7.92 \cdot 10^{-2}$	2239	77
DL-PHE	$1.29 \cdot 10^{-1}$	1412	82
DL-TRP	$3.44 \cdot 10^{-1}$	1148	95
DL-VAL	$2.22 \cdot 10^{-2}$	1549	34

Table 5.25 K_t, K_c and K_{ex} for the extraction of amino acids from water to ethanol by 18-Crown-6, at 298.15 K

Amino Acid	K_t	K_c	K_s
DL-ALA	$6.82 \cdot 10^{-4}$	4898	3
GLY	$3.51 \cdot 10^{-4}$	6456	2
DL-ILE	$1.89 \cdot 10^{-2}$	2570	48
DL-LEU	$1.39 \cdot 10^{-2}$	4168	58
DL-PHE	$1.51 \cdot 10^{-2}$	2291	34
DL-TRP	$4.47 \cdot 10^{-2}$	2630	117
DL-VAL	$2.51\ 10^{-2}$	2570	6

Table 5.26 K_t, K_c and K_{ex} for the extraction of amino acids from water to methanol by Cryptand-222, at 298.15 K

Amino Acid	K_t	K_c	K_e
DL-ALA	$4.79 \cdot 10^{-3}$	1659	8
GLY	$1.36 \cdot 10^{-3}$	2290	3
DL-ILE	$1.22 \cdot 10^{-3}$	6456	787
DL-LEU	$7.92 \cdot 10^{-2}$	2398	190
DL-PHE	$1.29 \cdot 10^{-1}$	2951	380
DL-TRP	$3.44 \cdot 10^{-2}$	5248	1805
DL-VAL	$2.22 \cdot 10^{-2}$	2398	190

Table 5.27 K_t, K_c and K_{ex} for the extraction of amino acids from water to ethanol by Cryptand-222, at 298.15 K

Amino Acid	K_t	K_c	K_e
DL-ALA	$6.82\ 10^{-4}$	2399	2
GLY	$3.51\ 10^{-4}$	2691	1
DL-ILE	$1.89\ 10^{-2}$	7413	140
DL-LEU	$1.39\ 10^{-2}$	2138	29
DL-PHE	$1.51\ 10^{-2}$	1445	22
DL-VAL	$2.51\ 10^{-3}$	1585	4

CHAPTER 6

EXTRACTION OF AMINO ACIDS FROM METHANOL BY RESINS CONTAINING DIBENZO-18-CROWN-6 AS ANCHOR GROUPS

6.1 Generalities

By incorporating macrocyclic ligands into a polymeric matrix, Blasius[170-178] and co-workers prepared a new type of extracting agents capable of forming complexes with inorganic and organic species. The structure of some of these agents which mainly contain crown ethers and cryptands as anchor groups have been thoroughly investigated (Figure 6.1). The notation § was introduced by Blasius to indicate the resin phase.

Polymeric resins of this type have numerous advantageous properties[174]. They are highly resistant to chemicals, temperature and radiolysis. They have neutral ligands as anchor groups and the electrical neutrality is maintained by the simultaneous uptake of cations and anions. The cations and anions usually loose at least a part of their solvation shell when uptaken by the resin. They actually complex with the resin in a similar manner than with the monomer ligands. Therefore, the stability of the complexes formed with the resin depends also on the type of ion, the solvent, the size of the crown ether ring, the number, type and basicity of the hetero atoms of the ligand.

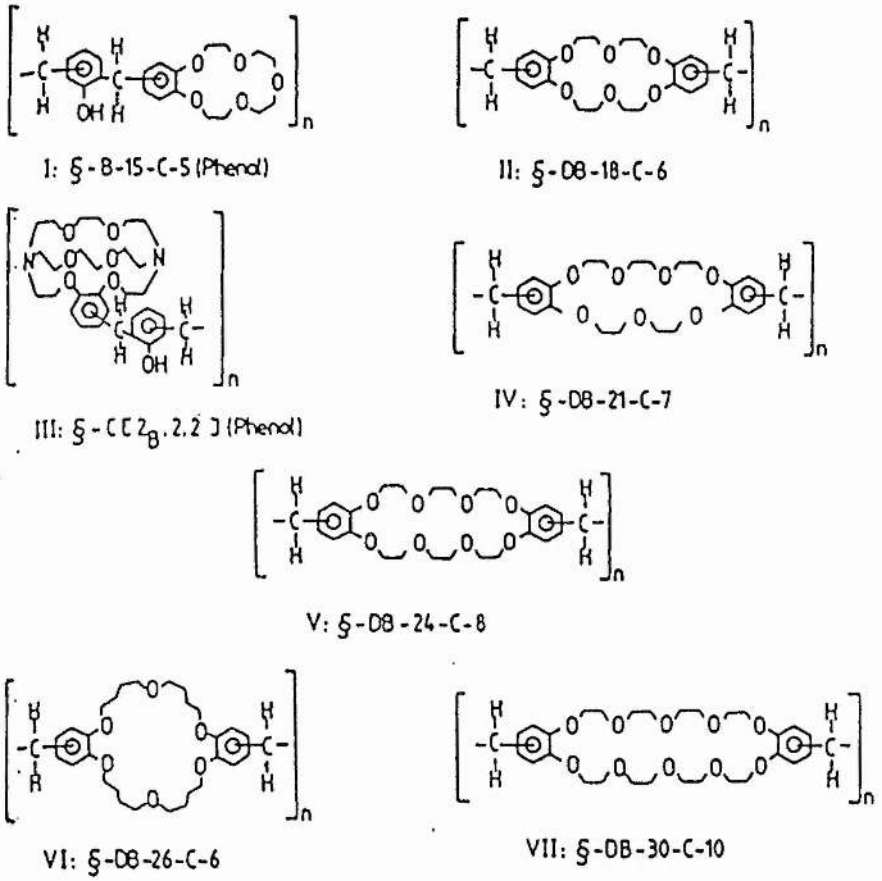

Exchangers with cyclic polyethers as anchor groups. Hetero atoms: O, N. I = Benzo-15-crown-5; II = dibenzo-18-crown-6; III = cryptate [2B.2.2]; IV = dibenzo-21-crown-7; V = dibenzo-24-crown-8; VI = dibenzo-26-crown-6; VII = dibenzo-30-crown-10.

Figure 6.1 Structure of polymeric resins containing cyclic polyethers and cryptands as anchor groups

The major advantage of the use of these resins is the possibility of recycling them, by a simple wash with water. This leads to an economic way of using the macrocyclic ligands as extracting agents.

Resins with macrocyclic ligands as anchor groups have many possible applications in inorganic and organic chemistry (Table 6.1)[174].

Table 6.1 Applications of exchangers with cyclic polyethers as anchor groups

Analytical Chemistry

Separation of cations (e.g. alkali and alkaline
earth metals,
heavy and precious metals)
Separation of anions (e.g. halides and pseudo halides)
Separation of organic compounds
Trace enrichment (e.g. radionuclides)
Determination of water in inorganic and organic compounds

Column chromatography, thin-layer chromatography
Electrophoresis
Ion-sensitive membrane

Preparative Chemistry

Salt conversions (e.g. preparation of iodides and thiocyanates)
Catalysis of organic reactions with activated anions: nucleophilic substitutions, eliminations, additions, saponifications, carbonyl reactions, oxidations, reductions, Wittig reactions, organometallic reactions, rearrangements, extrusions (CO_2, N_2), isomerizations, polymerizations

The resins have also been used as extracting agents for the hydrogen bonding species. Interactions between urea, thiourea and phenol in aqueous solutions and §DB18C6 were studied by Danil de Namor and Sigstad[175]. The results indicate that 1:1 thiourea-crown ether and 4:1 phenol-crown ether complexes are formed in the resin phase. The extraction processes were in all cases enthalpy favoured and entropy unfavoured.

As a continuation of the study involving the complexation of amino acids with macrocyclic ligands, the interaction of these amino acids with the polymeric crown ethers has been considered.

6.2 Capacities of §DB18C6 with Amino Acids in Methanol at 298.15 K

Resins containing Dibenzo-18-Crown-6 (§DB18C6) are commercially available (Poly-Dibenzo-18-Crown-6, Fluka). Their water content (1.25 %) was removed by heating them up to 130°C in a drying pistol. The resins were then left in a desiccator containing phosphorus pentoxide as drying agent for several days. Microanalysis showed that almost all the water has been removed (Table 6.2).

Table 6.2 Microanalysis of §DB18C6

	%C	%H	%O
calculated	68.39	6.73	24.87
found	68.02	7.01	24.97

The first step in this study was to determine the capacity of §DB18C6. It is important to distinguish between the total capacity (c_T) and the effective capacity (c_E) of an exchanger. The total capacity of the resin is a measure of the number of moles of crown ether units per gram of resin, whereas the effective capacity is referred to the actual number of moles of molecules uptaken by the resin under specified conditions. In general the total and the effective capacities are different.

The value of the total capacity of §DB18C6 reported by Blasius[176] was of $2.59 \cdot 10^{-3}$ mol.g^{-1}. In this work the value has been derived from the microanalytical data (Table 6.2) and is found to be $2.60 \cdot 10^{-3}$ mol.g^{-1}. The effective capacities (c_E) of §DB18C6 were determined for a number of amino acids in methanol at 298.15 K. The experimental procedure followed is

described in Section 3.10. These results obtained by triplicate are reported in Table 6.3.

Table 6.3 Effective capacities (c_E) of §DB18C6 for a series of amino acids in methanol at 298.15 K

Amino Acid	c_E/mol.g^{-1}
DL-ALA	$1.27 \cdot 10^{-3}$
GLY	$1.62 \cdot 10^{-3}$
DL-ILE	$9.86 \cdot 10^{-4}$
DL-LEU	$9.81 \cdot 10^{-4}$
DL-PHE	$7.91 \cdot 10^{-4}$
DL-VAL	$9.48 \cdot 10^{-4}$

The results show that §DB18C6 can be used as extracting agent for the amino acids in methanol. The amount uptaken by the resin varies with the nature of the amino acid. In the series studied, the effective capacity is highest for glycine and lowest for DL-phenylalanine. These differences may certainly be attributed to steric hindrances of the amino acid side chain. The structural aspects of the resin must also be taken into consideration; the resin being a compact framework, its crown ether units can therefore not undergo rearrangements or reorientation to adapt themselves to the guest molecules. Thus, the role of the amino acid side chain is more important in the process studied here than in the complexation process of the amino acids with the free ligand in solution (Chapter 5). The capacity of §DB18C6 for the amino acids in methanol decreases in the following order:

$$GLY > ALA > LEU \approx ILE \approx VAL > PHE$$

This sequence corresponds also to the order of increase of the bulkiness of the amino acid side chain.

Steric hindrances may also be responsible for the unsaturation of the resin with the amino acids. In the systems studied here, the capacity of §DB18C6 does not reach its maximum saturation state ($2.60 \cdot 10^{-3}$ mol.g^{-1}). Hidden crown ether units in the resin framework may not be accessible to the amino acids, especially those having bulky side chains like DL-phenylalanine. Blasius[174] also observed that in methanol, the maximum capacities reached for different guest molecules are between 1 and 2 millimole per gram of resin.

6.3 Distribution of the Amino Acids between §DB18C6 and Methanol at 298.15 K.

The distribution coefficient (D) of the amino acids between §DB18C6 and methanol were obtained using the following expression:

$$D = c_{\S DB18C6}/[HAa]_e \qquad 6.1$$

where $[HAa]_e$ ($mol.dm^{-3}$) is the equilibrium concentration of the amino acid in the methanolic solution and, $c_{\S DB18C6}$ ($mol.g^{-1}$) is the amount of the amino acid in the resin phase, as determined by

$$c_{\S DB18C6} = \frac{([HAa]_i - [HAa]_e) \cdot V}{W_r} \qquad 6.2$$

In expression 6.2, $[HAa]_i$ represents the initial molar concentration of amino acid in methanol, W_r (g) the amount of resin used and V (dm^3) the volume of the solution.

The concentration dependence of the distribution coefficients at 298.15 K is shown in Figure 6.2. The data to calculate these values were taken from Tables 6.7-6.12.

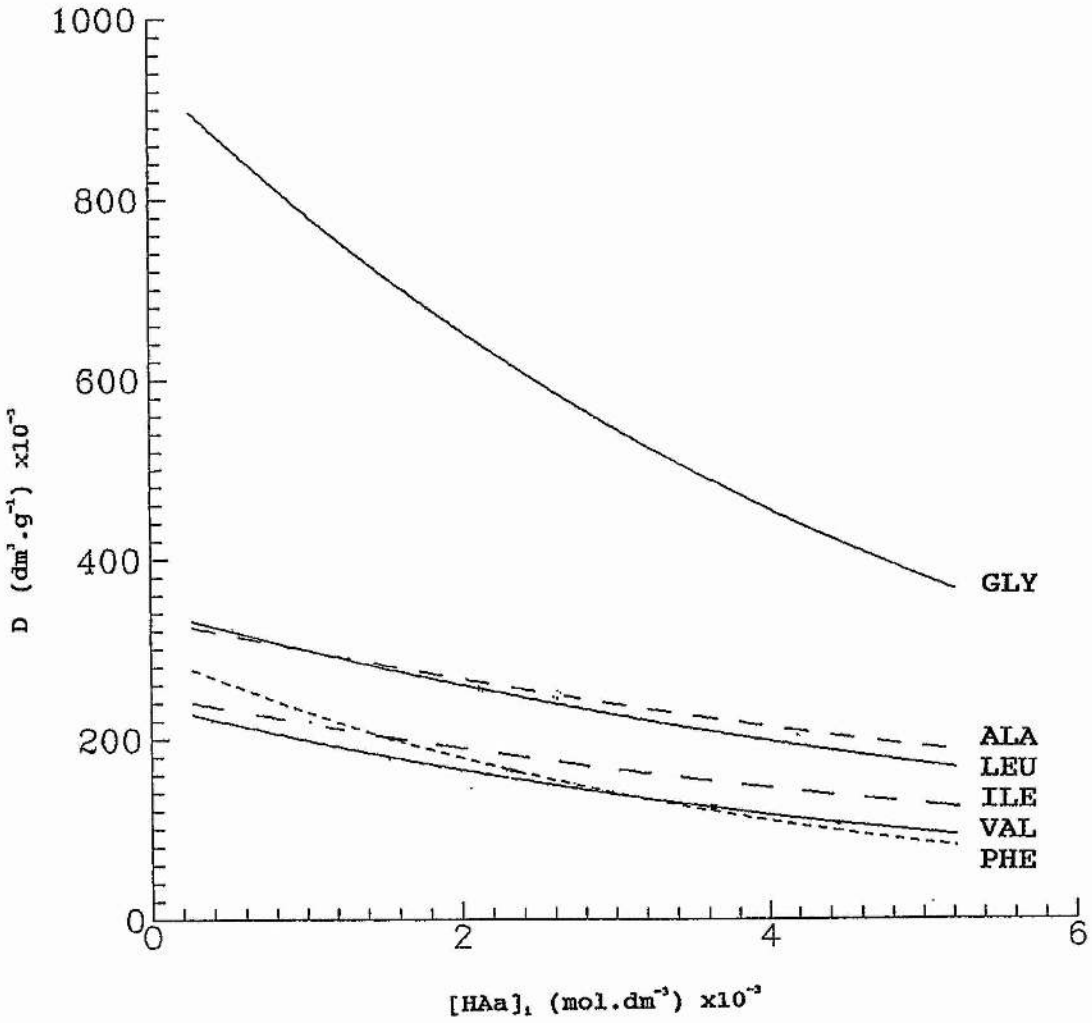

Figure 6.2 Variation of the distribution coefficient of the amino acids between §DB18C6 and methanol as a function of the initial concentration of amino acid, at 298.15 K

The distribution coefficients are strongly dependent on the initial concentration of the amino acid in the methanolic phase. Distribution values generally decreases with increasing solution concentration, this effect being more pronounced for glycine than for the other amino acids. This decrease could be attributed to an increase in interaction in the resin phase as the number of sites available for extraction decreases.

In order to investigate the possibility of selectively extracting the different amino acids, it seems relevant to compare the separation factor for two amino acids at different initial concentrations. The separation factor between an amino acid A and an amino acid B is given by:

$$S_B^A = \frac{D_A}{D_B} \qquad 6.3$$

where D_A and D_B are the distribution coefficient of the amino acids A and B respectively. It has been suggested[176] that a good separation between two species can be achieved if the separation factor differs at least 0.2 units from 1. Figure 6.2 shows that the separation factor for glycine with the other amino acids is at least equals to 2 up to a concentration of $4 \cdot 10^{-3}$ $mol.dm^{-3}$. Therefore, it can be concluded that glycine could be separated from the other amino acids in this range of concentrations. It can also be observed that the distribution coefficients for DL-Alanine and DL-Leucine are slightly higher than those for DL-Isoleucine, DL-Valine and DL-Phenylalanine leading to a separation factor of about 1.5. Thus, separation of the former amino acids from the latter ones could be achieved.

6.4 Equilibrium Constant for the extraction of Amino Acids from Methanol by §DB18C6 at 298.15 K

The extraction of an amino acid (HAa) from methanol (MeOH) by §DB18C6 can be represented as:

$$HAa_{(MeOH)} + n.\overline{DB18C6} \rightleftharpoons \overline{DB18C6_nHAa} \qquad 6.4$$

where the barred formula refers to the resin phase. n is the fraction of units of DB18C6 occupied by the amino acid and corresponds to the ratio between the total capacity and the effective capacity of the resin:

$$n = c_T/c_E \qquad 6.5$$

Process 6.4 is characterized by the apparent extraction constant K_{ex}:

$$K_{ex} = \frac{\overline{x}_{(LnHAa)}}{[HAa]_e.[1-n.\overline{x}_{(LnHAa)}]^n} \qquad 6.6$$

$x_{(LnHAa)}$ and $[1-n.x_{(LnHAa)}]$ are respectively the mole fractions of the amino acid and the free ligand in the resin phase. $[HAa]_e$ is the molar equilibrium concentration of amino acid in methanol. $x_{(LnHAa)}$ can be defined as:

$$\overline{x}_{(LnHAa)} = \frac{c_{\S DB18C6}}{c_T} \qquad 6.7$$

where $c_{\S DB18C6}$ is the amount of amino acid uptaken per gram of dry resin, in a volume V (ml) of solvent and for a weight W_r (g) of resin as defined by Expression 6.2.

Table 6.4 Extraction constants (log K_{ex}) of amino acids form methanol by §DB18C6 at 298.15 K. Corresponding n value

Amino Acid	log K_{ex}	n
DL-ALA	2.52 ± 0.26	2.04
GLY	2.89 ± 0.21	1.60
DL-ILE	2.31 ± 0.18	2.64
DL-LEU	2.68 ± 0.29	2.65
DL-PHE	2.62 ± 0.20	2.91
DL-VAL	2.39 ± 0.28	2.74

The extraction isotherms are shown in Figure 6.3. The extraction constant is usually the relevant parameter for discussing the selectivity of extraction. It can nevertheless be seen from Eqn. 6.6. that K_{ex} is very much dependent on the n value. When the n value is higher (lower capacity), a higher value for log K_{ex} is found. For comparison purposes between the different extraction constants of the amino acids, the n value should be similar. K_{ex} is therefore not an absolute parameter in the discussion of the selectivity of extraction.

6.5 Thermodynamic Parameters for the Extraction of Amino Acids from Methanol by §DB18C6 at 298.15 K

The thermodynamic parameters ($\Delta_{ex}G$, $\Delta_{ex}H$, $\Delta_{ex}S$) associated with the extraction process represented by *Eqn. 6.4* have been determined for a series of amino acids. It must be emphasized that these parameters are only apparent due to the difficulty to define the standard state in the resin phase. The free energy of extraction was derived from the extaction constant:

$$\Delta_{ex}G = -RT.\ln K_{ex} \qquad 6.8$$

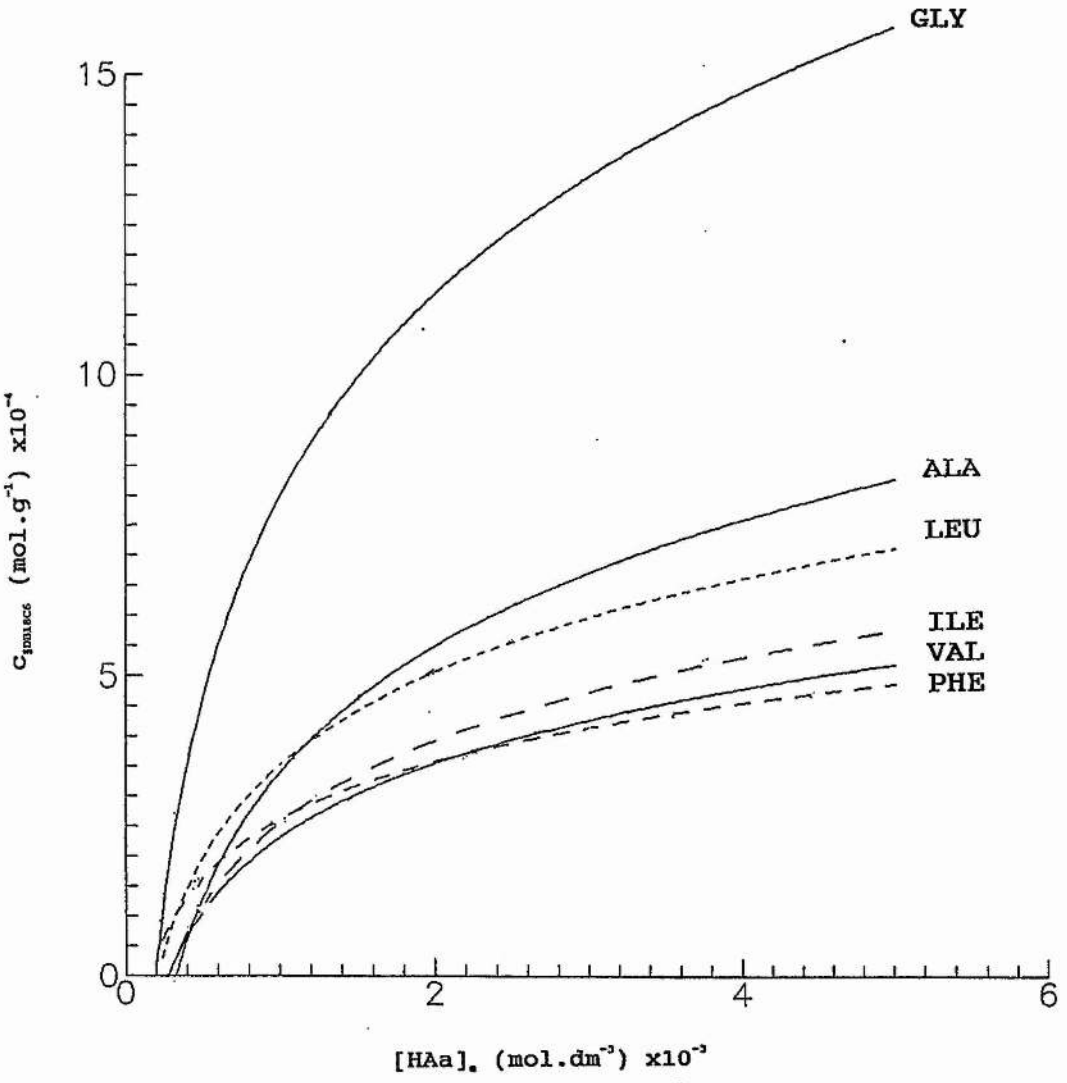

Figure 6.3 Extraction isotherms of amino acids from methanol by §DB18C6 at 298.15 K

The enthalpy of extraction was obtained by measuring the heats of reaction between the resin and a solution of amino acid in methanol. The experimental procedure was described in Section 3.4. The reaction was started by breaking a glass ampoule containing the resin in a methanolic solution of amino acid, therefore the measured heat (Q) was first corrected for the heat of ampoule-breaking (see section 3.4.4.3). The heat of reaction obtained (Q_r), after corrections with ampoule-breaking, corresponds not only to the actual heat of extraction (Q_{ex}) but also to the heat of immersion (Q_I) of the resin in methanol and the heat of dilution (Q_D). The heat of extraction has therefore been calculated as:

$$Q_{ex} = Q_r - Q_I - Q_D \qquad 6.9$$

The ($Q_I + Q_D$) values were determined as the intercepts of the plots Q_r versus $c_{\S DB18C6}$ (Figure 6.4). The values found are reported in Table 6.6, the average value being equal to -41.08 $J.g^{-1}$. The enthalpy for the extraction was then calculated as:

$$\Delta_{ex}H = Q_{ex}/c_{\S DB18C6} \qquad 6.10$$

These values are reported in Table 6.5. The entropy of extraction obtained by combining the free energy and the enthalpy data are also included in Table 6.5.

The data in Table 6.5 show that the extraction process of the amino acids from methanol by §DB18C6 is favoured enthalpically ($\Delta_{ex}H < 0$). The unfavourable entropy term observed for this process ($\Delta_{ex}S < 0$) might be an indication that the compact framework of the resin converts the amino acids into more rigid structures when these are uptaken by §DB18C6.

Table 6.5 Free energy, enthalpy and entropy of extraction of amino acids from methanol by §DB18C6 at 298.15 K

Amino Acid	$\Delta_{ex}G$/kJ.mol^{-1}	$\Delta_{ex}H$/kJ.mol^{-1}	$\Delta_{ex}S$/J.K^{-1}.mol^{-1}
DL-ALA	-7.16	-8.32 ± 0.84	-4.7
GLY	-6.24	-11.66 ± 1.22	-18.2
DL-LEU	-6.64	-10.70 ± 0.91	-13.6
DL-ILE	-5.72	-10.69 ± 0.50	-16.6
DL-PHE	-6.49	-6.18 ± 0.41	1.0
DL-VAL	-5.92	-7.88 ± 0.97	-6.5

Table 6.6 Extrapolated ($Q_I + Q_D$) values for the §DB18C6 in methanol at 298.15 K. Results derived from the plots in Figure 6.4

($Q_I + Q_D$) /J.g^{-1}	Plot
-39.978	1
-39.134	2
-41.827	3
-41.752	4
-41.221	5
-42.199	6

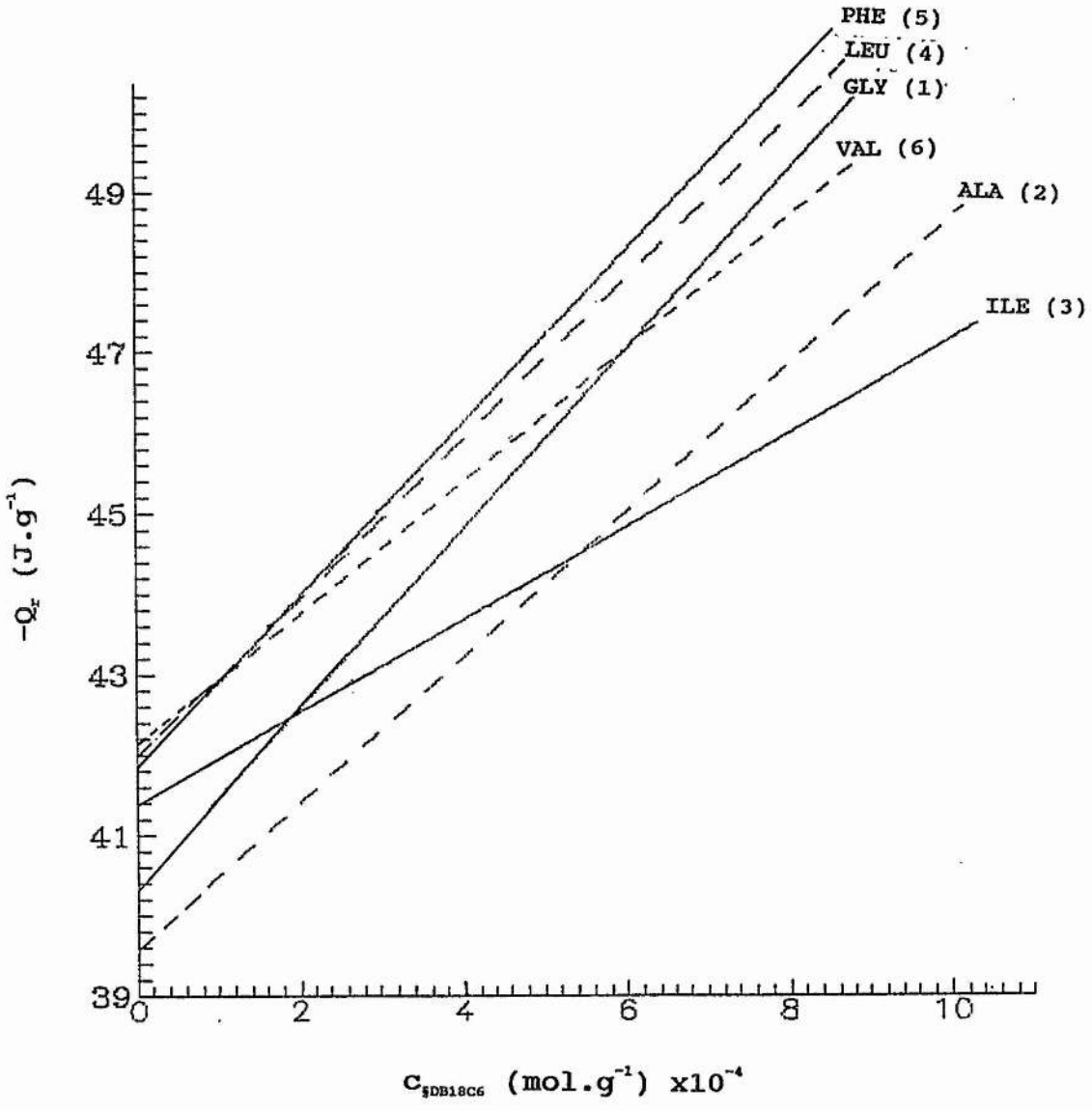

Figure 6.4 Plots of Q_r versus $c_{\$DB18C6}$ for amino acids in methanol at 298.15 K

Table 6.7 Data used for the calculation of the extraction constant (log K_{ex}), the enthalpy of extraction ($\Delta_{ex}H$) and the distribution coefficient (D) for the extraction of Glycine from methanol by §DB18C6 at 298.15 K

Weight of Resin (g)	c_i (mol.dm^{-3})	c_e	$c_{\S DB18C6}$ mol.g^{-1}	$x_{(LnHAa)}$	$\log K_{ex}$	Q_r J.g^{-1}	Q_{ex} J.g^{-1}	$\Delta_{ex}H$ kJ.mol^{-1}	D dm^3.g^{-1}
0.01110	$1.81\cdot10^{-3}$	$1.58\cdot10^{-3}$	$1.04\cdot10^{-3}$	0.4000	3.11	-51.944	-11.966	-11.51	0.658
0.00693	$1.45\cdot10^{-3}$	$1.32\cdot10^{-3}$	$9.38\cdot10^{-4}$	0.3601	3.03	-51.279	-11.301	-12.04	0.711
0.01034	$1.08\cdot10^{-3}$	$8.99\cdot10^{-4}$	$8.75\cdot10^{-4}$	0.3365	3.11	-48.969	-8.991	-10.27	0.973
0.01065	$9.05\cdot10^{-4}$	$7.89\cdot10^{-4}$	$5.44\cdot10^{-4}$	0.2092	2.71	-46.996	-7.018	-12.90	0.689
0.01048	$7.24\cdot10^{-4}$	$6.22\cdot10^{-4}$	$4.87\cdot10^{-4}$	0.1873	2.73	-46.308	-6.330	-12.99	0.783
0.01101	$3.62\cdot10^{-4}$	$3.02\cdot10^{-4}$	$2.72\cdot10^{-4}$	0.1046	2.67	-42.764	-2.786	-10.24	0.901

Table 6.8 Data used for the calculation of the extraction constant (log K_{ex}), the enthalpy of extraction ($\Delta_{ex}H$) and the distribution coefficient (D) for the extraction of DL-Alanine from methanol by §DB18C6 at 298.15 K

Weight of Resin (g)	c_i (mol.dm^{-3})	c_e	$c_{\S DB18C6}$ mol.g^{-1}	$x_{(LnHAa)}$	logK_{ex}	Q_r J.g^{-1}	Q_{ex} J.g^{-1}	$\Delta_{ex}H$ kJ.mol^{-1}	D dm^3.g^{-1}
0.01276	$5.24\cdot10^{-3}$	$5.01\cdot10^{-3}$	$9.01\cdot10^{-4}$	0.3479	2.94	-47.925	-7.947	-8.82	0.179
0.01160	$4.19\cdot10^{-3}$	$4.09\cdot10^{-3}$	$8.19\cdot10^{-4}$	0.3162	2.80	-47.622	-7.644	-9.33	0.200
0.01137	$3.14\cdot10^{-3}$	$3.01\cdot10^{-3}$	$5.79\cdot10^{-4}$	0.2235	2.41	-44.212	-4.234	-7.31	0.192
0.00845	$2.62\cdot10^{-3}$	$2.51\cdot10^{-3}$	$6.25\cdot10^{-4}$	0.2413	2.58	-44.668	-4.690	-7.51	0.249
0.01286	$2.09\cdot10^{-3}$	$1.97\cdot10^{-3}$	$4.45\cdot10^{-4}$	0.1718	2.32	-43.371	-3.393	-7.62	0.226
0.01366	$1.05\cdot10^{-3}$	$9.57\cdot10^{-4}$	$3.40\cdot10^{-4}$	0.1313	2.41	-42.852	-2.874	-8.45	0.335
0.01614	$5.24\cdot10^{-4}$	$4.74\cdot10^{-4}$	$1.55\cdot10^{-4}$	0.0595	2.21	-41.409	-1.431	-9.23	0.327

Table 6.9 Data used for the calculation of the extraction constant (log K_{ex}), the enthalpy of extraction ($\Delta_{ex}H$) and the distribution coefficient (D) for the extraction of DL-Isoleucine from methanol by §DB18C6 at 298.15 K

Weight of Resin (g)	c_i (mol.dm^{-3})	c_e	$c_{\S DB18C6}$ mol.g^{-1}	$x_{(LnHAa)}$	logK_{ex}	Q_r J.g^{-1}	Q_{ex} J.g^{-1}	$\Delta_{ex}H$ kJ.mol^{-1}	D dm^3.g^{-1}
0.01351	$2.57 \cdot 10^{-3}$	$2.44 \cdot 10^{-3}$	$4.81 \cdot 10^{-4}$	0.1857	2.65	-46.923	-5.096	-10.59	0.197
0.00824	$2.06 \cdot 10^{-3}$	$2.01 \cdot 10^{-3}$	$3.03 \cdot 10^{-4}$	0.1169	2.18	———	———	———	0.151
0.01187	$2.06 \cdot 10^{-3}$	$1.92 \cdot 10^{-3}$	$2.94 \cdot 10^{-4}$	0.1135	2.18	-45.019	-3.192	-10.86	0.153
0.00957	$1.54 \cdot 10^{-3}$	$1.49 \cdot 10^{-3}$	$2.61 \cdot 10^{-4}$	0.1008	2.18	-44.559	-2.732	-10.47	0.175
0.01150	$1.28 \cdot 10^{-3}$	$1.21 \cdot 10^{-3}$	$3.04 \cdot 10^{-4}$	0.1174	2.41	-45.313	-3.485	-11.46	0.251
0.00922	$1.03 \cdot 10^{-3}$	$9.99 \cdot 10^{-4}$	$2.16 \cdot 10^{-4}$	0.0834	2.20	———	———	———	0.216
0.01061	$1.03 \cdot 10^{-4}$	$9.75 \cdot 10^{-4}$	$2.56 \cdot 10^{-4}$	0.1023	2.38	-44.413	-2.587	-10.10	0.262

Table 6.10 Data used for the calculation of the extraction constant (log K_{ex}), the enthalpy of extraction ($\Delta_{ex}H$) and the distribution coefficient (D) for the extraction of DL-Leucine from methanol by §DB18C6 at 298.15 K

Weight of Resin (g)	c_i (mol.dm^{-3})	c_e	$c_{\S DB18C6}$ mol.g^{-1}	$x_{(LnHAa)}$	logK_{ex}	Q_r J.g^{-1}	Q_{ex} J.g^{-1}	$\Delta_{ex}H$ kJ.mol^{-1}	D dm^3.g^{-1}
0.01684	$2.67\cdot10^{-3}$	$2.48\cdot10^{-3}$	$5.64\cdot10^{-4}$	0.2178	2.92	-47.668	-5.916	-10.49	0.227
0.01675	$2.14\cdot10^{-3}$	$1.97\cdot10^{-3}$	$5.07\cdot10^{-4}$	0.1959	2.83	-47.208	-5.455	-10.76	0.257
0.01179	$1.60\cdot10^{-3}$	$1.49\cdot10^{-3}$	$4.66\cdot10^{-4}$	0.1801	2.82	-46.493	-4.740	-10.17	0.312
0.01538	$1.33\cdot10^{-3}$	$1.18\cdot10^{-3}$	$4.58\cdot10^{-4}$	0.1768	2.89	-45.981	-4.228	-9.23	0.388
0.01149	$1.07\cdot10^{-3}$	$1.01\cdot10^{-3}$	$2.61\cdot10^{-4}$	0.1008	2.35	-44.789	-3.037	-11.64	0.258
0.01875	$5.34\cdot10^{-4}$	$4.91\cdot10^{-4}$	$1.14\cdot10^{-4}$	0.0470	2.09	-43.116	-1.363	-11.96	0.232
0.01542	$2.67\cdot10^{-4}$	$2.39\cdot10^{-4}$	$9.08\cdot10^{-5}$	0.0350	2.27	-42.723	-0.970	-10.69	0.380

Table 6.11 Data used for the calculation of the extraction constant (log K_{ex}), the enthalpy of extraction ($\Delta_{ex}H$) and the distribution coefficient (D) for the extraction of DL-Phenylalanine from methanol by §DB18C6 at 298.15 K

Weight of Resin (g)	c_i ($mol.dm^{-3}$)	c_e	$c_{\S DB18C6}$ $mol.g^{-1}$	$x_{(LnHAa)}$	$\log K_{ex}$	Q_r $J.g^{-1}$	Q_{ex} $J.g^{-1}$	$\Delta_{ex}H$ $kJ.mol^{-1}$	D $dm^3.g^{-1}$
0.00858	$4.55 \cdot 10^{-3}$	$4.47 \cdot 10^{-3}$	$4.66 \cdot 10^{-4}$	0.1792	2.86	-44.087	-2.866	-6.15	0.104
0.01255	$3.64 \cdot 10^{-3}$	$3.53 \cdot 10^{-3}$	$4.38 \cdot 10^{-4}$	0.1684	2.82	-43.831	-2.610	-5.96	0.124
0.00918	$2.73 \cdot 10^{-3}$	$2.65 \cdot 10^{-3}$	$4.15 \cdot 10^{-4}$	0.1596	2.57	-43.922	-2.701	-6.51	0.156
0.00833	$2.27 \cdot 10^{-3}$	$2.21 \cdot 10^{-3}$	$3.60 \cdot 10^{-4}$	0.1385	2.45	-43.251	-2.030	-5.64	0.163
0.01149	$1.07 \cdot 10^{-3}$	$1.01 \cdot 10^{-3}$	$2.61 \cdot 10^{-4}$	0.1008	2.43	-42.954	-1.733	-6.64	0.161

Table 6.12 Data used for the calculation of the extraction constant (log K_{ex}), the enthalpy of extraction ($\Delta_{ex}H$) and the distribution coefficient (D) for the extraction of DL-Valine from methanol by §DB18C6 at 298.15 K

Weight of Resin (g)	c_i (mol.dm^{-3})	c_e	$c_{\S DB18C6}$ mol.g^{-1}	$x_{(LnHAa)}$	logK_{ex}	Q_r J.g^{-1}	Q_{ex} J.g^{-1}	$\Delta_{ex}H$ kJ.mol^{-1}	D dm^3.g^{-1}
0.01333	$3.90\cdot10^{-3}$	$3.75\cdot10^{-3}$	$5.34\cdot10^{-4}$	0.2062	2.72	-47.027	-4.827	-9.04	0.142
0.01199	$2.34\cdot10^{-3}$	$2.25\cdot10^{-3}$	$3.75\cdot10^{-4}$	0.1448	2.40	-45.375	-3.176	-8.47	0.166
0.01229	$1.95\cdot10^{-3}$	$1.84\cdot10^{-3}$	$4.47\cdot10^{-4}$	0.1726	2.73	-44.986	-2.786	-6.33	0.242
0.01216	$1.56\cdot10^{-3}$	$1.46\cdot10^{-3}$	$2.90\cdot10^{-4}$	0.1120	2.32	-44.329	-2.129	-7.34	0.199
0.01480	$7.80\cdot10^{-4}$	$7.51\cdot10^{-4}$	$1.65\cdot10^{-4}$	0.0637	2.15	-43.595	-1.396	-8.46	0.219
0.00840	$3.90\cdot10^{-4}$	$3.75\cdot10^{-4}$	$8.48\cdot10^{-5}$	0.0327	2.05	-42.854	-0.652	-7.69	0.225

CHAPTER 7

CONCLUSIONS

Enthalpy data obtained by calorimetry for processes involving lanthanide cryptates in dipolar aprotic media have never been reported before. The availability of these parameters, as well as the free energy and entropy values, enabled a detailed interpretation of the complexation reactions of tervalent lanthanide cations with Cryptand-221 and Cryptand-222 in acetonitrile and propylene carbonate.

It was found that:

i) In these solvents, the cryptands form complexes of very high stabilities with the tervalent lanthanide cations. However, these ligands do not exhibit any selectivity towards these cations. It was therefore concluded that the cryptands are not suitable for separating the lanthanide cations.

ii) The complexation reaction is enthalpy favoured for all the lanthanide cryptates as a result of strong electrostatic interactions between the tervalent cations and the donor atoms of the ligand. This process is generally entropy unfavoured.

iii) The enthalpies of complexation of the lanthanide(III) cryptates in acetonitrile were found to be similar to those in propylene carbonate.

Single-ion transfer values based on the Ph_4AsPh_4B assumption were obtained from three independent measurements of heats of solution of *a)* the lanthanide triflates *b)* the lanthanide 221-cryptates and *c)* the lanthanide 222-cryptates. In the latter two cases the single-ion values for

the tervalent lanthanides have been derived from calculations involving a thermodynamic cycle, taking into account the complexation data. It was shown that the transfer of lanthanide(III) cations from propylene carbonate to acetonitrile is largely enthalpically favoured. It was also noted that the lanthanide(III) cryptates undergoe the same changes in interaction with the solvent (as reflected by the enthalpy term) during the transfer process than the corresponding free lanthanide. Therefore, it was concluded that these solvents are able to recognize selectively the lanthanide cations whether through the ligand or by direct interaction. Consequently, the cryptate conventions used for the calculation of single-ion values for the transfer of monovalent cations among dipolar aprotic media are not valid for the tervalent cations in these solvents.

This part of the thesis has been the subject of a paper published in the Journal of the Chemical Society[177].

In the second part of this work, the thermodynamics of interaction of macrocyclic ligands with amino acids were studied[178]. It was shown that the amino acids are capable to interact not only with the crown ethers but also with the cryptands in the alcohols.

The results indicate that:

i) The active site of the amino acid as guest molecule for macrocyclic hosts is the protonated amino group (NH_3^+), forming three hydrogen bonds with the oxygen atoms of the macrocyclic ligands. In general, 1:1 amino acid-macrocyclic ligand complexes have been observed. The complexes formed in methanol and ethanol are stable enough ($3<\log K_s<4$) to give isolable compounds.

ii) No selectivity between the primary amino acids occurs. However, it has been shown that the selectivity is mainly dependent on the number of hydrogen bonds available for interaction. Therefore,

proline (forming two hydrogen bonds) and lysine (capable of a forming 2:1 complex) have slightly different stability constants than the other amino acids.

iii) The similarity in the stability constants of the amino acid complexes in methanol and ethanol are the result of an enthalpy-entropy compensation effect.

The transfer process between methanol and ethanol of a series of amino acids was studied. It was shown that the transfer data are closely related to the complexation data. For a given ligand, the differences observed in the thermodynamic parameters of complexation are due to the differences in the solvation of the amino (NH_3^+) group of the amino acid. A linear correlation between the enthalpies of transfer of the amino acids from methanol to ethanol and the difference of the corresponding complexation parameters in methanol and ethanol were observed. Therefore, this work also illustrates the importance of the transfer data among different solvents for the host and guest molecules in the interpretation of the complexation processes in these solvents involving these species. The importance of the transfer parameters has also been emphasized in a recent publication by Danil de Namor[179].

Resins containing Dibenzo-18-Crown-6 as anchor groups have been used to extract a series of amino acids form methanol. It has been shown that there is a possibility of separating glycine and also, to a slighter extent, DL-Alanine and DL-Leucine from the other amino acids. These findings may have important applications, notably because the resins have the advantadge to be recyclable.

REFERENCES

1. E. FISCHER, Ber. Dtsch. Chem. Ges., 1894, *27*, 2985
2. C.J. PEDERSEN, J. Am. Chem. Soc., 1967, *89*, 2495,7017
3. B.C. PRESSMAN, Fed. Proc. Fed. Am. Soc. Exp. Biol., 1968, *27*, 1283 and references cited therein
4. C. MOORE, B.C. PRESSMAN, Biochem. Biophys. Res. Commun., 1964, *15*, 562
5. C.J. PEDERSEN, J. Am. Chem. Soc., 1970, *92*, 386, 391
6. J.M. LEHN, J.P. SAUVAGE, Tetrahedron Lett., 1969, 2885
7. J.M. LEHN, Struct. & Bonding (Berlin), 1973, *16*, 1
8. D.J. CRAM, T. KANEDA, P.C. HELGESON, G.H. LEIN, J. Am. Chem. Soc., 1979, *101*, 6752
9. K.N. TRUEBLOOD, C.B. KNOBLER, E. MAVERICK, H.C. HELGESON, S.H. BROWN, D.J. CRAM, J. Am. Chem. Soc., 1981, *103*, 5594
10. K.E. KOENIG, G.M. LEIN, P. STRÜCKLER, T. KANEDA, D.J. CRAM, J. Am. Chem. Soc., 1984, *106*, 2160
11. D.J. CRAM, S.P. HO, C.B. KNOBLER, E. MAVERICK, K.N. TRUEBLOOD, J. Am. Chem. Soc., 1985, *107*, 2989
12. E. WEBER, F. VÖGTLE, Chem. Ber., 1976, *109*, 1803
13. F. VÖGTLE, E. WEBER (Eds), Top. Curr. Chem., 1981, *98*; ibid. 1982, *101*; ibid. 1984, *121*
14. D.J. CRAM, G.M. LEIN, J. Am. Chem. Soc., 1985, *107*, 3657
15. D.J. CRAM, Angew. Chem. Int. Ed. Engl., 1986, *25*, 1039
16. S.S PEACOCK, D.M. WALBA, F.C.A. GAETA, R.C. HELGESON, D.J. CRAM, J. Am. Chem. Soc., 1980, *102*, 2043
17. D.S. LINGENFELTER, R.C. HELGESON, D.J. CRAM, J. Am. Chem. Soc., 1981, *46*, 393
18. J.M. LEHN, Pure & Applied Chem., 1979, *51*, 979
19. H.K. FRENSDORFF, J. Am. Chem. Soc., 1971, *95*, 4684
20. M. KIRCH, J.M. LEHN, Angew. Chem. Int. Ed. Engl., 1975, *14*, 1555

21. J.D. LAMB, J.J. CHRISTENSEN, J.L. OSCARSON, B.L. NIELSON, B.W. ASAY, R.M. IZATT, J. Am. Chem. Soc., 1980, *102*, 6820
22. A.F. DANIL de NAMOR, E. SIGSTAD, Polyhedron, 1986, *5*, 839
23. M.W. HOSSEINI, J.M. LEHN, J. Chem. Soc., Chem. Comm., 1988, 397
24. M.W. HOSSEINI, J.M. LEHN, J. Chem. Soc., Chem. Comm., 1985, 1155
25. M.W. HOSSEINI, J.M. LEHN, J. Am. Chem. Soc., 1987, *109*, 7047
26. D.J. CRAM, H.E. KATZ, J. Am. Chem. Soc., 1983, *105*, 135
27. J.M. LEHN, C. SIRLIN, J. Chem. Soc., Chem. Comm., 1978, 949
28. J.M. LEHN, C. SIRLIN, New J. Chem., 1987, *11*, 693
29. Y.A. OVCHINNIKOV, V.T. IVANOV, A.M. SHKROB, Membrane-Active complexones, Elsevier, Amsterdam, 1974
30. P. MUELLER, D.O. RERDIN, Biochem. Biophys. Res. Comm., 1967, *26*, 398
31. E. EYAL, G.A. RECHNITZ, Anal. Chem., 1972, *43*, 1090
32. G.A. RECHNITZ, E. EYAL, Anal. Chem., 1972, *44*, 320
33. R.M. IZATT, J.S. BRADSHAW, S.A. NIELSEN, J.D. LAMB, J.J. CHRISTENSEN, Chem. Rev., 1985, *85*, 271
34. J.C. BUNZLI, D. WESSNER, Coord. Chem. Rev., 1984, *60*, 191
35. F. VÖGTLE, W.M. MÜLLER, W.M. WATSON, Top. Curr. Chem., 1984, *125*, 231
36. L.F. LINDOY, "The Chemistry of Macrocyclic Ligand Complexes", Cambridge University Press, 1989
37. M.R. TRUTER, Struc. & Bonding, 1973, *16*, 71
38. N.K. DALLEY in "Synthetic Multivalent Macrocyclic Compounds" (R.M. Izatt, J.J. Christensen, Eds), Academic Press, 1978, 207
39. D. MORAS, B. METZ, R. WEISS, Acta Crystallogr. Sect. B, 1973, *29*, 383 and 388
40. D. MORAS, R.WEISS, Acta Crystallogr. Sect. B, 1973, *29*, 396, 400, 1059
41. B. METZ, D. MORAS, R. WEISS, Acta Crystallogr. Sect. B, 1973, *29*, 1377, 1382, 1388
42. B. METZ, R. WEISS, Inorg. Chem., 1974, *13*, 2094

43. B. METZ, D. MORAS, R. WEISS, J. Chem. Soc., Perkin Trans. II, 1976, 423

44. F. MATHIEU, R. WEISS, J. Chem. Soc., Chem. Comm., 1973, 816

45. J.D. LAMB, R.M. IZATT, J.J. CHRISTENSEN, D.L. EATOUGH in "Coordination Chemistry of Macrocyclic Compounds" (G.A. Nelson, Ed) Plenum Press, New York, 1979

46. R.D. SHANNON, Acta Crystallogr. Sect. A, Found. Crystallogr., 1976, *32*, 751

47. F. MATHIEU, B. METZ, D. MORAS, R. WEISS, J. Am. Chem. Soc., 1978, *100*, 4412

48. G. ANDEREGG, Helv. Chim. Acta, 1975, *58*, 1218

49. F. ARNAUD-NEU, B. SPIESS, M.J. SCHWING-WEILL, J. Am. Chem. Soc., 1982, *104*, 5641

50. B.G. COX, N. van TRUONG, H. SCHNEIDER, J. Am. Chem. Soc., 1984, *106*, 1273

51. A.F. DANIL de NAMOR, M.C. RITT, J. KRÖBER, unpublished results

52. R.M. IZATT, D.J. EATOUGH, J.J. CHRISTENSEN, Struct. & Bonding, 1973, *16*, 161

53. R.M. IZATT, R.E. TERRY, B.L. HAYMORE, L.D. HANSEN, N.K. DALLEY, A.G. AVONDET, J.J. CHRISTENSEN, J. Am. Chem. Soc., 1976, *98*, 7620

54. F. ARNAUD-NEU, R. YAHYA, M.J. SCHWING-WEILL, J. Chimie Physique, 1986, *83*, 403

55. B.G. COX, N. van TRUONG, J. GARCIA-ROSAS, H. SCHNEIDER, J. Phys. Chem., 1984, *88*, 996

56. R.M. IZATT, R.E. TERRY, T.E. JENSEN, B.L. HAYMORE, Inorg. Chim. Acta, 1978, *30*, 1

57. H.K. FRENSDORFF, J. Am. Chem. Soc., 1971, *95*, 153

58. D.J. CRAM, R.C. HELGESON, L.R. SOUSA, J.M. TIMKO, M. NEWCOMB, P. MOREAU, F. DEJONG, G.W. GOKEL, P.H. HOFFMAN, L.A. DOMEIR, S.C. PEACOCK, K. MADAM, Pure & Applied Chem., 1975, *43*, 327

59. M.A. BUSH, M.R. TRUTER, J. Chem. Soc., Perkin Trans.II, 1972, 345
60. H.E. SIMMONS, C.H. PARK, J. Am. Chem. Soc., 1968, *90*, 2428
61. A.F. DANIL de NAMOR, F.R. FERNANDEZ-SALAZAR, J. Chem. Soc., Faraday Trans. I, 1988, *90*, 2428
62. A.F. DANIL de NAMOR, F.R. FERNANDEZ-SALAZAR, P. GREENWOOD, J. Chem. Soc., Faraday Trans. I, 1987, *83*, 2663
63. B. DIETRICH, J.M. LEHN, J.P. SAUVAGE, J. Chem. Soc., Chem. Comm., 1973, *15*, 1973
64. H.K. FRENSDORFF, J. Am. Chem. Soc., 1971, *95*, 600
65. B.G. COX, P. FIRMAN, I. SCHNEIDER, H. SCHNEIDER, Inorg. Chim. Acta, 1981, *49*, 153
66. B.G. COX, J. GARCIA-ROSAS, H. SCHNEIDER, J. Am. Chem. Soc., 1981, *103*, 1384
67. V. GUTMANN, E. WYCHERA, Inorg. Nucl. Chem. Letters, 1966, *2*, 257
68. M.H. ABRAHAM, A.F. DANIL de NAMOR, W.H. LEE, J. Chem. Soc., Chem. Comm., 1977, 893
69. J. GUTKNECHT, H. SCHNEIDER, J. STROKA, Inorg. Chem., 1978, *17*, 3326
70. M.F. LEJAILLE, M.H. LIVERTOUX, G. GUIDON, J. BESSIERE, Bull. Soc. Chim. Fr., 1978, 373
71. J. BESSIERE, M.F. LEJAILLE, Anal. Lett., 1979, *12*, 753
72. M.K. CHANTOONI, I.M. KOLTHOFF, J. Soln. Chem., 1985, *14*, 1
73. A.F. DANIL de NAMOR, L. GHOUSSEINI, W.H. LEE, J. Chem. Soc., Faraday Trans. I, 1985, *81*, 2495
74. A.F. DANIL de NAMOR, L. GHOUSSEINI, J. Chem. Soc., Faraday Trans. I, 1984, *80*, 2349
75. A.F. DANIL de NAMOR, L. GHOUSSEINI, J. Chem. Soc., Faraday Trans. I, 1985, *81*, 781
76. A.F. DANIL de NAMOR, L. GHOUSSEINI, J. Chem. Soc., Faraday Trans. I, 1986, *82*, 3275

77. A.F. DANIL de NAMOR, T. HILL, R.A.C. WALKER, E. CONTRERAS-VIGURIA, H. BERROA de PONCE, J. Chem. Soc., Faraday Trans. I, 1988, *84*, 2551
78. A.F. DANIL de NAMOR, J. Chem. Soc., Faraday Trans.I, 1988, *84*, 2441
79. J.M. LEHN, J.P. SAUVAGE, J. Chem. Soc., Chem. Comm., 1971, 440
80. D.K. CABBINESS, D.W. MARGERUM, J. Am. Chem. Soc., 1969, *91*, 6540
81. G. CHAPUT, G. JEMINET, J. JUILLARD, Can. J. Chem., 1975, *53*, 2240
82. J.M. LEHN, J.P. SAUVAGE, J. Am. Chem. Soc., 1975, *97*, 6700
83. E. KAUFFMAN, J.M. LEHN, J.P. SAUVAGE, Helv. Chim. Acta, 1976, *59*, 1099
84. M. CIAMPOLINI, P. DAPPORTO, N. NARDI, J. Chem. Soc., Chem. Comm., 1978, 78
85. F.A. HART, M.B. HURTSHOUSE, K.H.A. MALIK, S. MOORHOUSE, J. Chem. Soc., Chem. Comm., 1978, 549
86. R.M. IZATT, J.D. LAMB, J.J. CHRISTENSEN, B.L. HAYMORE, J. Am. Chem. Soc., 1977, *99*, 8344
87. G. GUILLAIN, P. BARTHELEMY, J. MASSAUX, J.F. DESREUX, J. Chem. Soc., Dalton Trans., 1984, 2847
88. J.H. BURNS, C.F. BAES Jr, Inorg. Chem., 1981, *20*, 616
89. I. MARROLEAU, J.P. GISSELBRECHT, M.GROSS, F. ARNAUD-NEU, M.J. SCHWING-WEILL, J. Chem. Soc., Dalton Trans, 1989, 367
90. R. PIZER, R. SELZER, Inorg. Chem., 1983, *22*, 1359
91. E.L. YEE, O.A. GANSOW, M.J. WEAVER, J. Am. Chem. Soc., 1980, *102*, 2278
92. M.C. ALMASIO, F. ARNAUD-NEU, M.J. SCHWING-WEILL, Helv. Chim. Acta, 1983, *66*, 1296
93. F. ARNAUD-NEU, E.L. LOUFOUILOU, M.J. SCHWING-WEILL, J. Chem. Soc., Dalton Trans, 1986, 2624
94. D.J. CRAM, K.N. TRUBLOOD, Top. Curr. Chem., 1981, 98, *43*

95. R.M. IZATT, J.D. LAMB, N.E. IZATT, B.E. ROSSITER Jr, J.J. CHRISTENSEN, B.L. HAYMORE, J. Am. Chem. Soc., 1979, *101*, 6273
96. B. GOSSE, A. DENAT, Electroanalytical Chem. and Interfacial Electrochem., 1974, *56*, 5129
97. J. MASSAUX, G. DUYCKAERTS, Anal. Chim. Acta, 1974, *73*, 41
98. Methodes de Dosage par les Titriplex, Merck Manual.
99. A. SEMINARA, A. MUSUMECI, Inorg. Chim. Acta, 1980, *39*, 9
100. E.L. YEE, O.A. GANSOW, M.J. WEAVER, J. Am. Chem. Soc., 1979, *101*, 4408
101. A. SEMINARA, E. RIZZARELLI, Inorg. Chim. Acta, 1980, *40*, 249
102. A. SABATINI, A. VACCA, P. GANS, Talanta, 1974, *21*, 53
103. I. WADSÖ, Quart. Rev. Biophysics, 1970, *3*, 383
104. I. WADSÖ, Science Tools, 1966, *13*, 33
105. S.R. GUNN, J. Chem. Thermodynamics, 1971, *3*, 19
106. H.C. DICKINSON, Bull. Nat. Standards, 1914, *11*, 189
107. A.R. CHALLOWER, H.A. GUNDRY, A.R. MEETHAM, Phil. Trans. Roy. Soc. London, 1955, *A247*, 553
108. L.K.B. 8700 Precision Calorimetric System, Instruction Manual, LKB Produkter, Stockholm, Sweden
109. S. SUNNER, I. WADSÖ, Science Tools, 1966, *13*, 1
110. J.J. CHRISTENSEN, R.M. IZATT, I.D. HANSEN, Rev. Sci. Instrum., 1965, *36*, 779
111. K.P. MISCHENKO, Y.Y. KAGANOVICH, Zhur. Prikled. Khim., 1949, *22*, 1078 (Chem. Abstract, 1950, *44*, 921a)
112. R.J. IRVING, I. WADSÖ, Acta Chem. Scand. 1964, *11*, 189
113. R.J. IRVING, I. WADSÖ, Acta Chem. Scand., 1964, *18*, 195
114. S.R. GUNN, J. Phys. Chem., 1965, *69*, 6902
115. G. OJELUND, I. WADSÖ, Acta Chem. Scand., 1967, *21*, 1838
116. J.O. HILL, G. OJELUND, I. WADSÖ, J. Chem. Therm., 1969, *1*, 111
117. H. NAGHIBI-BIDOKHTI, PhD Thesis, University of Surrey, UK, 1977
118. L. GHOUSSEINI, PhD Thesis, University of Surrey, UK, 1985
119. R. TRABOULSSI, PhD Thesis, University of Surrey, UK, 1990

120. A.I. VOGEL, Elementary Practical Organic Preparation, revised by B.V. Smith and N.H. Waldron, 3rd edition, 1980, 87
121. J.J CHRISTENSEN, J. RUCKMAN, D.J. EATOUGH, R.M. IZATT, Thermochim. Acta, 1972, *3*, 203
122. J.J CHRISTENSEN, J. RUCKMAN, D.J. EATOUGH, R.M. IZATT, Thermochim. Acta, 1972, *3*, 219
123. J.J. CHRISTENSEN, J. RUCKMAN, D.J. EATOUGH, R.M. IZATT, Thermochim. Acta, 1972, *3*, 233
124. J.D. LAMB, Brigham Young University, Utah, USA, personal communication
125. V.P. PARKER, Thermal Properties of Aqueous Univalent Electrolytes, Nat. Bur. Stand., NRSDS-NBS2, Govt. Printing Office, Washington D.C., 1965
126. F.D. ROSSINI, D.D. WAGMAN, W.H. EVANS, S. LEVINE, I. JAFFER, Selected Values of Chemical Thermodynamic Properties, Nat. Bur. Stand., Circ. 500, U.S. Govt. Printing Office, Washington D.C. 1952
127. D.D. WAGMAN, W.H. EVANS, V.P. PARKER, I. HALLOW, S.M. BAILEY, R.H. SCHWUN, Selected Values of Chemical Thermodynamic Properties, Nat. Bur. Stand., Technical Note 270-3, U.S. Govt. Printing Office, Washington D.C., 1968
128. R.K. McMULLAN, W. SAENGER, J. FAYES, D. MOOTZ, Carbohydr. Res., 1973, *31*, 211
129. C.E. VANDERZEE, J.A. SWANSEN, J. Phys. Chem., 1963, *67*, 2608
130. D.J. HALE, R.M. IZATT, J.J. CHRISTENSEN, J. Phys. Chem., 1963, *67*, 2608
131. L.D. HANSEN, E.A. LEWIS, J. Chem. Therm., 1971, *3*, 35
132. T. MOELLER, The Chemistry of the Lanthanides, Reinhold Publishing, New York, 1963
133. C.M. CRISS, M. SALOMON, in "Physical Chemistry of Organic Solvent Systems", A.K. Covington and T. Dickinson, (Plenum Press, London, 1973)
134. B.G. COX, A.J. PARKER, J. Am. Chem. Soc., 1973, *95*, 402

135. R. ALEXANDER, A.J. PARKER, J. Am. Chem. Soc., 1967, *89*, 5549
136. O. POPOVYCH, A. GIBOFSKY, D.H. BERNE, Anal. Chem., 1972, *44*, 811
137. E. GRUNWALD, G. BAUGHAM, G. KOHNSTAN, J. Am. Chem. Soc., 1960, *82*, 5801
138. H. STREHLOW, H.M. KOEPP, Z. Electrochem., 1958, *62*, 373
139. O. POPOVYCH, R. TOMKINS, in "Non-Aqueous Solution Chemistry", Wiley-Intersc., 1981, 399
140. R. ALEXANDER, A.J. PARKER, J.H. SHARP, W.E. WAGHORNE, J. Am. Chem. Soc., 1972, *94*, 1148
141. Y. MARCUS, "Ion Solvation", Wiley-Intersc., 1985
142. B.G. COX, H. SCHNEIDER, Pure & Applied Chem., 1989, *61*, 171
143. I. MARROLEAU, Personal Communication
144. V.A. BIDZILYA, L.P. OLEKSENKO, Russian J. Phys. Chem., English Translation, 1985, *55*, 1168
145. V.A. BIDZILYA, L.P. OLEKSENKO, Russian J. Phys. Chem., English Translation, 1985, *55*, 214
146. V.A. BIDZILYA, L.P. GOLOVKOVA, Z.Z. ROZHKOVA, Russian J. Phys. Chem., English Translation, 1988, *58*, 1645
147. R.M. IZATT, J.D. LAMB, B.E. ROSSITER, N.E. IZATT, J.J. CHRISTENSEN, B.L. HAYMORE, J. Chem. Soc., Chem. Comm., 1978, 386
148. O. NAGANO, A. KOBAYASHI, Y. SASAKI, Bull. Chem. Soc. Jpn., 1978, *51*, 790
149. I. GOLDBERG, J. Am. Chem. Soc., 1980, *102*, 4106
150. M.J. BOVILL, D.J. CHADWICK, I.O. SUTHERLAND, J. Chem. Soc., Perkin Trans., 1980, 1529
151. M. NEWCOMB, S.S. MOORE, D.J. CRAM, J. Am. Chem. Soc., 1977, *99*, 6405
152. D.J. CRAM, K.N. TRUEBLOOD, Top. Curr. Chem., 1981, *98*, 43
153. K.N. TRUEBLOOD, C.B. KNOBLER, D.S. LAWRENCE, R.V. STEVENS, J. Am. Chem. Soc., 1982, *104*, 1355

154. J.M. TIMKO, S.S. MOORE, D.M. WALBA, P.C. HIBERTY, D.J. CRAM, J. Am. Chem. Soc., 1974, *96*, 4207
155. J.G. VINTER, A. DAVIS, M.R. SAUNDERS, J. Comp. Aided Molecular Design, 1987, *1*, 31
156. R. LUMRY, S. RAJENDER, Biopolymers, 1970, *9*, 1125
157. E.A. LEWIS, L.D. HANSEN, J. Am. Chem. Soc., 1973, *95*, 2081
158. S. TAKAGI, T. KIMURA, M. MAEDAR, Therm. Acta, 1985, *88*, 247
159. A.F. DANIL de NAMOR, R. TRABOULSSI, D.F.V. LEWIS, J. Am. Chem. Soc., 1990, *112*, 8447
160. Y. INOUE, T. HAKUSHI, J. Chem. Soc., Perkin Trans., 1985, 935
161. J.M. TIMKO, R.C. HELGESON, M. NEWCOMB, G.W. GOKEL, D.J. CRAM, J. Am. Chem. Soc., 1974, *96*, 7097
162. M. NEWCOMB, J.M. TIMKO, D.M. WALBA, D.J. CRAM, J. Am. Chem. Soc., 1977, *99*, 6392
163. R.C. HELGESON, T.C. TARNOWSKI, J.M. TIMKO, D.J. CRAM, J. Am. Chem. Soc., 1977, *99*, 6411
164. B.P. DEY, S.C. LAHIRI, Indian J. Chem., 1986, *25*, 136
165. E.J. COHN, T.L. McMEEKIN, J.T. EDSALL, J.M. WEARE, J. Am. Chem. Soc., 1934, *56*, 2270
166. T.L. McMEEKIN, E.J. COHN, J.M. WEARE, J. Am. Chem. Soc., 1936, *58*, 2173
167. A.F. DANIL de NAMOR, Personal Communication
168. C.H. LING, PhD Thesis, University of Surrey, UK, 1981
169. J.B. DALTON, C.C.A. SCHMIDT, J. Biol. Chem., 1933, *103*, 549
170. E. BLASIUS, W. ADRIAN, K.P. JANZEN, G. KLAUTKE, J. Chromatogr., 1974, *96*, 89
171. E. BLASIUS, K.P. JANZEN, G. KLAUTKE, J. Anal. Chem., 1975, *277*, 374
172. E. BLASIUS, P.G. MAURER, J. Chromatogr., 1976, *125*, 511
173. E. BLASIUS, P.G. MAURER, Makromol. Chem., 1977, *178*, 649
174. E. BLASIUS, K.P. JANZEN, H. LUXEMBURGER, V.B. NGUYEN, H. KLOTZ, J. STOCKEMER, J. Chromatogr., 1978, *167*, 307

175. E.E. SIGSTAD, PhD Thesis, University of Surrey, UK, 1985
176. E. BLASIUS, K.P. JANZEN, M. KELLER, H. LAUDER, T. NGUYEN-TIEN, G. SCHOTTER, Talanta, 1980, *27*, 107
177. A.F. DANIL de NAMOR, M.C. RITT, M.J. SCHWING-WEILL, F. ARNAUD-NEU, J. Chem. Soc., Faraday Trans., 1990, *86*, 89
178. A.F. DANIL de NAMOR, M.C. RITT, M.J. SCHWING-WEILL, F. ARNAUD-NEU, D.F.V. LEWIS, J. Chem. Soc., Chem. Comm., 1990, 116
179. A.F. DANIL de NAMOR, Pure & Applied Chem., 1990, *62* (11), 2441

APPENDIX A

This appendix contains the Infra-Red spectra of Cryptand-221 and Cryptand-222, as well as an example of the spectra of the lanthanide triflates and their cryptates.

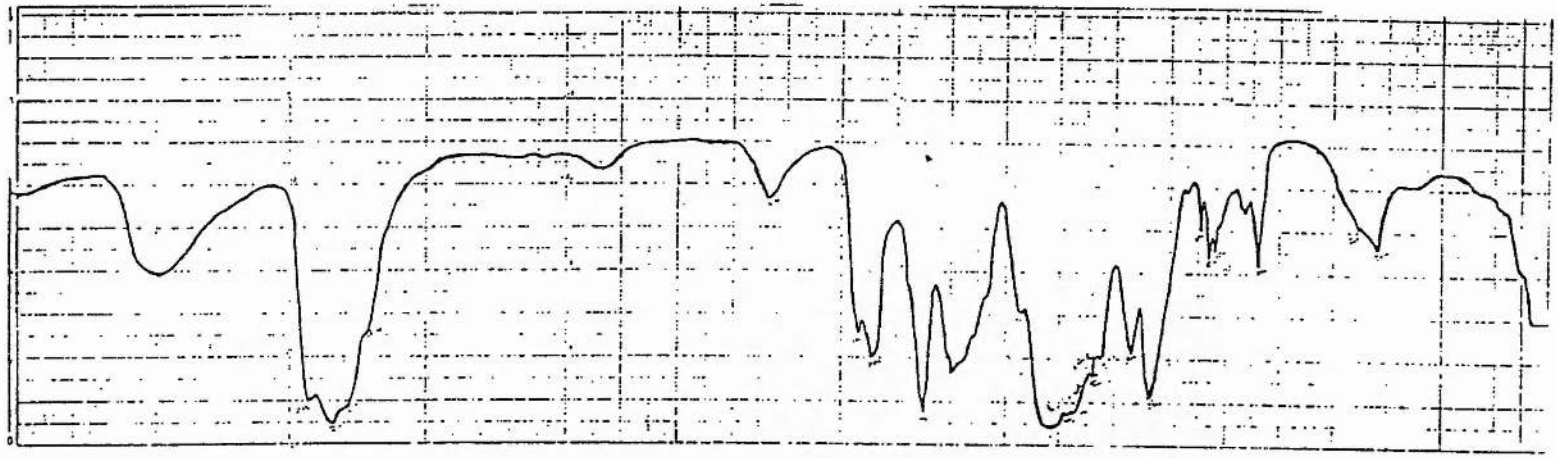

IR Spectrum of Cryptand 221

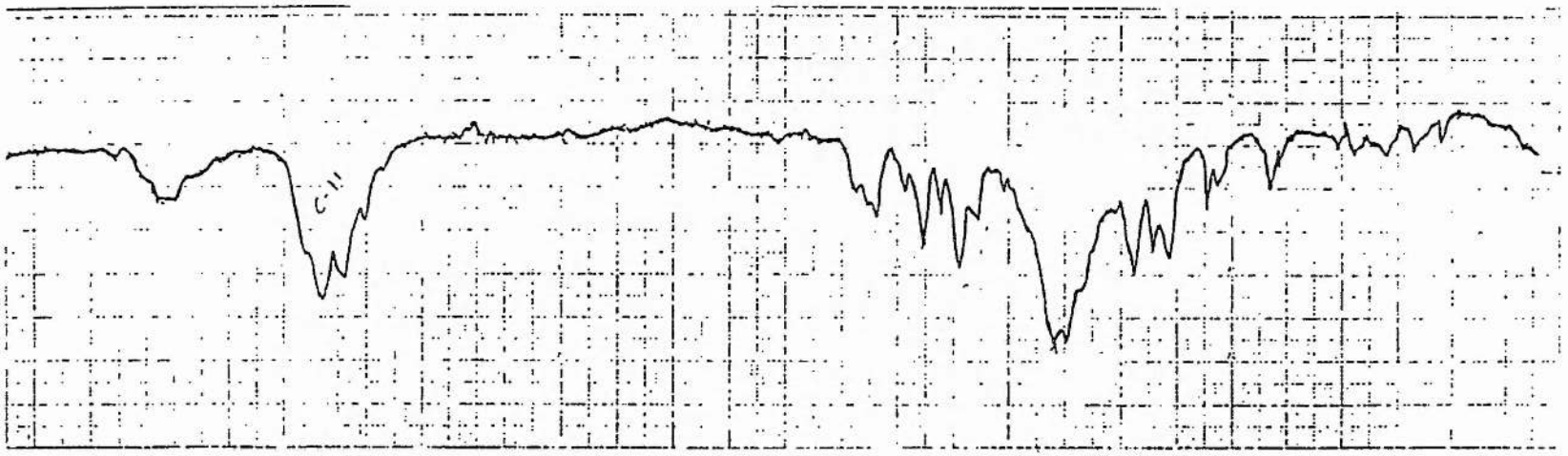

IR Spectrum of Cryptand 222

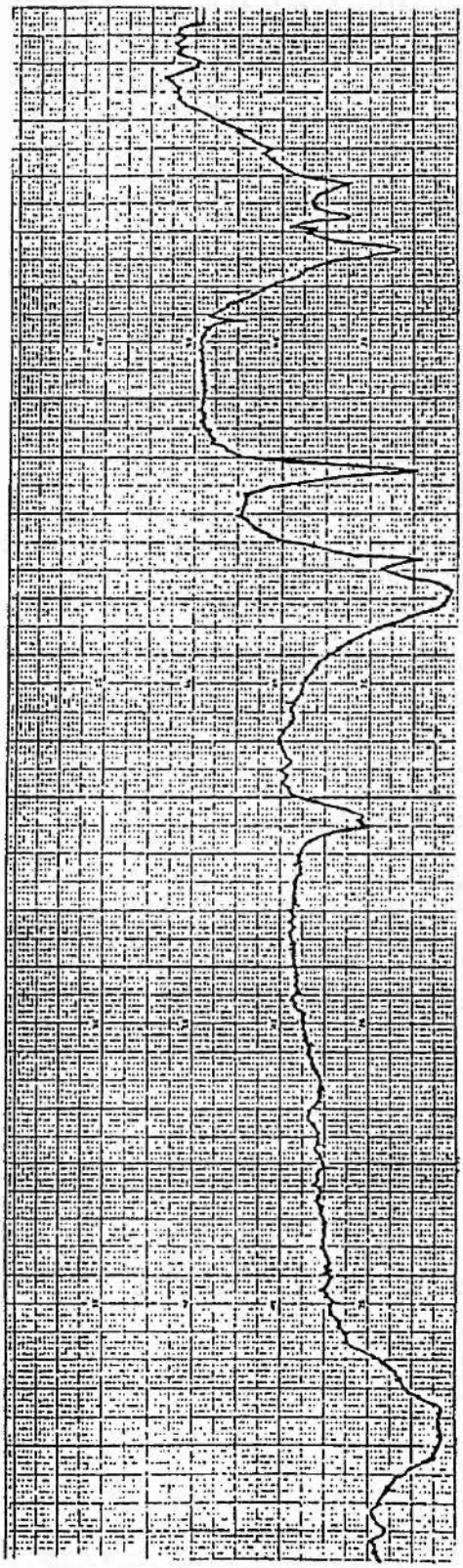

IR Spectrum of $La(CF_3SO_3)_3$

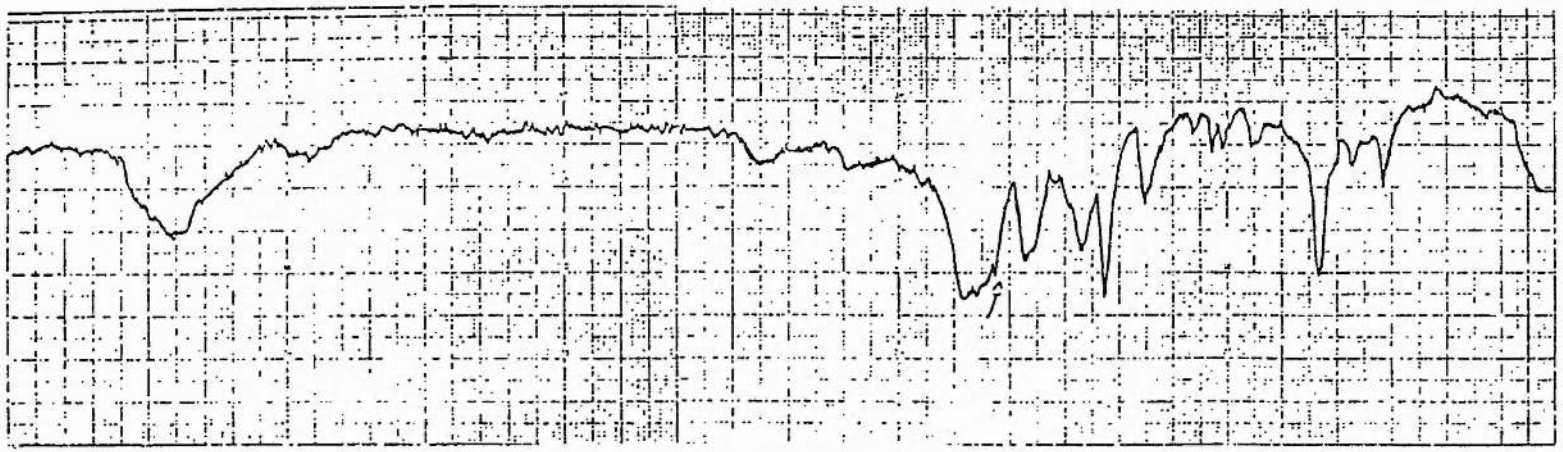

IR Spectrum of La221$(CF_3SO_3)_3$

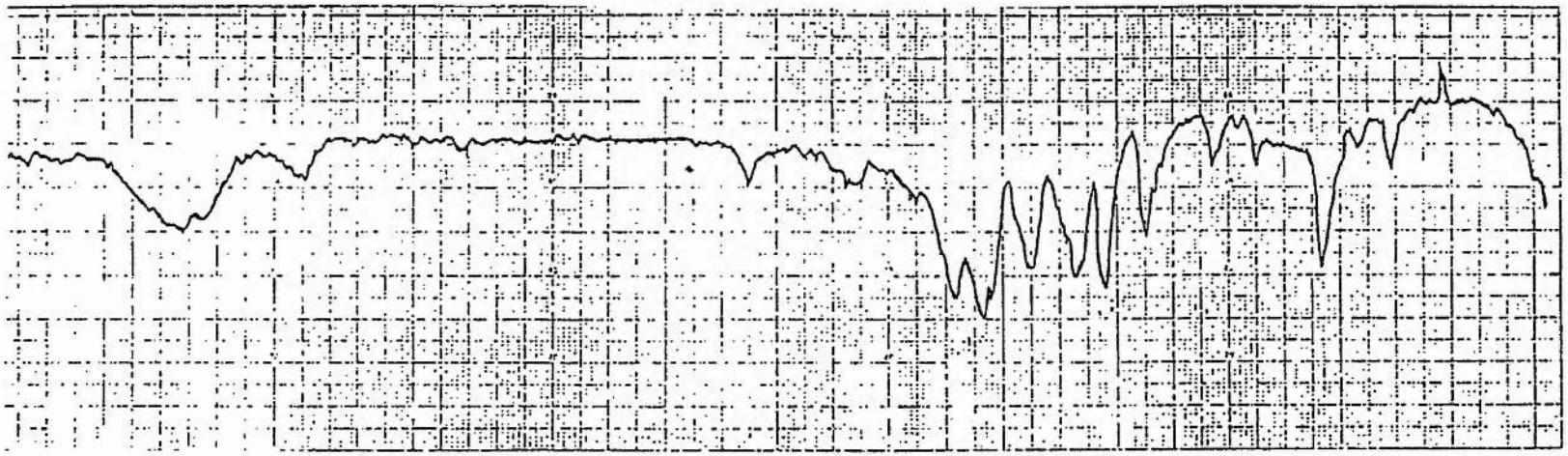

IR Spectrum of La222$(CF_3SO_3)_3$

APPENDIX B

Simultaneous Determination of Equilibrium Constants (K_c, $\Delta_c G°$) and Changes in Enthalpies ($\Delta_c H°$) and Entropies ($\Delta_c S°$)

If the equilbrium constant is not too high ($K \leq 10^6$), it is possible to determine K-values by calorimetric titration. Usually the titration is performed stepwise. This method can be used for the study of the binding between metal ions and ligands, or between macromolecules and ligands. It is mainly simple 1:1 equilibria which are of interest. More complex equilbria are difficult to resolve by calorimetry alone.

For a complexation process between a ligand (L) and a guest species (G) in a solvent (s), the equilibrium can be written as:

$$G_{(s)} + L_{(s)} \rightleftharpoons GL_{(s)} \qquad 1$$

The equilibrium constant is expressed, in terms of activities, as:

$$K_c = \frac{a_{GL}}{a_G . a_L} \qquad 2$$

or in terms of concentrations and activity coefficients:

$$K_c = \frac{[GL]}{[M].[L]} . \frac{f_{GL}}{f_G . f_L} \qquad 3$$

If $[G]_o$ and $[L]_o$ are the initial concentrations of the guest species and the ligand respectively, the mass balance equations at equilibrium may be written as:

$$[G]_o = [G] + [GL] \quad 4$$

$$[L]_o = [L] + [GL] \quad 5$$

By replacing [G] and [L] into expression 3.:

$$K_c = \frac{f_{GL}}{f_g} \cdot \frac{[GL]}{([L]_o - [GL]).([G]_o - [GL])} \quad 6$$

This leads to a quadratic equation:

$$[GL]^2 - ([G]_o + [L]_o + \frac{f_{GL}}{f_G} \cdot \frac{1}{K_c}).[GL] + [GL]_o.[L]_o = 0 \quad 7$$

which can be solved for [GL], the number of moles of complex formed:

$$[GL] = \frac{[G]_o + [L]_o + \frac{f_{GL}}{f_G} \cdot \frac{1}{K_c} \pm [[([G]_o + [L]_o + \frac{f_{GL}}{f_G} \cdot \frac{1}{K_c})^2 - 4.[G]_o.[L]_o]]^{1/2}}{2} \quad 8$$

Computer programs have been developed to calculate for a given value of K_c the molar concentration (corrected for the activity coefficients of G and GL) of the complex (GL). For the initial calculation, γ_{GL} and γ_G are assumed to be unity. Once [GL] is estimated, [G] can be obtained from $[G]_o$ - [GL]. Values of [GL] and [G] are then used to estimate γ_{GL} and γ_G using the extended form of the Debye-Hückel equation. These values of γ_{GL} and γ_G are then

substituted back into euqation 8. using the same K_c to find another value for [GL] which again is used to calculate better values of γ_{GL} and γ_G. This iteration process will take place until [GL] converges. The final [GL] value is then used to calculate the $\Delta_c H°$ values as:

$$\Delta_c H^\circ = \frac{Q_c}{[GL].V} \qquad 9$$

V (ml) being the volume of ligand in the amino acid solution.

An example of calculation is given for the complexation reaction of DL-Alanine by 18-Crown-6 in methanol at 298.15 K. The following data were collected from the titration experiment.

[ALA] /mol.dm^{-3}	[18C6] /mol.dm^{-3}	Q_r/J	Volume /ml
$1.29 \cdot 10^{-3}$	$3.04 \cdot 10^{-4}$	-0.5042	0.1326
$1.29 \cdot 10^{-3}$	$6.09 \cdot 10^{-4}$	-0.9326	0.2652
$1.28 \cdot 10^{-3}$	$9.14 \cdot 10^{-4}$	-1.2769	0.3978
$1.28 \cdot 10^{-3}$	$1.22 \cdot 10^{-3}$	-1.5711	0.5304
$1.28 \cdot 10^{-3}$	$1.52 \cdot 10^{-3}$	-1.7983	0.6630
$1.27 \cdot 10^{-3}$	$1.82 \cdot 10^{-3}$	-1.9744	0.7956
$1.27 \cdot 10^{-3}$	$2.16 \cdot 10^{-3}$	-2.1087	0.9282

The program calculates for each assumed log K_c value, the concentration of GL and then the standard enthalpies of complexation for each Q_r entered. Thus for each log K_c value, there will be an averaged $\Delta_c H°$ value and a standard deviation $\sigma(\Delta_c H°)$. When the assumed log K_c value is far away from the correct value, the $\Delta_c H°$ values vary considerably, and hence give rise to a large standard deviation. The minimum deviation is observed when the assumed log K_c value coincides with the actual value.

The final K_c and $\Delta_c H°$ values selected for this reaction are:
log K_c = 3.59 and $\Delta_c H°$ = -39.693 ± 1.024. Among all log K_c values, the value of 3.59 gave the smallest standard deviation as illustrated in Figure 1, hence it is the most probable value. In general, the log K_c and the $\Delta_c H°$ values reported for a particular complexation reaction are taken as average of several independent titration runs.

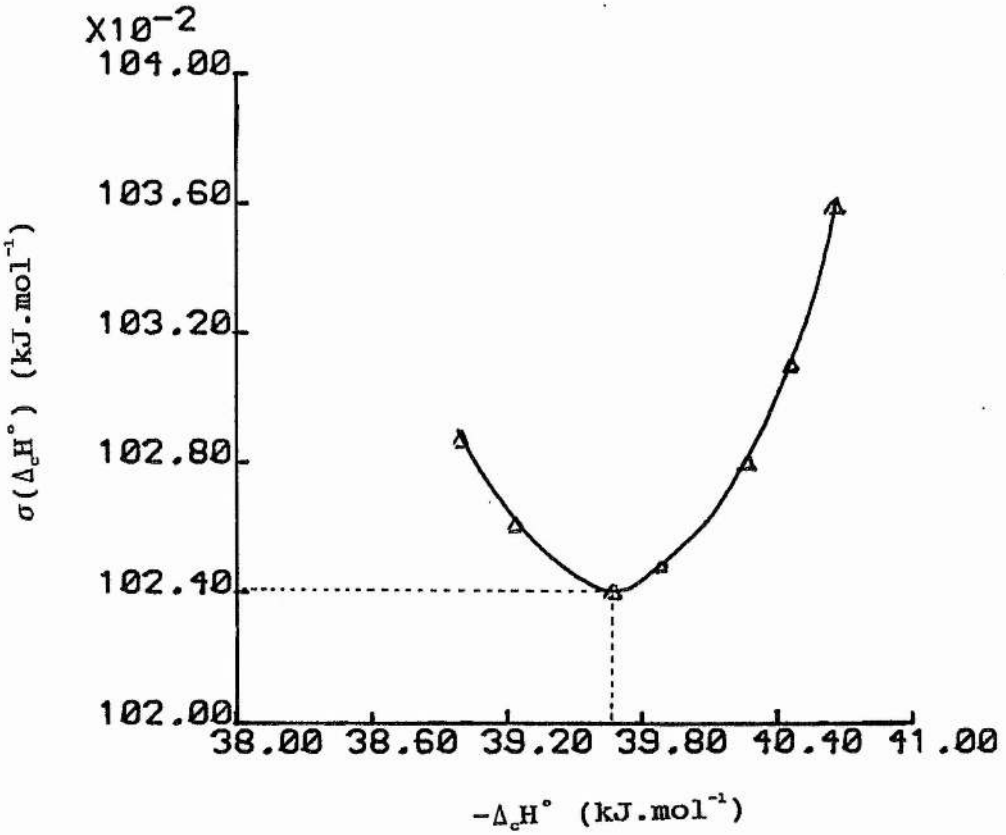

Figure 1 Estimation of $\Delta_c H°$ value from the variation of the standard deviation